DERIVATIVES OF INDOLE AND ANILINE AS ORGANIC CORROSION INHIBITORS OF LOW CARBON STEEL

By

Francis Kolawole OJO
MATRIC NUMBER: 146827

B.Sc. Industrial Chemistry (Jos), M.Sc. Industrial Chemistry (Ibadan)

A Thesis in the Department of Chemistry,
Submitted to the Faculty of Science
in partial fulfilment of the requirements for the Degree of

DOCTOR OF PHILOSOPHY

of the

UNIVERSITY OF IBADAN

JANUARY, 2020

ABSTRACT

Inorganic corrosion inhibitors are frequently used in protecting metals from acidic solutions often employed in industrial processes. However, their applications have been limited by high cost of production and toxicity.Thus, the search for alternatives which are affordable and with negligible environmental effects. Functional electronegative elements and π- electron conjugated double bonds which are important features in corrosion inhibition process are contained in heterocyclic compounds such as indole and aniline. However, the corrosion inhibition properties of indole and aniline have not been adequately investigated. Therefore, this study was designed to investigate the corrosion inhibition efficiencies and adsorption mechanism of some derivatives of indole and aniline on low carbon steel.

Derivatives of indole: 6-benzyloxyindole and 3-methylindole and aniline:2-nitroaniline, 3-nitroaniline and 4-nitroaniline were employed for the corrosion inhibition. The corrosion rates and inhibition efficiencies of these derivatives were determined by weight loss and potentiodynamic polarisation methods. Images of low carbon steel in the absence of inhibitor and acid, low carbon steel in the presence of acid only and low carbon steel in the presence of acid and inhibitors of concentration 10 x 10^{-5} M were recorded with the aid of Scanning Electron Microscopy (SEM).The concentration range of inhibitors employed was 2 x 10^{-5} M to 10 x 10^{-5} M in 1.0 M HCl at 303K - 333K. The derivatives of indole and aniline were optimised using density functional theory at the B3LYP/6-31G* level. The experimental inhibition efficiencies of the inhibitors were compared to their theoretical inhibition efficiencies. Data generated were analysed by using multiple regressions at $\alpha_{0.05}$.

The corrosion rates from weight loss (mg $cm^{-2}h^{-1}$ x 10^{-3}) and potentiodynamic polarisation (mmpy) methods followed the order: 6-benzyloxyindole (0.55, 34.62) < 3-methylindole (0.98, 69.93) < 2-nitroaniline (3.43, 242.14) < 3-nitroaniline (3.49, 244.98) < 4-nitroaniline (3.55, 248.53).Inhibition efficiencies of the inhibitors increased with decrease in temperature, with all the inhibitors having their highest inhibition efficiencies at 303 K and at the concentration of 10 x 10^{-5} M. The inhibition efficiencies obtained from weight loss and potentiodynamic polarisation methods followed the order: 6-benzyloxyindole (92.29% and 94.11%) > 3-methylindole (86.32% and 88.11%) > 2-nitroaniline (52.24% and 58.82%) > 3-nitroaniline (51.37% and 58.34%) > 4-nitroaniline (50.50% and 57.74%). Potentiodynamic polarisation

curves revealed that the organic inhibitors acted as mixed-type inhibitors. The SEM images revealed that the corrosion reaction did not take place homogeneously over the surface of low carbon steel in 1 M HCl solution. However, the surface of the low carbon steel was protected by these organic inhibitors. The activation energies (12.21 – 55.40 kJ) and the Gibb's free energy values (-4.51 − -8.80 kJ) obtained from the weight loss method supported a physical adsorption mechanism. The adsorption was found to obey Langmuir adsorption isotherm. A good fit (R^2 = 0.9957) between the experimental and theoretical inhibition efficiencies was observed.

The 6-benzyloxyindole and 3-methylindole inhibited the corrosion of low carbon steel in hydrochloric acid and the process was through physical adsorption mechanism.Hence, these indole derivatives could serve as alternatives to inorganic corrosion inhibitors.

Keywords: Potentiodynamic polarisation, Langmuir adsorption isotherm, Indole derivatives, Aniline derivatives.

Word count: 499

CERTIFICATION

I certify that this work was carried out by Ojo, Francis Kolawole in the Department of Chemistry, University of Ibadan and has not been submitted elsewhere.

.....

Supervisor

I.A. Adejoro,

B.Sc., M.Sc., Ph.D. (Ibadan)

Reader, Department of Chemistry,

University of Ibadan, Nigeria.

ACKNOWLEDGEMENTS

My profound gratitude goes first and formost to God Almighty for sustaining me all the way.Thank you JesusChrist, for all you have done, you are doing and will continuously do in my life, Amen!

I am grateful to my Supervisor, Dr I. A. Adejoro for accepting me. Worthy to commend is your calm way of receiving me and your words of encouragement are of no less effect. Sir, i am grateful. With a heart of gratitude, I also appreciate Professor J. A. Lori for his fatherly guidance that has triggered meto fire on progressively.Thank you sir.

My immense appreciation goes to the Head of Department, Prof T. I. Odiaka and members of staff both teaching and non-teaching in the Department of chemistry, University of Ibadan for the enabling environment to carry out my research work. Special thanks to Dr A.R. Ipeaiyeda, Prof G. O. Adewuyi and Prof I. A. Oladosu. May God guide and protect you always. Amen.

My gratitude also goes to all members of staff of Chemical sciences department, Bingham university, Karu, Nasarawa State, for their support and provision of a conducive atmosphere for my research.

My profound gratitude goes to Eng. Toyin Fayakin, Eng. TukdatDabugat and Eng. Rinde Iroko. Thank you so much for all the love and support.

I also appreciate the members of Ibadan Varsity Christian Union (IVCU) postgraduate fellowship and all believers for their love and prayers. May God continue to strengthen us in his love.

My sincere gratitude also goes to my friends and colleagues, too numerous to mention for their love and support. I love you. May God bless you all. Amen.

Finally to my loved ones, my wife (Ojo Patience Atule), my son (Ojo David), my father (Mr Clement Ojo), my mother (Mrs Ojo Janet), my mother in law (Mrs AmoduRoselin), my siblins (Jumoke, Lanre, Lekan and Kayode) and my very own uncle Sule. Thanks for praying all through and supporting me. I love you all. May God in His infinite mercy bless you all, Thanks and thanks so much.

DEDICATION

This project work is dedicated primarily to God Almighty, The Alpha and Omega, The Author and Finisher of my faith. The one who was, who is and will forever be. Secondly to my beloved daughter and son who have gone to be with my lord, Jesus Christ. Amen!

TABLE OF CONTENTS

Title

Page

CHAPTER THREE:EXPERIMENTAL SECTIONS

CHAPTER FOUR: RESULTS AND DISCUSSION

LIST OF TABLES

LIST OF FIGURES

Figure No. Title

Page

CHAPTER ONE

INTRODUCTION

1.1 Background of the study

There has been a steady rise in the use of organic compounds as corrosion inhibitors of metals in aqueous environment. Tosafe guard metals against corrosion is very important. The use of Inhibitor is one of the practical means of preventing corrosion (Adejoro *et al.,* 2015). Inhibitors can protect metal surface by forming a barrieragainst corrosive agent in contact with metal. The effectiveness of inhibitors to offer protection against metals depends largely on the interaction between the inhibitor and the metal surface (Ameena, 2014). The inhibitors adsorbed on the metal surface could disturb the corrosion reaction, either by blocking the metal surface or by altering the activation barriers of the anodic and cathodic reactions of the corrosion process (Ebenso *et al.,* 2010a).

Electrons are donated to unoccupied d orbital of metal by organic compounds to form coordinate covalent bonds and these organic compounds can also accept free electrons from the metal by using their anti-bonding orbital to form feedback bonds, consequently creating excellent corrosion inhibitors. The organic inhibitors that are effective are those compounds containing hetero atoms like oxygen, sulfur, nitrogen and phosphorus (Barouni, 2014). The presence of aromatic rings and conjugated double bonds could further enhanced the effectiveness of these organic compounds as

excellent corrosion inhibitors (Adejoro *et al.,* 2016). The free electron pairs on heteroatom or π electrons are available for sharing to make bonds and behave as nucleophilic centers of organic molecules and help facilitate the adsorption process over the metal surface, whose atoms acts as electrophiles. The effectiveness of an inhibitor molecule in recent studies has been compared to its spatial and electronic structure with the aid of quantum chemical methods.These method provide in depth information into the inhibitor – surface interaction (Ebenso *et al.,* 2010b; Musa and Kamal, 2015). The use of quantum chemical parameters offers threekey

advantages: Based on the molecular structure, compounds with respect to the parent compound, substituents and various fragments can be directly characterized. Also, in terms of chemical reactivityof the compounds under study the proposed mechanism of action can be directly accounted for (Issa *et al.,* 2009; Valdez *et al.,* 2005), and lastly, novel organic inhibitors could be simulated (Stoyanova and Peyerimhoff, 2002). The theoretical calculation of the inhibition efficiency of organic molecules in selecting excellent corrosion inhibitors have continuously gained popularity especially with the significant progress in the building of sophisticated software packages which has been employed in quantum mechanical calculations (Gokhan, 2008). The use of some indole derivatives and nitro aniline compounds as effective organic inhibitors is interesting and can offer a great deal of solution to the unending corrosion challenge. However, it has not been extensively reported as such few reports exist in literature to date (Fouda *et al.,* 2014).

1.2 Statement of the problem

Corrosion has been a major threat to diverse industries including metallurgical and refinery industries. A huge sum of fund is directed towards an effective and cheap method of preventing and controlling this physio-chemical deterioration every year thereby increasing the cost of production. Several attempts made towards corrosion prevention include galvanization, passivation, anodization and inhibition by inorganic compounds. Most inorganic compounds such as phosphates, nitrites, hydrazines and chromates adopted as corrosion inhibitors proved to be carcinogenic and hazardous to the environment thus necessitating the need for the search of affordable, easily available and green corrosion inhibitors. This study is therefore directed to carry out experimental research and theoretical investigation on some indole derivatives and nitro aniline derivatives.

1.3 Significance of the study

This research will be a good predictive tool for engineers and other fields of science that find metals and their alloys especially low carbon steel, aluminium and copper very useful.

Building and construction industries that make use of iron rods, low carbon steel, aluminium and other metals in making materials like reinforced concrete, roofing sheet, bridges and sophisticated machines need a cost effective approach in

maintaining and preserving their equipment and products. This will enhance the durability and shelf life of these metal products. The result of this study will likely provide a cost effective modality which will invariably give a room for increased profit, increase employment rate and preserve the quality of materials. Furthermore, researchers and students in other related science-based fields may find the results of this research work useful in carrying out further studies on the molecules.

1.4 Justification for the study

The impact of corrosion effects on the safety and operation efficiency of equipment are often more severe than the mere loss of metal mass which may eventually lead to breakdowns of different kinds and the need for costly replacements.Damaging effects of corrosion include decrease of mechanical strength as a result of loss of metal mass and structural failure or collapse, material value reduction due to deterioration of appearance and loss of time in availability of profile-making industrial equipment.

Acids play a very major role in industrial processes such as industrial acid cleaning, oil well acidizing, acid pickling,acid descaling, cleaning of oil refinery equipment, chemical and electrochemical etching(Popoola*et al.,* 2013). In all of these industrial processes metals and their alloys are exposed to the action of acids. In oil well acidizing for instancemineral acids are pumped into the well to counter formation of plugging by clays and fines or dissolved carbonates and to remove scale from the bore well and other downward equipment for improved oil recovery. Exposures of these metals or metal alloys to acids could be damagingbut in many situations, corrosion inhibitors are extensively used in curbing the corrosion rates of metals/metal alloys in these acidic environment (Popova*et al.,* 2004). The main problem in using low carbon steel in acidic solution is that of uniform corrosion.

Corrosion has led to various dangers or damages as a result of structural breakdown in aircraft,industrial plants, pipe lines, bridges, cars, etc. Also other harmful effects of corrosion includes perforation of vessels and pipes permitting escape of contents and possible harm to the environment, loss of important surface properties of a metale.g electrical conductivity of contacts, contamination of fluids in vessels and pipes e.g cloudiness of beer when trace quantities of heavy metals are released into it by corrosion. A likely way out to protect low carbon steel from acidic environment is the introduction of corrosion inhibitors (Solmaz,2010).

Chromates, nitrites, hydrazines and phosphates are some of the adopted inorganic compounds used, however they are to be harmful to the environment. This necessitated the search for alternatives which are non-toxic, organic compounds having one or more hetero atoms and π electrons have shown to be effective in combatting corrosion(Babic-Samardzija et al., 2005).

Despite the usefulness of experimental methods in explaining the corrosion inhibition mechanism they are often time consuming and costly because they are based on trial – and error experiments (Gece, 2008). Nevertheless, steady progress in computer software and hardware advances have created unlimited access for great use of computational chemistry (theoretical chemistry) in research involving corrosion inhibition (Gokhan, 2008).

The work in this project largely has to do with the study of the corrosion inhibitive effect of some heterocyclic organic compounds namely 6 benzyl oxy indole, 3 methyl indole, 2 nitro aniline, 3 nitro aniline and 4 nitro aniline for low carbon steel in aqueous hydrochloric acid environments. This work is important because the organic inhibitors are affordable, non-toxic, easy to synthesize and inhibitors have not been reported as corrosion inhibitors.

For this reason this research is sets out to investigate:

i. The corrosion inhibition efficiencies of these indole derivatives and nitro aniline compounds by the use of gravimetric, gasometric, electrochemical and theoretical method.
ii. To establish the inhibition mechanism by the use of gravimetric, gasometric, electrochemical and theoretical method.
iii. To correlateexperimental inhibition efficiencies to some of the quantum chemical parameters.

1.5 Scope and limitation of the study

This research covers the corrosion inhibition studies of low carbon steel in 1 M HCl with some indole derivatives (Set A inhibitors) and nitro aniline derivatives (Set B inhibitors) namely 6 benzyl oxy indole, 3 methyl indole, 2 nitro aniline, 3 nitro aniline and 4 nitro aniline using weight loss method (gravimetric), hydrogen evolution method (gasometric), potentiodynamic polarization method (electrochemical) and quantum chemical studies (theoretical). In the case of fairly effective corrosion inhibitors, synergistic effect with iodide ions would be undertaken. The scanning electron microscope (SEM) will also be employed to clearly show the rate of corrosion.

1.6 Aim of Study

This study is therefore aimed at investigating the inhibitory potential of some derivatives of indole and aniline.

1.7 Objectives

i. To evaluate the inhibition efficiencies of some derivatives of indole and aniline for low carbon steel corrosion
ii. To effectively characterize the inhibitive mechanism of the corrosion process.
iii. To apply scanning electron microscopy to study surface morphology of low carbon steel in the absence and presence of the said inhibitors
iv. To correlate the quantum chemical parameters of some indole and aniline derivatives with their experimental corrosion inhibition efficiency.

CHAPTER TWO

LITERATURE REVIEW

2.1 Corrosion

The word corrosion came from the Latin term *corrodere* meaning gnaw or to gnaw. It is a process which results from a reaction between the environment and a metal/ metal alloy. Metals naturally occur in the combined state as minerals (Erika, 2012).

Corrosion does not only occur in metals, as perceived by lay men. Rather, the corrosion engineers consider corrosion in both metals and nonmetals. For instance, molten metal could attack solid metal (i.e. liquid metal corrosion), fluxing of the lining of a steelmaking furnace and deterioration of paint and rubber by chemicals or sunlight are kinds of corrosion. Nonetheless, metal corrosion is the most common type of corrosion.Corrosion reactions are usually electrochemical reactions (Mohd, 2010).

An electrochemical reaction is characterized by the absorption and emission of electrons and is summarized by equations 2.1, 2.2, 2.3 and 2.4.

$$Ox + ne^- \overset{OxRed}{\longleftrightarrow} Red \qquad 2.1$$

Anodic reaction is oxidation of a metal and the reduction is called cathodic reaction.Oxis an oxidizing agent,Redis a reducing agent and n is the number of electrons (e^-)in the reaction. In an electrochemical reaction electrons moves between anode and cathodewhereas ions move within thesolution.

The rate of corrosion depends on the dynamics of the anodic and cathodic reaction, the conduction of the solution and additionally the electronic conductivity within the solid phases.An anodic reaction on metal surface (M) is described in equation [2.2]

$$M \longrightarrow M^{n+} + ne^- \qquad 2.2$$

Equation [2.2]is usually balanced by oxygen reduction in equation [2.3] as a result of oxygen in the atmosphere

$\frac{1}{2}O_2 + H_2O + 2e^- \longrightarrow 2OH^-$ 2.3

This reaction in equation 2.3 is a cathodic reaction.

With reference to Figure1,iron is oxidized at the anode while oxygen is reduced at the cathode. Rust is then formed due to reaction between Fe^{2+} and OH^- (Erika, 2012).

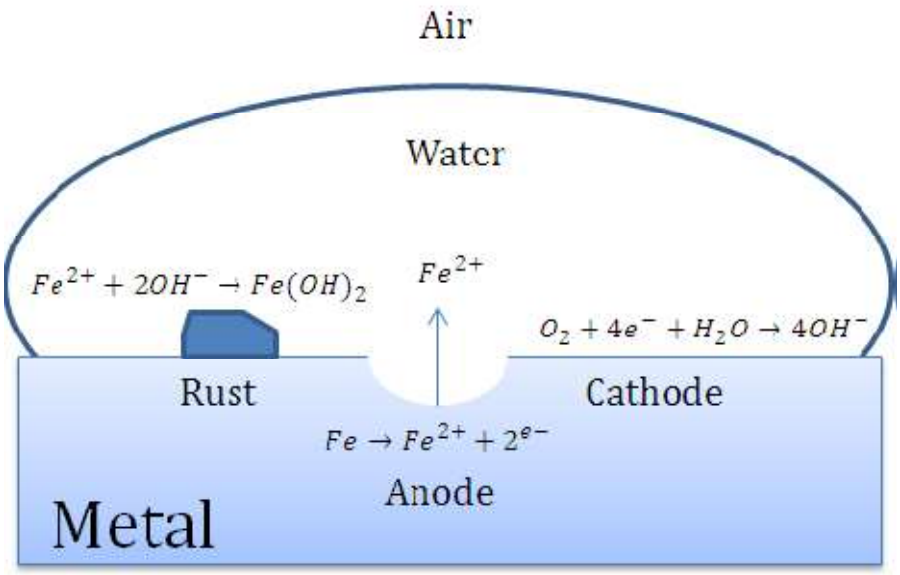

Figure 2.1: Illustration of the corrosion process on a surface of iron.

Source: Erika, 2012

2.2 Oxide Layer Formation

An oxide layer is formed on metal when in contact with moist air. An excess of negatively charged oxygen will then be produced when electrons in the oxidation process move toward the air-oxide interface (equation 2.4) while excess of positive ions is created at

$\frac{1}{2}O_2 + e^-$ O^{2-} $\longrightarrow$ 2.4

the metal-oxide interface. Potential difference between adsorbed oxygen and metal ion is important in oxide layer formation which is strengthened by a strong field due to metal ions driving through the oxide layer towards the oxide ions at a greater force.

The oxide layer acts as a barrier to the anodic dissolution reaction. However the layer is thin and will eventually atrophy,thus exposing the metal to corrosion attack. (Erika, 2012)

2.3 Forms of Corrosion

We have variouskinds of corrosion which principally depends on the environment and metal: (Mohd, 2010)

2.3.1 General (Uniform) Corrosion

Thisiscorrosiveattackevenly coveringalargefractionorthewholesurfacearea. Thinning ofthemetalprogressesuntilfailure.Thisisthemostimportantformof corrosionwhenconsidering tonnage waste.However,disastersseldomoccursbecause uniformcorrosioniseasily anticipatedandmeasured.Uniformcorrosioncanbe practicallycontrolledbycathodicprotection,useofcoatings,orsimplybyspecifyinga corrosion allowance(Matson, 1996).

2.3.2 Pitting Corrosion

Thiskindofcorrosionislocalizedsuchthatcavitiesare made inthematerial.The damagefrompittingisconsideredtobemorehazardousthanuniformcorrosionbecause itismoredifficultto predict,detectanddesignagainst.Corrosionproductsoften cover the pits. Pittingis initiated by:

a)Localizedchemicalormechanicaldamage totheprotectiveoxidefilm;factorssuch aslowdissolvedoxygenconcentrations,highconcentrationsofchlorideandacidity can causebreakdown of apassivefilmand renderaprotectiveoxide film moreunstable.

b) Protective coatingcould be poorlyused whichcan lead to localized damage.

c)Metalpartofthecomponentcouldcontainnon-uniformitiesforinstancenonmetallic inclusions (Marcus *et al.,*2008).

2.3.3 Stress Corrosion

Thiscracking isasaresultofthecombinedinfluenceoftensilestressandacorrosive environment.Thegravityofthistypeofcorrosiononamaterialisfrequently between drycrackingandthefatiguethresholdofthatmaterial.Therequiredtensilestressesmay bedirectform of appliedstresses orin themannerofresidual stresses(Sieradzki *et al.,*198).

2.3.4 CreviceCorrosion

Itisalocalizedformofcorrosioncommonly linkedwithastandingsolutiononthe micro-environmentallevelwhichoccur increvicesshielded areassuchasinsulation material,gaskets, washers and clamps (Theodore,2000).

2.3.5 Intergranular Corrosion

Thistypeofcorrosioniscommonly linkedwitheffectsfromchemicalsegregation implying thatimpuritieshaveatendencytobeenrichedatgrainboundariesorspecific phases precipitated on thegrain boundaries.Thecorrosionattacktakeplace favorably onthegrain-boundaryphase,orinaregionclosetoitthathaslostanelementnecessary foradequatecorrosionresistance.Inanycasethemechanicalpropertiesofthestructure willbegrosslyaffected (Marcus *et al.,* 2008).

2.3.6 Galvanic Corrosion

Thiscorrosiondamageisinducedwhentwodifferentmaterialsarecombined ina corrosiveelectrolyte.When agalvaniccoupleforms,oneof themetals in thecouplebecomestheanodeandcorrodesfasterthanitwouldallby itselfreverseis the caseforthecathode.Forgalvaniccorrosion totakeplace, these conditions must be present:

a. Electrochemically different metals must be present.

b. These metals must be connected electrically.

c. The metals must be in contact with an electrolyte.

Therelativedignity ofamaterialcanbeanticipated bydeterminingitscorrosion potential.Thegalvanicserieslistst herelativenobility ofsomematerialsinseawater. Asmallanodeorcathodearearatioishighly undesirable.Inthiscase,thegalvanic currentisconcentratedontoa smallanodicarea.Rapidreductioninthicknessofthe dissolvinganodetendstotakeplaceunderthesecondit ions.Gooddesignsshouldbethe ultimate waytoavoid theseproblems(Song*et al.,* 2004).

2.4 Corrosioncontrolinthe oilandgas industry

Oilfieldcorrosionissuesarenotfixedoccurrences.Overtimefluidcharacteristicschanges,le ading to systemsbecoming lessopentorecognized

corrosionmitigationprograms(Popoola *et al.,*2013).Technicaloptions adoptedinthe domainof corrosioncontrolinthe oilandgasproductionincludes material selection,useofprotective coatings, useof inhibitors, cathodicprotection and corrosion monitoring(Nalli, 2010).

2.4.1 Selection ofappropriatematerials

Popoola*et al.,*(2013)stressedtheneedtochangethematerialsofconstructionandselect othermaterialstosuitthetargetrequirementswhenitisnoticedthatthematerialsinuse are disposedtoattackfromcorrosion.Smith,(1999)proposedsomecorrosion-resistant alloysthatcanbeusedintheoilandgasindustrytoinclude825nickelalloy,625nickel alloy,2550nickelalloy,13Cr, Super 13Cr, 22Cr duplex,25Cr duplex,28Cr stainless steelandC276nickelalloy.Whilespecialty stainlesssteel e.gLDX2101,254SMO and654SMOwasproposed byJohansson*et al.,*(2010)forsolvingcorrosionproblemsintheoilandgasindustry.These stainlesssteelsprovedtobe excellent materials in resistingcorrosion.

2.4.2 Useofinhibitors

Thesearechemicalsthatare usedtoshieldthemetalsurfaceinordertoprotectthem fromcorrosioninoilandgasindustries.Metalsareprotectedeitherby theinhibitors combiningwiththemor by inhibitorsreactingwiththeimpuritiesintheenvironment that couldlead tocorrosion(Rajeev *et al.,*2012). Corrosion inhibitorcouldwork in differentways:Itmay block active sitesonthe metalsurface,thuslimiting the rate of theanodicorcathodicreaction,itmay causethemetaltoenterintothepassivation regionwhereanaturaloxidefilmisformedbyraisingthepotentialofthemetalsurface.
Furthermore someinhibitorshelpsinthecreationof a thinlayer onthemetalsurface whichsuppressestheprocessofcorrosion(Graeme,2010).Environmentalfriendliness, availability andcostarefactorstobeconsideredbeforeusingacorrosioninhibitorin the oilandgasindustry.Inthe lightof these factors,organic corrosioninhibitors are preferredtoinorganiccompoundsforprotectionofsteelsinacidmedia(Rajeev*et al.,*2012).

2.4.3 Useof protectivecoatings

Thelifeofamaterialwillbeenhancedby placingaprotectivelayeronthematerialto evadedirectcontactwiththemedia.Paint,coatings,metalliclining ormetallicsheets, fiberglass,glassflake, epoxy,andrubbercould actasthebarrieror layer.Sometimes

cadmium,nickelandzinccoatingsarepreferredoncertaincomponentslikeflangesand bolting(Nalli, 2010).

2.4.4 Cathodic protection technique

Thismethodhelptoreducecorrosionbyminimizingthedifferenceinpotentialbetween anodeandcathode.Thisisrealizedby applyingcurrenttothestructure tobeprotected from an externalsource. Whensufficient current is applied, the whole structurewillbe atonepotential;thus,anodeandcathodesiteswillnotexist(Guyer,2009).Itisnormally usedinconjunctionwithcoatingsandcanbeconsideredasa secondary corrosion control technique.

2.4.5 Adequatecorrosionmonitoring andinspection

Corrosionmonitoringisthepracticeofmeasuringthecorrosivity ofprocessstream conditionsby theuseofprobes(mechanical,electrical,orelectrochemicaldevices) whichareplacedintotheprocessstreamandconstantly opentotheprocessstream condition.Corrosionmonitoring techniquesaloneprovidedirectandonline measurement ofmetal loss/corrosion rate in oiland process system. One ofthemethodsistocarryouttheon-streaminspectionbyundertakingthewallthickness measurementsperiodicallyonfixedandvulnerablelocationsontheequipment,piping, andpipelinestoassessthematerialconditionsandcorrosionrates(Popoola*et al.,*2013).

2.5 Theuseofacidsinthe acidizing procedure

Thetreatmenton underground reservoirusuallyinvolves theinjection ofdifferent acid at 15%concentration (sometimes from 5% to28%)(Quraishiand Jamal, 2000; Quraishi*et al.,*2002).Themostcommonconventionalacidsare HCl,HF,acetic,and formicacids.Themajority ofacidizingtreatmentscarriedoututilizeHClat concentrationsof 5–28% (Smith*et al.,*1978).HClhasanadvantage over the other mineralacidsintheacidizing operationbecauseitformsmetalchlorides, whichareverysolubleintheaqueousphaseunlikesulphate,nitrate,andphosphatesalts whichhavelowersolubility(Jayaperumal,2010).HCliswidely usedforstimulating carbonate-basedreservoirssuchaslimestone anddolomite.HClrepresentsthemost economicalacidfordissolving$CaCO_3$ inpicklingapplications.However,thefast reactionratewithrocks,thecorrosionrate,andthepittingtendency ofmaterialsvary considerably withHClconcentration,whichcancauseproblems. Additionally,another

disadvantage ofusing HClisitshighcorrosivenesstosteel, aluminium,orchromium-platedequipment.Insummary,thecorrosionofpipelinesand otherequipmentinvolvedintheoilandgasindustryrepresentalargeprobleminthe acidizing process and consequentlyalargepart ofthe total cost and potential danger to the personnel involved. Thus, theselection ofnon-corrosive orlow-corrosiveinhibited acid solution is crucial.

2.6 Application methods.

The selectionofaninhibitorisofprimeimportance,buttheproperapplicationofan inhibitor isevenmore important.Ifaninhibitordoesnotreachthecorrosiveareas,it cannotbe effective.Maximumcorrosionprotectioncanbe achievedby continuous injection ofinhibitor through adual tubingstring (kill string), acapillarytubing, aside mandrelvalve,orevenperforatedtubing.Anyofthesemethodswillsupply a continuousresidualof inhibitor tomaintaincorrosionprotection(French etal,1993). Many gaswellsarenotequippedwithfacilitiesforcontinuoustreatmentandmustbe treated by sometypeofbatchorslugtreatment.Themostcommonly usedmethodis thebatchorshort-batchtreatmentinwhichavolumeofinhibitorsolution(typically 2 to 10%)is injectedinto ashut-in wellandallowedto fallto thebottom. Fall rates are a functionofsolutionviscosity.Thecommonfailure ofthismethodisnotallowing sufficienttimefortheinhibitortoreachthehole bottom.Avariationon thismethodis thetubingdisplacementtreatmentinwhichtheinhibitorsolutionispushedtothebottom by dieselorcondensate.Thisguaranteestheinhibitorreachingbottomhole,butitcan killlow-pressurewells.Sometimesa shortbatchisforceddownwitha nitrogen displacementor compressedgastospeedupthe fallrateandreduce shut-intime.An inhibitor squeeze issometimesusedtogetalonger returntime andsimulate a continuoustreatment.However,there isalwaysthe concernofformation damagewith squeezes and with tubing displacements.

2.7 Quantitative Structural Activity Relationship (QSAR)

QSAR was developed to relate the structure activity relationship of moleculardescriptors from quantum chemical calculations of organic compounds ascorrosion inhibitors. In this method of analysis, the model quality depends on the

fitting andprediction ability. On this account, it is suitable to form several quantum chemical descriptorssuch as log *P* (substituent constant), polarization, E_{HOMO} - E_{LUMO}, softness, hardness, molecular volume, weight e.t.c. and attempt to correlate thesequantum chemical parameters to the experimentally determined inhibition efficiencies. In thisapproach, a relationship in the form of an equation is sought, which correlates the molecularparameters/descriptors to the observed activity. The linear equation shown equation 2.5is often used in the study of corrosion inhibitors to correlate the quantum moleculardescriptors with the experimental inhibition efficiency of the inhibitors (Lukovits, *et al.,* 2001).

$$\%IE = \acute{\alpha} + \beta_1 \times_1 + \beta_2 \times_2 \ldots\ldots\ldots \beta_n \times_n \qquad 2.5$$

Where ά and ß are constants i.e regression coefficients determined through regression analysis,X1, X2.... Xnare quantum chemical index characteristic of the molecule 1,2...n.

2.8Reviewofsome corrosioninhibitors forhydrochloricacidsolutions

Asmentionedabove,among acidsolutions,HCl(at5–28%(Smith*et al.,*1978)isthe mostwidely usedfortheacidizingprocedureandthatiswhy themainfocusisonthis acid.AlsoHClconcentrationslowerthantheminimumcommonlyemployed(5%) are alsoincluded.However,Itmustbe pointedoutthatthe followingreviewcannotcover allaspects of corrosion inhibitorsusein HCl solutions.

Abiola, 2006 reportedthat 3-(4-amino-2-methyl-5-pyrimidylmethyl)-4-methyl thiazoliumchlorideeffectively reducedcorrosionrateoflowcarbonsteelin0.5moldm^{-3}and 5 moldm-^{3}HClat 30^{O}C.

AitChikh*et al.,*2005found outthat1,12-bis(1,2,4-triazolyl)dodecaneforcarbon steel in1moldm^{-3}HCl.actedasagoodcathodic-typeinhibitor.Theyinferedthatadsorption of thiscompoundoccursviasynergisticeffectbetweenchloride ionsandthepositive quaternaryammoniumion moietypresent in the inhibitor molecule.

Aljourani*et al.,*2009showedthatthetrendofI.E% forthecorrosioninhibitorsinthe following order:2-mercaptobenzimidazole>2-methylbenzimidazole>benzimidazole forlowcarbonsteelin1moldm^{-3} HClat25^{O}C.TheI.E%ofall3corrosioninhibitors decreased with increasingtemperaturefrom 25 to55^{O}C.

Babic-Samardzija*et al.,*2005studied2-butyn-1-ol,3-butyn-1-ol,3-pentyn-1-ol,and4-pentyn-1-olascorrosioninhibitorsforironin1moldm^{-3} HClatambienttemperatures. They

reportedthattheorganiccompoundsbehavedasmixed-typeinhibitorsandalso showed that theirI.E%depends on thetriplebondposition and chain length.

Baddini*et al.,* 2007 found that tributylamine,aniline,n-octylamine,diphenylamine, dodecylamine,di-n-butylamine,cyclohexylamine,1,3-dibutyl-2-thiourea are themost effective corrosion inhibitorsamongthe 23compounds studied.

Cruz*et al.,*(2004)revealedtheI.E%inthefollowing order:1-(2-ethylamino)-2-methylimidazoline ~N-[3-(2-aminoethylaminoethyl)]-acetamide>1-(2-ethylamino)-2-methylimidazolidineforcarbonsteelatroomtemperatureindeaerated0.5moldm^{-3}HCl.

Cruz*et al.,*(2005)studied2-aminomethylbenzimidazoleandbis(benzimidazol-2-ylethyl) sulphideascorrosioninhibitorsforcarbonsteelindeaerated0.5moldm^{-3}HCl.Theyfound outthattheformeractsasa cathodic typeinhibitor andthelatterasamixed-type inhibitor.

Elachouri*etal.,* (1995)employed2-(alkyl(CnHn+1) dimethylamonio)butanolbromides (n=11–15)ascorrosioninhibitorsforFe(purity99.5%)andrevealedthatthey are effective cathodic-typecorrosioninhibitor.TheirI.E% increasedwithanincrease inhibitor concentration.

Flores*et al.,*(2011)revealedthattheInhibitionefficiency ofsodiumNalkyl-phthalamates(alkyl=n-C_6H_{13},n-$C_{10}H_{21}$,n-$C_{14}H_{29}$)ascorrosioninhibitorsforSAE1018carbonsteelin0.5moldm^{-3} HClisreliantonontheconcentrationandalkylchain length.Theresearchalsoshowedthat allthe inhibitorsactedasmixed-type inhibitors and followed aphysisorption typeof adsorption.

Itaand Offiong,(1997)reportedthata-pyridoinis moreeffectivethan2,2 0-pyridilasa corrosioninhibitorforlowcarbonsteelin0.5moldm^{-3} HClat30and40^{O}C.Healso showedthatthesecompoundsinhibithydrogenevolutionin8moldm^{-3}HCl.Furthermore,theI.E% ofthesecorrosioninhibitorsincreaseswithincreasedconcentrationandwith increasingtemperature.

ItaandOffiong,(2001)researchedonbenzoinandbenzilcompoundsascorrosion inhibitorsforlowcarbonsteelinHClsolutionat30and40^{O}C.Theinhibition efficiency (I.E %) of these compounds followed the order benzoin >

benzoin-(4-phenylthiosemicarbazone) > benzyl > benzyl-(4-phenylthiosemicarbazone).Jayaperumal,(2010)reportedthatoctylalcoholandpropargylalcoholareexcellent inhibitors for low carbonsteel in 15% HCl at 30 and 105^{O}C. Popova *et al.,*(2003)examinedbenzimidazole, 2-aminobenzimidazole, 2-mercaptobenzimidazole, 1-benzylbenzimidazol, and1,2-dibenzylbenzimidazoleas corrosioninhibitorsforlowcarbonsteelindeaerated1moldm^{-3}HClsolution.Theyfound out that allfivediazoles havestrong corrosion inhibition properties.

Popova*et al.,*(2004)reportedthattheI.E%of8benzimidazolederivativesincreaseswith increasedconcentrationandactasmixed-typeinhibitorsforlowcarbonsteelin1moldm^{-3} HCl at 20^{O}C.

Popova*et al.,*(2007)studied5differentazolecompoundsas corrosioninhibitorsforlow carbonsteelin1moldm^{-3} HClat20^{O}C.TheI.E%ofthesecompoundswasreportedto havethefollowing order:indole~1H-benzotriazole~benzothiazole>benzimidazole. The authorsreportedthattheI.E% of thesecompoundsincreaseswithincrease in concentration and that theyact as mixed-typeinhibitors.

Tang *et al.,*(2005)reportedthat1-(2-pyridylazo)-2-naphtholisaneffectivemixed-type corrosioninhibitorforcarbonsteelin1moldm^{-3}HClat25–50^{O}C.I.E%decreaseswith increasingtemperature.

Vishwanatham andHaldar, (2008) stated thatfurfurylalcohol isan effectivemixed-type corrosioninhibitorforN80steelin15% HCl.ItsI.E%increasedwithincreasing concentration, but decreased with increaseintemperature(T)from 30 to 110^{O}C.

2.9 ReviewofsomeorganiccorrosionInhibitorsviatheoreticalmethod mainly density functional theory (DFT).

Issa*et al.,*(2009)investigatedtheanti-corrosivepropertiesofsomeantipyrineSchiffbases (a)(benzylidineamino)antipyrine(b)4-hydroxy3-(benzylidineamino)antipyrine(c)2-hydroxy3-(benzylidineamino)antipyrineand(d)2-hydroxy3-(naphthylidineamino) antipyrineusingdensity functionaltheory attheB3LYP/6-31G*level.The computationalcalculationswere performedtofinda relationbetweentheir electronic andstructuralpropertiesandtheinhibitionefficiency.Thecalculatedquantumchemical parameterscorrelatedtotheinhibition efficiency are,thehighestoccupiedmolecular orbital(HOMO), the lowestunoccupiedmolecular orbital(LUMO),the separation energy (ΔE),thedipolemoment(m),thesoftness(s),thetotalnegativechargeonthe whole

molecule (TNC),the totalcharge ontheazomethine moiety,themolecular volume(Vi),andthetotalenergy (TE).Agoodcorrelationbetweenthequantum chemical parameters andthe experimental inhibition efficiencywasfound.

According toEbensoetal(2010a),Somequantumchemicalparametersofthree thiosemicarbazides,namely 2-(2-aminophenyl)-Nphenylhydrazinecarbothioamide (AP4PT),N,2-diphenylhydrazinecarbothioamide(D4PT) and2-(2-hydroxyphenyl)-N-phenylhydrazinecarbothioamide(HP4PT),werecalculatedusingdifferentmethodsand were foundtocloselycorrelatewith the experimental %IE.

IranandHossein,(2009)studiedthequantitativestructurepropertyrelationship(QSPR) analysisofsomeorganiccompounds.TheycalculatedEHOMO,ELUMO,ELUMO – HOMO, dipolemoment,Volumeofcompound,lengthofC=N,thelengthofO-H,thenetcharge onthe nitrogeninthe imine group, the netchargeonthe oxygenatominthe hydroxyl groupandtheionisationpotentialby usingthesemi-empericalAM1method.The theoretical predictions and experimental datacloselyagreed.

Awad*et al.,*(2009)employedtheuseofDensity FuntionalTheory inperforming theoreticalcalculationsonsomeTriazole Schiffbasesascorrosioninhibitors.A good agreement was established betweenexperimentaland theoretical data.

Nnabuketal,(2009)employedthe useofsemiempiricalandDFTmethodatlevelof B3LYP/6-31Gincalculatingsomequantumindicesof Tetracyclineforthecorrosionof lowcarbonsteelin0.1MH_2SO_4.They foundoutthatvaluesobtainedforthequantum indicescomparedfavorably withvaluesobtainedforotherinhibitors,andestablished that theoretical data andexperimental data agrees.

Musaand Kamal,(2015)usethedensityfunctionaltheory(DFT)attheB3LYP/6-31G*/6-31+g(d) basissetslevelandsemi-empiricalAM1methodsonfourBenzimidazole (BZL)andsubstitutedbenzimidazole namely 2-aminobenzimidazole(ABZL),2-mercaptobezimidazole (MBZL)and2-phenylbenzimidazole (PhBZL) ascorrosion inhibitorsfor(70/30)brassin1MHClO4,tostudythecorrelationbetweenitsmolecular structureandthecorrespondinginhibitionefficiency(%IE).Agoodcorrelationbetween the theoretical data and the experimental resultswas established.

Inthesamevein corrosioninhibitionefficiencyofthreePhenyltetrazolesubstituted compounds, namely 5-phenyl-1H-tetrazole(PT),5-p-tolyl-1H-tetrazole(M-PT)and5-

(4-methoxyphenyl)-1H-tetrazole (MO-PT) onlow carbonsteelwasevaluatedby quantumchemicalcalculationsbasedon densityfunctionaltheory(DFT)method at the B3LYP/6-31G(d,P) basis set level in order to investigate the relationship between their molecular and electronic structure and inhibition efficiency. The quantumchemicalpropertiesmostrelevanttotheir potentialactionascorrosion inhibitors such as E_{HOMO}, E_{LUMO}, energy gap (ΔE), dipole moment (μ), hardness(η),softness(S),theabsoluteelectronegativity(χ),thefractionsofelectrons transferred (ΔN) and theelectrophilicityindex(ω)were calculated.
Thelocalreactivity hasbeenanalyzedthroughthe Fukuifunctionandcondensed softness indices in order tocompare the possible sitesfor nucleophilic and electrophilicattacks.Thetheoreticalresultsobtainedusing DFTbasedreactivity indexes,werefoundtobeconsistentwiththeexperimentalresults(Udhayakala*et al.,*2013). Corrosioninhibition ofcopperthroughsixbipyrazoliccompoundshasbeenelucidated by meansofdensityfunctionaltheory(DFT)-derivedreactivity indexes.Thequantum chemistry calculationswereperformedattheB3LYP/6-31G(d)level.Thetheoretical resultsobtainedareingoodagreementwithexperimentalresults(Boussalah*et al.,*2012).

The adsorption mechanism and inhibition efficienciesof two pyrimidine derivatives 6- methyl-4-phenyl-4,5-dihydropyrimidine-2-thiol(THPT1) and 4,6-diphenyl4,5-dihydropyrimidine-2-thiol (THPT2)werestudied as corrosion inhibitors usingDensity functionaltheory(DFT)attheB3LYP/6-31G(d,p)basissetlevel.Thetheoreticalresults werefoundtobeincloseagreementwiththeexperimentalresults(Udhayakala*et al.,*2013).

CHAPTER THREE

EXPERIMENTAL SECTIONS

3.1 Inhibitors used for study

Set A inhibitors namely 6 benzyl oxy indole and 3 methyl indole were obtained from Manchester organics while pure samples of set B inhibitors namely ortho, meta and 4 nitro aniline were obtained from chemical sciences department, Bingham university, Karu, Nasarawa state and used without further purifications. Names and molecular structures of the inhibitors investigated are presented in Figure 3.1

3.2 Materials used

The steel metal rods were obtained from building and material market, Maraba, Karu, Nasarawa state. Test were performed on freshly prepared cylindrical rods of low carbon steel of the following composition (wt. %): 0.012 % Ni, 0.017% Mo, 0.040% Cr, 0.168% C, 0.154 % Mn, 0.207% Si, 0.008% P and balance Fe. Specimen used in the weight loss technique and hydrogen evolution method (gasometric) were mechanically press-cut into cylindrical rods, each of dimension 30mm length and 1.45mm diameter. The rods were degreased by washing in absolute ethanol and acetone, dried under room temperature and stored in a moisture free desiccator. Subsequently, the initial weight of each rod was carefully measured (Adejoro*et al.,* 2013) with an Ohahus Pioneer™ analytical weighing balance. Specimen used in the electrochemical method were carefully cut into many cylindrical working electrodes of dimension 80mm length and 1.45mm. The upper part of the working electrode (4cm) was covered with Teflon and epoxy coating, the top most end (2cm) was left uncovered and the exposed surface of working electrodes (2cm) were polished using emery papers of finer grade, degreased by washing in ethanol and acetone, dried under room temperature and stored in a desiccator free of moisture.

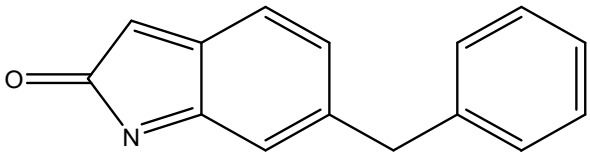

6 benzyl oxy indole

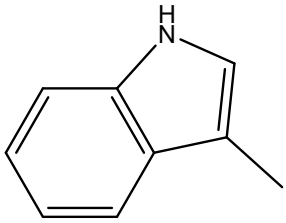

3 methyl indole

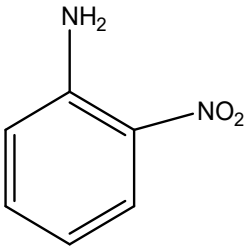

2 nitro aniline

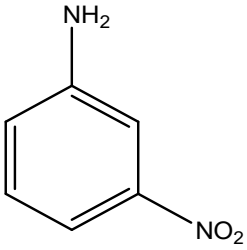

3 nitro aniline

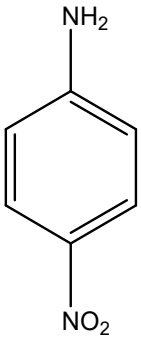

4 nitro aniline

Figure 3.1 Chemical structures and names of Inhibitors

3.3 Preparation of solutions.

Thesolutions, 1 mol/dm^3 HCl were made by dilution of analytical grade 98% HCl with bidistilled H_2O. All chemicals and reagents were of analytical grade. The measurements were performed in 1mol/dm^3 HCl without and with the presence of investigated compounds (inhibitors) in the concentration range from 2 x 10^{-5} to 10 x10^{-5}mol/dm^3

3.4 Weight loss method (Gravimetric method)

In the weight loss experiment, a previously weighed metal (low carbon steel) cylindrical rod was immersed completely in 50ml of the test solution in an open beaker. The beaker was placed into a water bath kept at 30^{o}C for 8hours. The product from corrosion reaction was removed by washing each rod in a solution containing 50 % NaOH and 100 g of zinc dust (Eddy, 2010). The washed rod was rinsed in acetone and dried in the air before re-weighing. The experiment was also carried out at 40^{o}C, 50^{o}C and 60^{o}C. In each case, the difference in weight at intervals of 2hrs for a period of 8hrs was taken as the total weight loss. From the weight loss results, the inhibition efficiency (I.E%) of the inhibitor, degree of surface coverage and corrosion rates were calculated using equations 3.1, 3.2 and 3.3 respectively.

$$\%\text{I. E} = \left(1 - \frac{W_1}{W_2}\right) x\ 100 \qquad 3.1$$

$$\Theta = 1 - \frac{W_1}{W_2} \qquad 3.2$$

$$CR(mgh^{-1}cm^{-2}) = {}^{W}/_{At} \qquad 3.3$$

Where W_1 and W_2 are the weight losses (g) for low carbon steel in the presence and absence of the inhibitor solution, Θ is the degree of surface coverage of the inhibitor, A is the total surface area of the low carbon steel rod (cm^2), t is the period of immersion (hours) and W is the weight loss of low carbon steel after time (t). All the measurements were performed in triplicate and the mean value recorded.

3.5 Hydrogen gas evolution method (Gasometric method)

The gasometric method was carried out at 303K as described by Ebenso *et al.,* 2004. From the hydrogen gas liberated per minute, corrosion inhibition efficiencies were calculated by means of equation 3.4 below

$$\%I.E = \left(1 - \frac{V_{Ht}^{1}}{V_{Ht}^{0}}\right) x100 \quad 3.4$$

Where $V^{1}_{Ht}$and V^{0}_{Ht} are the volumes of H_2 gas (cm^3) evolved at time (minutes) for inhibited and uninhibited solutions respectively.

3.6 Electrochemical measurements

Versa stat 4 electrochemical system stationed at Federal University of Technology, Akure (FUTA) was used for the test. A standard three –electrode system was used and temperature was maintained at 303K. The reference electrode was silver/silver chloride, counter electrode was platinum and working electrode was low carbon steel. The open circuit potential (OCP) test lasted for 30 minutes in order to attain a stable value. The Tafel polarization was performed in the potential range of ±250 mV vs potential (E) at scan rate of 0.5 mV/s. Each test was repeated at least two times in order to verify the reproducibility. The inhibition efficiency (I.E%) was calculated by using the formula 3.5:

$$\%IE = \left(1 - {icorr_{inh}}/{icorr_{free}}\right) \times 100 \quad 3.5$$

Whereicorr(free) and icorr(inh) are the corrosion current densities in the absence and presence of inhibitor, respectively.

3.7 Scanning electron microscopy (SEM)

The analysis of the morphology of the low carbon steel surface after 72 hours of immersion time was carried out in Chemical Engineering Department, ABU Zaria using scanning electron microscopy (SEM), operated in the contact mode under ambient conditions using JSM-6010LA analytical scanning electron microscope. Images of the specimens were recorded after exposure as follows: (a) low carbon steel in the absence of inhibitor and acid, (b) low carbon steel in the presence of acid only and (c) low carbon steel in the presence of acid and inhibitors of concentration 10 x 10^{-3} M.

3.8 Quantum Measurements

All the quantum measurements were done with SPARTAN'14 V1.0

The full optimization was initially achieved by using molecular mechanicforce fields (MMFF). The results from MMFF were further selected as input and re-optimized using Semi empirical AM1.

The Semi empirical AM1 structures were selected as input and were re-optimized using Density Functional Theory (DFT) at the level of B3LYP methods which uses the exchange functional proposal by Becke and all the correlations functional given by Lee, Yang and Parr.

The b-31G* basis set has been used in conjunction with DFT method because it has the advantage of being flexible enough to guarantee reliable theoretical results and being small enough for rapid calculations. It represents an excellent compromise between completeness and economy.

The molecular geometry was fully optimised without any constraint using analytical gradient procedure implemented within the program package.

The quantum parameters considered are as follow: the energy of the highest occupied molecular orbital (E_{HOMO}), the energy of the lowest unoccupied molecular orbital (E_{LUMO}), separation energy ($E_{LUMO} - E_{HOMO}$), dipole moment (μ), Log P, and Polarizability of the various Indole derivatives.

Statistical analysis were performed using SPSS program version 17.0 for windows. The linear equation proposed by (Lukovits, et al., 2001) refer to equation 2.5 is usually used in the study of corrosion inhibitors to correlate the quantum molecular descriptors with the experimental inhibition efficiency of the inhibitors.

3.9 Chemical reactivity parameters obtained from density functional theory (DFT)

DFT is considered a very useful method to probe the inhibitor/surface interaction as well as to analyze the experimental data. Density functional theory has been found to be successful in providing understandings into the chemical reactivity and selectivity, in low carbon steel of global parameters such as electronegativity (χ), hardness (η) and softness *(S)*(Gokhan, 2008). Thus, for an *N*-electron system with total electronic energy (*E*) and an external potential (v (r)); chemical potential (μ)known as the negative of electronegativity (χ), has been defined as the first derivative of the *E* with respect *N* at v (r) refer to equation 3.6:

$$\chi = -\mu = -\left(\frac{\partial E}{\partial N}\right)_{v(r)} \quad 3.6$$

Hardness (ɳ) has been defined within the DFT as the second derivative of the *E* withrespect to *N* at *v*(*r*), and it is a property which measures both the stability and reactivity of a molecule refer to equation 3.7:

$$\eta = \left(\frac{\partial^2 E}{\partial N^2}\right)_{v(r)} = \left(\frac{\partial \mu}{\partial N}\right)_{v(r)} \quad 3.7$$

Where E is the electronic energy, N is the number of electrons, and v (r) is the external potential due to the nuclei and μ is chemical potential.

The number of transferred electrons *(*Δ*N*) from the inhibitor molecule to the metal surface can be calculated by using equation 3.8:

$$\Delta N = \frac{\chi_{fe} - \chi_{inh}}{[2(n_{fe+} n_{fe})]} \quad 3.8$$

Where χ_{fe} and χ_{inh}represent the absolute electronegativity of iron and the inhibitor molecule, respectively; nfe and n_{in} represent the absolute hardness of iron and the inhibitor molecule, respectively.

I and *A* are related in turn to E_{HUMO} and E_{LUMO} using equations 3.9 and 3.10:

$$I = -E_{HOMO} \quad 3.9$$

$$A = -E_{LUMO} \quad 3.10$$

These quantities are related to electron affinity (*A*) and ionization potential (*I*),referto equations3.11, 3.12 and 3.13:

$$\chi = \frac{I+A}{2} \quad 3.11$$

$$\chi = -\frac{E_{LUMO}+E_{HOMO}}{2} \quad 3.12$$

$$n = \frac{I-A}{2}$$

$$n = -\frac{E_{LUMO}+E_{HOMO}}{2} \quad 3.13$$

Recently, a new global chemical reactivity parameter has been introduced and is called an electrophilicity index (ω). Refer to equation 3.14:

$$\omega = \frac{\mu^2}{2n} \qquad 3.14$$

This was proposed as a measure of the electrophilic power of a molecule.

Global softness can be calculated using equation 3.15:

$$S = \frac{1}{n} \qquad 3.15$$

CHAPTER FOUR

RESULTS AND DISCUSSION

4.1 Weight loss measurements for 6 benzyl oxy indole and 3 methyl indole (Set A inhibitors)

Hydroxyl accelerated mechanism has gained awesome acceptance from many research on the anodic dissolution of Fe in acidic solutions (Ebenso*et al.,* 2008). Refer to equations 4.1, 4.2 and 4.3:

$$Fe + H_2O \leftrightarrow FeOH_{ads} + H^+ + e^- \quad 4.1$$

$$FeOH_{ads} \rightarrow FeOH^+ + e^- \quad \text{(rate determining step)} \quad 4.2$$

$$FeOH^+ + H^+ \leftrightarrow Fe^{2+} + H_2O \quad 4.3$$

It has been suggested that anions such as SO_4^{2-}, I^-, Cl^- and S^{2-} may also precipitate in forming reaction intermediates on the corroding metal surface, which either inhibit or aid corrosion (Umoren and Ebenso, 2008). It is important to recognize that the suppression or stimulation of the dissolution process is initiated by the specific adsorption of the anions on the metal surface.

Bockris mechanism as earlier outlined suggests that Fe electro- dissolution in acidic sulphate solutions depends primarily on the adsorbed intermediate $FeOH_{ads}$.Ebenso*et al.,* (2008) proposed the following mechanism involving two adsorbed intermediates to account for the retardation of Fe anodic dissolution in the presence of an inhibitor. Refer to equations 4.4 to 4.10:

$$Fe + H_2O \leftrightarrow FeH_2O_{ads} \quad 4.4$$

$$FeH_2O_{ads} + M \leftrightarrow FeOH^-_{ads} + H^+ + M \quad 4.5$$

$$FeH_2O_{ads} + M \leftrightarrow FeM_{ads} + H_2O$$

$$4.6 FeOH^-_{ads} \rightarrow FeOH_{ads} + e^- \quad \text{(rate determining step)}$$

4.7

$FeM_{ads} \leftrightarrow FeM^{+}_{ads} + e^{-}$ 4.8

$FeOH_{ads} + FeM^{+}_{ads} \leftrightarrow FeM_{ads} + FeOH^{+}$ 4.9

$FeOH^{+}\ H^{+} \leftrightarrow Fe^{2+} + H_2O$ 4.10

Where M represents the inhibitor species.

Metal surfaces are heterogeneous in natureduetothe presence of lattice defects and dislocations, a metal surface that is corroding is largelyconsidered to have multiple adsorption sites, having activation energies and heats of sites having suitable adsorption enthalpies. Inthe mechanism above, substitution of some adsorbed water molecules on the metal surface by inhibitor species to yield the adsorbed intermediate FeM_{ads} (Eq. (4.6)), reduces the amount of the species $FeOH_{ads}$ available for the rate determining steps and thus retards Fe anodic dissolution.

The gravimetric method of measuring corrosion rate is suitable because of its simple application and reliability (Obot *et al.,* 2009). Weight loss of low carbon steel, in mg, was measured at different time intervals in the absence and presence of different concentrations of the inhibitors studied. Figs. 4.1 - 4.12 show the weight loss-time curves obtained for low carbon steel in 1 mol/dm^3 HCl in the absence and presence of different concentrations of 6 benzyl oxy indole and 3 methyl indole at 303-333K. The figures show that the presence of the inhibitors falls significantly below that of the free acid. The corrosion rates (CR) and inhibition efficiency (%I.E) values calculated from gravimetric measurements for various concentrations of 6 benzyl oxy indole and 3 methyl indole in 1mol/dm^3 HClafter 8 hours immersion at 303-333 K are listed in Tables 4.1 – 4.3. It is evident from these tables and figures that the corrosion rate reduced with rising inhibitor concentration but rose with increase in temperature. Tables 4.1- 4.3 also show that the inhibition efficiency (%I.E) rose with rising inhibitor concentration, gettingto a maximum of 92.29 and 86.32 % for 6 benzyl oxy indole and 3 methyl indole respectively. This could be attributed to the adsorption of these compounds onto the surface of thelow carbon steel through non-bonding electron pairs of nitrogen and oxygen as well as the π-electrons of the aromatic rings. The high inhibitive performance of 6 benzyl oxy indole when compared to 3 methyl indole may be attributed to the presence of oxygen atom in addition to the nitrogen atom and thus leading to a higher bonding ability of the inhibitor to the low carbon steel surface. Similar observation has been reported (Adejoro et al., 2015).

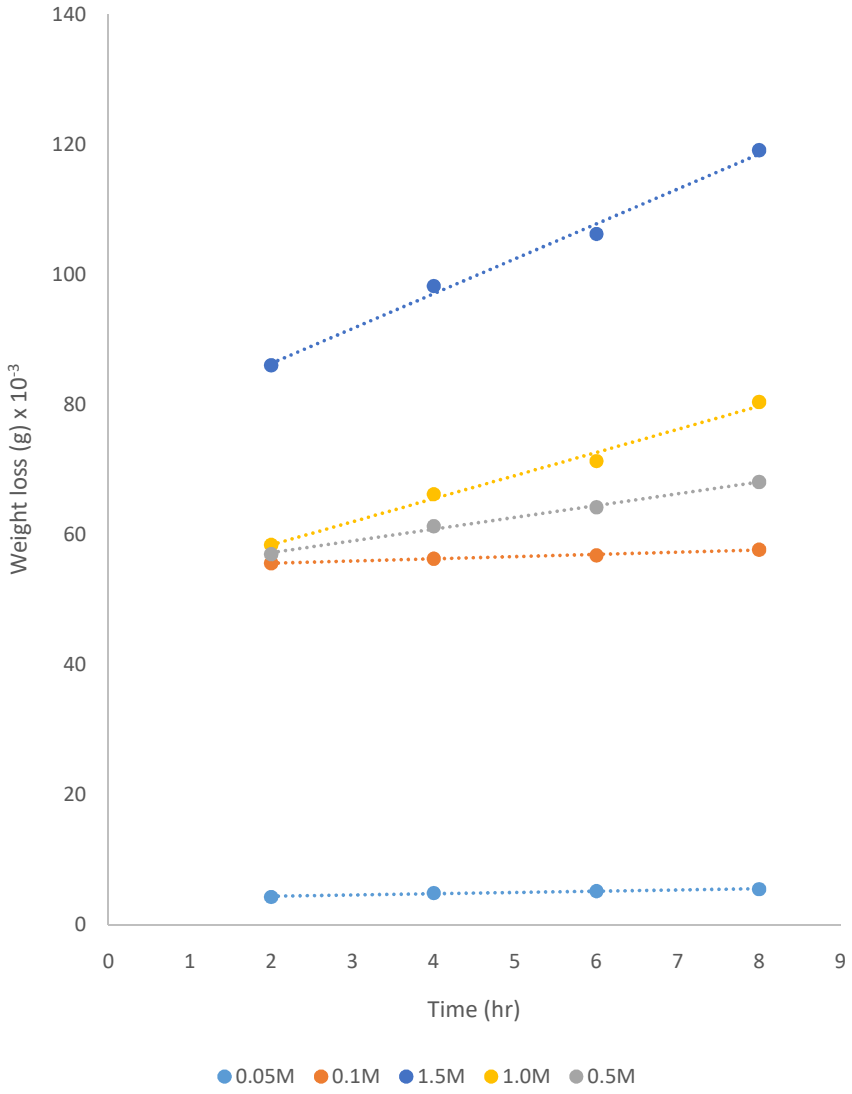

Fig 4.1: Weight loss vs time for low carbon steel corrosion in different concentrations of HCl(0.05 mol/dm^3-1.5 mol/dm^3) at 303K.

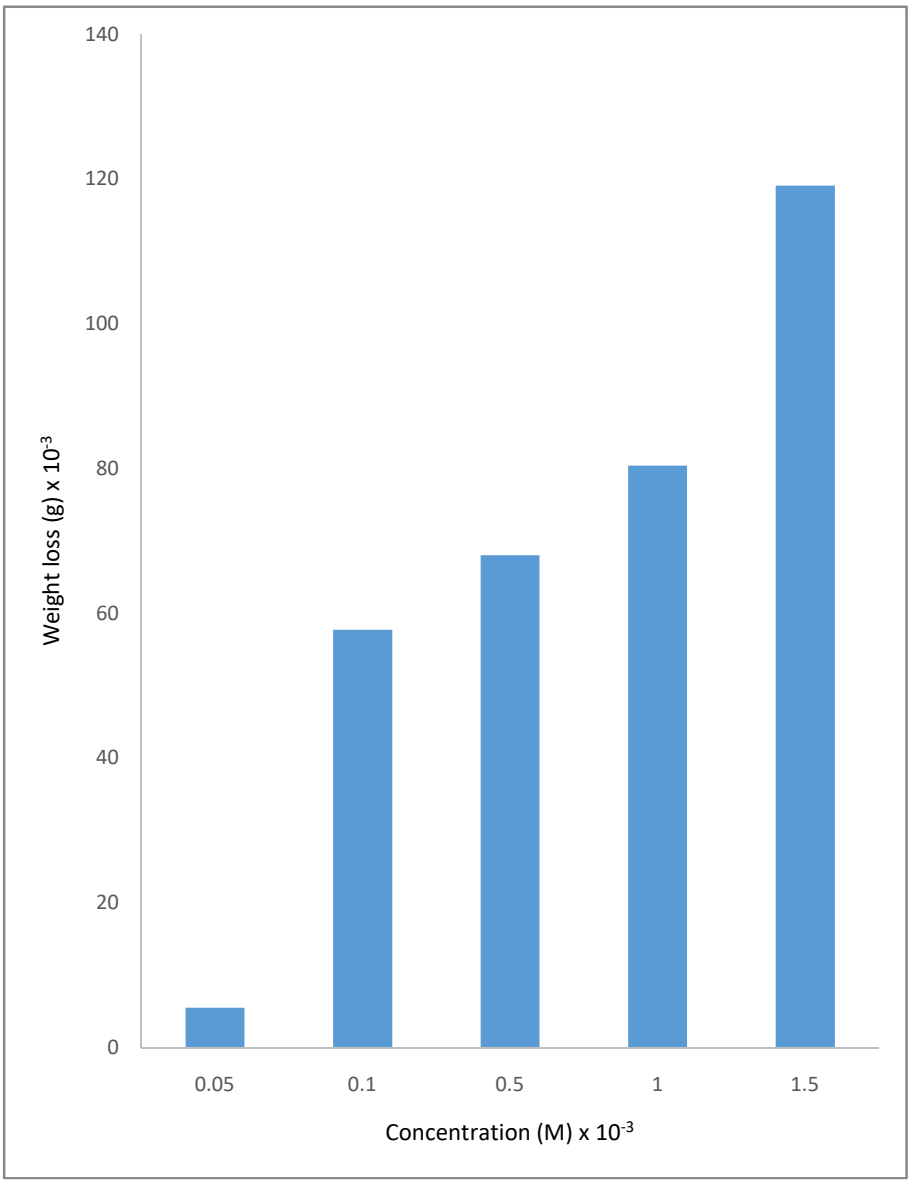

Fig 4.2: Weight loss values against different concentrations of HCl(0.05 mol/dm^3-1.5 mol/dm^3) of low carbon steel corrosion after 8hours immersion time at 303K.

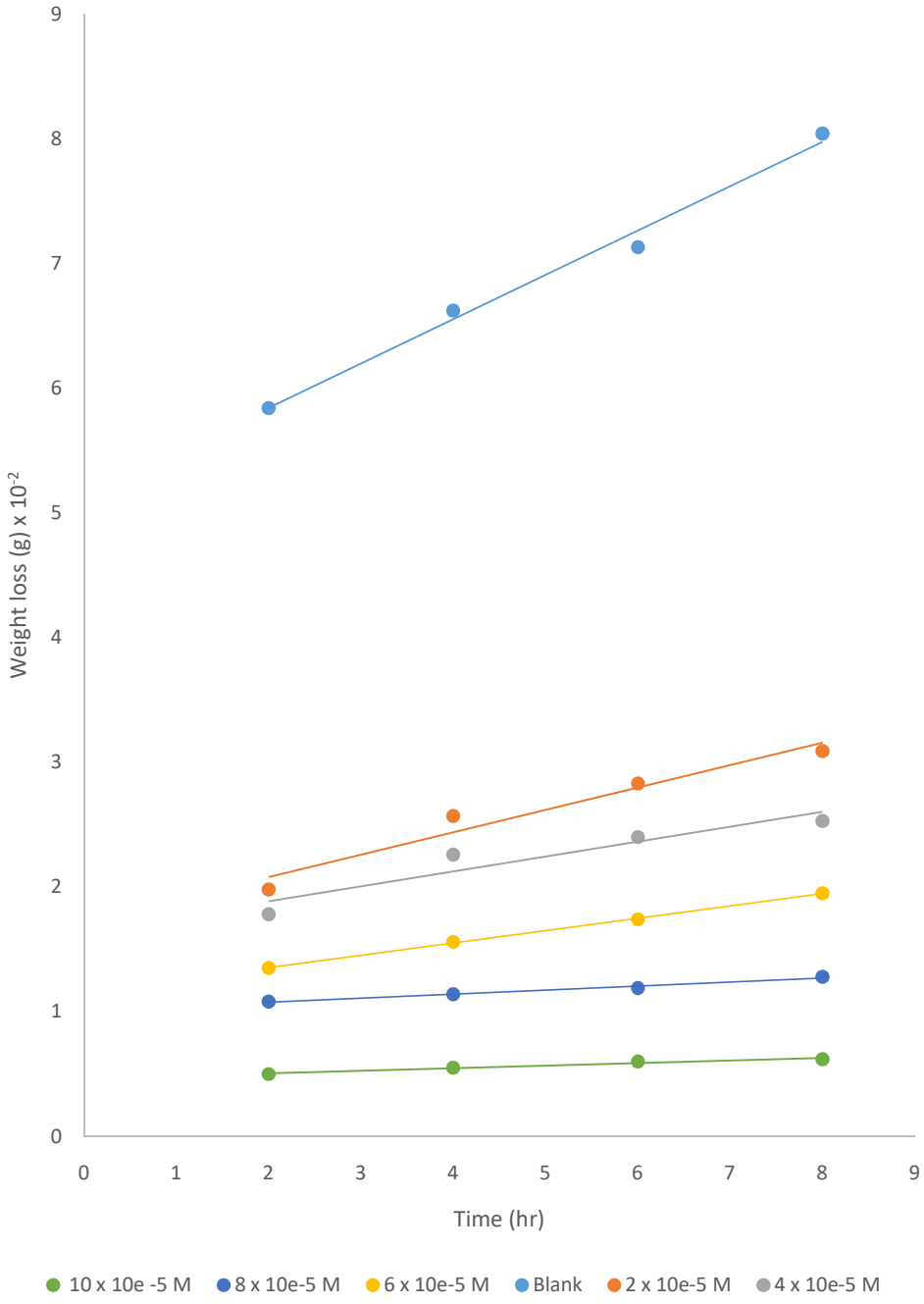

Fig 4.3: Weight loss vs time for low carbon steel corrosion in 1 mol/dm^{3}HCl in the presence of various concentrations of 6 benzyl oxy indole at 303K.

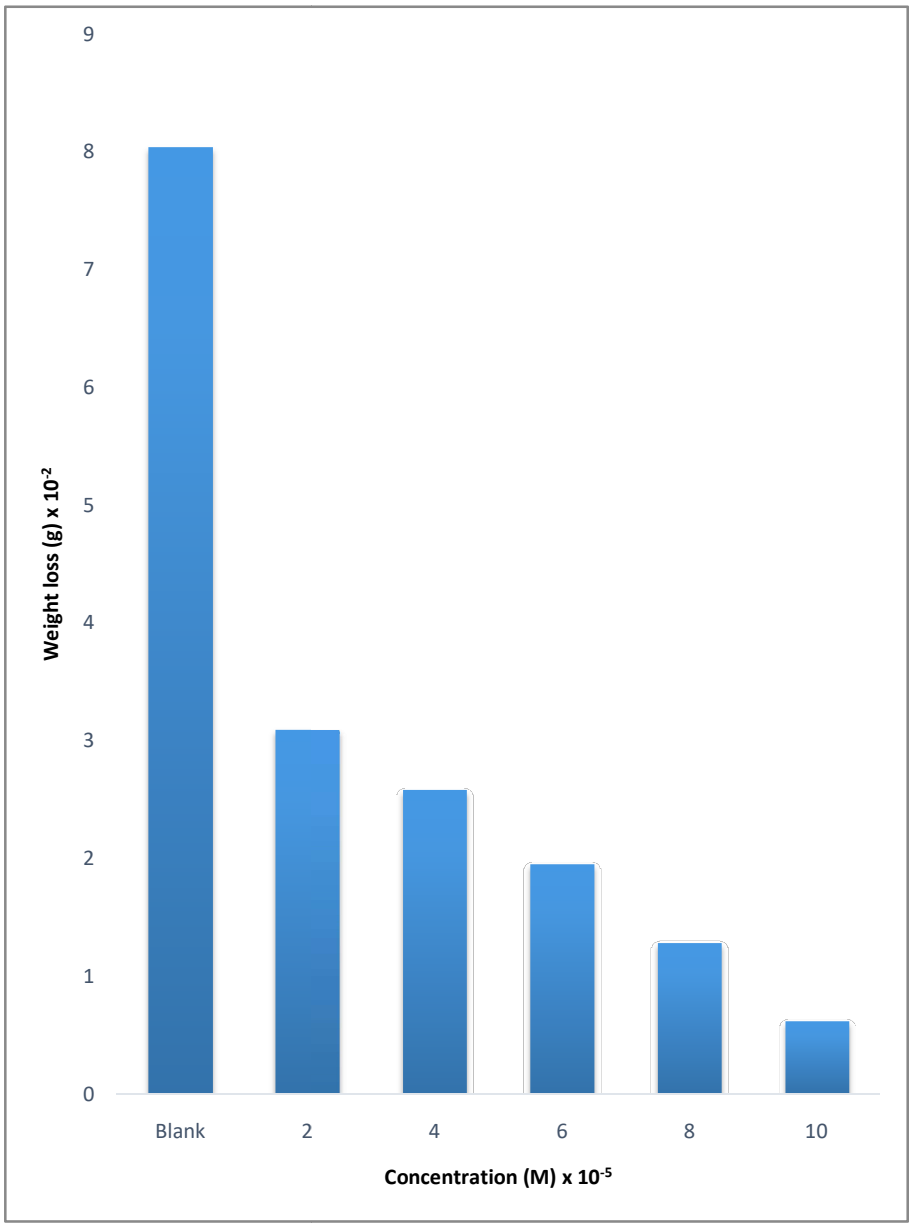

Fig 4.4: Weight loss values against different concentrations of 6 benzyl oxy indole in 1 mol/dm^3 HClof low carbon steel corrosion after 8hours immersion time at 303K.

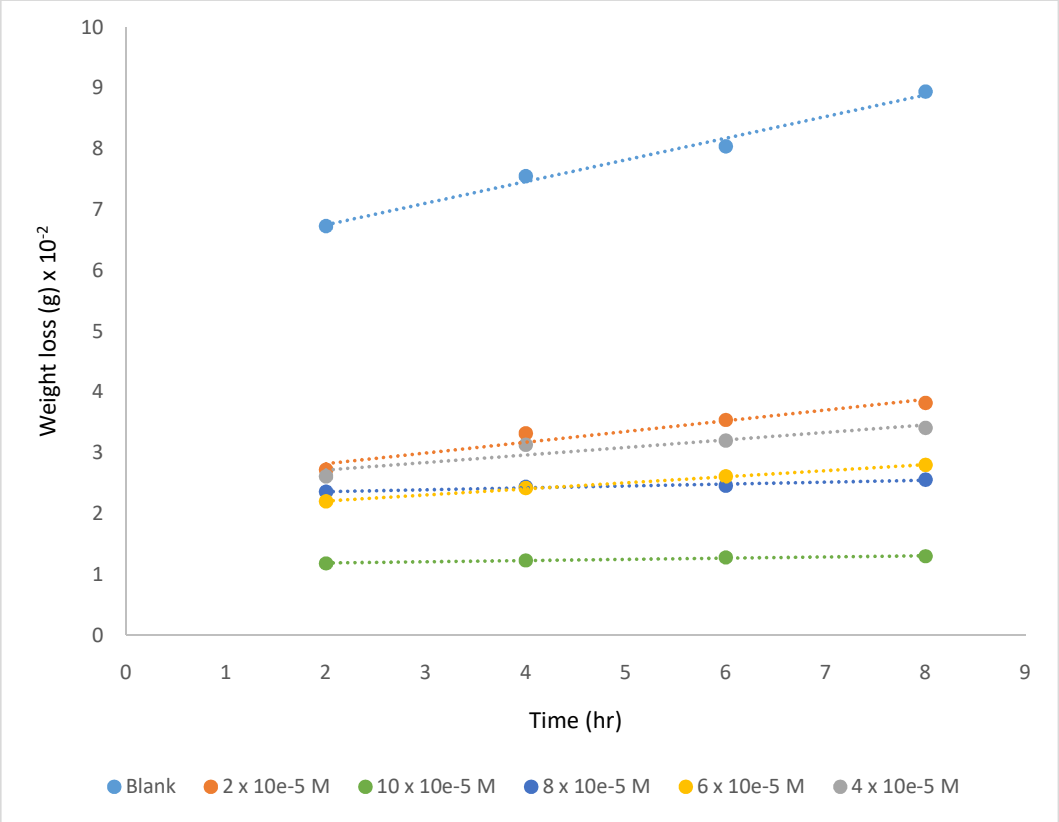

Fig 4.5: Weight loss vs time for low carbon steel corrosion in 1 mol/dm^3 HCl in the presence of various concentrations of 6 benzyl oxy indole at 313K.

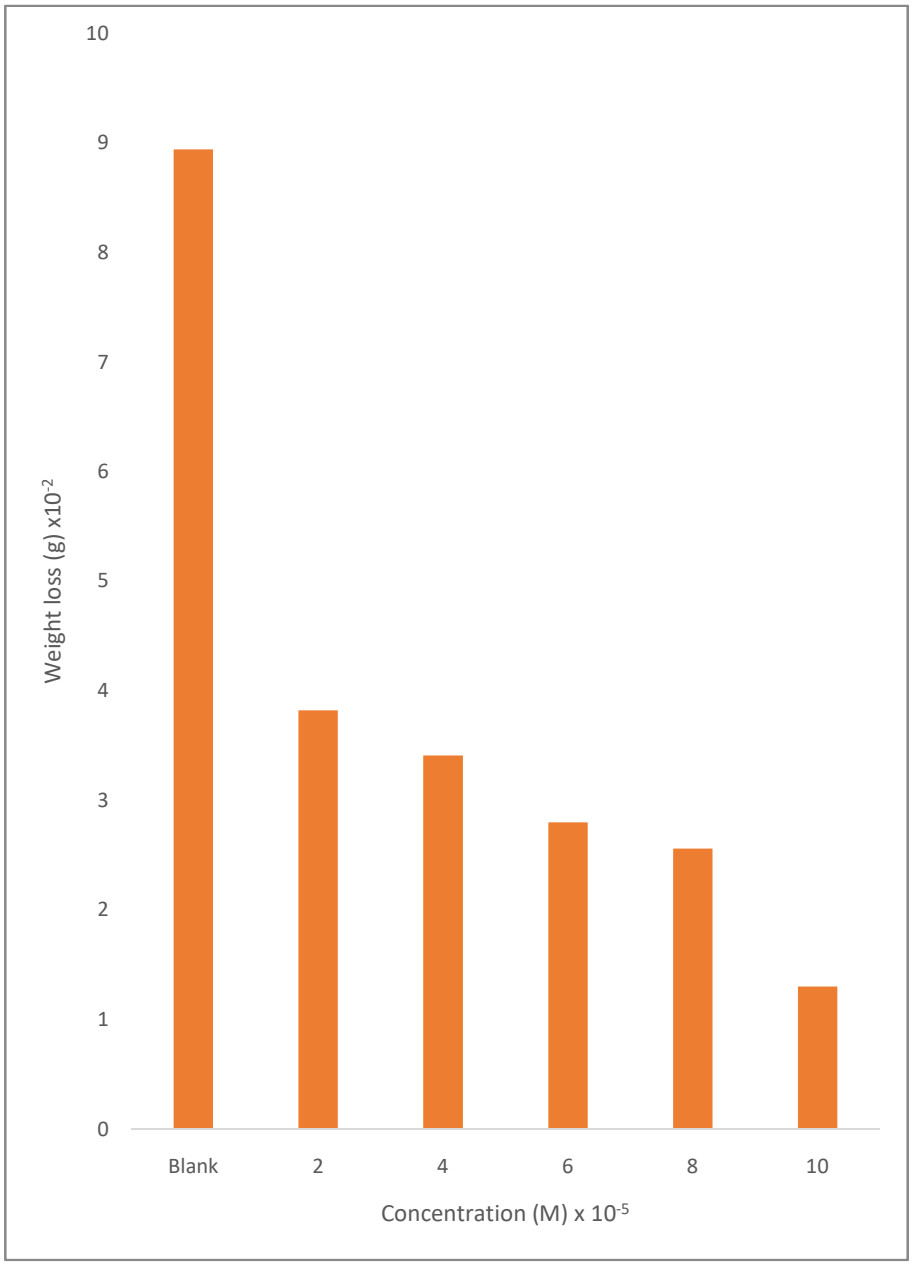

Fig 4.6: Weight loss values against different concentrations of 6 benzyl oxy indole in 1 mol/dm^3 HClof low carbon steel corrosion after 8hours immersion time at 313K.

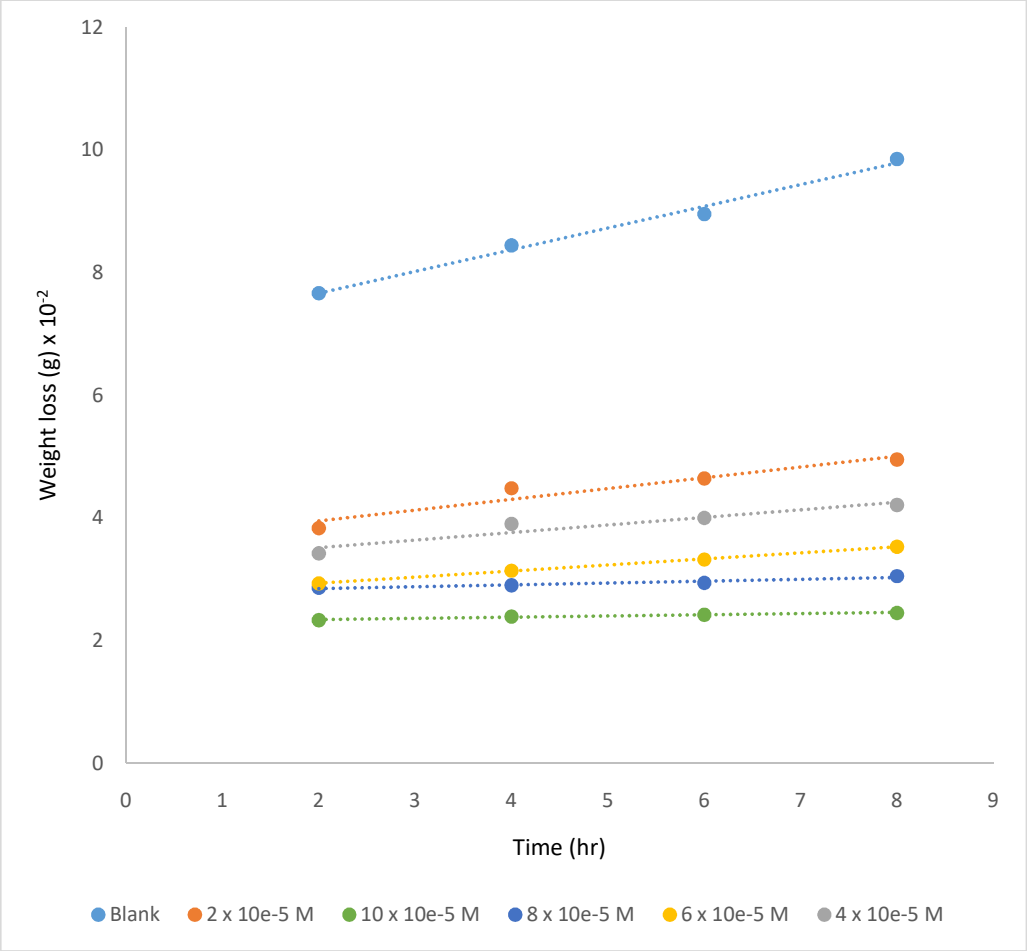

Fig 4.7: Weight loss vs time for low carbon steel corrosion in 1 mol/dm^{3}HCl in the presence of various concentrations of 6 benzyl oxy indole at 323K.

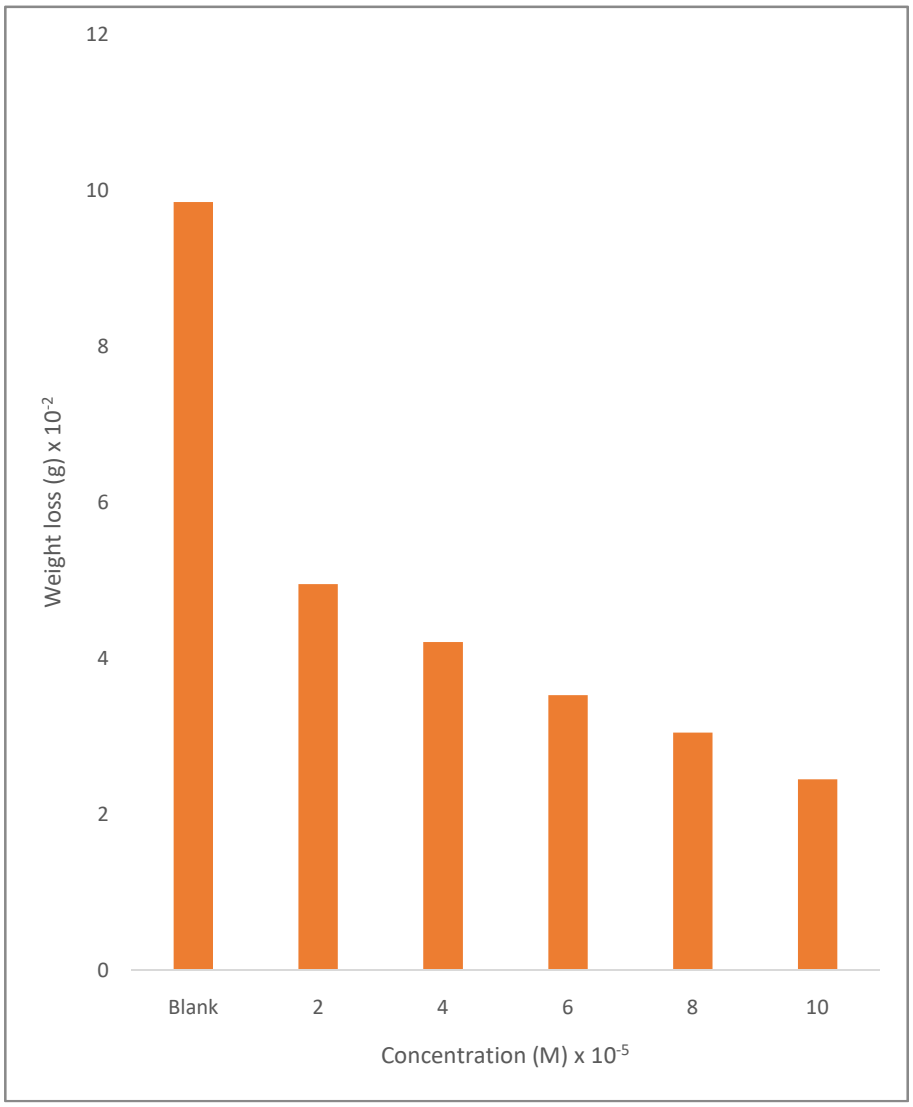

Fig 4.8: Weight loss values against different concentrations of 6 benzyl oxy indole in 1 mol/dm^3 HClof low carbon steel corrosion after 8hours immersion time at 323K.

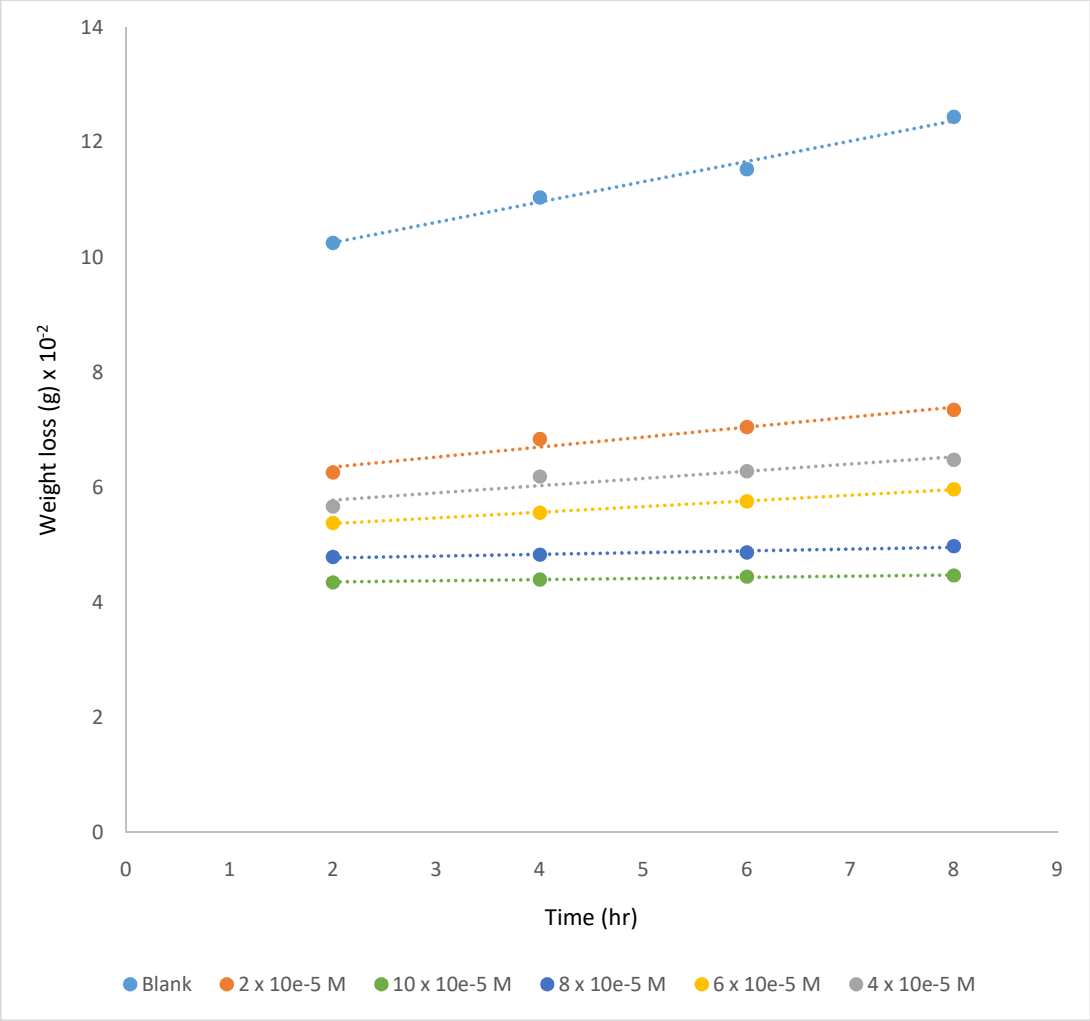

Fig 4.9: Weight loss vs time for low carbon steel corrosion in 1 mol/dm^3 HCl in the presence of different concentrations of 6 benzyl oxy indole at 333K.

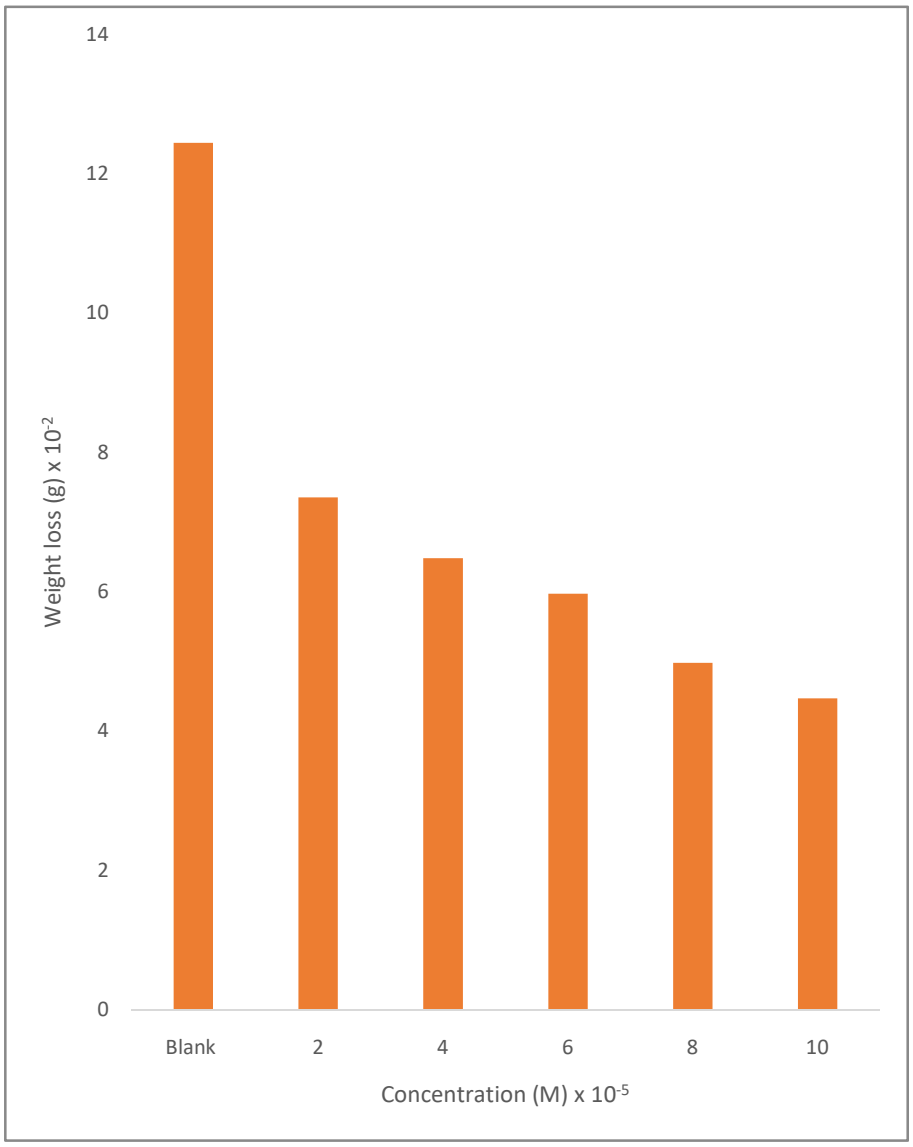

Fig 4.10: Weight loss values against different concentrations of 6 benzyl oxy indole in 1 mol/dm^3 HClof low carbon steel corrosion after 8hours immersion time at 333K.

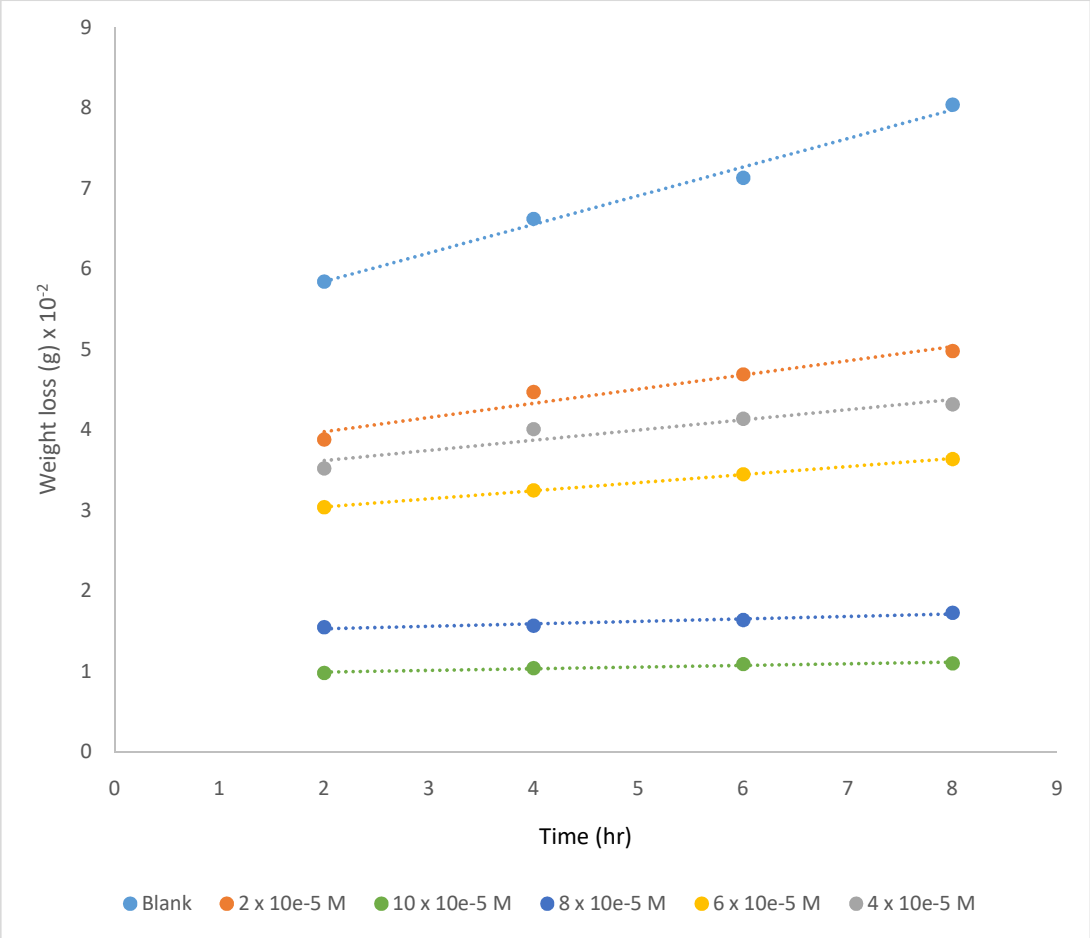

Fig 4.11: Weight loss vs time for low carbon steel corrosion in 1 mol/dm^{3}HCl in the presence of various concentrations of 3 methyl indole at 303K.

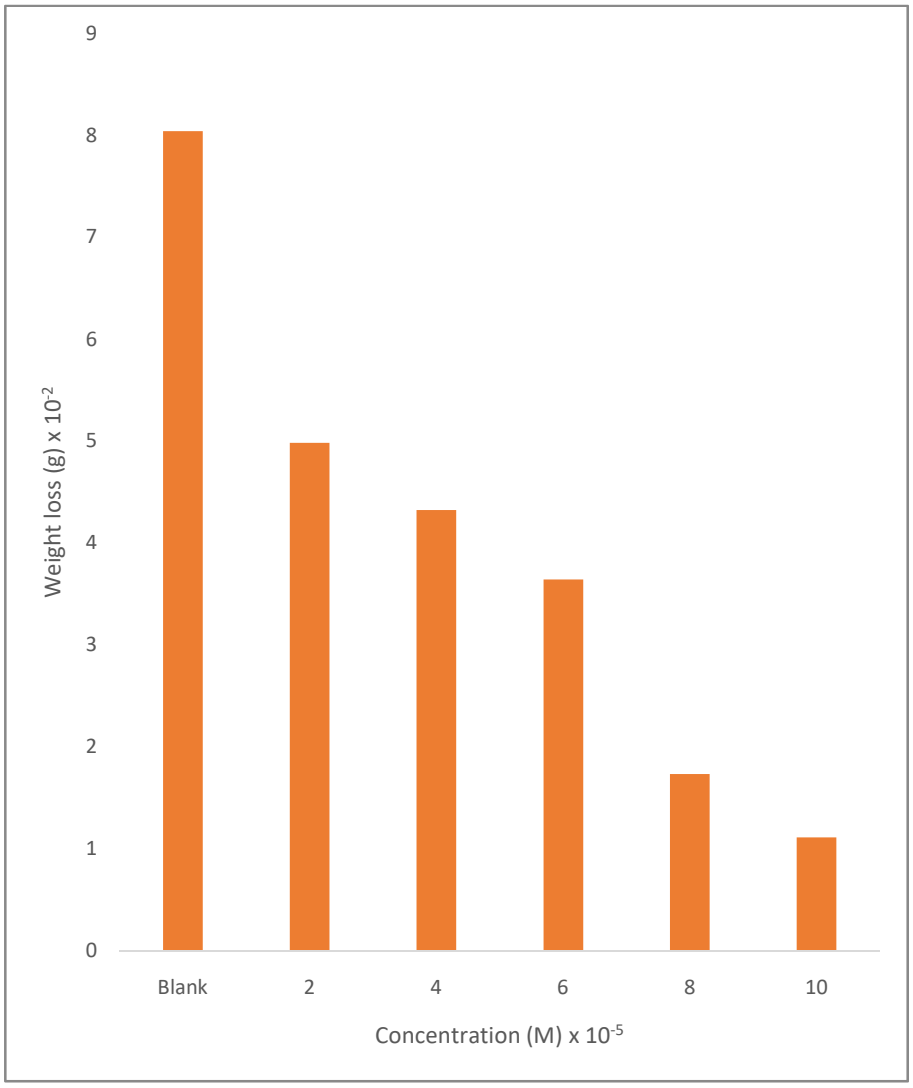

Fig 4.12: Weight loss values against different concentrations of 3 methyl indole in 1 mol/dm^3 HClof low carbon steel corrosion after 8hours immersion time at 303K.

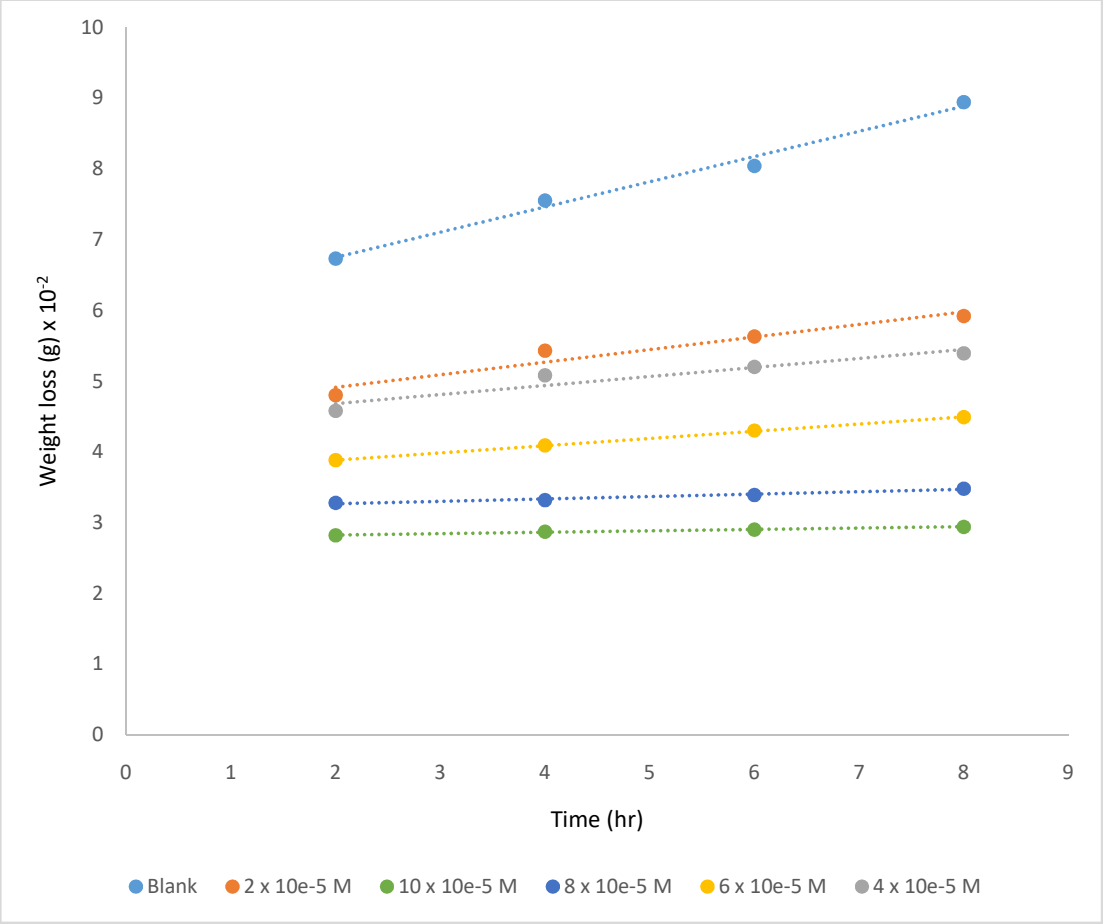

Fig 4.13: Weight loss vs time for low carbon steel corrosion in 1 mol/dm^{3}HCl in the presence of various concentrations of 3 methyl indole at 313K.

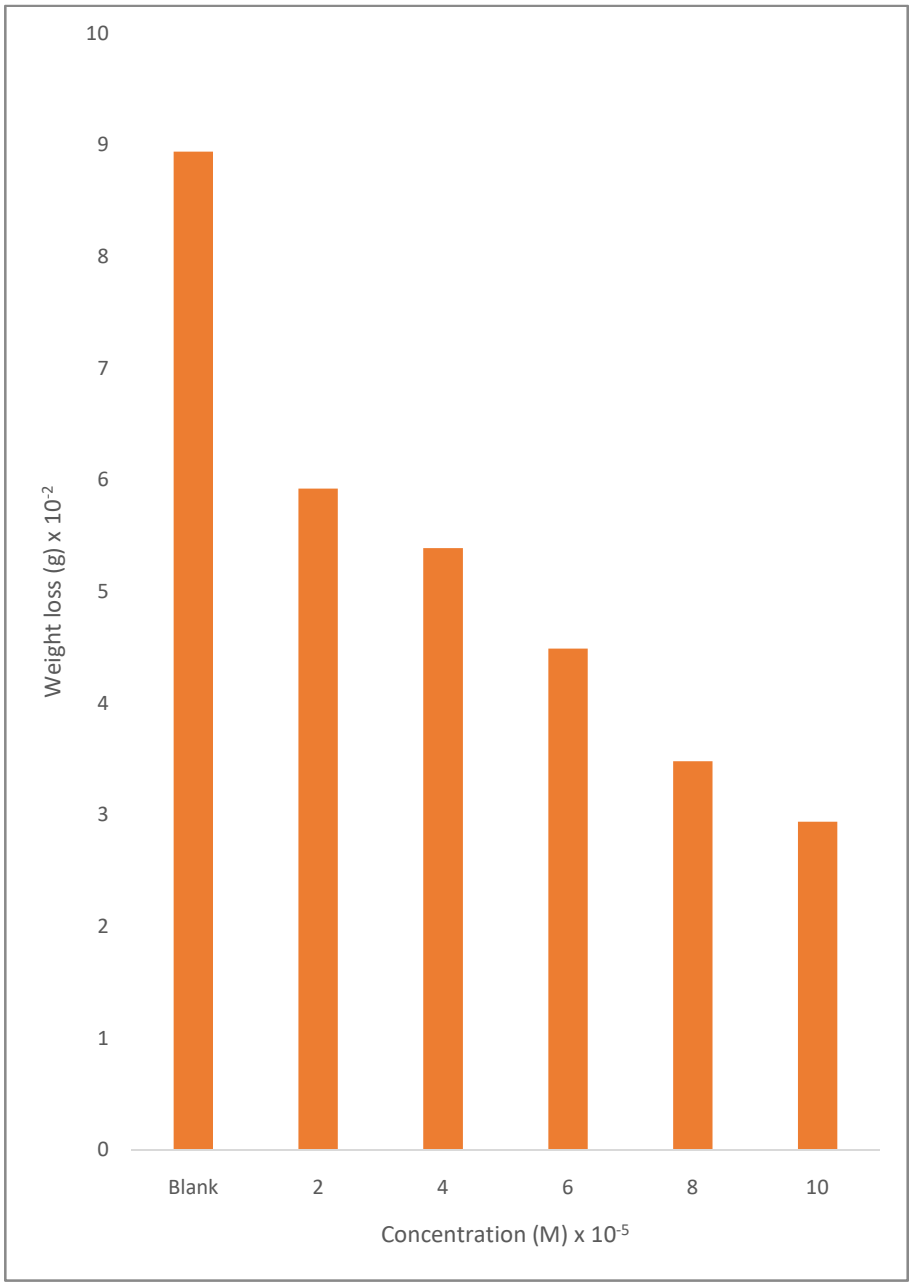

Fig 4.14: Weight loss values against different concentrations of 3 methyl indole in 1 mol/dm^3 HClof low carbon steel corrosion after 8hours immersion time at 313K.

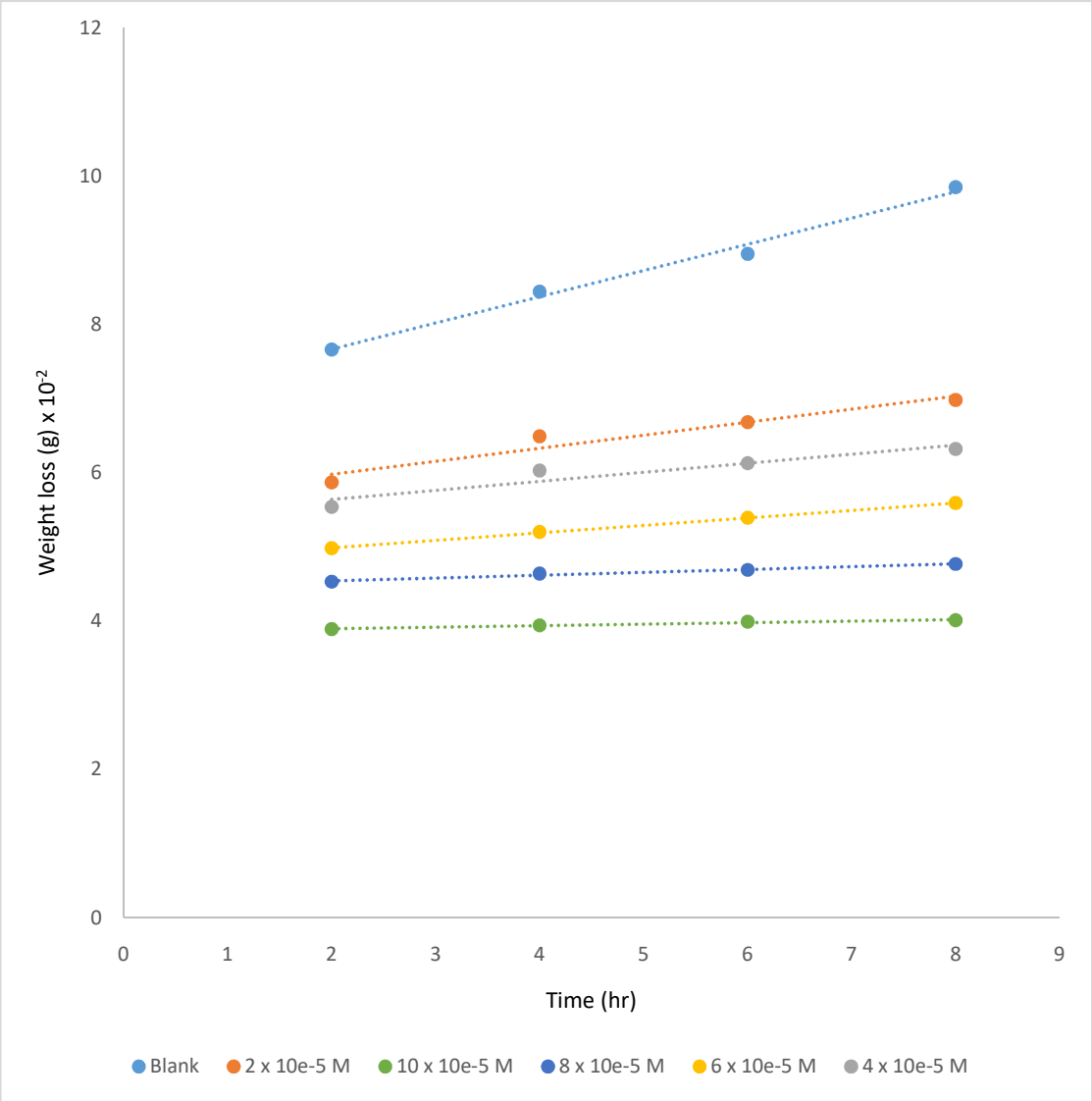

Fig 4.15: Weight loss vs time for low carbon steel corrosion in 1 mol/dm^{3}HCl in the presence of various concentrations of 3 methyl indole at 323K.

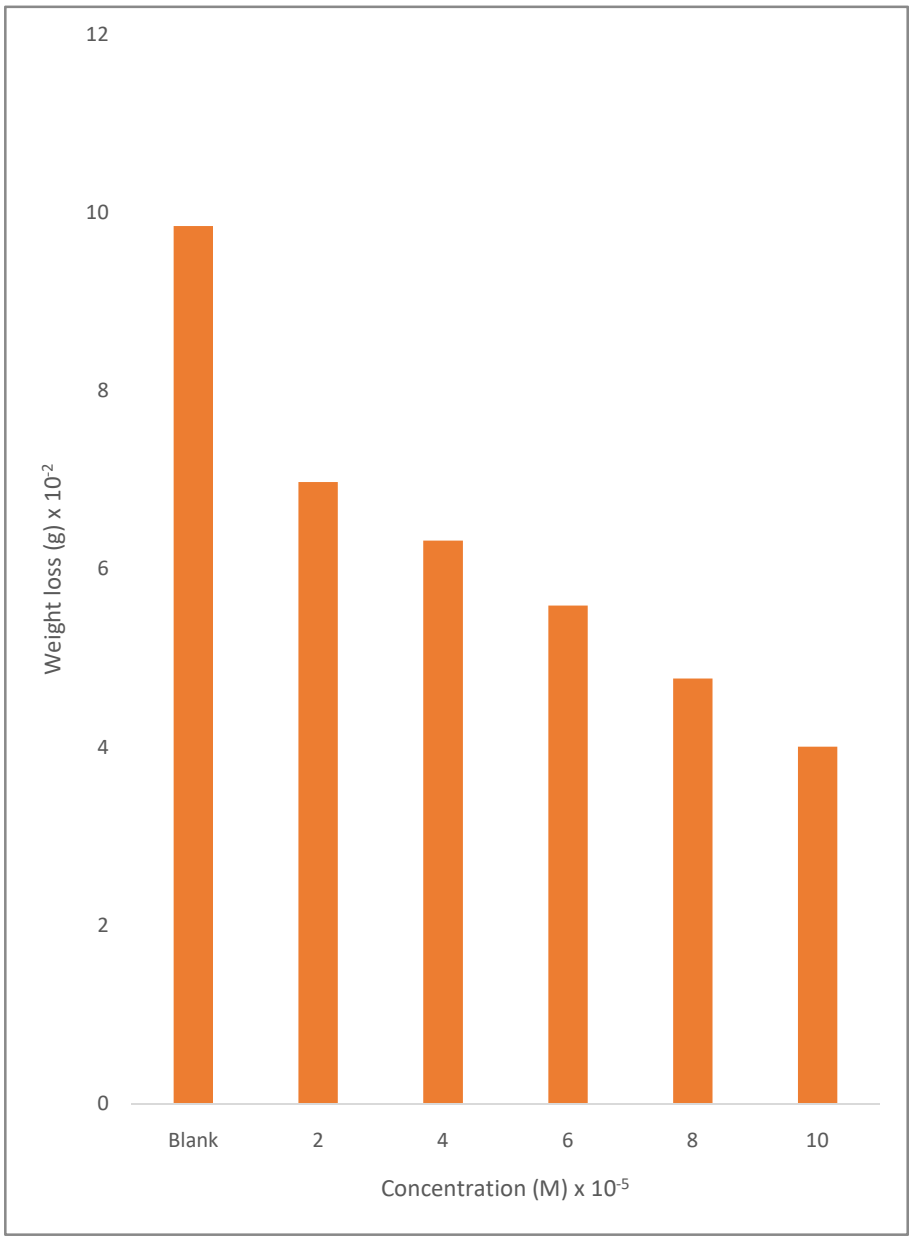

Fig 4.16: Weight loss values against different concentrations of 3 methyl indole in 1 mol/dm^3 HClof low carbon steel corrosion after 8hours immersion time at 323K.

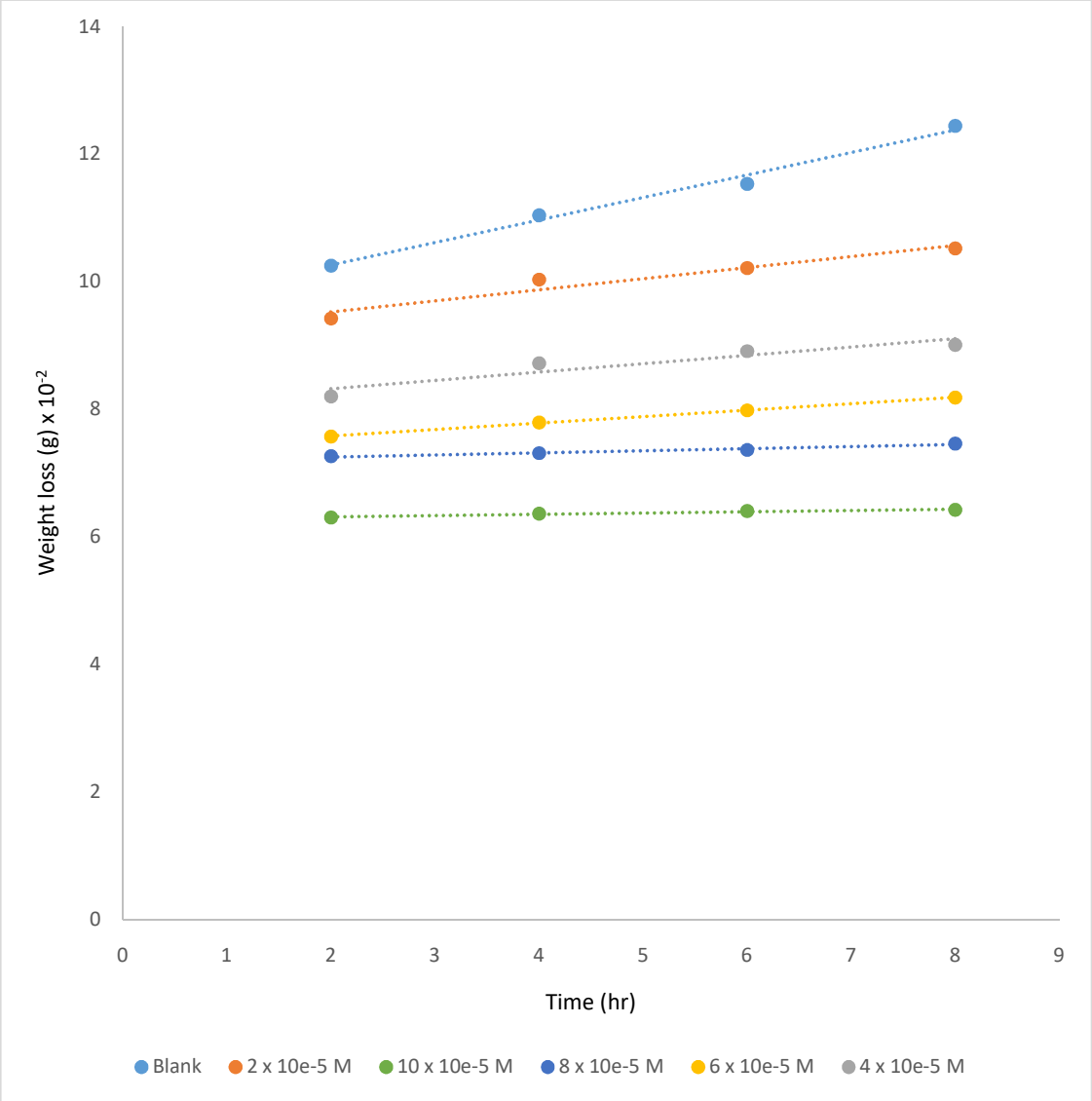

Fig 4.17: Weight loss vs time for low carbon steel corrosion in 1 mol/dm^{3}HCl in the presence of various concentrations of 3 methyl indole at 333K.

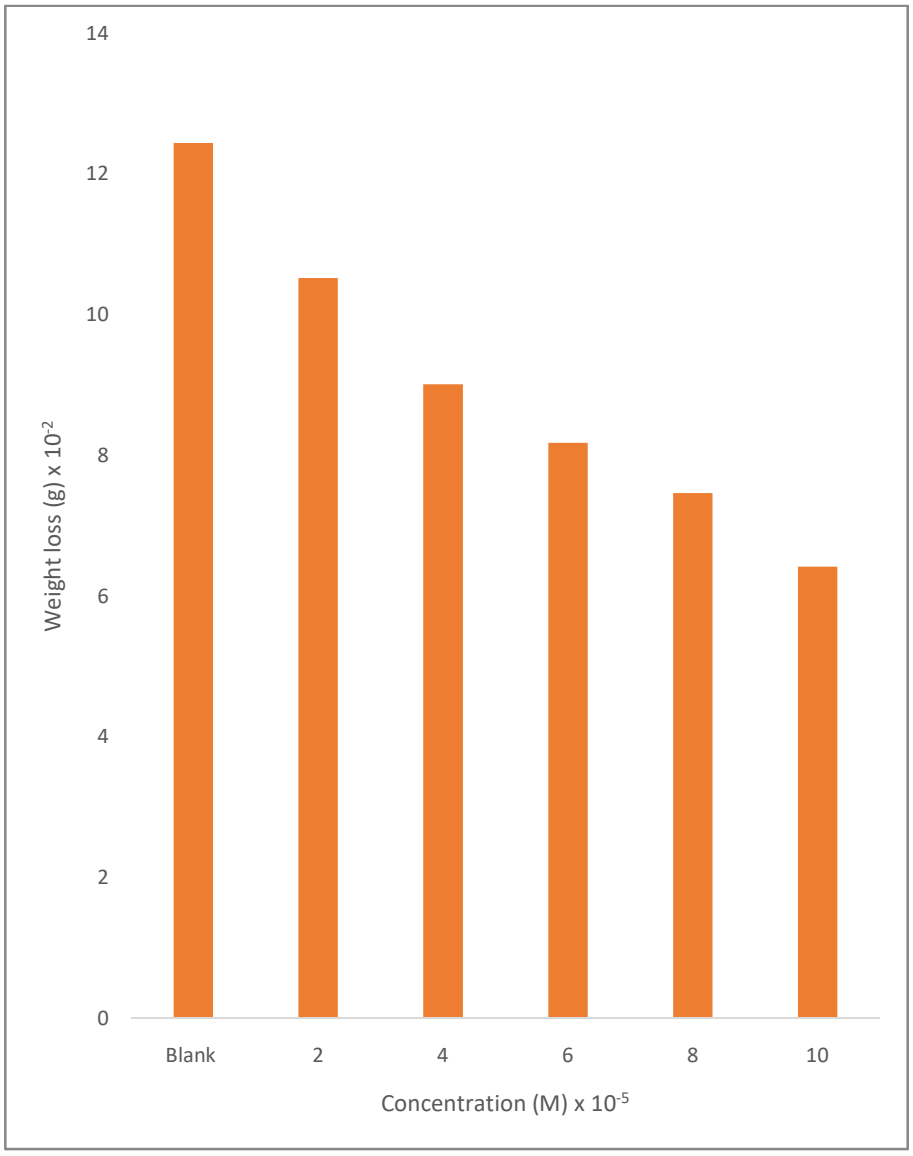

Fig 4.18: Weight loss values against different concentrations of 3 methyl indole in 1 mol/dm^3 HClof low carbon steel corrosion after 8hours immersion time at 333K.

Table 4.1: Inhibition efficiencies (I.E%) and corrosion rates for low carbon steel in 1 mol/dm^3 HCl in the presence and absence of various concentrations of 6 benzyl oxy indole at various temperatures viagravimetric method.

Concentration	**Corrosion Rate (Mg Cm^{-2}h^{-1}) x 10^{-3}**				**Inhibition Efficiency (%)**			
mol/dm^3	303K	313K	323K	333K	303K	313K	323K	333K
Blank	7.18	7.98	8.79	11.11	-	-	-	-
2 x 10^{-5}	2.76	3.41	4.42	6.56	61.57	57.27	49.75	40.92
4 x 10^{-5}	2.3	3.04	3.76	5.79	67.91	61.87	57.26	47.90
6 x 10^{-5}	1.74	2.50	3.15	5.33	75.75	68.68	64.16	52.01
8 x 10^{-5}	1.14	2.29	2.72	4.45	84.08	71.36	69.04	59.96
10 x 10^{-5}	0.55	1.16	2.19	3.99	92.29	85.46	75.13	64.06

Table 4.2: Inhibition efficiencies (I.E%) and corrosion rates for low carbon steel in 1 mol/dm^3 HCl in the presence and absence of various concentrations of 3 methyl indole at various temperatures viagravimetric method.

Concentration mol/dm^3	Corrosion rate (mg cm^{-2}h^{-1}) x 10^3				Inhibition efficiency (%)			
	303K	313K	323K	333K	303K	313K	323K	333K
Blank	7.18	7.98	8.79	11.11	-	-	-	-
2 x 10^{-5}	4.45	5.29	6.23	9.39	38.06	33.78	29.14	15.43
4 x 10^{-5}	3.85	4.81	5.64	8.04	46.27	39.71	35.84	27.57
6 x 10^{-5}	3.25	4.01	4.99	7.30	54.73	49.78	43.25	34.24
8 x 10^{-5}	1.54	3.11	4.23	6.66	78.48	61.07	51.57	40.03
10 x 10^{-5}	0.98	2.63	3.58	5.73	86.32	66.67	59.28	48.39

4.2 Effect of temperature and concentration on corrosion inhibition of 6 benzyl oxy indole and 3 methyl indole on low carbon steel

The corrosion rate of low carbon steel in the absence and presence of 6 benzyl oxy indole and 3 methyl indole at 303 – 333K was investigatedby means ofgravimetric method. Table 4.1 and Table 4.2 reveals the calculated values of corrosion rates ($mgcm^{-2}h^{-1}$), inhibition efficiency (IE%) and the degree of surface coverage (Θ) for dissolution of low carbon steel in $1mol/dm^3$ HCl in the presence and absence of 6 benzyl oxy indole and 3 methyl indole. It is obvious from the tables that percentage inhibition efficiency increases with rise in concentration of inhibitors but decreases with rise in temperature. The reduction in inhibition efficiency with rise in temperature is indicative of physical adsorption mechanism (Physiosorption) and may be due to increase in the solubility of the protective film of any of the reaction products precipitated on the surface of the low carbon steel that may otherwise impede the corrosion reaction. Another possible cause could be attributed to a likelyshift in the Adsorption-desorption equilibrium towards desorption of adsorbed inhibitor due to an increase in the kinetic energy of the molecules of the solution. Thus, as the temperature rises, the sum of adsorbed molecules reduces or desorption rate of the inhibitors from the low carbon steel surface increases, thus, leading to a reduction in the inhibition efficiency (Adejoro *et al.,* 2015).

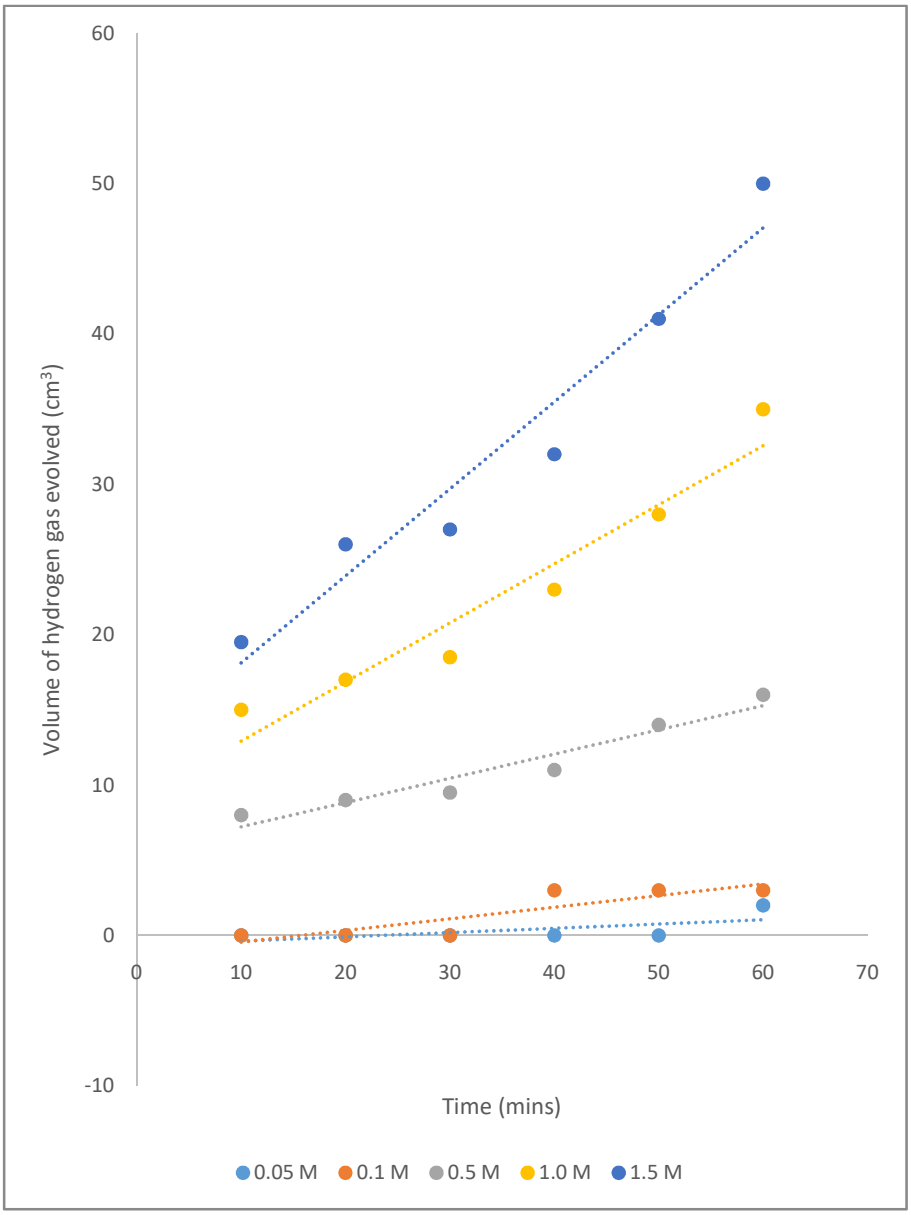

Fig 4.19: Volume of hydrogen gas liberated vs time for low carbon steel corrosion in various concentrations of HCl(0.05 mol/dm^3-1.5 mol/dm^3) at 303K.

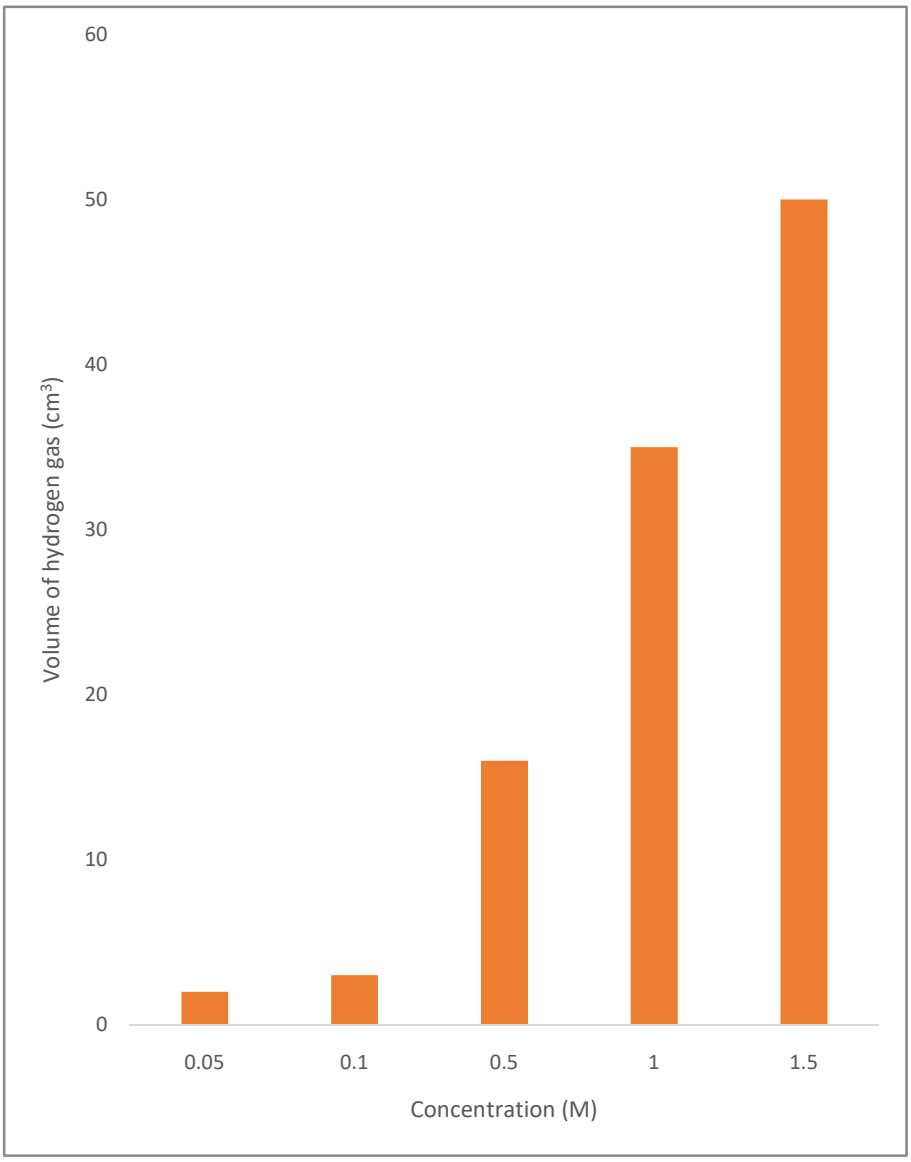

Fig 4.20: Volume of hydrogen gas liberated against different concentrations of HCl(0.05 mol/dm^3-1.5 mol/dm^3) of low carbon steel corrosion after 60 minutes reaction time at 303K.

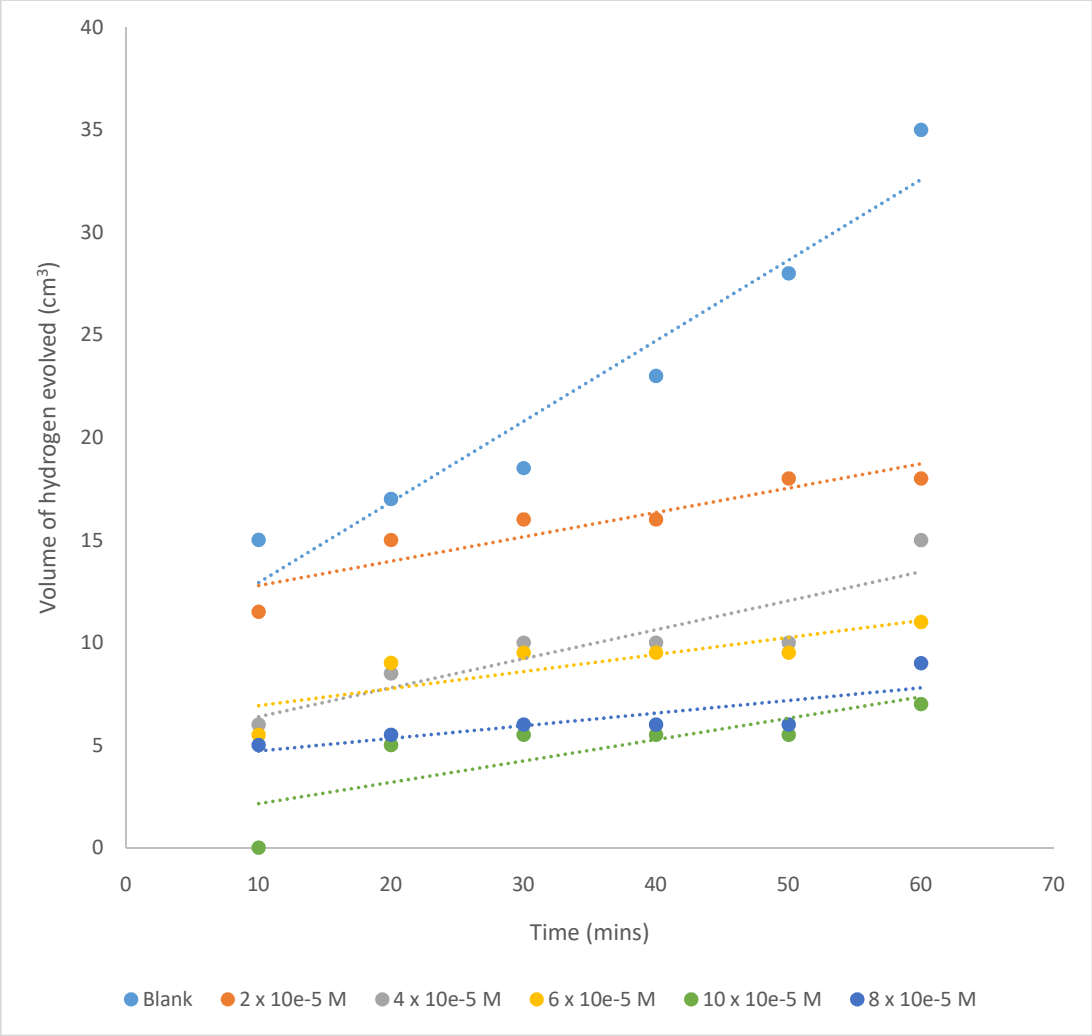

Fig 4.21: Volume of hydrogen gas liberated against time for low carbon steel corrosion in 1 mol/dm^{3}HCl in the presence of various concentrations of 6 benzyl oxy indole at 303K.

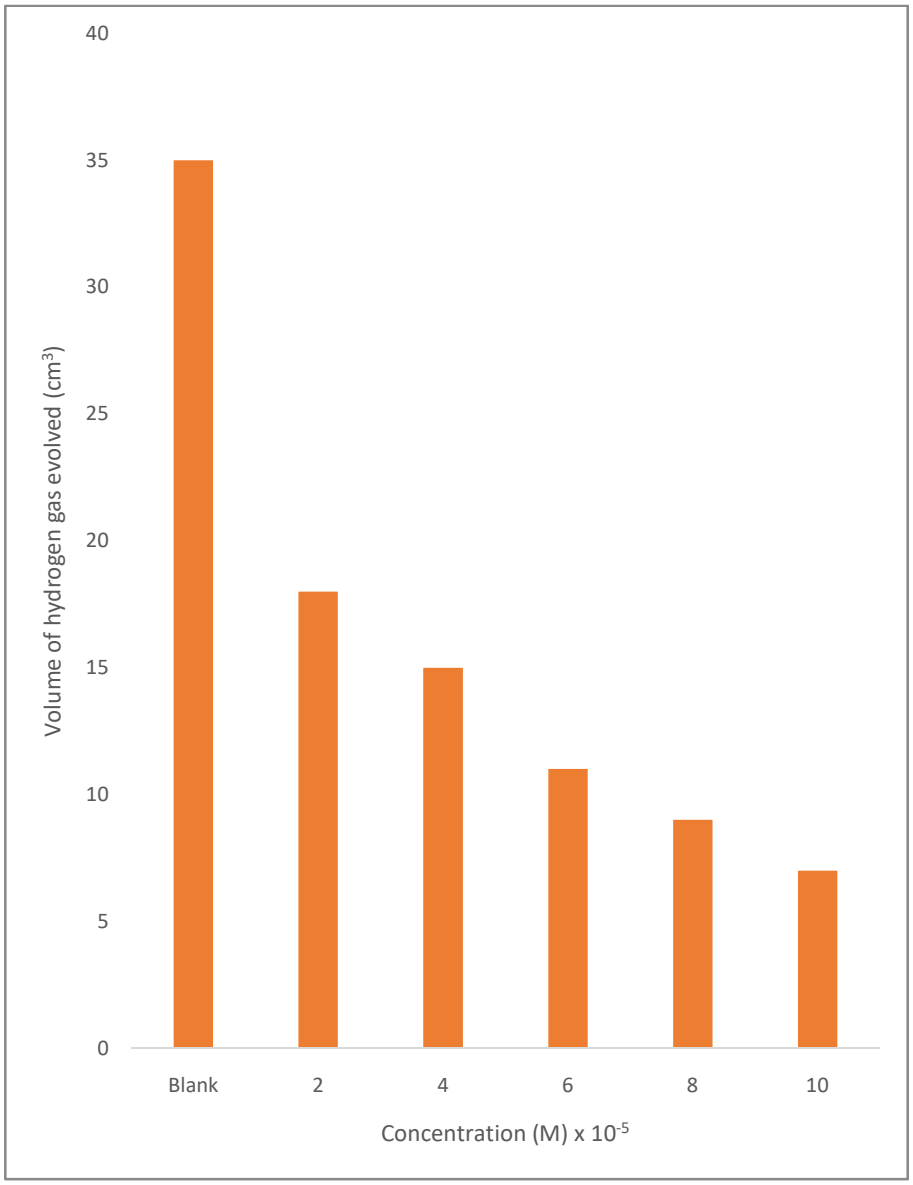

Fig 4.22: Volume of hydrogen gas liberated against different concentrations of 6 benzyl oxy indole in 1 mol/dm^3 HClof low carbon steel corrosion after 60 minutes reaction time at 303K.

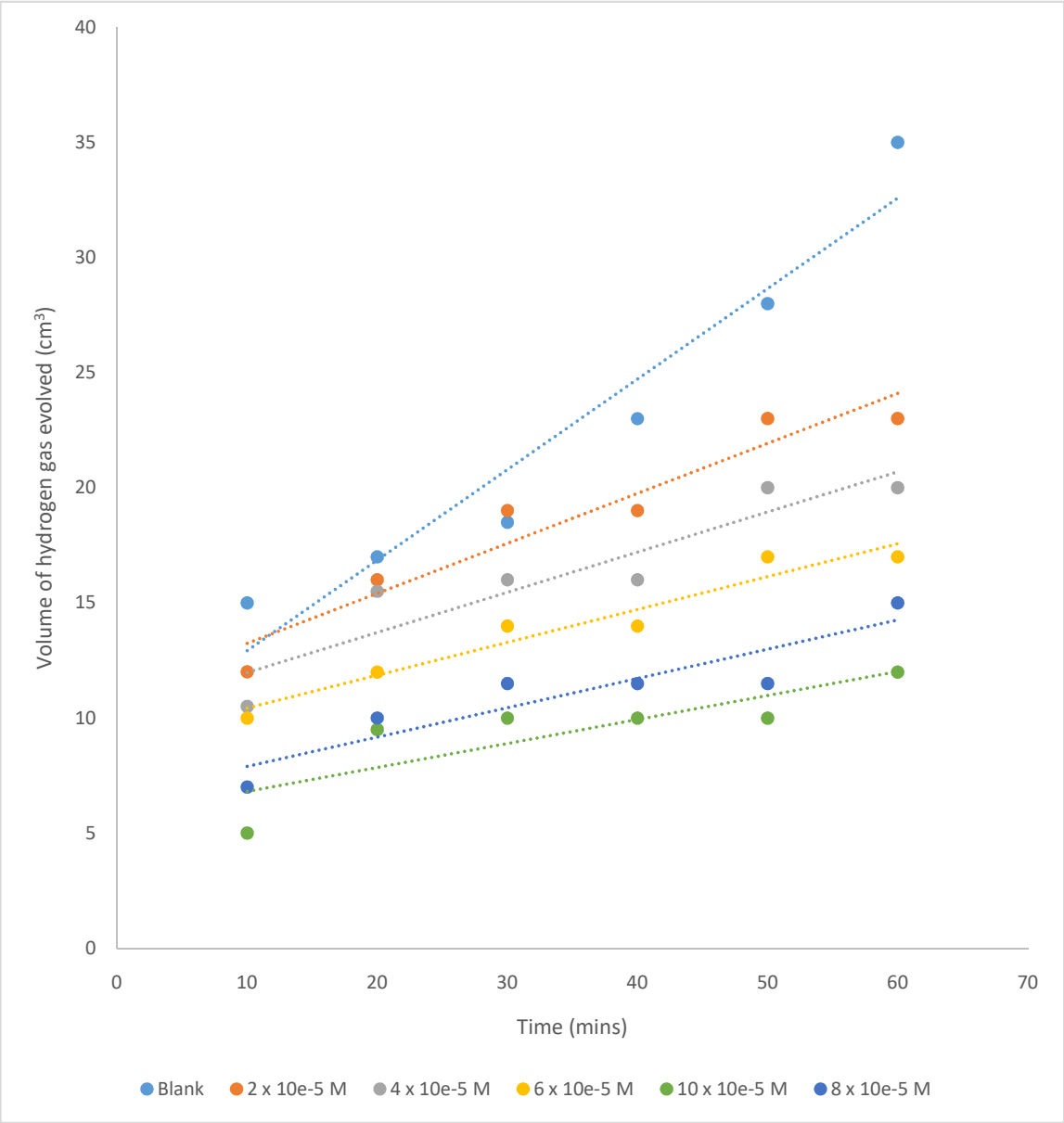

Fig 4.23: Volume of hydrogen gas liberated vs time for low carbon steel corrosion in 1 mol/dm^{3}HCl in the presence of various concentrations of 3 methyl indole at 303K.

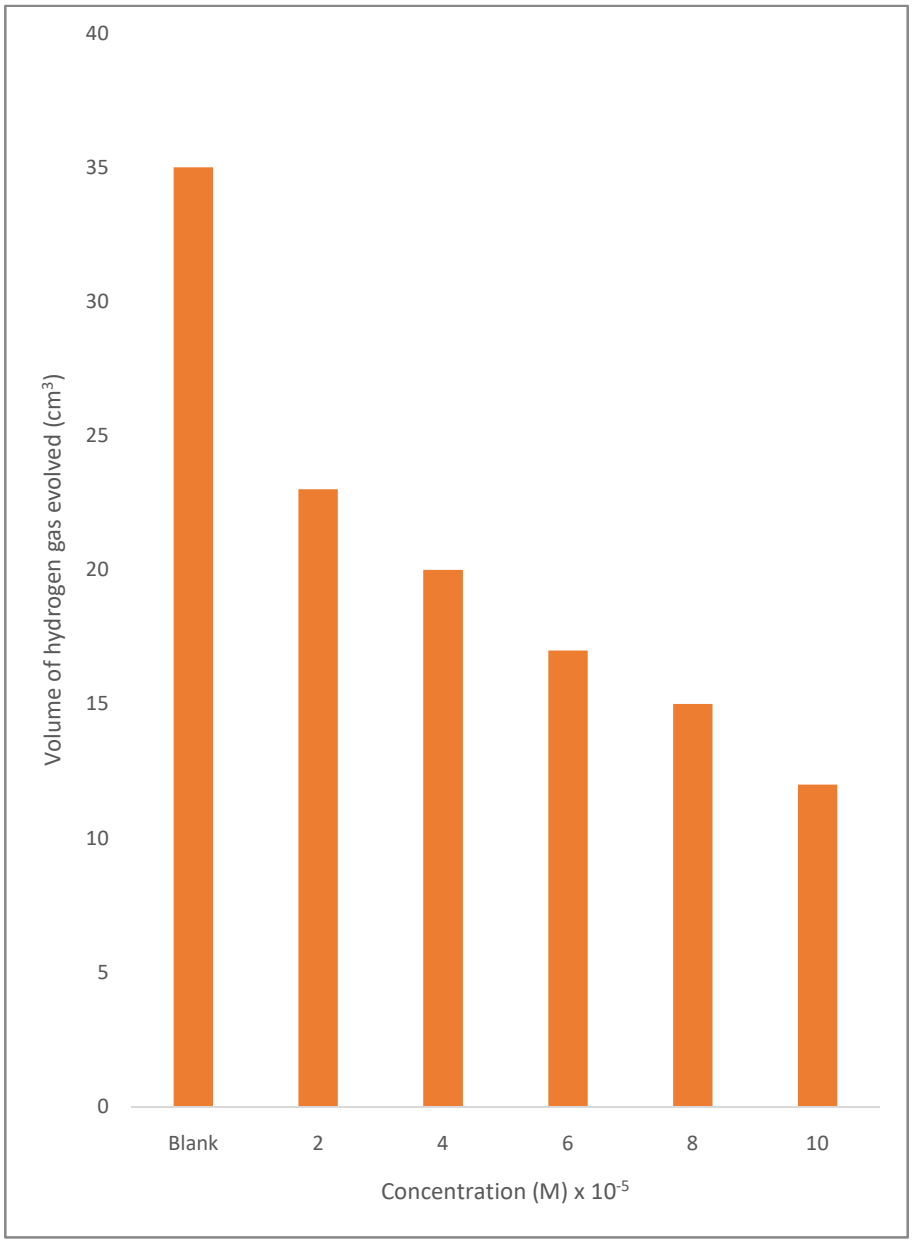

Fig 4.24: Volume of hydrogen gas liberated against different concentrations of 3 methyl indole in 1 mol/dm^3 HClof low carbon steel corrosion after 60 minutes reaction time at 303K.

Table 4.3: Inhibition efficiencies (I.E%), degree of surface coverage and corrosion rates for low carbon steel in 1 mol/dm^3 HCl in the presence and absence of various concentrations of 6 benzyl oxy indole at 30^oC using hydrogen evolution technique

Concentration mol/dm^3	Inhibition efficiency (I.E %)	Degree of surface coverage	Corrosion rate (cm^3min^{-1})
Blank	-	-	0.58
2 x 10^{-5}	48.57	0.49	0.30
4 x 10^{-5}	57.14	0.57	0.25
6 x 10^{-5}	68.57	0.69	0.18
8 x 10^{-5}	74.29	0.74	0.15
10 x 10^{-5}	80.00	0.80	0.12

Table 4.4: Inhibition efficiencies (I.E%), degree of surface coverage and corrosion rates for low carbon steel in 1 mol/dm^3 HCl in the presence and absence of various concentrations of 3 methyl indole at 30^{o}C using hydrogen evolution technique.

Concentration mol/dm^3	Inhibition efficiency (I.E %)	Degree of surface coverage	Corrosion rate (cm^{3}min^{-1})
Blank	-	-	0.58
2 x 10^{-5}	34.29	0.34	0.38
4 x 10^{-5}	42.86	0.43	0.33
6 x 10^{-5}	51.43	0.51	0.28
8 x 10^{-5}	57.14	0.57	0.25
10 x 10^{-5}	65.71	0.66	0.20

4.3 Hydrogen gas evolution measurements of indole derivatives

This method, aside its experimental rapidity, it ensures a more sensitive monitoring in situ of any perturbation by the inhibitor vis-à-vis gas evolution on the metal- corrodent interphase. Some authors have reported that comparable agreement exist between gasometric method and other methods of corrosion monitoring which includes gravimetric, polarization measurementand thermometric methods. (Solmaz, 2010.; Abdallah, 2004 and Umoren and Ebenso, 2008.)

Aydin and Koleli, 2006. Proposed the mechanisms for hydrogen gas evolution reaction on electrodes in acidic media. Refer to equations 4.12, 4.13 and 4.14:

i. A primary discharge step (Volume reaction)

$$M + H_3O^+ + e^- \leftrightarrow MH_{ad} + H_2O \qquad 4.12$$

ii. An electrochemical – desorption step (Heyrowsky reaction)

$$MH_{ad} + H_3O^+ + e^- \rightarrow M + H_2 + H_2O \qquad 4.13$$

iii. A recombination step (Tafel reaction)

$$MH_{ad} + MH_{ad} \rightarrow 2M + H_2 \qquad 4.14$$

For hydrogen gasliberation reaction, three different steps may be involve in the cathodic reaction as stated below:

First, H_2O molecule or H_3O^+ ion is released on electrode surface to produce hydrogen atom in acidic solution and an adsorbed hydrogen atom, MHads, is generated (Volmer reaction).

Second, one electron is transferred to a hydronium ion and the hydrogen evolution reaction occurs on metal surface (Heyrowsky reaction) or a recombination of the adsorbed hydrogen atom to liberate hydrogen gas subsequently (Tafel reaction)(Bhardwaj and Balasubramaniam, 2008).

Despite the necessity of the three states for the formulation of the mechanism, no one step of the three reactions occurs as a single step but combines with another i.e if volmer reaction is fast, Tafel and/or heprowsky reaction must be slow or vice versa. A fast step reaction is preceded by a slow step. So the presence of indole derivatives may

impede the formation of MH_{ads} and suppress reaction (Fekry and Ameer, 2010). Or hinder the electron transfer to H_3O^+ ion and suppress reaction (Abboud *et al.,* 2009).

The free corrosion of low carbon steel in 1 mol/dm^3 HCl was described by speedy effervescence as a result of the hydrogen gas liberated and corrosion rates in the absence and presence of the indole derivatives was calculated via hydrogen gasliberation method. As shown in Fig 4.21 - 4.24. the plots demonstrate the reduced deflection of hydrogen gas liberation rate on introduction of the indole derivatives into the corrodent, signifying that the indole derivatives actually inhibits corrosion of low carbon steel in 1 mol/dm^3 HCl when compared to the blank. The of hydrogen gas liberation rates were seen to reduce with rising indole derivatives concentration, indicating that the inhibition was concentration dependent. The results obtained for corrosion rates, surface coverage and inhibition efficiencies (Tables 4.3 and 4.4) are close to that obtained for weight loss method. It is indicative that these inhibitors are effective with 6 benzyl oxy indole being a more effective inhibitor than 3 methyl indole.

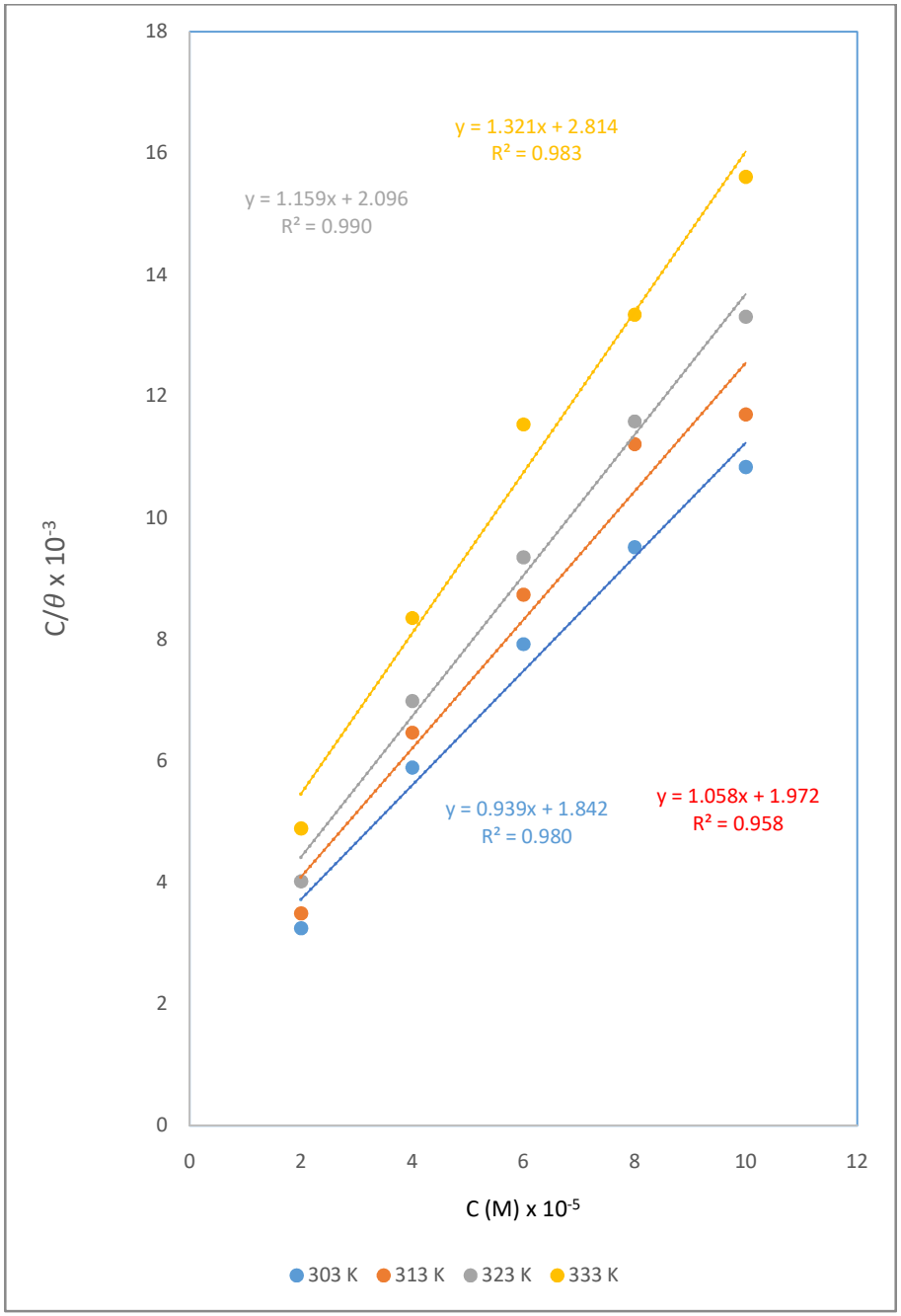

Fig 4.25: Langmuir isotherm plot for the adsorption of 6 benzyl oxy indole on low carbon steel in 1 mol/dm^3 HCl

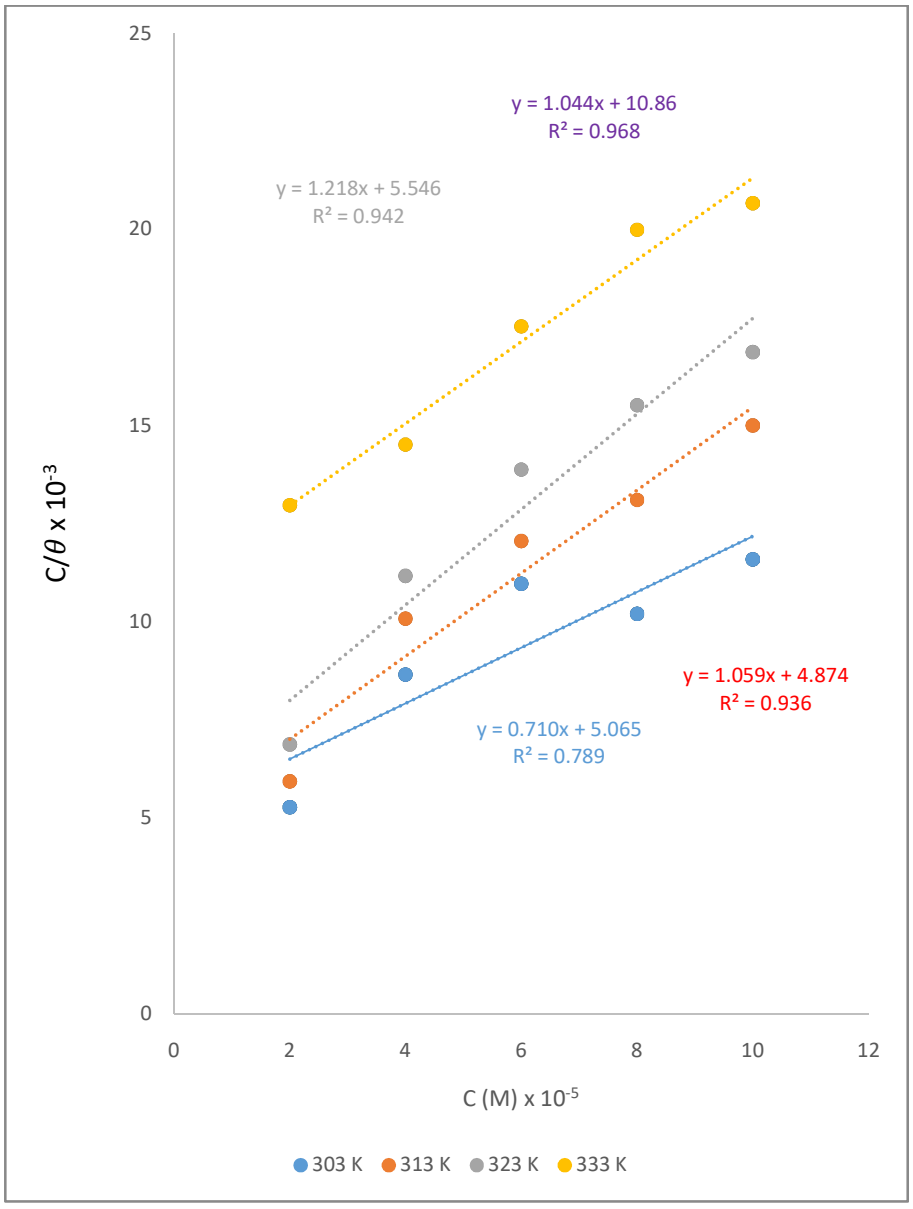

Fig 4.26: Langmuir isotherm plot for the adsorption of 3 methyl indole on low carbon steel in 1 mol/dm^3 HCl

Table 4.5: Langmuir parameters for the adsorption of 3 methyl indole on low carbon steel surface

Temperature (^oC)	K_{ads}	ΔG^o_{ads} (KJ)	Slope	R^2	R	Intercept
30	0.1974	-6.0305	0.7104	0.7895	0.8885	5.0657
40	0.2052	-6.3303	1.0592	0.9367	0.9678	4.874
50	0.1803	-6.1852	1.2182	0.9424	0.9708	5.5467
60	0.0920	-4.5139	1.0442	0.9681	0.9839	10.864

Where $\boldsymbol{R = \sqrt{R^2}}$

Table 4.6: Langmuir parameters for the adsorption of 6 benzyl oxy indole on low carbon steel surface

Temperature (^oC)	K_{ads}	ΔG^o_{ads} (KJ)	Slope	R^2	R	Intercept
30	0.5428	-8.5786	0.9399	0.9809	0.9904	1.8422
40	0.5071	-8.6847	1.0582	0.9589	0.9792	1.972
50	0.4770	-8.7978	1.1591	0.9908	0.9954	2.0964
60	0.3553	-8.2547	1.3219	0.9832	0.9916	2.8143

Where $\boldsymbol{R = \sqrt{R^2}}$

4.4 Adsorption Isotherm of indole derivatives

The adsorption mechanismdepends largelyon adsorption of solvent and other ionic species,the nature and charge of the metal surface, temperature of the corrosion reaction, electronic characteristic of the metal surface and the electrochemical potential at solution interface(Hmamou*et al.,* 2012).

When the interaction energy between the water molecule and the metal surface is higher than that betweenorganic molecule and metal surface then adsorption of the organic molecules takes place.

Langmuir isotherm was tested for its fit to the experimental data. Langmuir isotherm is given by equation 4.15.

$$C/\theta = 1/K_{ads} + C \qquad 4.15$$

Where θ is the degree of surface coverage, C the molar inhibitor concentration in the bulk solution and K_{ads} is the equilibrium constant of the process of adsorption. The graph of C/θ against C was linear as shown in Figures 4.25-4.26 having a correlation value bigger than 0.9, with aninsignificant deviation of the slopes from unity (Tables 4.5 and 4.6). This suggest that the Langmuir adsorption isotherm model can adequately describe the adsorption behavior. Langmuir isotherm assumes that:

iv. The number of adsorption sites on the metal surface is fixed and it is one adsorbate per site.
v. ΔG_{ads} is the equal for all sites and it does not dependon surface coverage (θ).
vi. Nointeraction between the adsorbates. (Maghraby and Soror, 2003).

The adsorption equilibrium constant values gotten from the intercept of the Langmuir adsorption isotherm of low carbon steel are connected to the free energy of adsorption via equation 4.16 (Ebenso *et al.,* 2010b) :

$$\Delta G^{o}_{ads} = -2.303RT \log (55.5\ K_{ads}) \qquad 4.16$$

Free energy of the adsorption is represented as ΔG^{o}_{ads}, R is the symbol of gas constant and temperature is represented as T. Free energy values are shown in Tables 4.5 and 4.6 The free energy values ranged from -8.80 to -8.25 KJ/mol^{-1} for 6 benzyl oxy indole and -6.33 to -4.51 KJ/mol^{-1} for 3 methyl indole.

ΔG^{o}_{ads} values up to -20kJmol^{-1} usually indicates physical adsorption, the inhibition comes to play as a result of electrostatic interaction between the charged molecules and the charged metal, while values up to or more than -40kJmol^{-1} indicates

chemisorption which occurs due to sharing or transfer of electrons from the organic molecules to the metal surface to form a coordinate type of bond (Ebenso *et al.,* 2010a). The values gotten from this research ranged from -8.80 to -4.514kJmol^{-1}, which agrees with the mechanism of physiosorption (Ashassi-Sorkhabi *et al.,* 2005).

Table 4.7: Thermodynamic parameters for the adsorption of 3 methyl indole via gravimetric method

Concentration mol/dm^3	Activation Energy (KJmol^{-1})	Heat of adsorption (Q_{ads}) KJ mol^{-1}
Blank	12.21	-
2 x 10^{-5}	20.88	-33.96
4 x 10^{-5}	20.52	-22.83
6 x 10^{-5}	22.63	-23.56
8 x 10^{-5}	40.95	-47.49
10 x 10^{-5}	49.39	-53.32

Table 4.8: Thermodynamic parameters for the adsorption of 6 benzyl oxy indole viagravimetric method

Concentration mol/dm^3	Activation Energy (KJmol^{-1})	Heat of adsorption (Q_{ads}) KJ mol^{-1}
Blank	12.20	-
2 x 10^{-5}	24.21	-23.45
4 x 10^{-5}	25.82	-23.32
6 x 10^{-5}	31.31	-29.61
8 x 10^{-5}	38.09	-35.25
10 x 10^{-5}	55.42	-53.26

4.5 Thermodynamic considerations of indole derivatives

The connectionconcerning thetemperature, activation energy and inhibition efficiency (IE%) of an inhibitor was given as follows (Niamein *et al.,* 2012):

i. Inhibitor whose IE (%) drops with rise in temperature. The value of activation energy (E_a) obtained is higher than that in the uninhibited solution.
ii. Inhibitors in which the IE (%) remains unchanged with change in temperature. The activation energy (E_a) does not change in the presence or absence of inhibitors.
iii. Inhibitors whose IE (%) is likely to increase with arise in temperature. The value of activation energy (E_a) obtained is lower than that of the uninhibited solution.

A greater value of the activation energy (E_a) of the corrosion process in the presence of inhibitor when compared to an uninhibited corrosion process suggest that the adsorption mode is physiosorption, while the other way round suggest chemisorption.

To further show that the indole derivatives adsorbed to low carbon steel through physiosorption, the values of activation energy (E_a) were calculated using Arrhenius equation(refer to equation 4.17)

$$\log(CR_2/CR_1) = E_a/2.303R\ (1/T_1 - 1/T_2) \qquad 4.17$$

Where $CR_1$and CR_2 represent the rates of corrosion at temperature T_1 and T_2, in that order. The values are as shown in Tables 4.1 and 4.2. Arise in the value of activation energy (E_a)when the indole derivatives are present as compared when they are absent and the reduction of its IE% with temperature rise can be understood as asign of physiosorption. With reference to Ameh *et al.,* 2012, it is likely that for chemisorption, the values of activation energy should be more than 80kJmol^{-1} for the mechanism of physiosorption. With the activation energy (E_a)values as shown in Table 4.7 (12.21-55.42kJmol^{-1}) for 6 benzyl oxy indole and Table 4.8 (12.21-49.39kJmol^{-1}) for 3 methyl indole, it further confirms the process of physical adsorption.

An estimation of heat of adsorption wascalculatedusing equation 4.18:

$$Q_{ads} = 2.303R\ [\log(\theta_2/1-\theta_2) - \log(\theta_1/1-\theta_1)] \times (T_1 \times T_2/T_2 - T_1)\ \text{kJmol}^{-1}. \qquad 4.18$$

The degrees of surface coverage are represented as θ_1 and θ_2 and temperatures are represented as T_1 and T_2.

The values calculated for Q_{ads} are shown in Tables 4.7 and 4.8. Calculated values of Q_{ads} using equation 6 ranged from -23.45 to -53.26kJmol^{-1} for 6 benzyl oxy indole and -33.96 to -53.32kJmol^{-1} for 3 methyl indole. The values obtained are negative signifying that the adsorption of these indole derivatives on low carbon steel is exothermic (Ameh *et al.,* 2012).

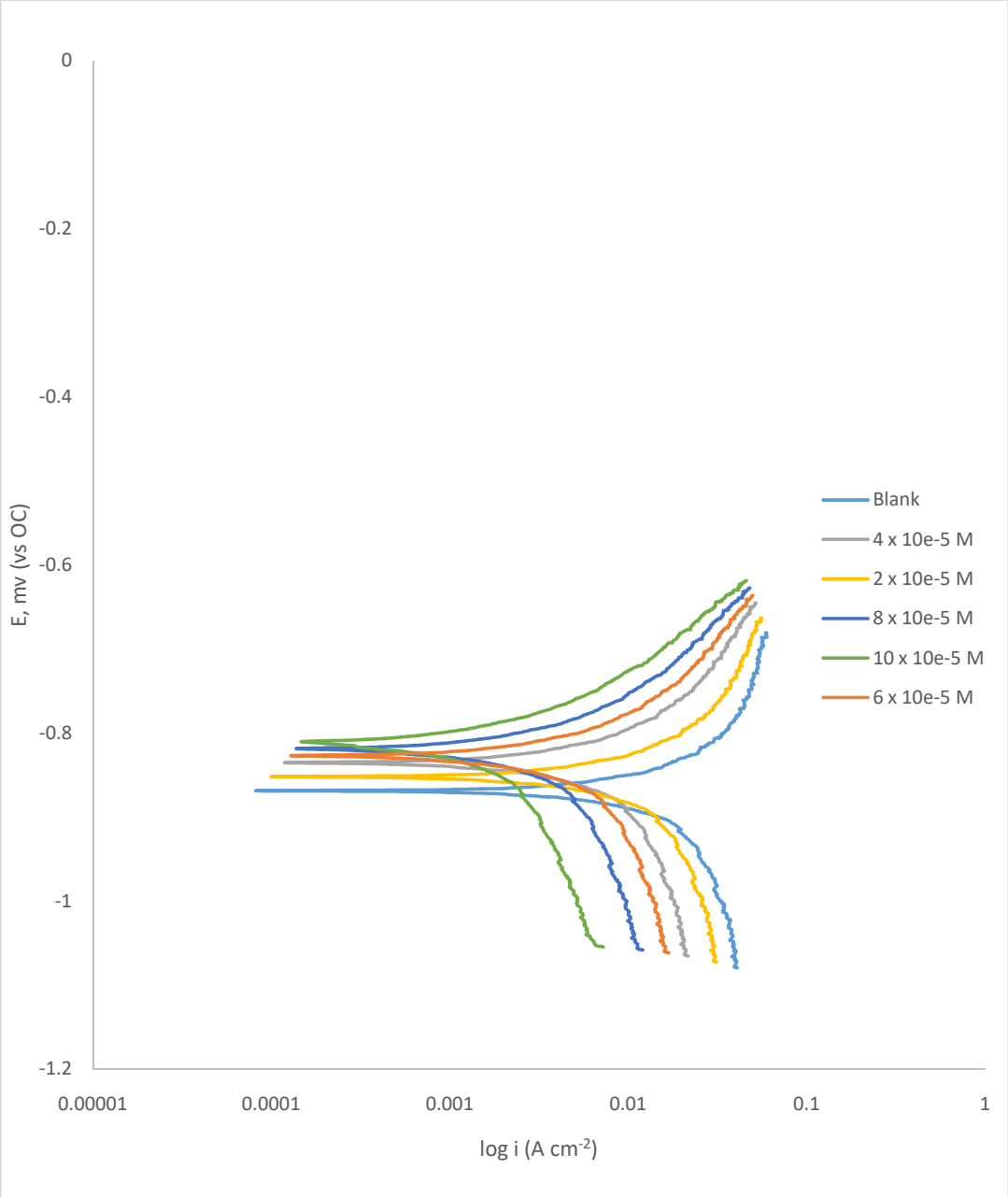

Figure 4.27: Potentiodynamic poilarization curves for low carbon steel in 1 mol/dm^3 **HCl containing various concentrations of 6 benzyl oxy indole**

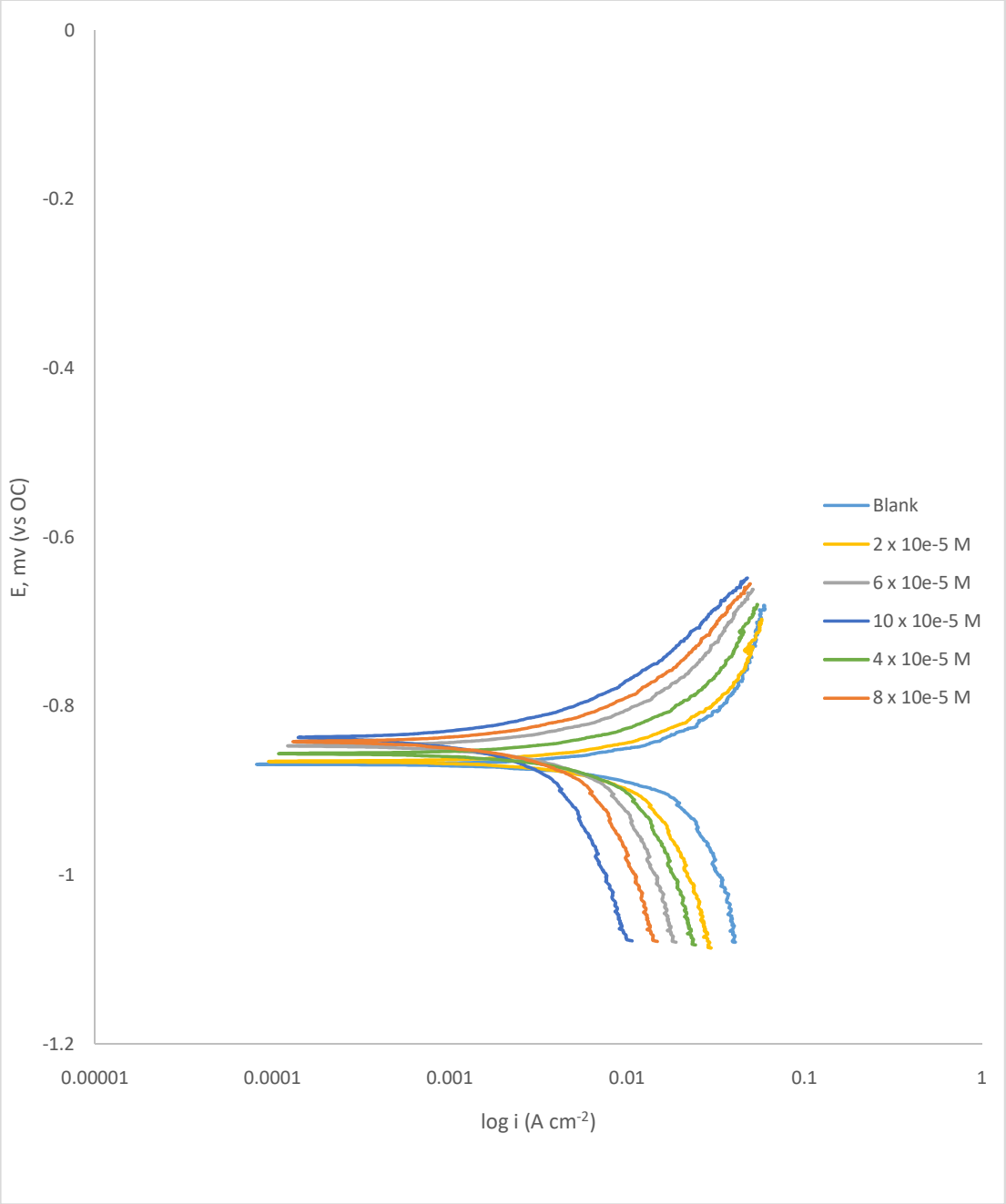

Figure 4.28: Potentiodynamic poilarization curves for low carbon steel in 1 mol/dm^3 HCl containing various concentrations of 3 methyl indole

Table 4.9: Potentiodynamic polarization parameters for low carbon steel in 1mol/dm^3 HCl with various concentrations of 6 benzyl oxy indole.

Concentration (mol/dm^3)	i_{cor} (A cm^{-2})	CR (mmpy)	I.E (%)	Θ
Blank	70.948	588.04	-	-
2 x 10^{-5}	19.197	159.120	72.94	0.729
4 x 10^{-5}	15.188	125.871	78.59	0.786
6 x 10^{-5}	12.573	104.209	82.28	0.823
8 x 10^{-5}	8.792	72.875	87.61	0.876
10 x 10^{-5}	4.176	34.616	94.11	0.941

Table 4.10: Potentiodynamic polarization parameters for low carbon steel in 1mol/dm^3 HCl with various concentrations of 3 methyl indole.

Concentration (mol/dm^3)	i_{cor} (A cm^{-2})	CR (mmpy)	I.E (%)	Θ
Blank	70.948	588.04	-	-
2 x 10^{-5}	38.521	319.274	45.71	0.457
4 x 10^{-5}	30.358	251.620	57.21	0.572
6 x 10^{-5}	22.751	188.567	67.93	0.679
8 x 10^{-5}	15.193	125.925	78.59	0.786
10 x 10^{-5}	8.437	69.930	88.11	0.881

4.6 Potentiodynamic Polarization Measurements of indole derivatives

Figures 4.27 and 4.28 illustratesthe Tafel polarization curves for low carbon steel in 1mol/dm^3 HCl in the absence and presence of different concentrations of indole derivatives at 303K, respectively. From Figures 4.27 and 4.28, it is shown that both anodic reaction (i.e metal dissolution) and cathodic reaction (i.e H_2evolution) were inhibited when indole derivatives were introduced to 1 mol/dm^3 HCl with the strength of inhibition increasing as inhibitor concentration increases. Tafel lines of inhibited systems in comparism with the uninhibited system are deflected to more negative and more positive potentials which increases with rise ininhibitor concentration. This actsuggest that the organic moleculesbehave as mixed-type inhibitors (Fouda *et al.,* 2006).

The results in Table 4.9 and 4.10 reveals that the rise in concentration of inhibitor leads to decrease in corrosion current density (icorr) and corrosion rates, (Migahed et al, 2009). The order of increasing I.E% of organic molecules under investigationis as follow: 6 benzyl oxy indole > 3 methyl indole.

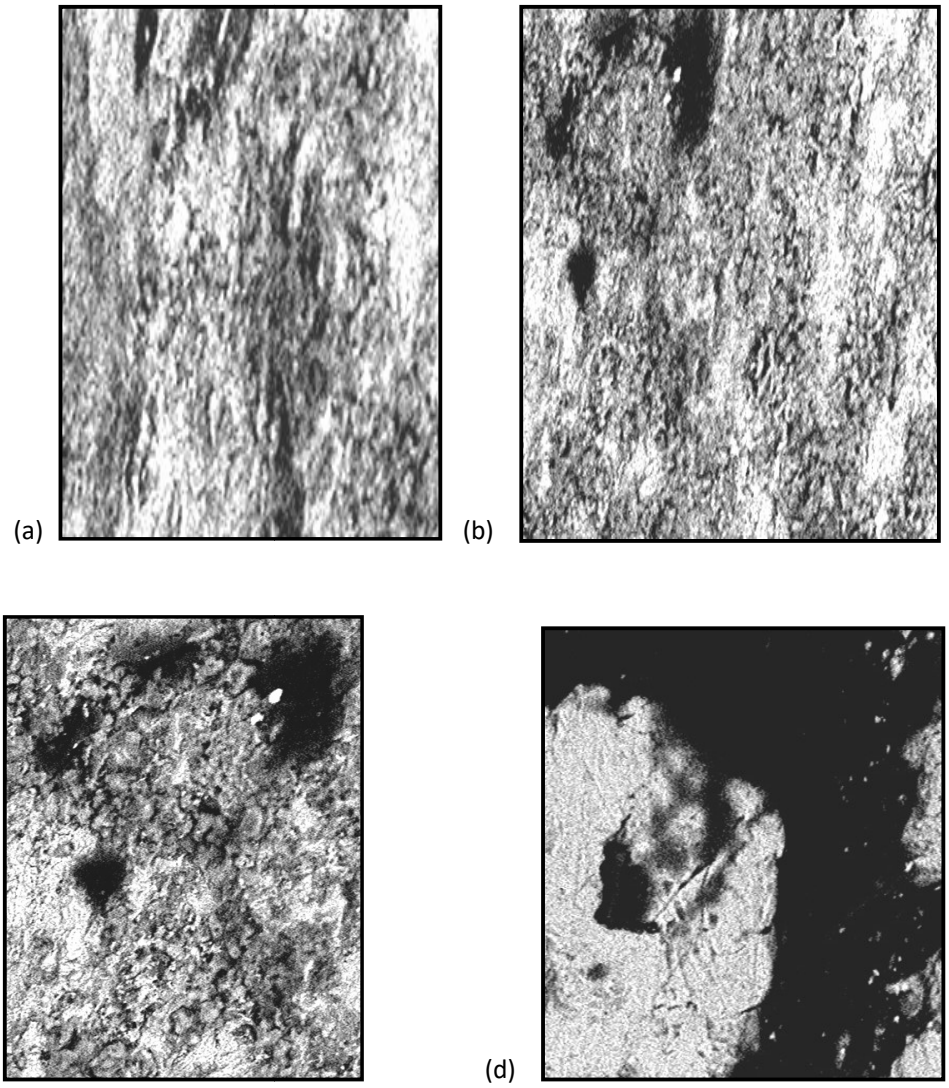

Fig 4.29: SEM characteristics of the low carbon steel in 1.0 mol/dm^3 HCl in (a) low carbon steel in the absence of inhibitor and acid, (b) low carbon steel in the presence of 6 benzyl oxy indole and acid, (c) low carbon steel in the presence of 3 methyl indole and (d) low carbon steel in the presence of acid only.

4.7 Scanning electron microscopy of indole derivatives

The scanning electron microscopy (SEM) image in Fig 4.29 reveals that corrosion does not occur homogeneously over the surface of low carbon steel in 1 mol/dm^3 HCl solution. However, the surface is significantly protected by the indole derivatives with 6 benzyl oxy indole being more effective than 3 methyl indole in comparism to the inhibitor – free solution.

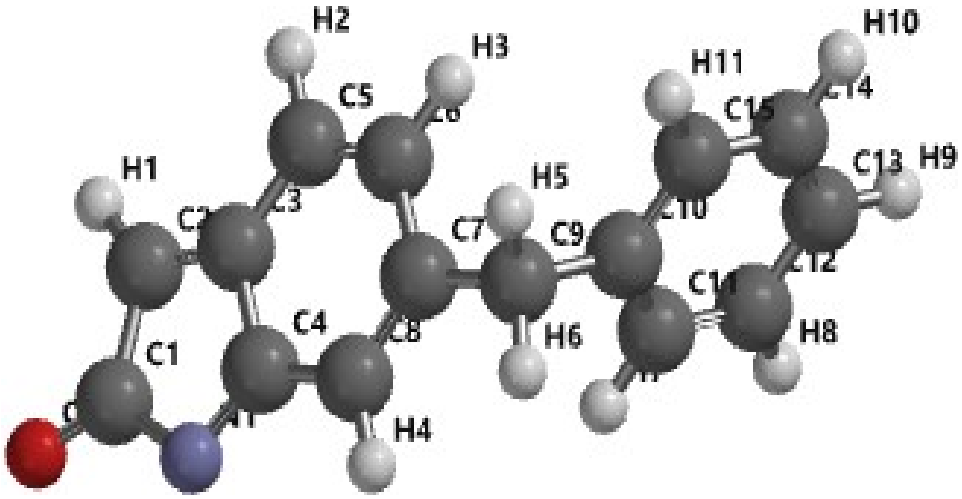

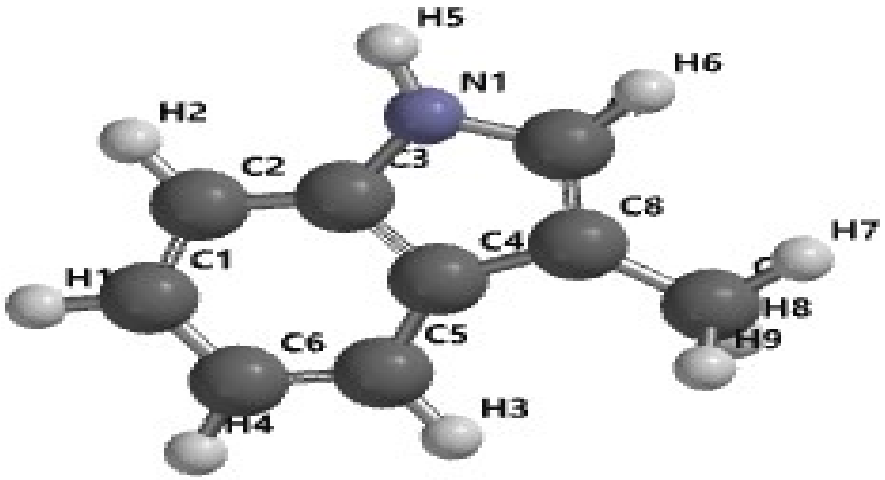

Figure 4.30: Labelled optimised structures

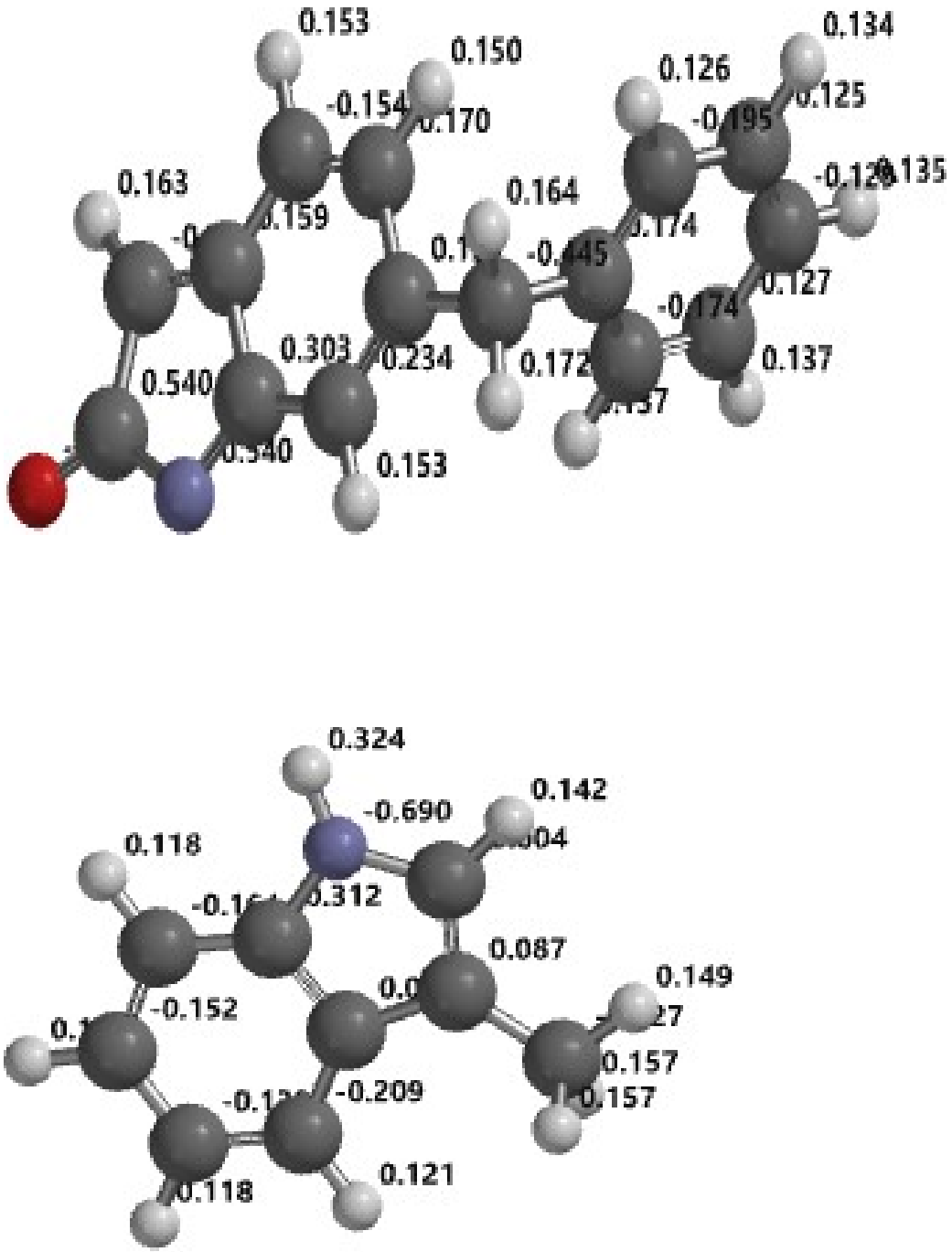

Figure 4.31: Optimised molecular structures of indole derivatives showing mulliken charges

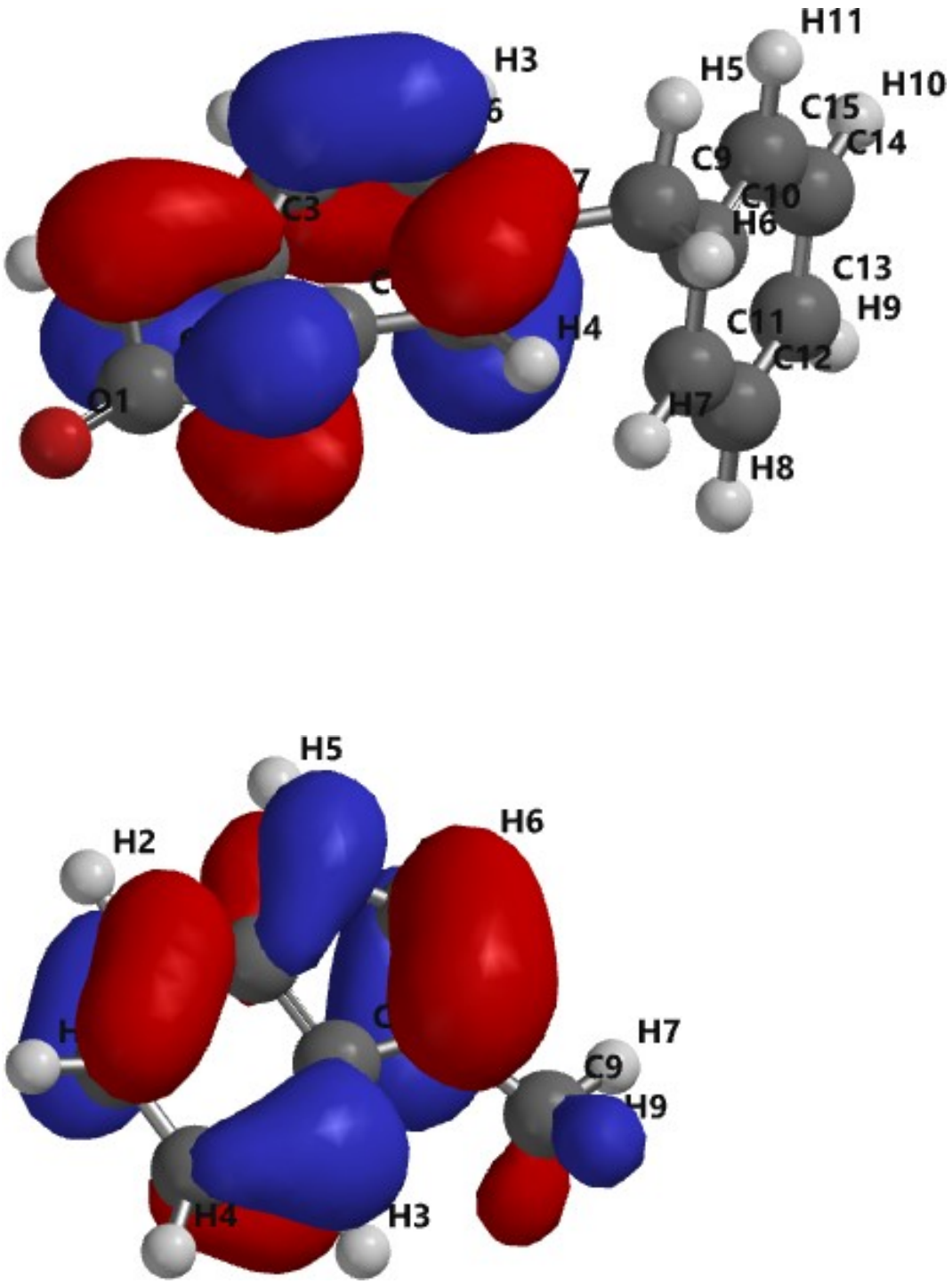

Figure 4.32: HOMO plot of optimised molecules

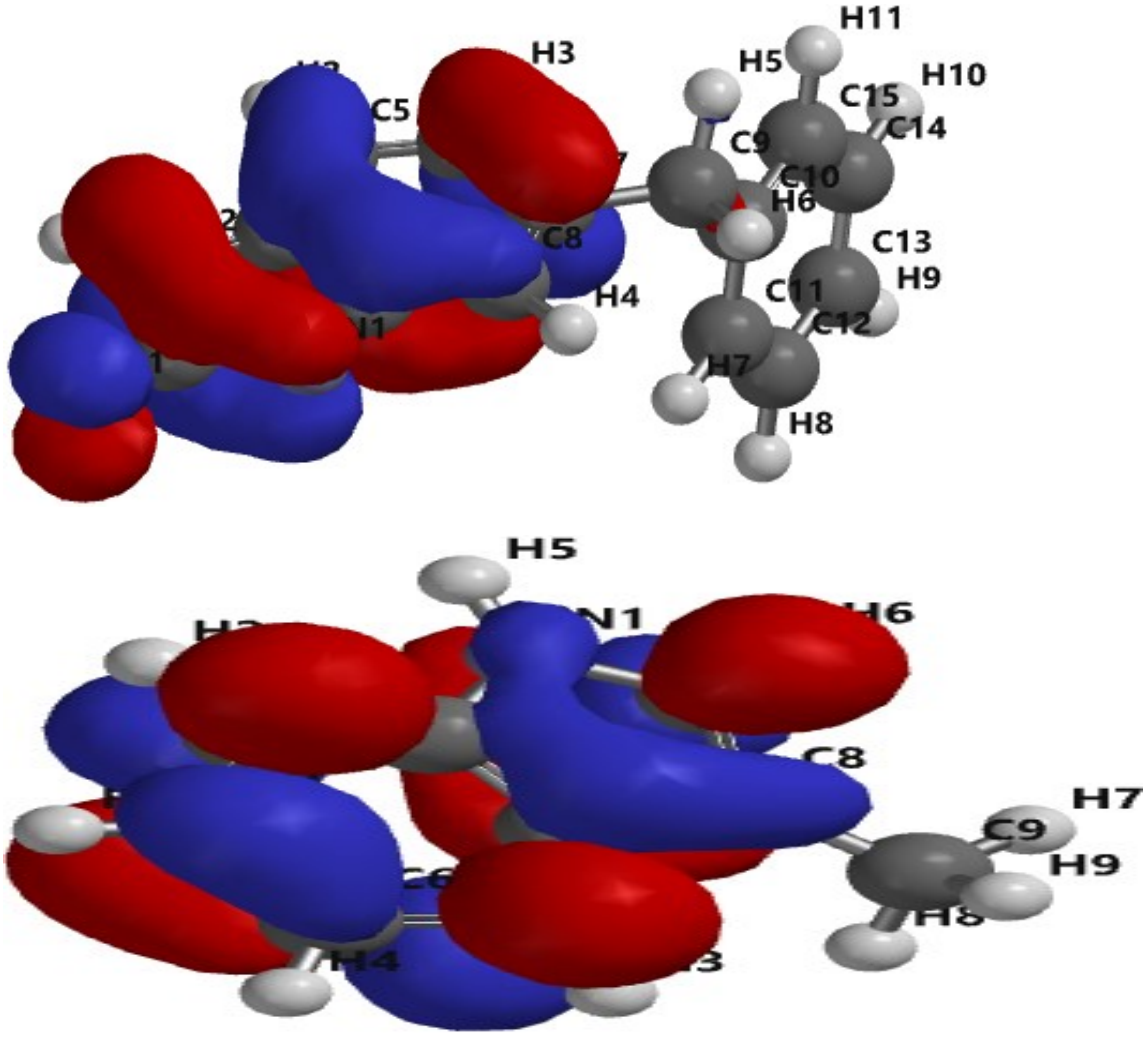

Figure 4.33: LUMO plot of optimised molecules

Table 4.11: Quantum chemical parameters of indole derivatives using DFT method

Quantum chemical parameters	6 benzyl oxy indole	3 methyl indole
E_{Homo} (eV)	-6.20	-5.25
E_{Lumo} (eV)	-3.49	-0.02
$E_{Lumo} - E_{Homo}$ (eV)	2.71	5.23
Dipole moment (μ)	6.44	2.05
Log P	2.08	0.32
Polarizability	59.99	52.35
Volume ($Å^3$)	237.32	150.53
Weight (amu)	221.26	131.18
Ionisation Potential (*I*)	6.20	5.25
Electron Affinity (*A*)	3.49	0.02
Hardness(η)	1.355	2.615
Softness (*S*)	0.738	0.382
Electronegativity(χ)	4.845	2.635
Chemical potential (μ)	-4.845	-2.635
Electrophilicity Index (ω)	8.662	1.3276

4.8 Quantum chemical study of 6 benzyl oxy indole and 3 methyl indole

The inhibition efficiency of the indole dreivatives have been measured experimentally. Quantum chemical indices calculated includes: energies of frontier molecular orbitals (E_{HOMO} and E_{LUMO}), separation energy ($E_{LUMO} - E_{HOMO}$), dipole moment, substituent constant (log p), polarizability, molecular volumes and molecular weights are tabulated in Table 4.11.

The E_{HOMO} is closely related with the electron giving ability of molecule (Xia *et al.,* 2008; Ebenso *et al.,* 2010a; Arslan *et al.,* 2009). Thus, rising values of E_{HOMO} suggestgreaterpropensity for donation of electrons to the suitable acceptor molecule with vacant molecular orbital and low energy, hence rising E_{HOMO}values aid the adsoption of the inhibitor (Ebenso *et al.,* 2010a). The E_{LUMO}signifies the capability of the molecule accepting electrons. Thus, the lesser the E_{LUMO}value the more seeming for the molecule accepting electrons (Adejoro *et al.,* 2015). The separation energy which connotes reactivity is thegap between the E_{HOMO} and E_{LUMO}. This energy gap also relates to how soft or hard a molecule is. The lower the energy gap the higher the reactivity towards a chemical specie. Hence, a hard molecule is less reactive than a soft molecule (Adejoro *et al.,* 2016). The extent to which an inhibitor binds to the metal surface improves with rising energy of HOMO, lowering energy of LUMO and low values of separating energy.

Dipole moment (μ)is alsoan important quantum chemical parameteruse in predicting the direction of corrosion inhibition. It is a way of measuring polarity in a bond and is associated withhow electrons are dispersed in a molecule. Even though literature is not consistent on the usage of dipole moment predicting the way a corrosion inhibition process goes, it is largely accepted that the adsorption of polar molecules having high dipole moments on the surface of the metal should result to improved inhibition efficiency (Mohamed, 2013).

The ratio of induced dipole moment to the intensity of the electric field is referred to as polarizability (Wang *et al.,* 2003).

The log p values obtained were observed to be closely related to the inhibition efficiencies of the molecules under investigation. Substituent constantsdon't depend

on the parent structure but differ with the substituent. Thus raising the log p values increases the corrosion inhibition efficiencies of organic molecules (Gece, 2011).

Molecular volume and weight are quantum parameters that determine molecular size and effective surface coverage. These invariably determine how effective a molecule can be adsorbed on and cover the surface of the metal, thusseparating it from the corroding setting. As the value of these parameters increase, so also the likely corrosion inhibition potentials of the molecules increase (Issa *et al.,* 2009).

The quantum indices calculated reveal that 6 benzyl oxy indole with E_{HOMO} and the E_{LUMO} at -6.08eV and -3.59eV, respectively and separation energy of 2.49eV this clearly marks 6 benzyl oxy indole a corrosion inhibitor with higher reactivity toward the metal surface as compared to 3 methyl indole with E_{HOMO} and the E_{LUMO}at -5.12eV and -0.09eV, respectively and separation energy of 5.03eV. This great inhibiting potential could also be attributed to the additional aromatic ring having sufficient π electrons thereby reducing the gap between theE_{HOMO} and the E_{LUMO}. Calculations show that its values for dipole moment, log p and polarizability are 6.48 debye, 2.08, 59.96 respectively which are well above that of 3 methyl indole, thus further enhancing its effectiveness towards inhibiting corrosion of low carbon steel in acidic medium.

6 benzyl oxy indole has a higher molecular volume, 236.34 $Å^3$ and molecular weight, 249.64amu, which most likely covers better the surface of the metal surface,thus suggest a higher value of inhibition efficiency for the organic molecule. These quantum chemical parameters results gotten are in agreement with the inhibition efficiency gotten for the studied molecules.

Furthermore some global reactivity parameters such as the electronegativity (χ), global chemical hardness(η), global softness(*S*) and Neucleophilicity index (□□ were calculated and presented in Table 4.13

Generallythe principle of HSAB predicts that hard acids favours co-ordinatingto hard bases and soft acids favours co-ordinating to soft bases(Obot and Obi-Egbedi, 2009). High HOMO-LUMO energy gap are often associated with hard molecules while alow HOMO-LUMO energy gap are associated with soft molecules. On the other hand, metal e.g low carbon steel are categorized as soft acids. Thus soft base molecules are

the most effective for metals in inhibiting corrosion (Masoud *et al.,* 2010). So, 6benzyl oxy indole is considered to have a better corrosion inhibition efficiency than 3 methyl indole judging from its values of lower energy gap, lower hardness and higher softness as presented Table 4.11(Ebenso *et al.,* 2010a). This observation is in agreement with the results gotten from experimental corrosion inhibition efficiencies.

The electrophilicity index ω, indicates the aptitude to which molecules can accept electrons.With reference to table 4.11, it shows that 6 benzyl oxy indole have a higher value of electrophilicity index. Thus, Fe atom can donate electrons to the anti-bonding orbitals of the inhibitor molecule to form back-donating bond. Also the inhibitor molecule can donate electrons to the vacant d orbitals of the Fe atom to form coordinate bond. This donation and back-donation actionsfurther enhances the adsorption of 6 benzyl indole onto the surface of the low carbon surface.

The Mulliken charge calculated as shown in Fig 4.31reveals that the nitrogen atom of the amine group and the oxygen atom could serve as active centres for the adsorption of the indole derivatives on the surface of the metal.

Molecular orbital calculations weredone to determine the coefficients of the HOMO and LUMO levels for the investigated indole derivatives as corrosion inhibitors to further throw more light on the mechanism of their adsorptions on the surface of the metal. Fig 4.32 shows the plot of the HOMO electronic density distribution for the indole derivatives. It is observed from calculations that the highest coefficients are found on the nitrogen atom, oxygen atom and the phenyl moiety which can be denoted as active adsorption sites of the inhibitors. The adsorption of 3 methyl indole took place via the lone pairs of electrons of the nitrogen (N_1) atom and π charges of the phenyl moiety and in the case of 6 benzyl oxy indole adsorption was effectedvia the lone pairs of electrons of the nitrogen (N_1) atom, oxygen atom, π charges of the phenyl moieties.

The LUMO plot is shown in Fig 4.33. The highest coefficient is localised on the nitrogen atom which can enable the back donation from the pyrrole group of the inhibitor to the metal. Thus increasing its adsorption on the surface of the metaland consequently the inhibition efficiency increases. The adsorption mechanism of the indole derivatives on the metal surface can be explained as electron donation from inhibitor molecule to the vacant d orbitals of the Fe atom and back donation from the

d-orbital of the Fe atom to the π antibonding counterpart of the organic molecule.In summary the results suggest that the indole derivatives are adsorbed on the surface of the metal via the highly electronegative nitrogen atom of the pyrrole group, the oxygen atom and the π charge of the phenyl moieties.

4.9 Weight loss measurements for ortho, meta and 4 nitro aniline (set B inhibitors)

Weight loss of low carbon steel, in mg, was measured at different time intervals in the absence and presence of different concentrations of the inhibitors studied. Figs. 4.39 - 4.62 show the weight loss-time curves obtained for low carbon steel in 1 mol/dm^3 HCl in the absence and presence of different concentrations of nitro aniline compounds at 303-333K. The figures show that the presence of the inhibitors falls significantly below that of the free acid. The corrosion rates (CR) and inhibition efficiency (%I.E) values calculated from gravimetric measurements for various concentrations of nitro aniline compounds in 1mol/dm^3 HClafter 8 hours immersion at 303-333 K are listed in Tables 4.1 1– 4.13. It is evident from these tables and figures that the corrosion rate reduced with rising inhibitor concentration but rose with increase in temperature. Tables 4.11- 4.13 also show that the inhibition efficiency (%I.E) rose with rising inhibitor concentration, getting to a maximum of 52.54 for 2 nitro aniline, 51.37 for 3 nitro aniline and 50.50 % for 4 nitro aniline respectively. This could be attributed to the adsorption of these compounds onto the surface of thelow carbon steel through non-bonding electron pairs of nitrogen and oxygen as well as the π-electrons of the aromatic rings. Similar observation has been reported (Adejoro *et al.,* 2016).

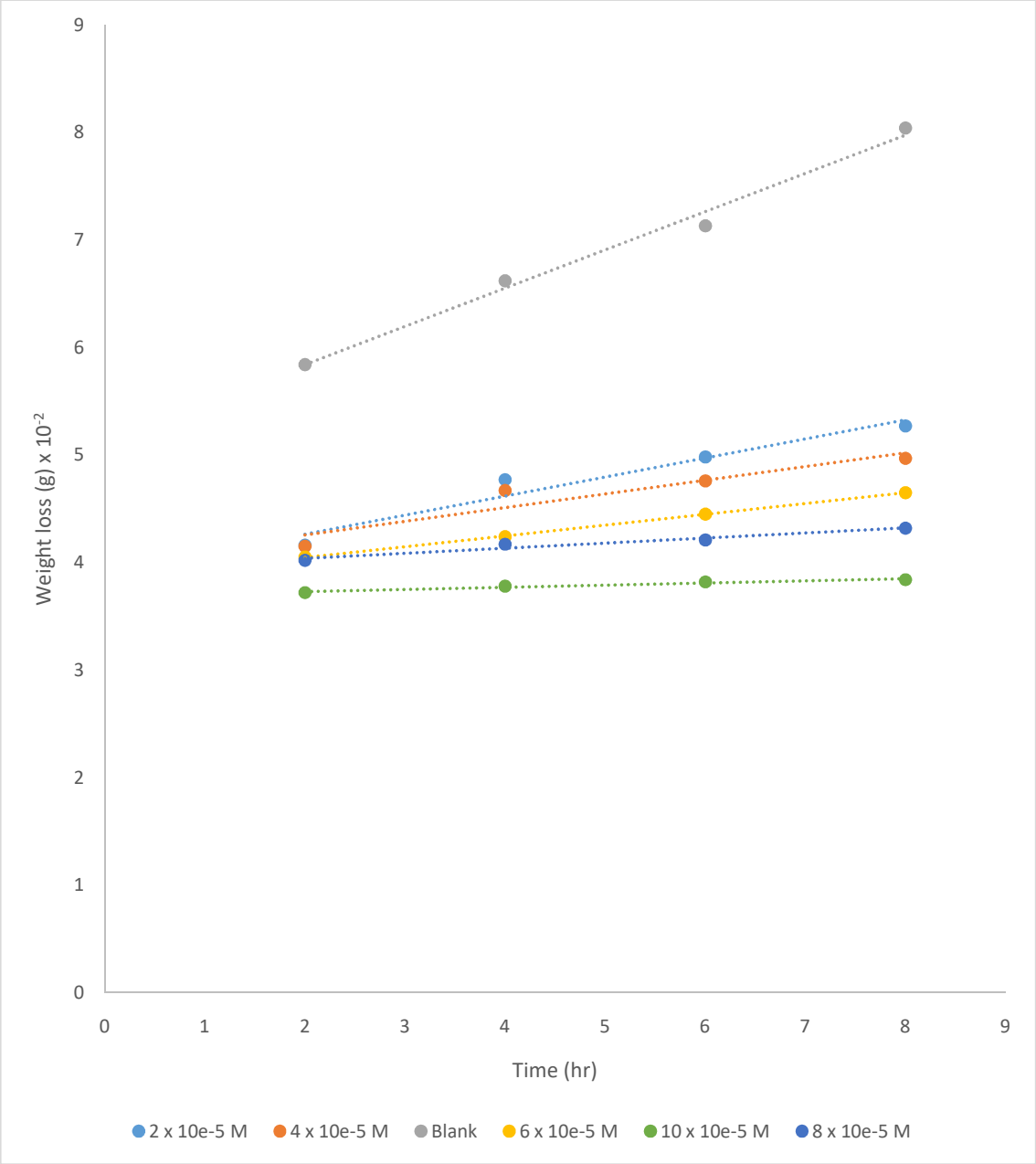

Fig 4.34: Weight loss versus time for low carbon steel corrosion in 1M HCl in the presence of various concentrations of 2 nitro aniline at 303K.

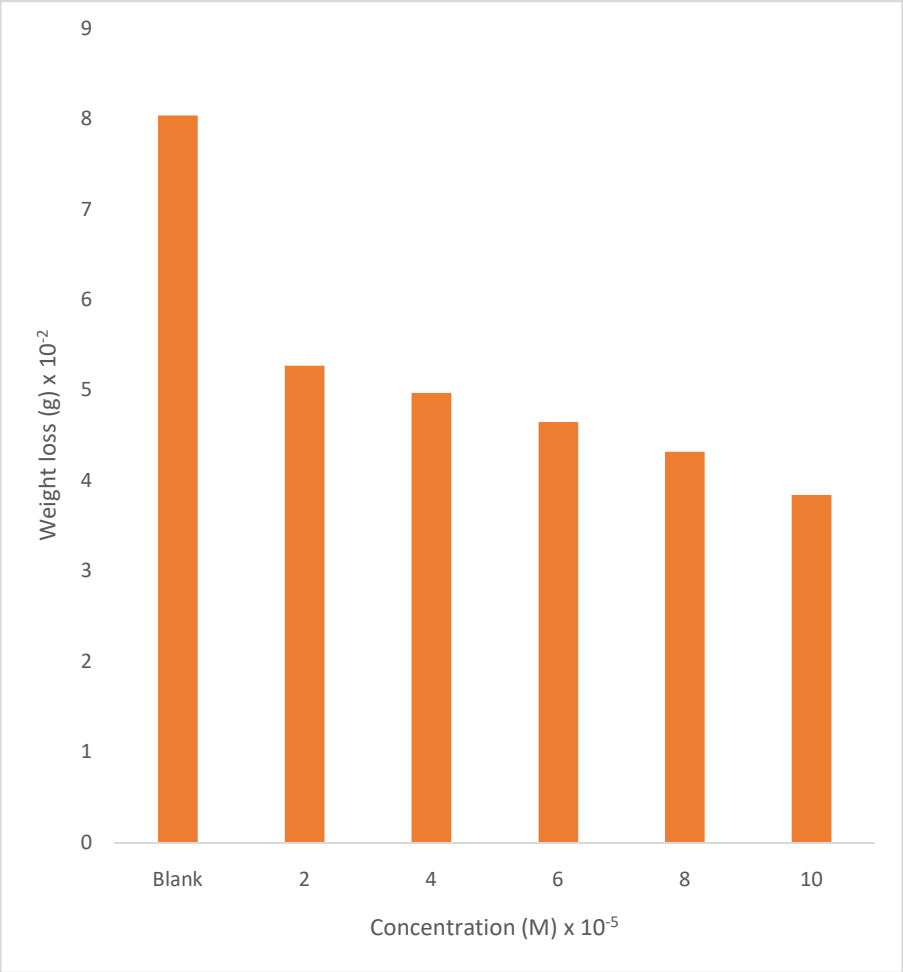

Fig 4.35: Weight loss values against different concentrations of 2 nitro aniline in 1 mol/dm^3 HClof low carbon steel corrosion after 8hours immersion time at 303K.

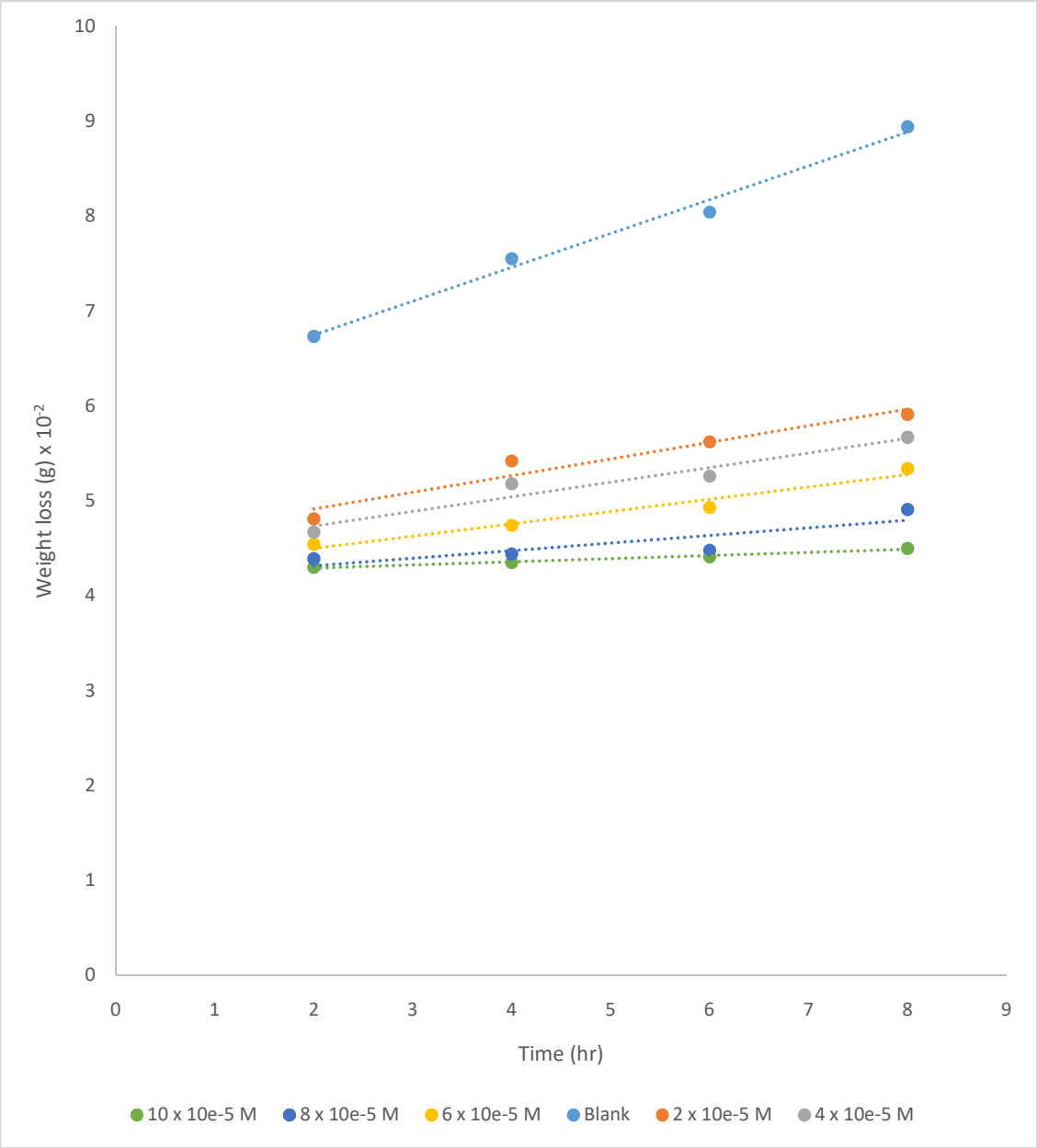

Fig 4.36: Weight loss versus time for low carbon steel corrosion in 1 mol/dm^{3}HCl in the presence of various concentrations of 2 nitro aniline at 313K.

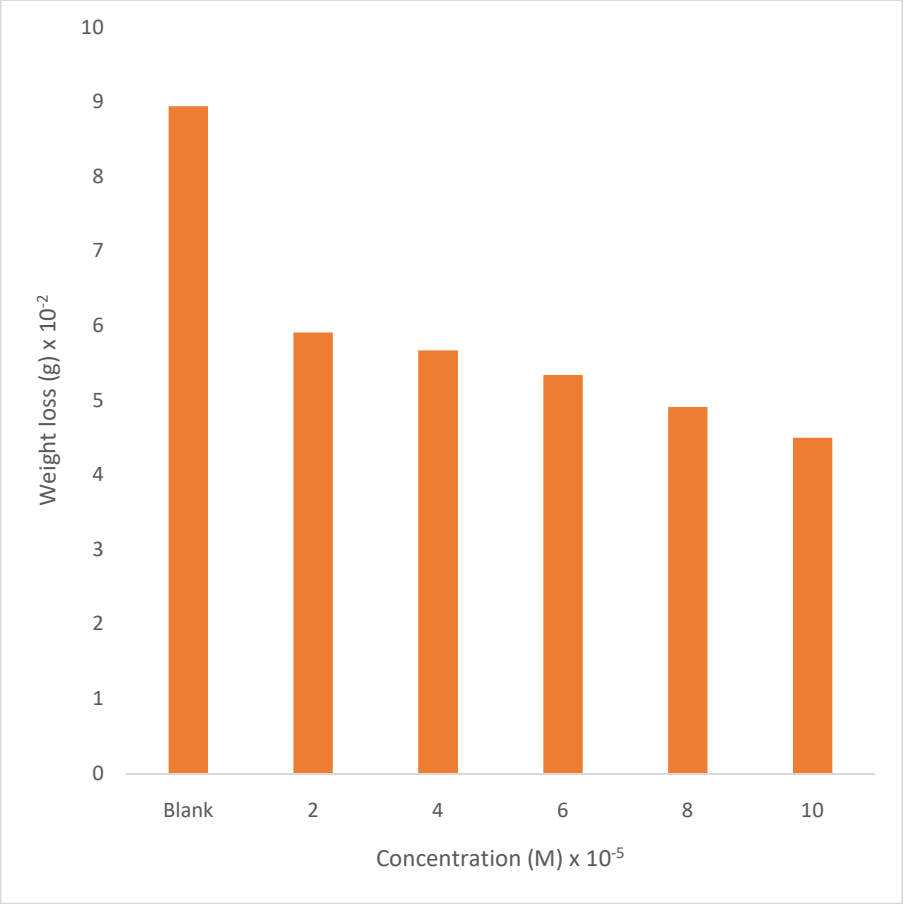

Fig 4.37: Weight loss values against different concentrations of 2 nitro aniline in 1 mol/dm^3 HClof low carbon steel corrosion after 8hours immersion time at 313K.

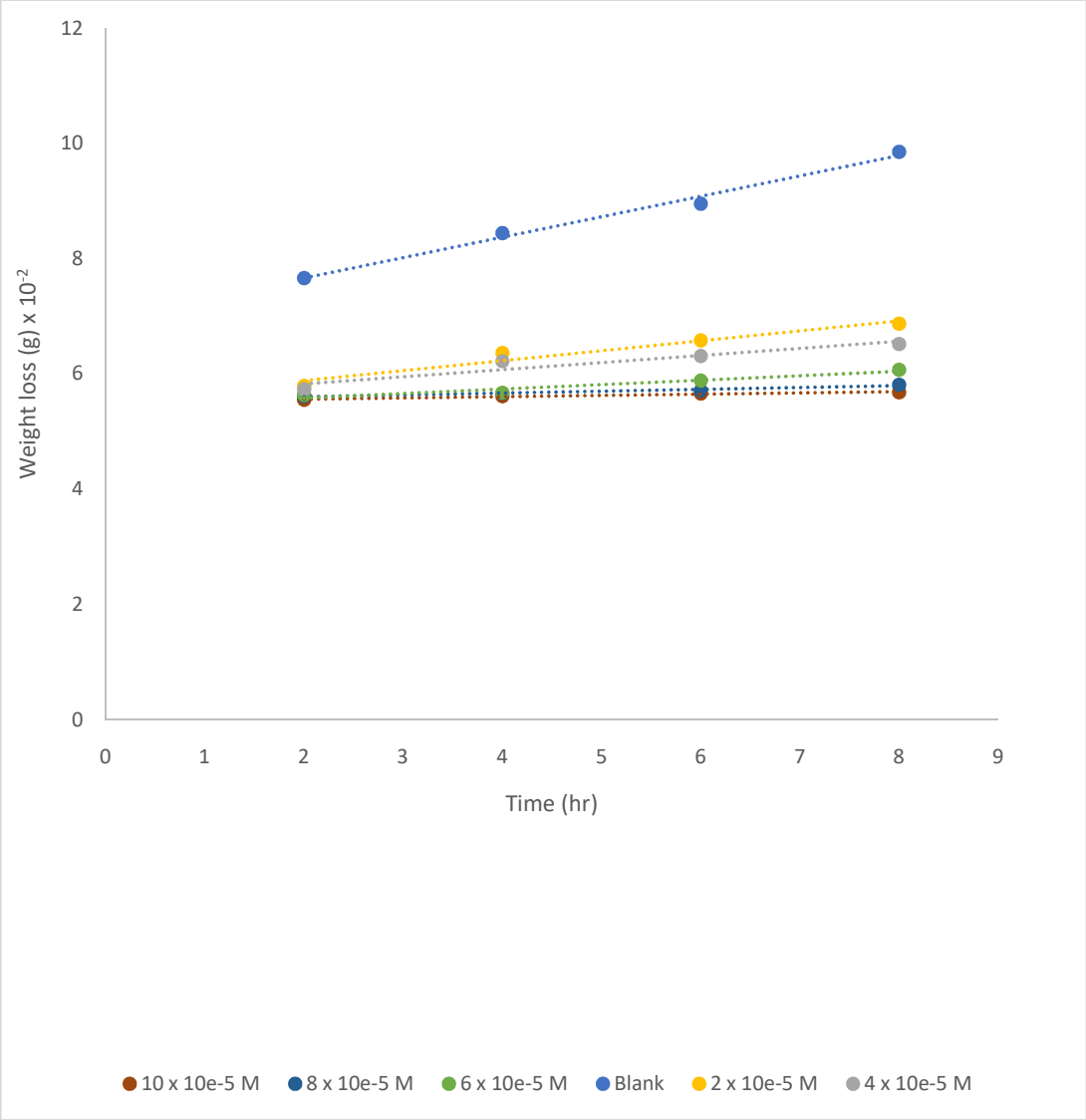

Fig 4.38: Weight loss versus time for low carbon steel corrosion in 1 mol/dm^{3}HCl in the presence of various concentrations of 2 nitro aniline at 323K.

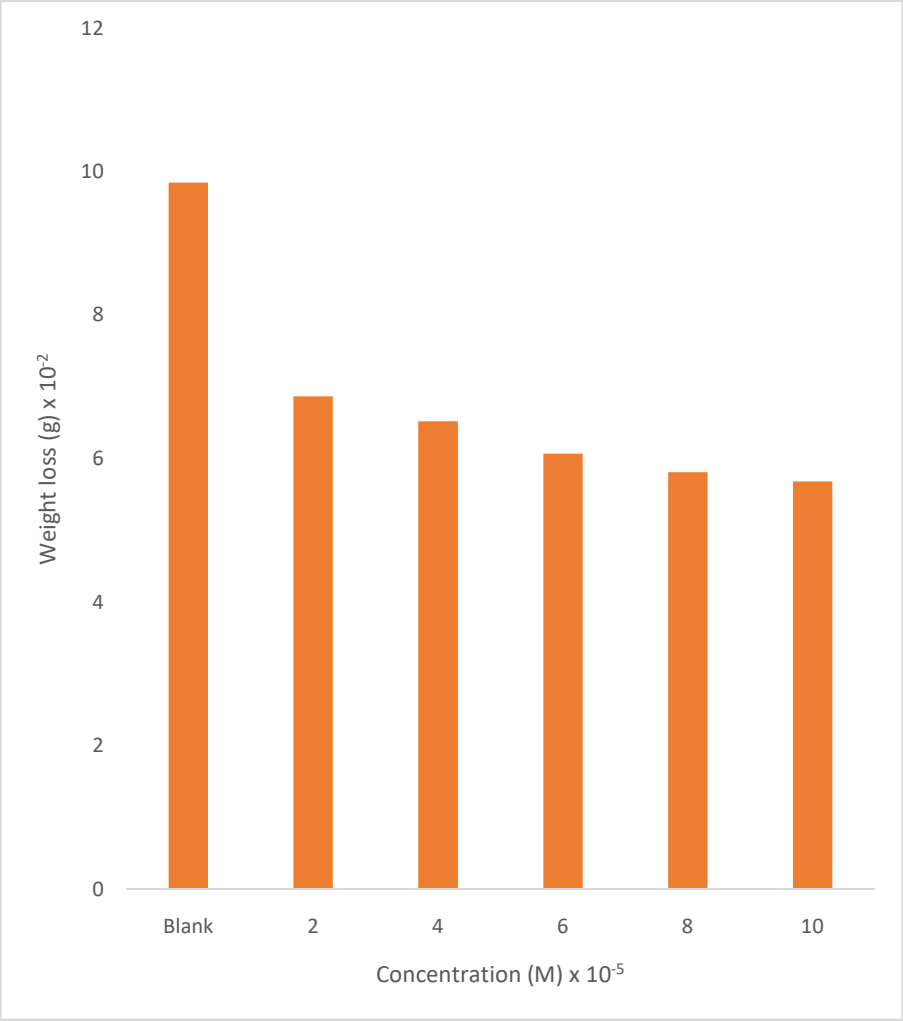

Fig 4.39: Weight loss values against different concentrations of 2 nitro aniline in 1 mol/dm^3 HClof low carbon steel corrosion after 8hours immersion time at 323K.

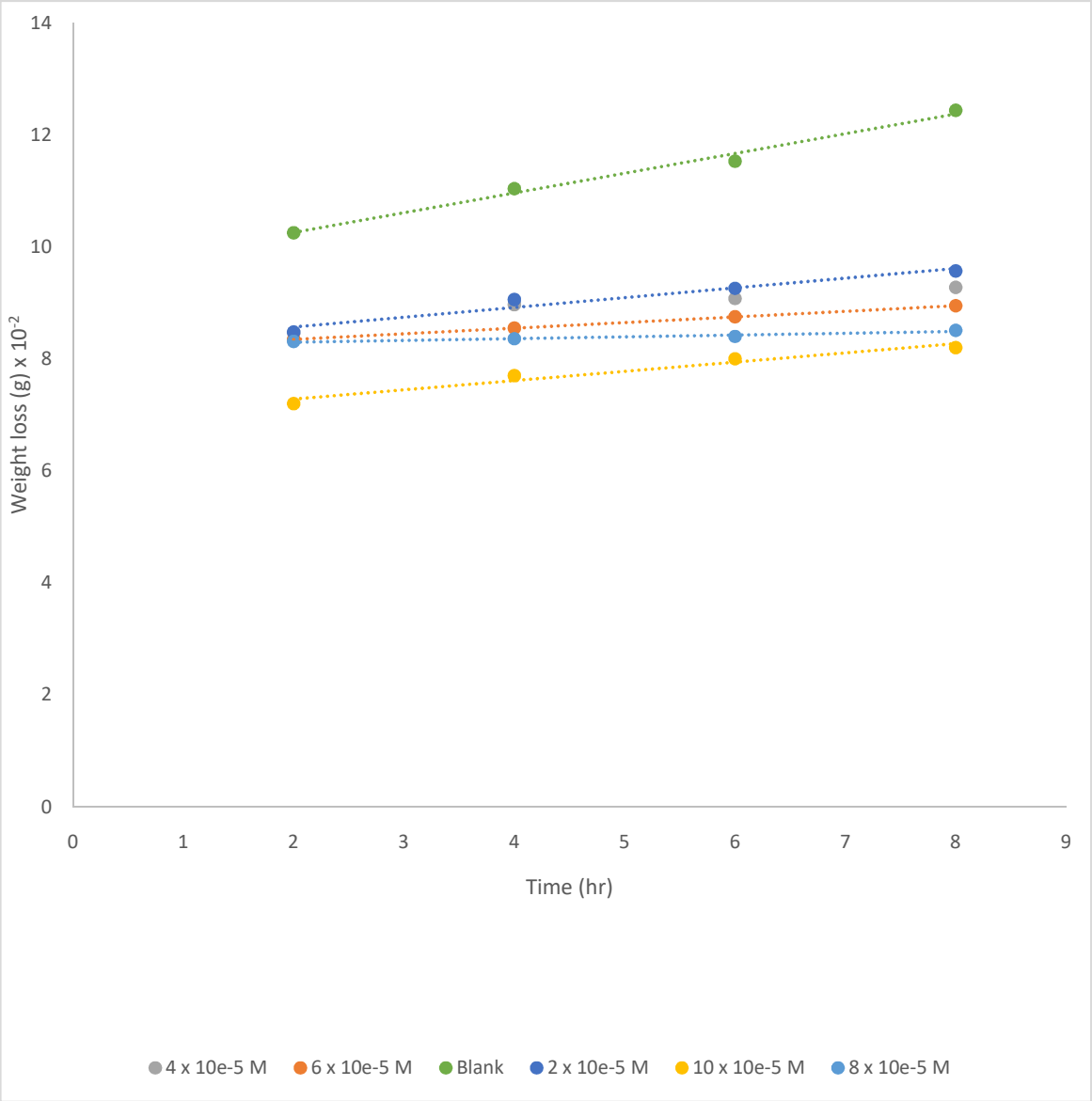

Fig 4.40: Weight loss versus time for low carbon steel corrosion in 1 mol/dm^{3}HCl in the presence of various concentrations of 2 nitro aniline at 333K.

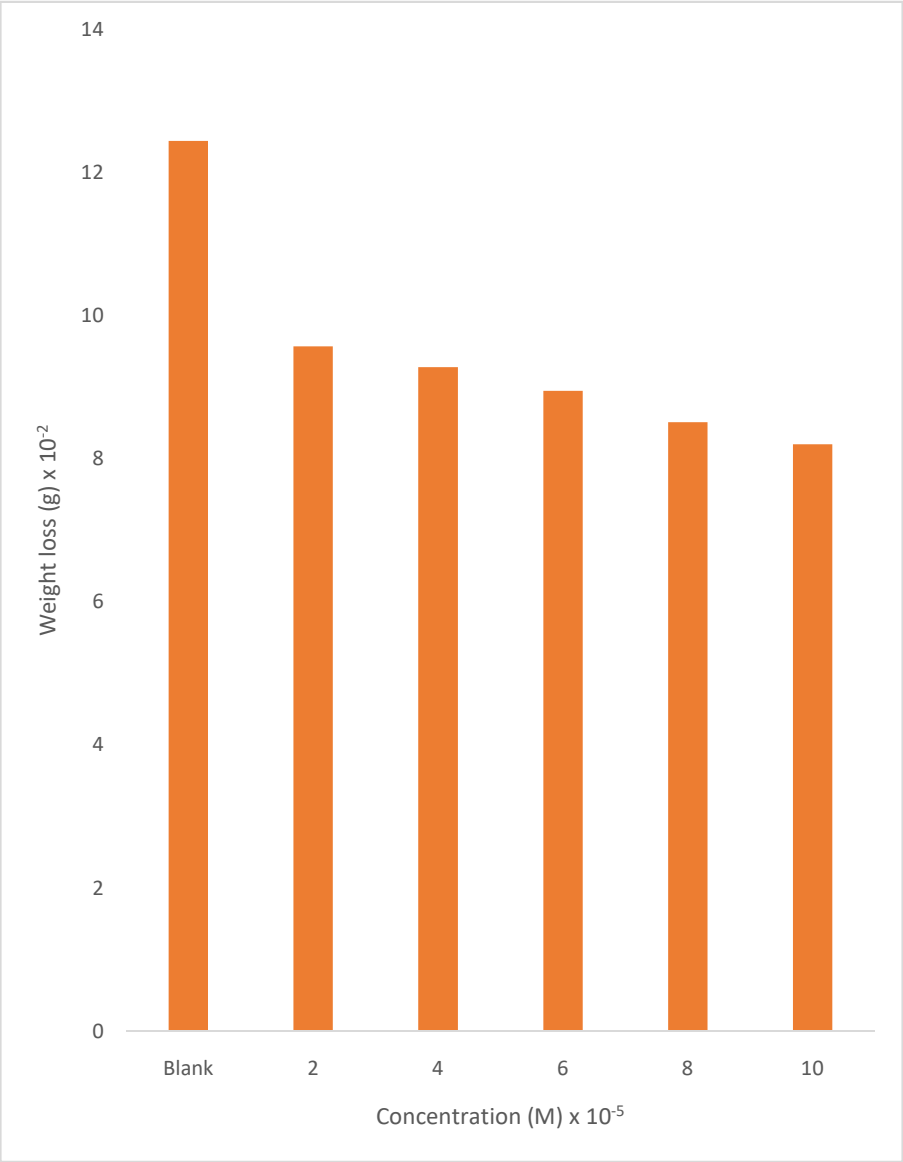

Fig 4.41: Weight loss values against different concentrations of 2 nitro aniline in 1 mol/dm^3 HClof low carbon steel corrosion after 8hours immersion time at 333K.

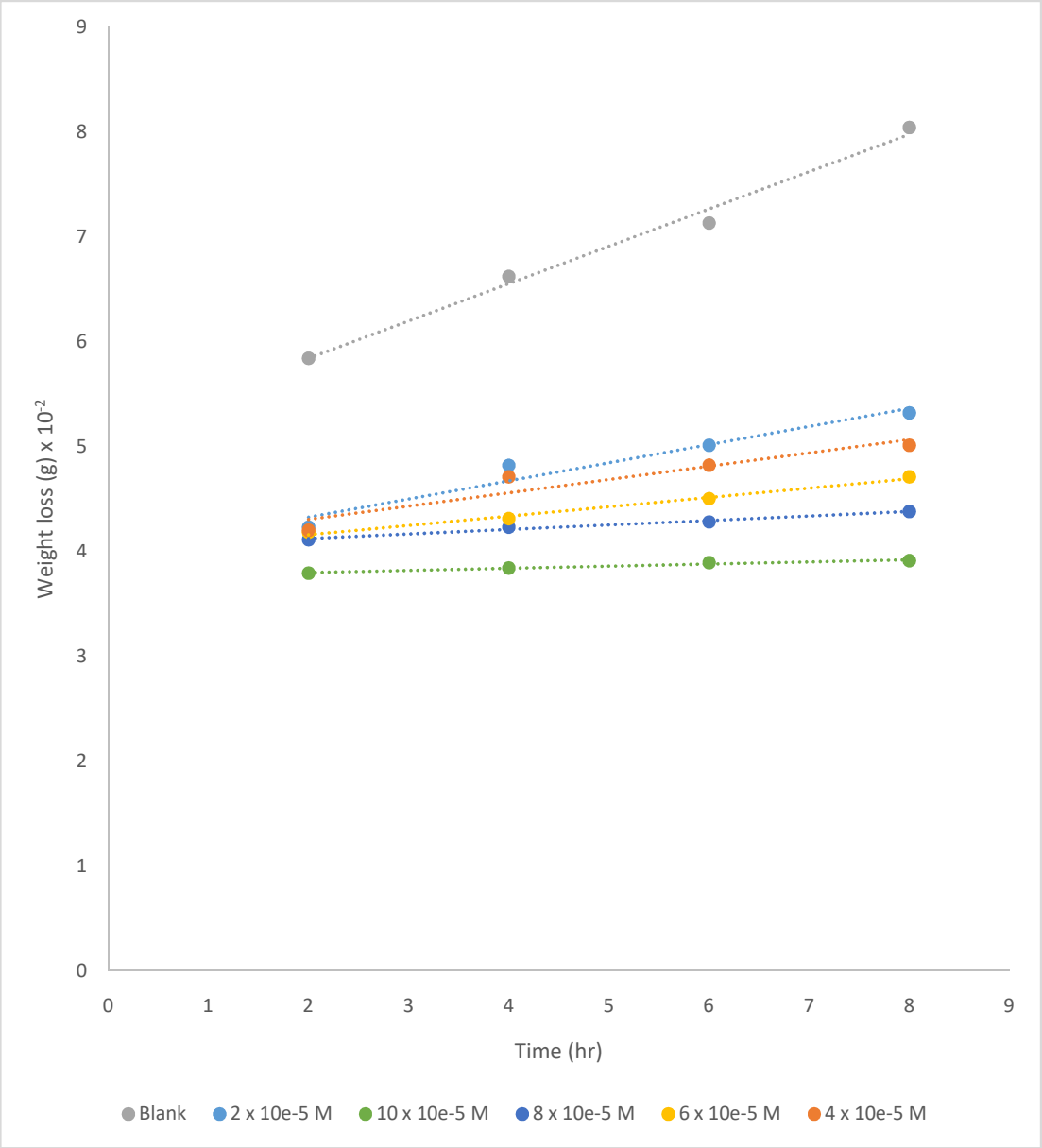

Fig 4.42: Weight loss vs time for low carbon steel corrosion in 1 mol/dm^{3}HCl in the presence of various concentrations of 3 nitro aniline at 303K.

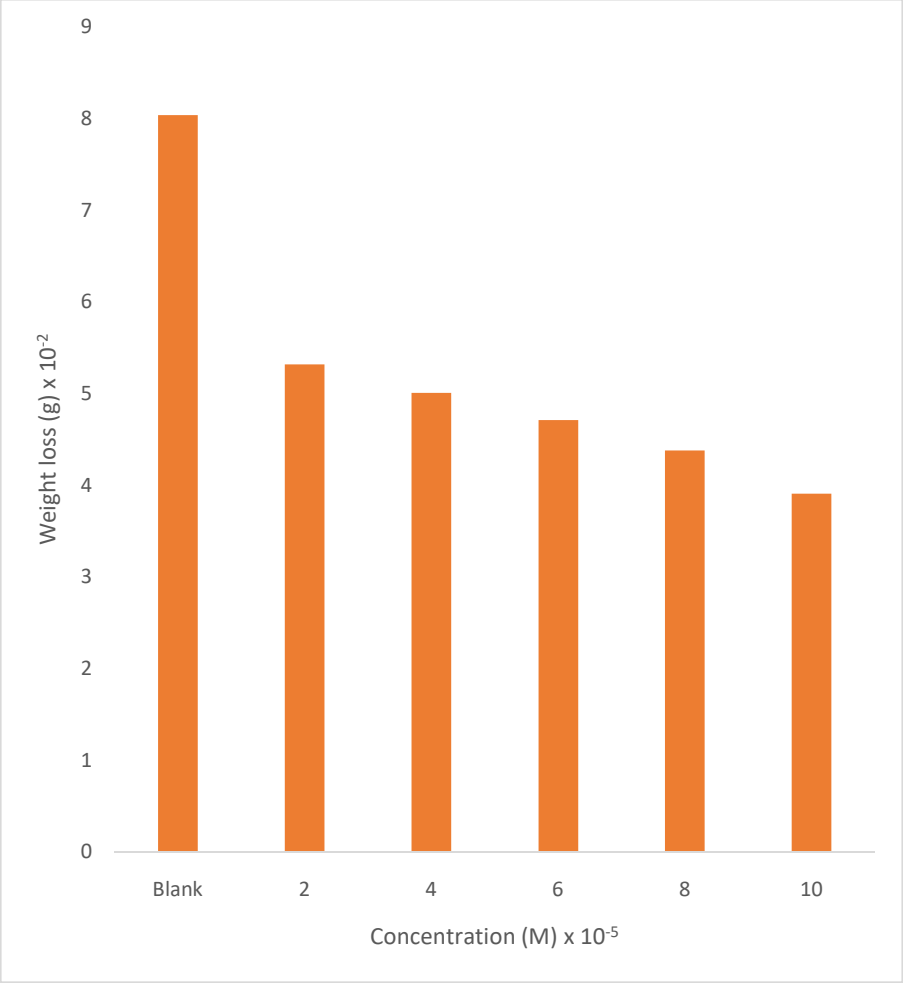

Fig 4.43: Weight loss values against different concentrations of 3 nitro aniline in 1 mol/dm^3 HClof low carbon steel corrosion after 8hours immersion time at 303K.

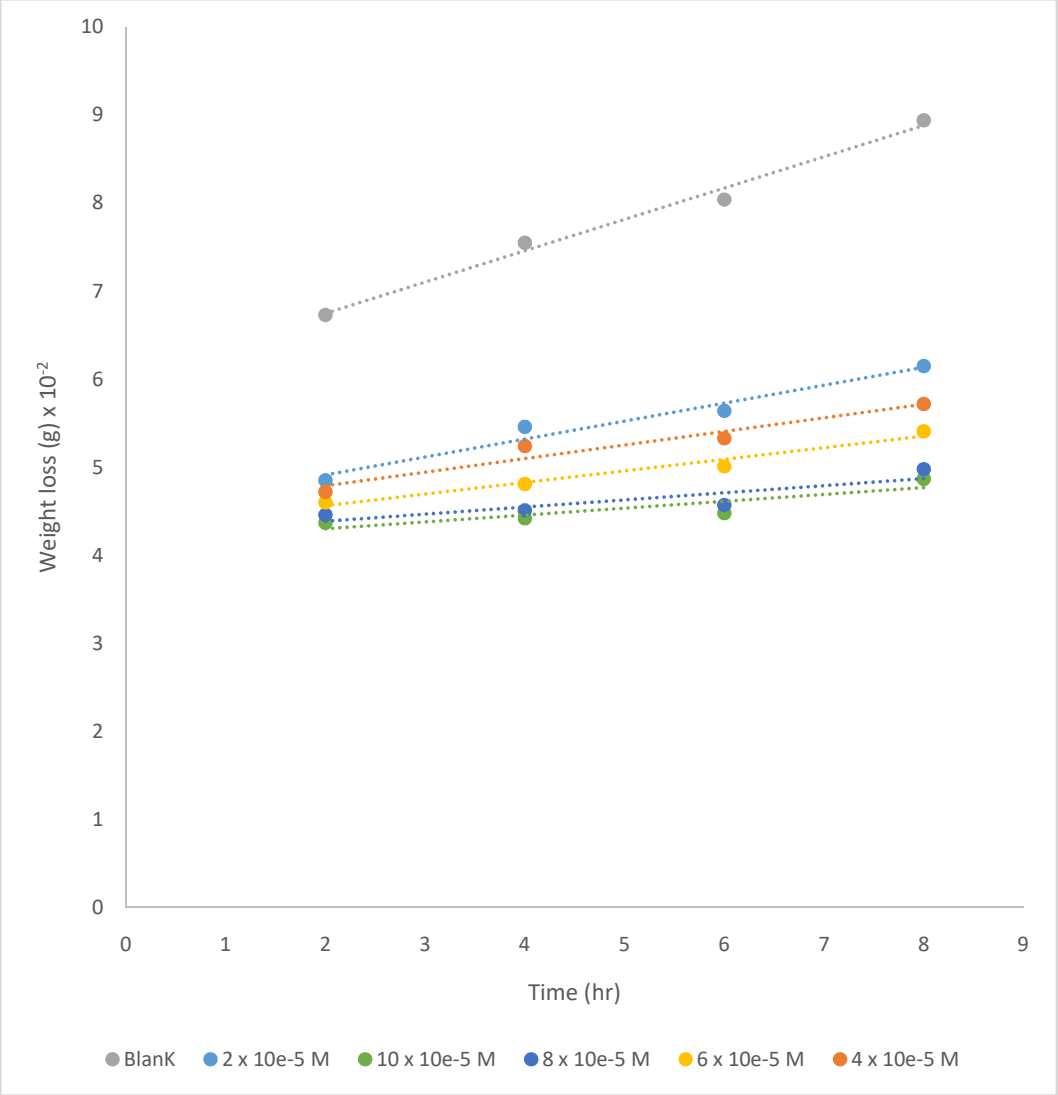

Fig 4.44: Weight loss vs time for low carbon steel corrosion in 1 mol/dm^{3}HCl in the presence of various concentrations of 3 nitro aniline at 313K.

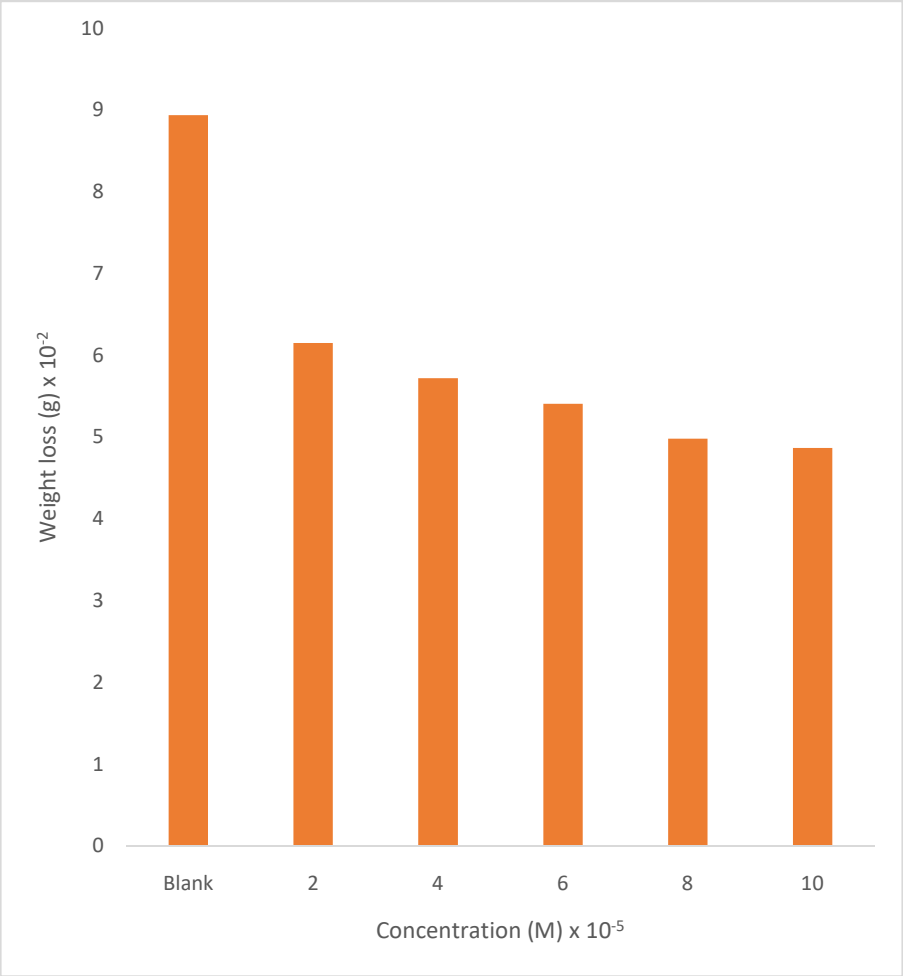

Fig 4.45: Weight loss values against different concentrations of 3 nitro aniline in 1 mol/dm^3 HClof low carbon steel corrosion after 8hours immersion time at 313K.

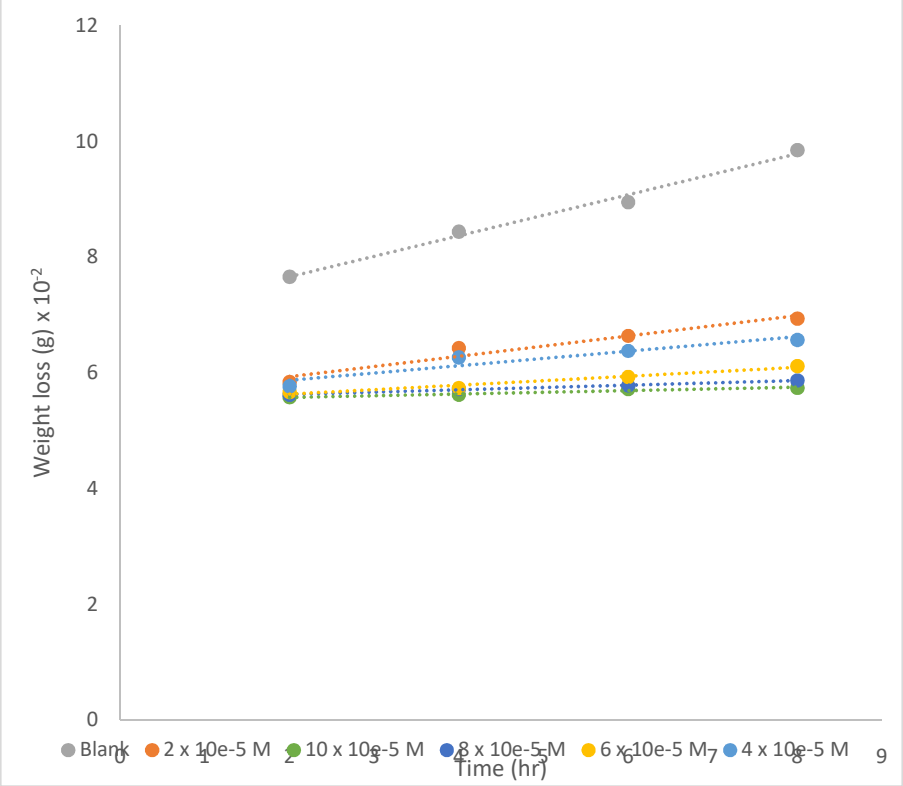

Fig 4.46: Weight loss vs time for low carbon steel corrosion in 1 mol/dm^{3}HCl in the presence of various concentrations of 3 nitro aniline at 323K.

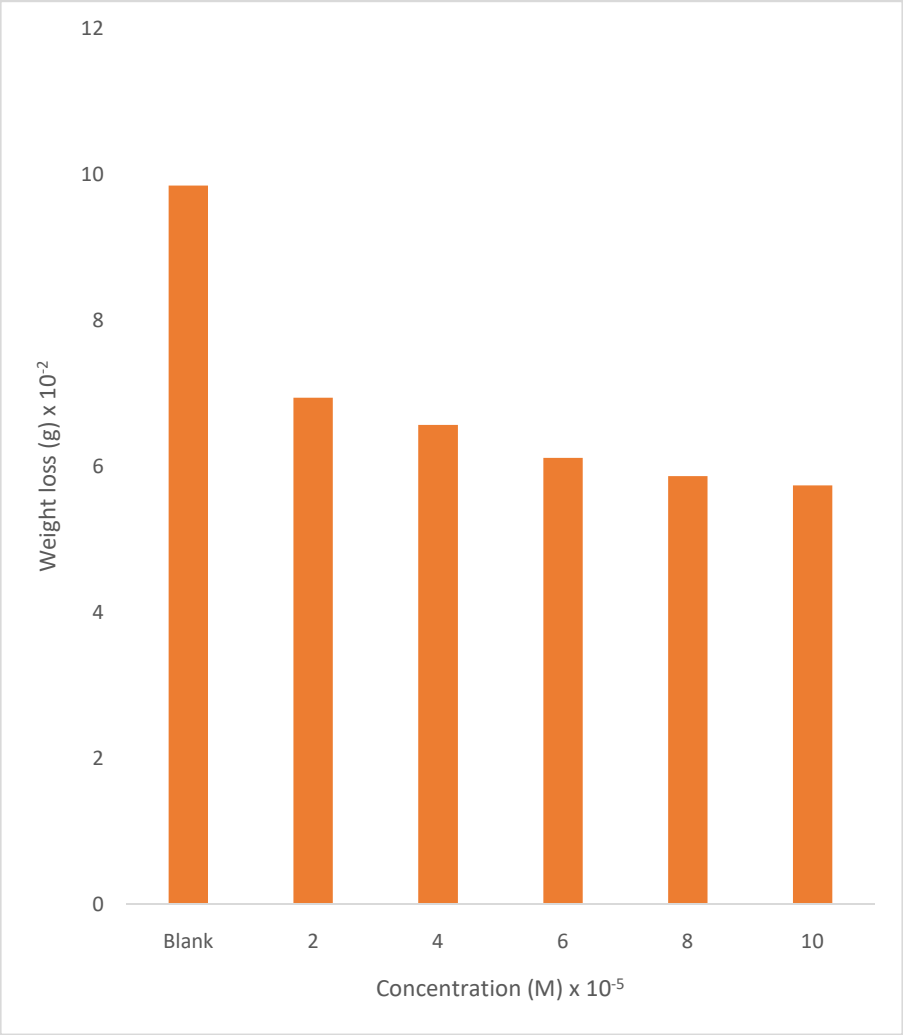

Fig 4.47: Weight loss values against different concentrations of 3 nitro aniline in 1 mol/dm^3 HClof low carbon steel corrosion after 8hours immersion time at 323K.

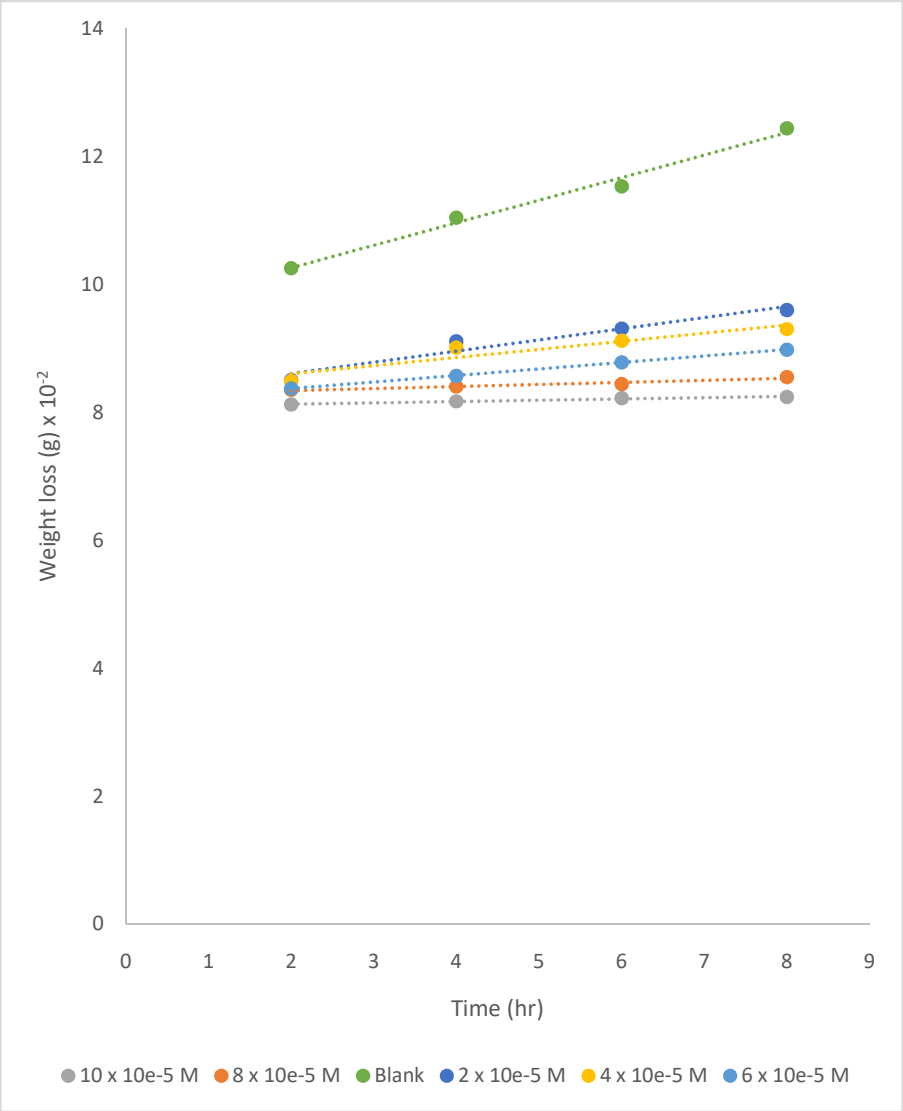

Fig 4.48: Weight loss vs time for low carbon steel corrosion in 1 mol/dm^{3}HCl in the presence of various concentrations of 3 nitro aniline at 333K.

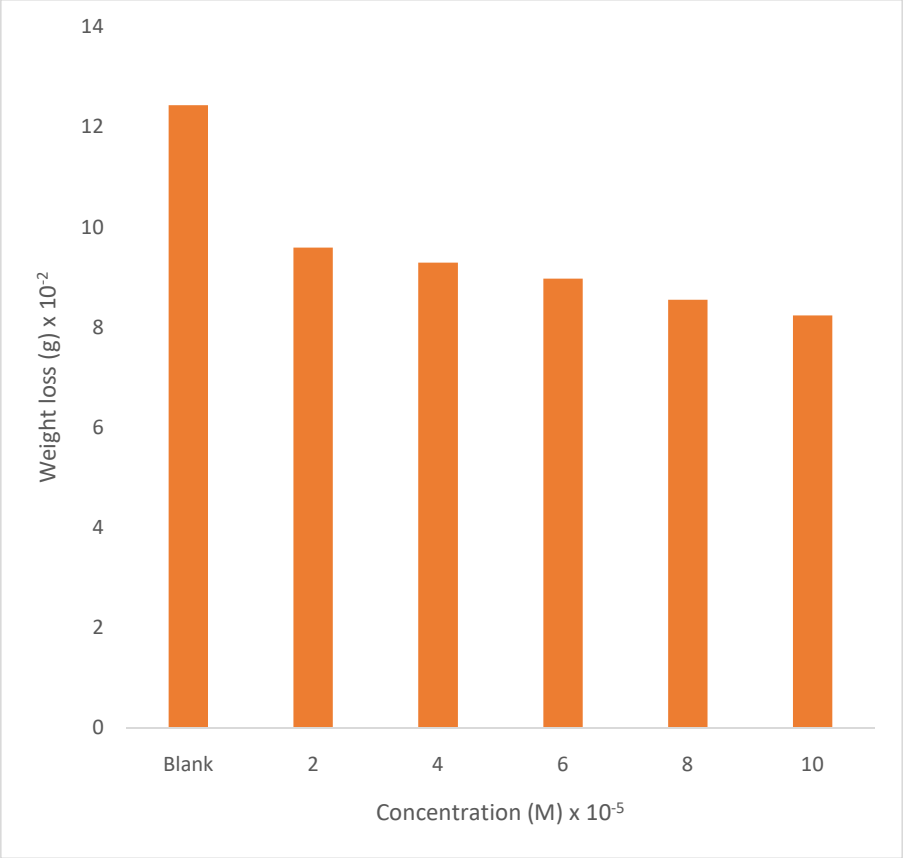

Fig 4.49: Weight loss values against different concentrations of 3 nitro aniline in 1 mol/dm^3 HClof low carbon steel corrosion after 8hours immersion time at 333K.

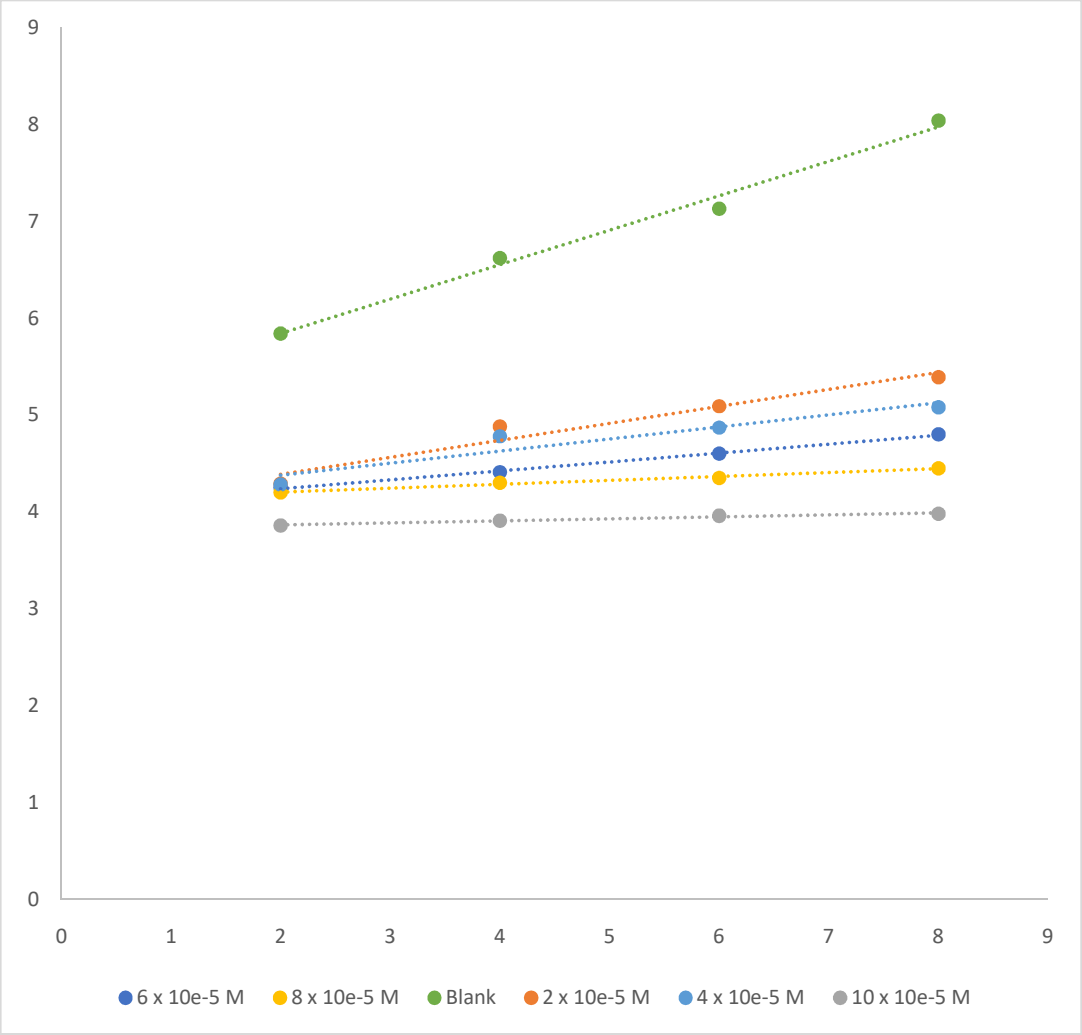

Fig 4.50: Weight loss vs time for low carbon steel corrosion in 1 mol/dm^3 HCl in the presence of various concentrations of 4 nitro aniline at 303.

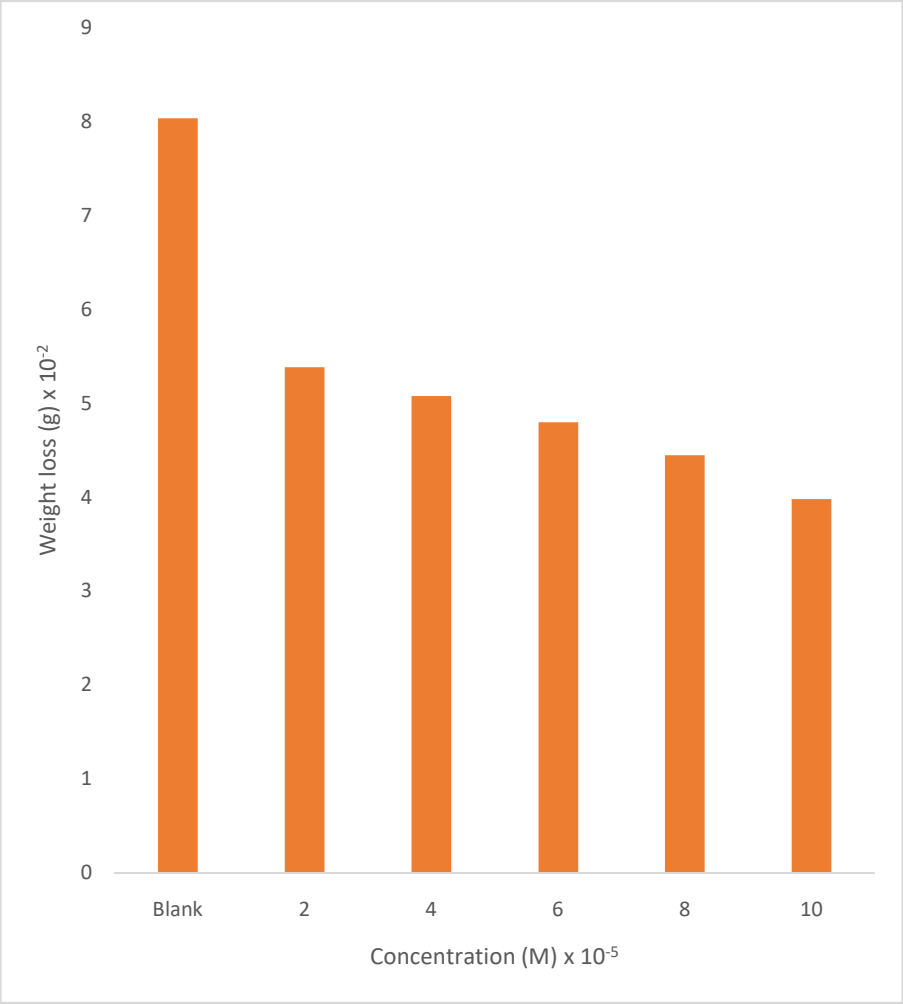

Fig 4.51: Weight loss values against different concentrations of 4 nitro aniline in 1 mol/dm^3 HClof low carbon steel corrosion after 8hours immersion time at 303K.

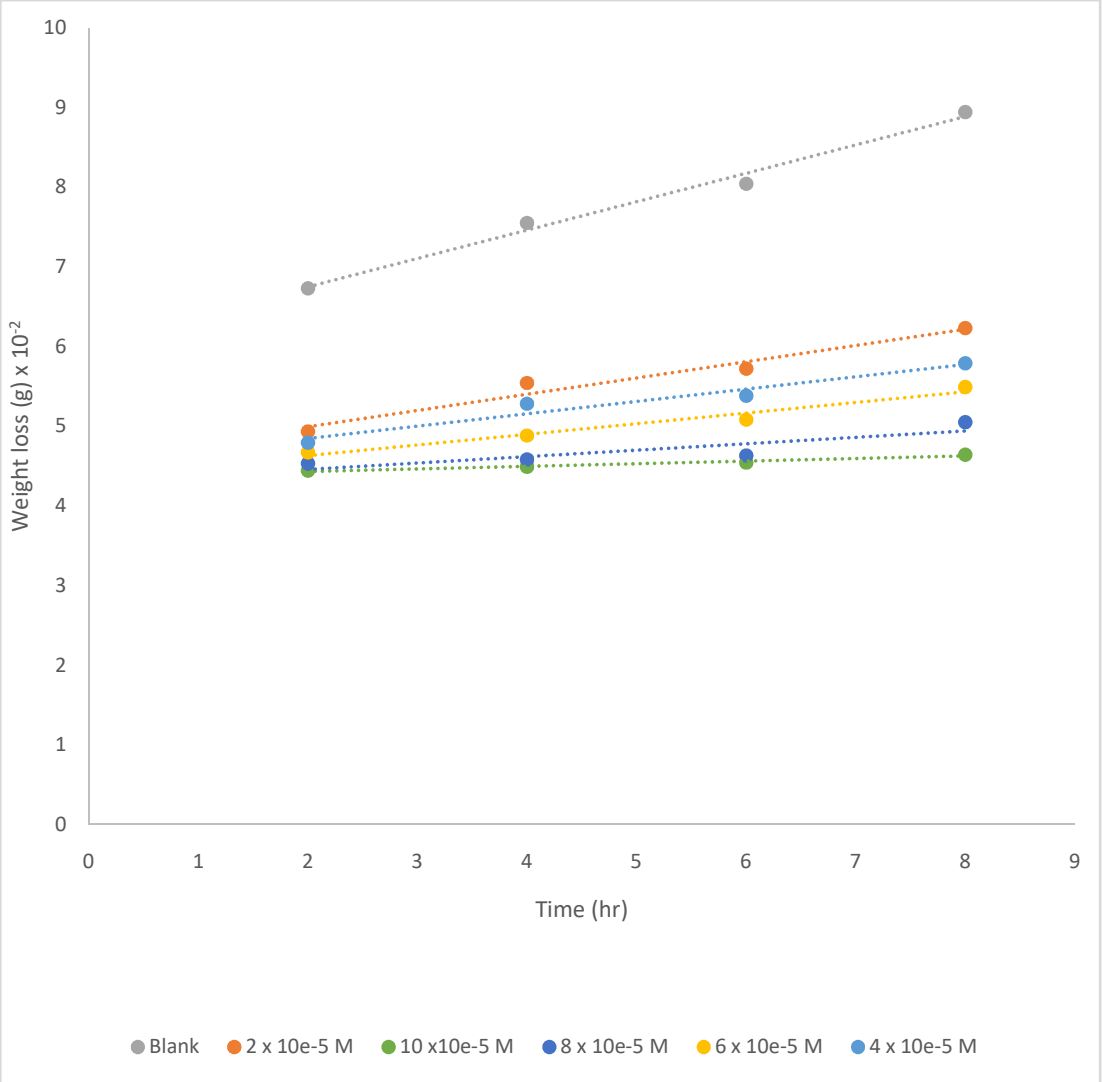

Fig 4.52: Weight loss vs time for low carbon steel corrosion in 1 mol/dm^{3}HCl in the presence of various concentrations of 4 nitro aniline at 313.

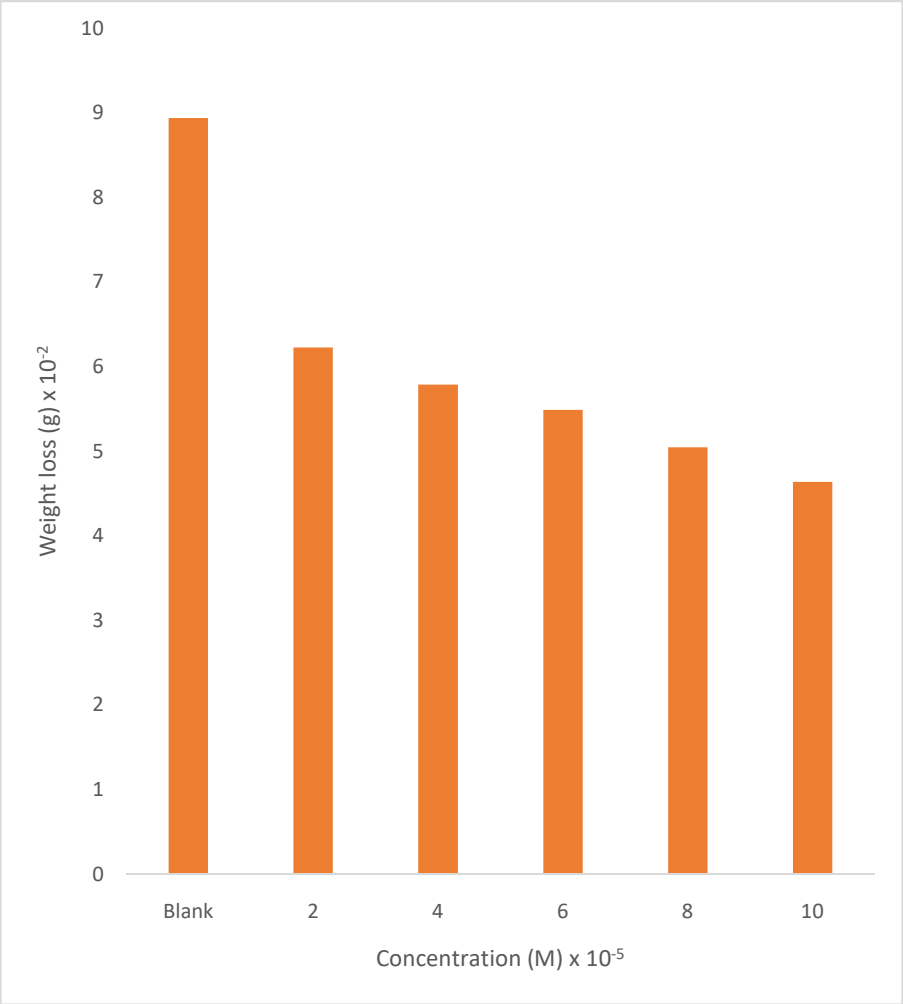

Fig 4.53: Weight loss values against different concentrations of 4 nitro aniline in 1 mol/dm^3 HClof low carbon steel corrosion after 8hours immersion time at 313K.

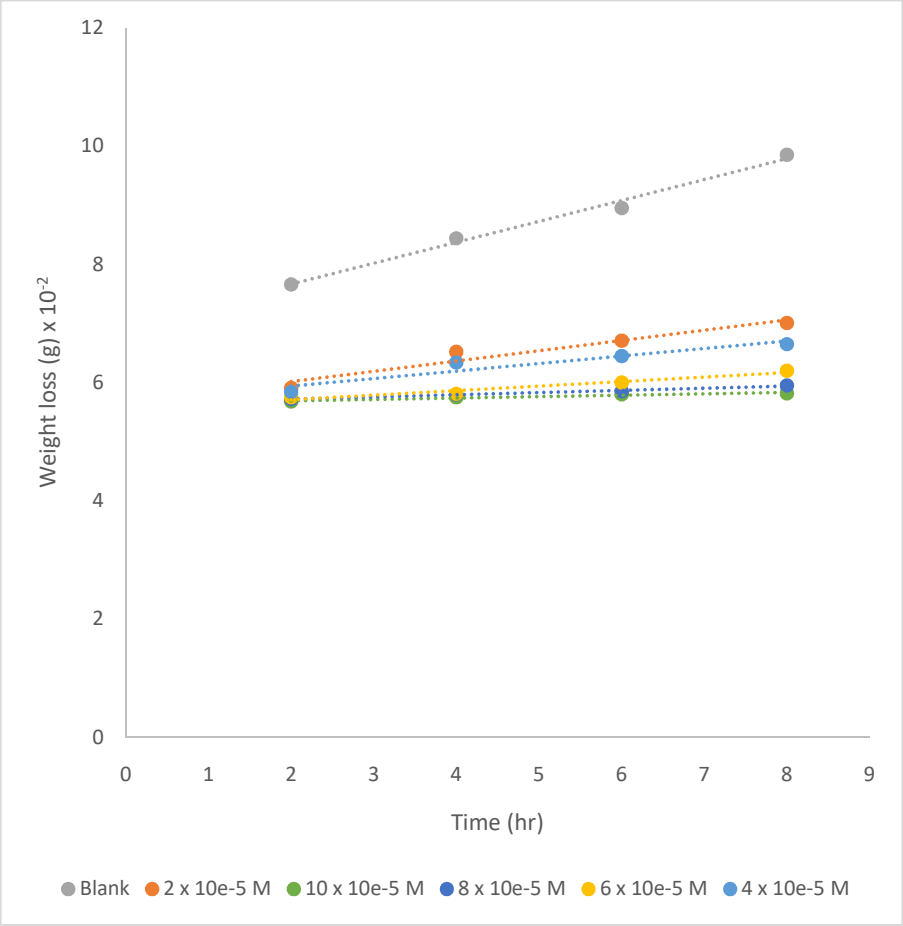

Fig 4.54: Weight loss vs time for low carbon steel corrosion in 1 mol/dm^{3}HCl in the presence of various concentrations of 4 nitro aniline at 323 K.

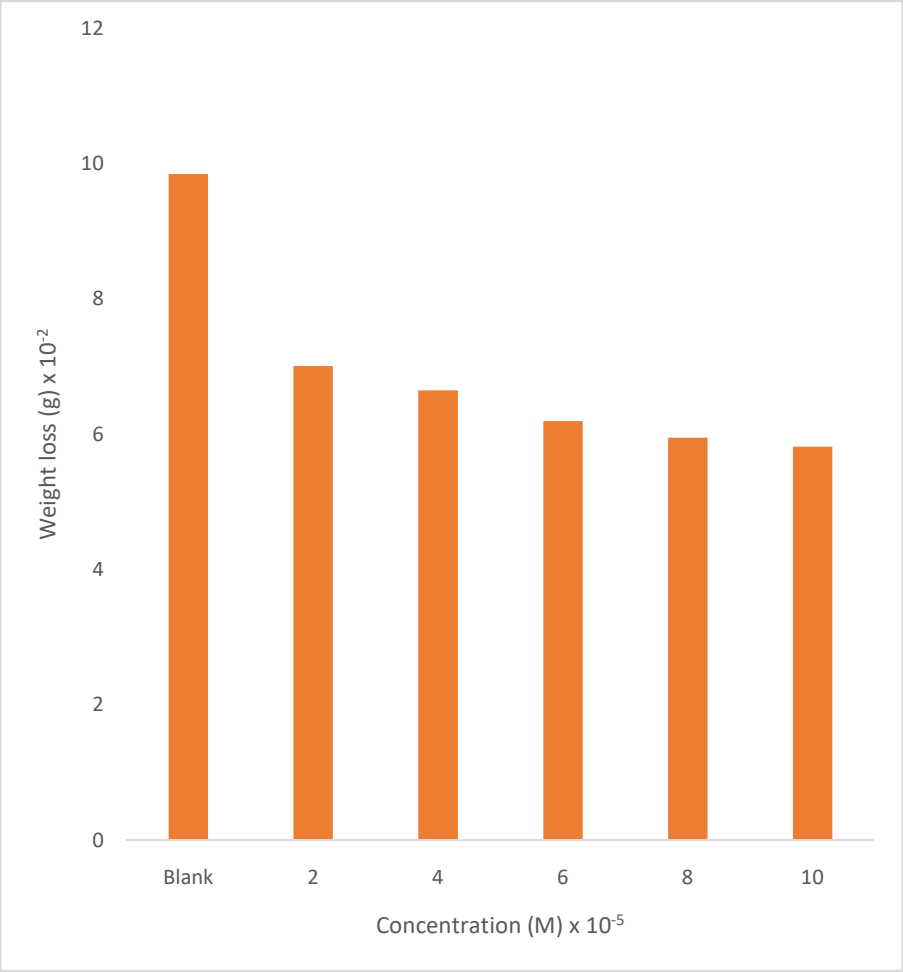

Fig 4.55: Weight loss values against different concentrations of 4 nitro aniline in 1 mol/dm^3 HClof low carbon steel corrosion after 8hours immersion time at 323K.

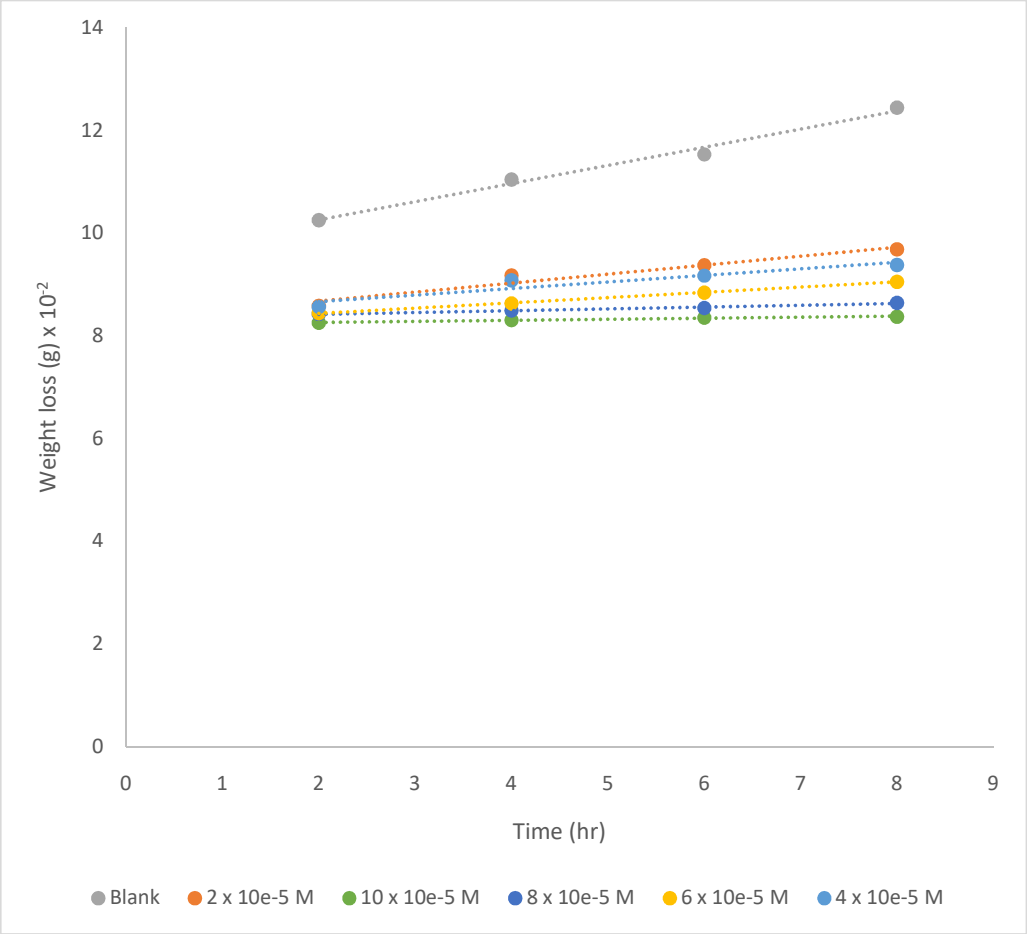

Fig 4.56: Weight loss vs time for low carbon steel corrosion in 1M HCl in the presence of various concentrations of 4 nitro aniline at 333 K.

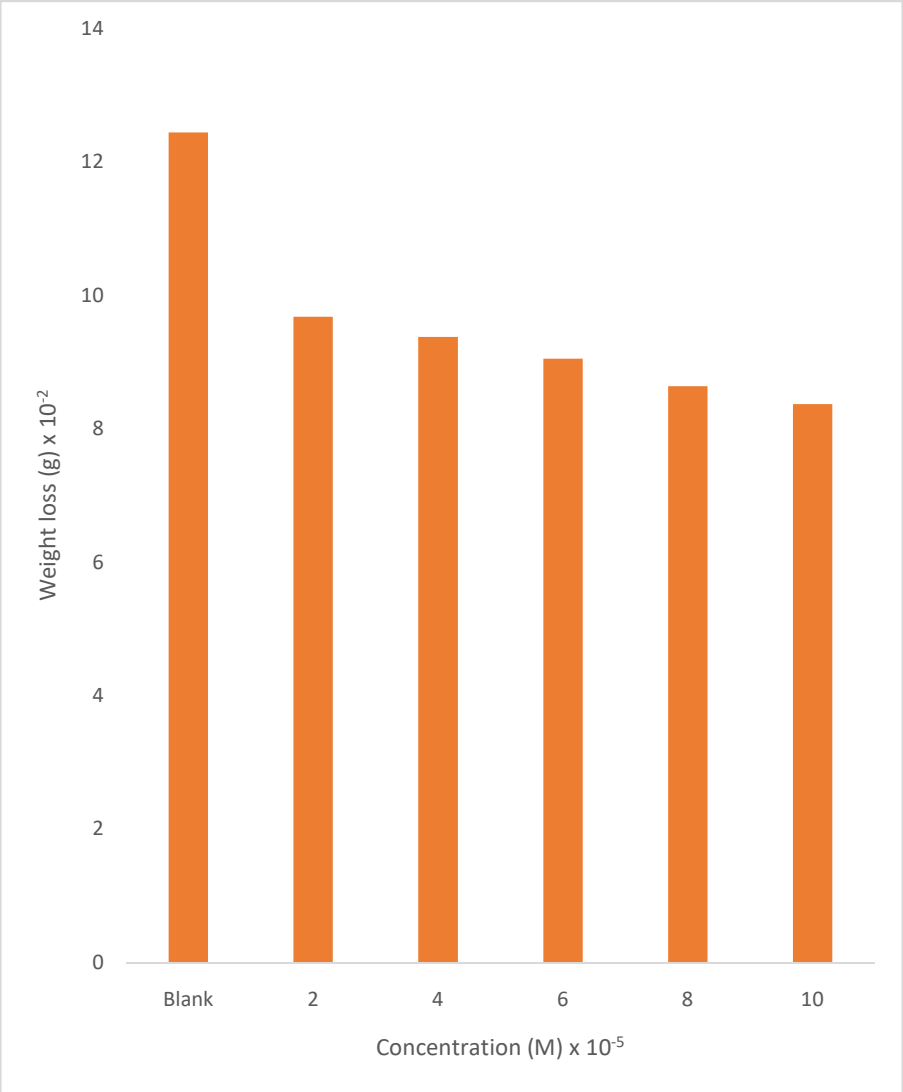

Fig 4.57: Weight loss values against different concentrations of 4 nitro aniline in 1 mol/dm^3 HClof low carbon steel corrosion after 8hours immersion time at 333K.

Table 4.12: Inhibition efficiencies (I.E%) and corrosion rates for low carbon steel in 1 mol/dm^3 HCl in the presence and absence of various concentrations of otho nitro aniline at various temperatures viagravimetric technique.

Concentration	**Corrosion Rate (Mg Cm^{-2}h^{-1}) x 10^{-3}**				**Inhibition Efficiency (%)**			
mol/dm^3	303K	313K	323K	333K	303K	313K	323K	333K
Blank	7.18	7.98	8.79	11.11	-	-	-	-
2 x 10^{-5}	4.71	5.28	6.13	8.54	34.45	33.89	30.25	23.07
4 x 10^{-5}	4.44	5.06	5.82	8.23	38.18	36.58	33.81	25.40
6 x 10^{-5}	4.15	4.77	5.42	7.99	42.16	40.27	38.38	28.05
8 x 10^{-5}	3.86	4.38	5.19	7.60	46.27	45.08	41.02	31.59
10 x 10^{-5}	3.43	4.03	5.07	7.32	52.24	49.66	42.36	34.08

Table 4.13: Inhibition efficiencies (I.E%) and corrosion rates for low carbon steel in 1 mol/dm^3 HCl in the presence and absence of various concentrations of3 nitro aniline at various temperatures viagravimetric technique.

Concentration	**Corrosion Rate (Mg Cm^{-2}h^{-1}) x 10^{-3}**				**Inhibition Efficiency (%)**			
mol/dm^3	303K	313K	323K	333K	303K	313K	323K	333K
Blank	7.18	7.98	8.79	11.11	-	-	-	-
2 x 10^{-5}	4.75	5.49	6.20	8.57	33.83	31.21	29.54	22.83
4 x 10^{-5}	4.47	5.11	5.87	8.30	37.69	36.01	33.30	25.24
6 x 10^{-5}	4.21	4.83	5.46	8.02	41.42	39.49	37.87	27.81
8 x 10^{-5}	3.91	4.45	5.24	7.63	45.52	44.30	40.41	31.27
10 x 10^{-5}	3.49	4.08	5.13	7.36	51.37	48.88	41.73	33.76

Table 4.14: Inhibition efficiencies (I.E%) and corrosion rates for low carbon steel in 1 mol/dm^3 HCl in the presence and absence of various concentrations of4 nitro aniline at various temperatures via gravimetric technique.

Concentration	**Corrosion Rate (Mg $Cm^{-2}h^{-1}$) x 10^{-3}**				**Inhibition Efficiency (%)**			
mol/dm^3	303K	313K	323K	333K	303K	313K	323K	333K
Blank	7.18	7.98	8.79	11.11	-	-	-	-
2 x 10^{-5}	4.81	5.56	6.26	8.64	32.96	30.31	28.83	22.19
4 x 10^{-5}	4.54	5.17	5.94	8.38	36.82	35.23	32.49	24.60
6 x 10^{-5}	4.29	4.90	5.54	8.08	40.30	38.59	37.06	27.25
8 x 10^{-5}	3.97	4.51	5.31	7.71	44.65	43.51	39.56	30.55
10 x 10^{-5}	3.55	4.14	5.20	7.47	50.50	48.10	40.91	32.72

4.10 Effect of temperature and concentration on corrosion inhibition of nitro aniline compounds on low carbon steel.

The corrosion rate of low carbon steel in the absence and presence of nitro aniline compounds at 303 – 333K was investigated by means of gravimetric method. Table 4.12, Table 4.13 and Table 4.14reveals the calculated values of corrosion rates ($mgcm^{-2}h^{-1}$), inhibition efficiency (IE%) and the degree of surface coverage (Ɵ) for dissolution of low carbon steel in 1 mol/dm^3 HCl in the presence and absence ofnitro aniline compounds. It is obvious from the tables that percentage inhibition efficiency increases with rise in concentration of inhibitors but decreases with rise in temperature. The reduction in inhibition efficiency with rise in temperature is indicative of physical adsorption mechanism (Physiosorption) and may be due to increase in the solubility of the protective film of any of the reaction products precipitated on the surface of the low carbon steel that may otherwise impede the corrosion reaction. Another possible cause could be attributed to a likely shift in the Adsorption-desorption equilibrium towards desorption of adsorbed inhibitor due to an increase in the kinetic energy of the molecules of the solution. Thus, as the temperature rises, the sum of adsorbed molecules reduces or desorption rate of the inhibitors from the low carbon steel surface increases, thus, leading to a reduction in the inhibition efficiency (Adejoro *et al.,* 2015).

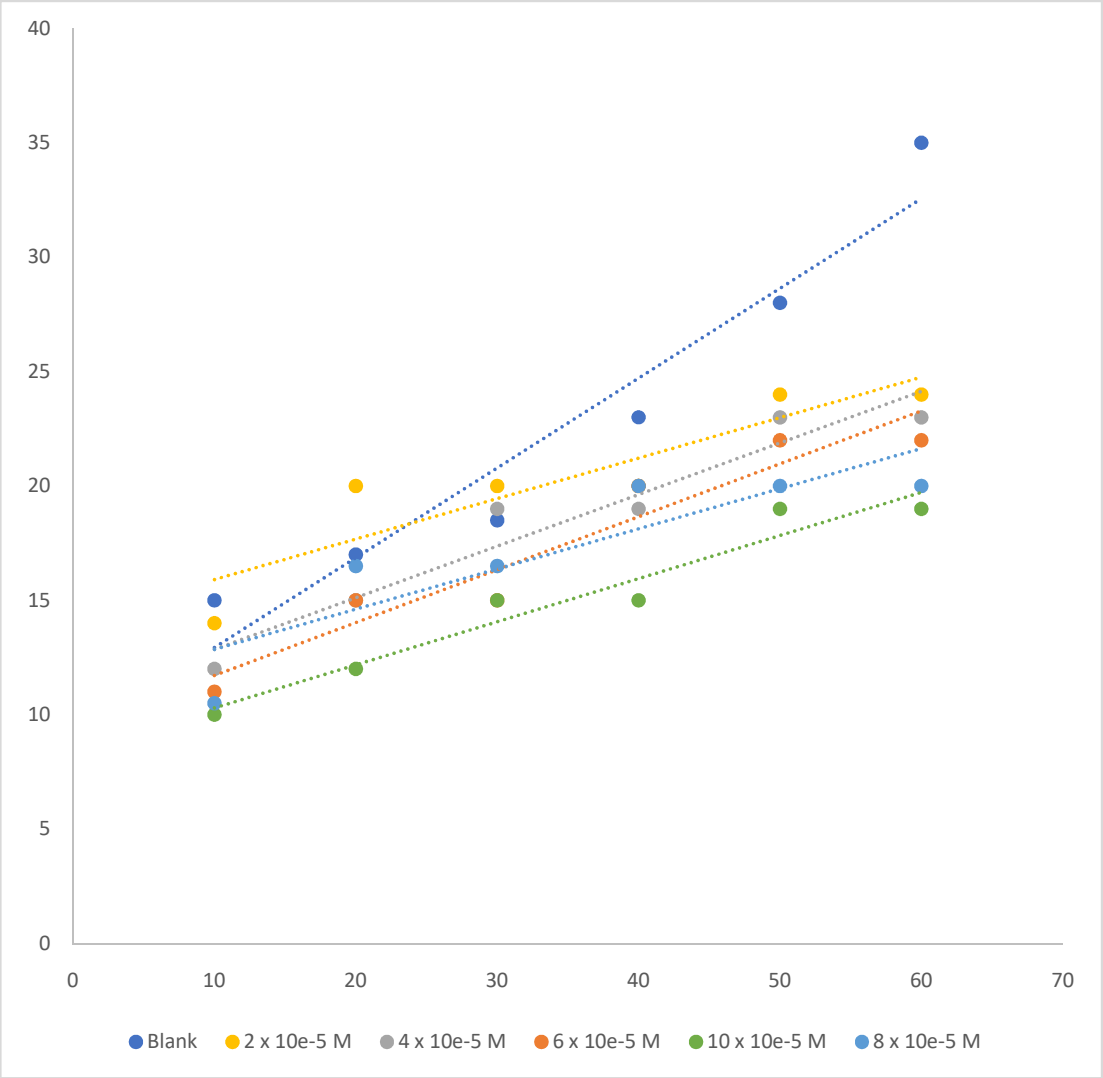

Fig 4.58: Volume of hydrogen gas liberated vs time for low carbon steel corrosion in 1 mol/dm^{3}HCl in the presence of various concentrations of 2 nitro aniline at 303K.

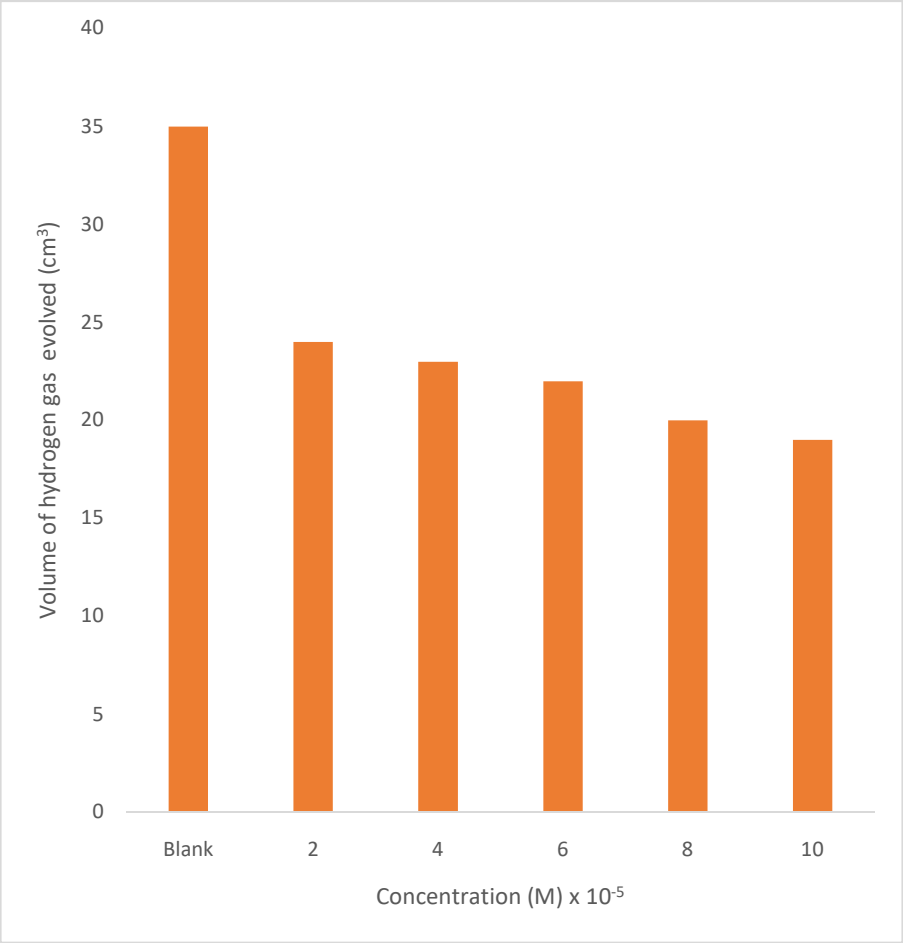

Fig 4.59: Volume of hydrogen gas liberated against different concentrations of 2 nitro aniline in 1 mol/dm^3 HClof low carbon steel corrosion after 60 minutes reaction time at 303K.

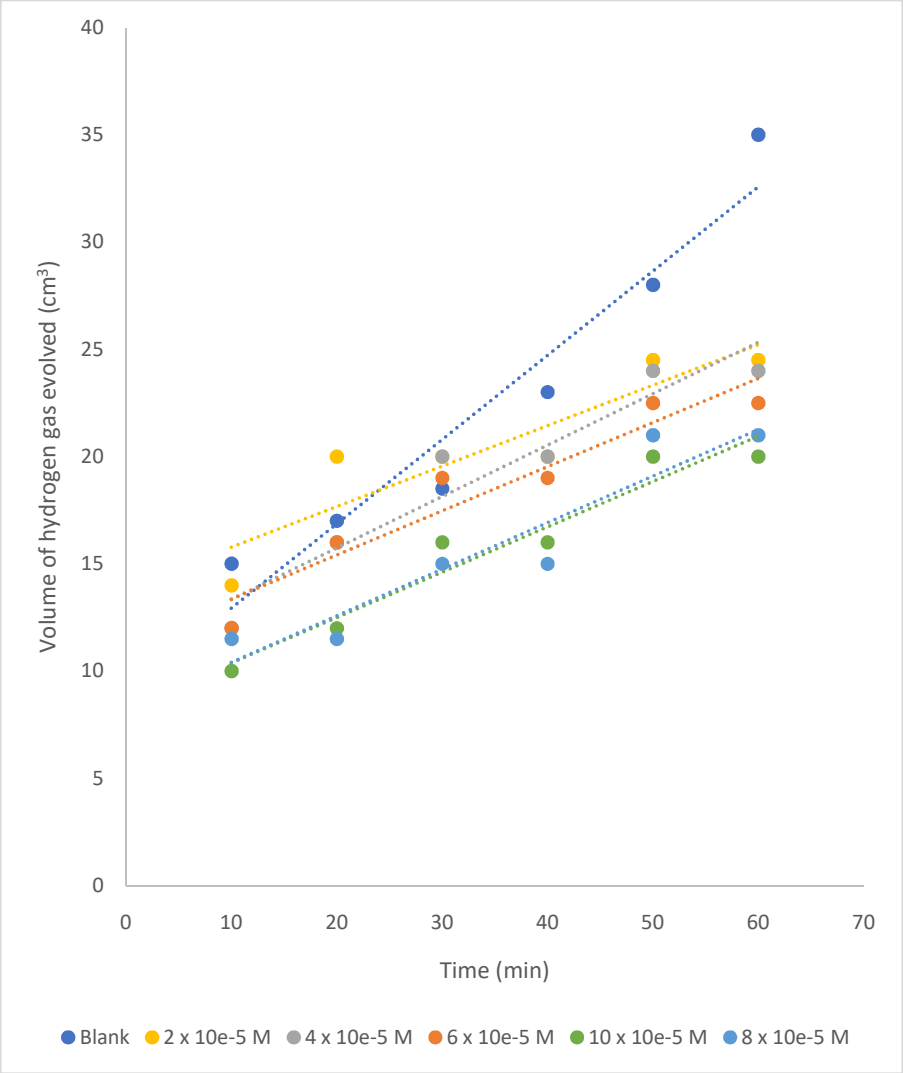

Fig 4.60: Volume of hydrogen gas liberated vs time for low carbon steel corrosion in 1 mol/dm^{3}HCl in the presence of various concentrations of 3 nitro aniline at 303K.

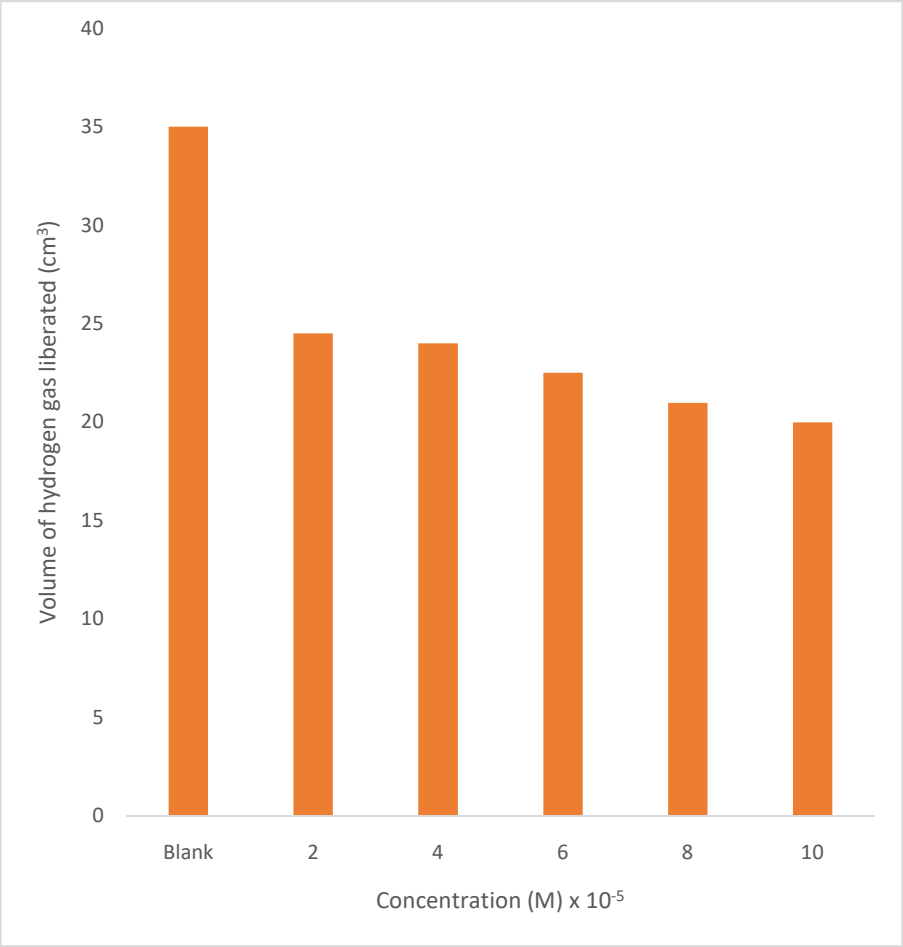

Fig 4.61: Volume of hydrogen gas liberated against different concentrations of 3 nitro aniline in 1 mol/dm^3 HClof low carbon steel corrosion after 60 minutes reaction time at 303K.

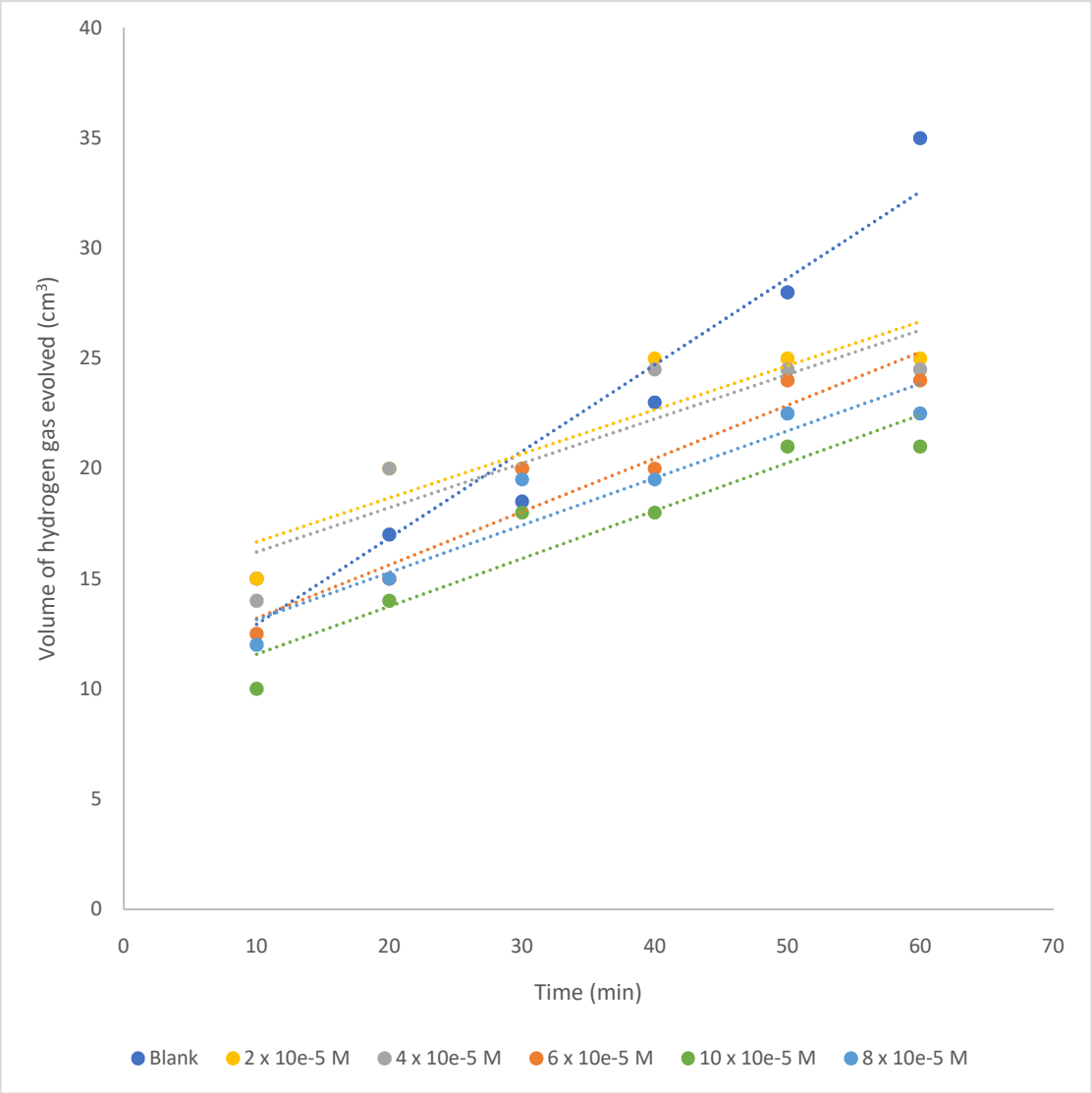

Fig 4.62: Volume of hydrogen gas liberated vs time for low carbon steel corrosion in 1 mol/dm^{3}HCl in the presence of various concentrations of 4 nitro aniline at 303K.

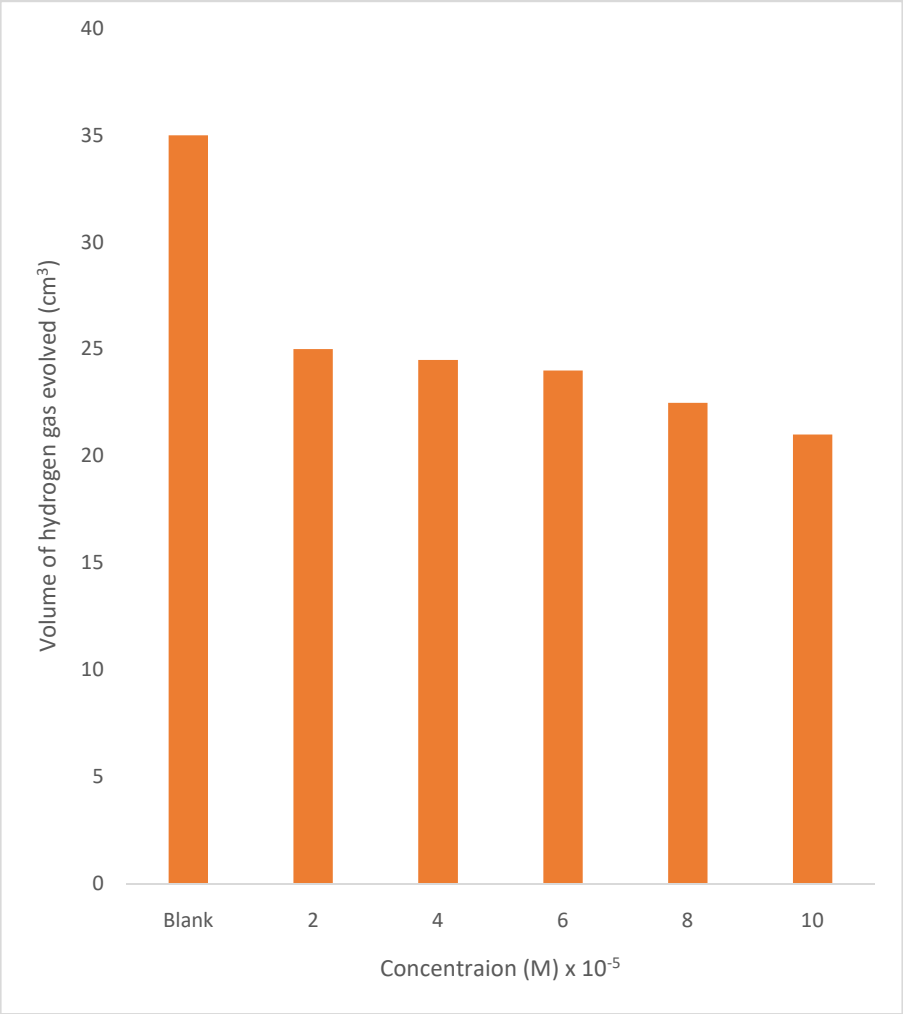

Fig 4.63: Volume of hydrogen gas liberated against different concentrations of 4 nitro aniline in 1 mol/dm^3 HClof low carbon steel corrosion after 60 minutes reaction time at 303K.

Table 4.15: Inhibition efficiencies (I.E%), degree of surface coverage and corrosion rates for low carbon steel in 1 mol/dm^3 HCl in the presence and absence of various concentrations of 2 nitro aniline at 30^{o}C using hydrogen evolution technique

Concentration mol/dm^3	Inhibition efficiency (I.E %)	Degree of surface coverage	Corrosion rate (cm^{3}min^{-1})
Blank	-	-	0.58
2 x 10^{-5}	31.43	0.31	0.40
4 x 10^{-5}	34.23	0.34	0.38
6 x 10^{-5}	37.14	0.37	0.37
8 x 10^{-5}	42.86	0.43	0.33
10 x 10^{-5}	45.71	0.46	0.32

Table 4.16: Inhibition efficiencies (I.E%), degree of surface coverage and corrosion rates for low carbon steel in 1 mol/dm^3 HCl in the presence and absence of various concentrations of 3 nitro aniline at 30^oC using hydrogen evolution technique

Concentration mol/dm^3	Inhibition efficiency (I.E %)	Degree of surface coverage	Corrosion rate (cm^3min^{-1})
Blank	-	-	0.58
2 x 10^{-5}	30.00	0.30	0.41
4 x 10^{-5}	31.43	0.31	0.40
6 x 10^{-5}	35.71	0.36	0.38
8 x 10^{-5}	40.00	0.40	0.35
10 x 10^{-5}	42.86	0.43	0.33

Table 4.17: Inhibition efficiencies (I.E%), degree of surface coverage and corrosion rates for low carbon steel in 1 mol/dm^3 HCl in the presence and absence of various concentrations of 4 nitro aniline at 30^oC using hydrogen evolution technique.

Concentration mol/dm^3	Inhibition efficiency (I.E %)	Degree of surface coverage	Corrosion rate (cm^3min^{-1})
Blank	-	-	0.58
2 x 10^{-5}	28.57	0.29	0.42
4 x 10^{-5}	30.00	0.30	0.41
6 x 10^{-5}	31.43	0.31	0.40
8 x 10^{-5}	35.71	0.36	0.38
10 x 10^{-5}	40.00	0.40	0.35

4.11 Hydrogen gas evolution measurements of nitro aniline compounds

The free corrosion of low carbon steel in 1 mol/dm^3 HCl was described by speedy effervescence as a result of the hydrogen gas liberated and corrosion rates in the absence and presence of the nitro aniline compounds was calculated via hydrogen gasliberation method. As shown in Fig 4.58 - 4.63. the plots demonstrate the reduced deflection of hydrogen gas liberation rate on introduction of the indole derivatives into the corrodent, signifying that the indole derivatives actually inhibits corrosion of low carbon steel in 1 mol/dm^3 HCl when compared to the blank. The of hydrogen gas liberation rates were seen to reduce with rising nitro aniline compounds concentration, indicating that the inhibition was concentration dependent. The results obtained for corrosion rates, surface coverage and inhibition efficiencies (Tables 4.15, 4.16 and 4.17) are close to that obtained for weight loss method. It is indicative that these nitro aniline compoundsas inhibitors are fairly effective.

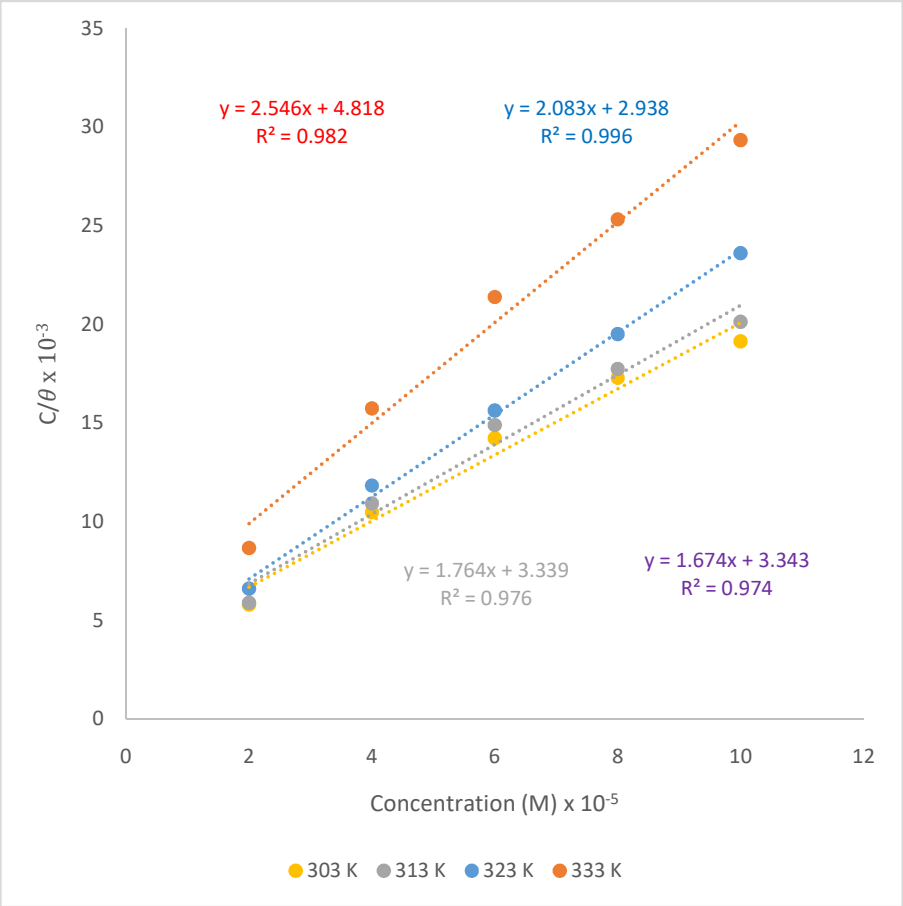

Fig 4.64: Langmuir isotherm for the adsorption of 2 nitro aniline on low carbon steel in 1 mol/dm^3 HCl

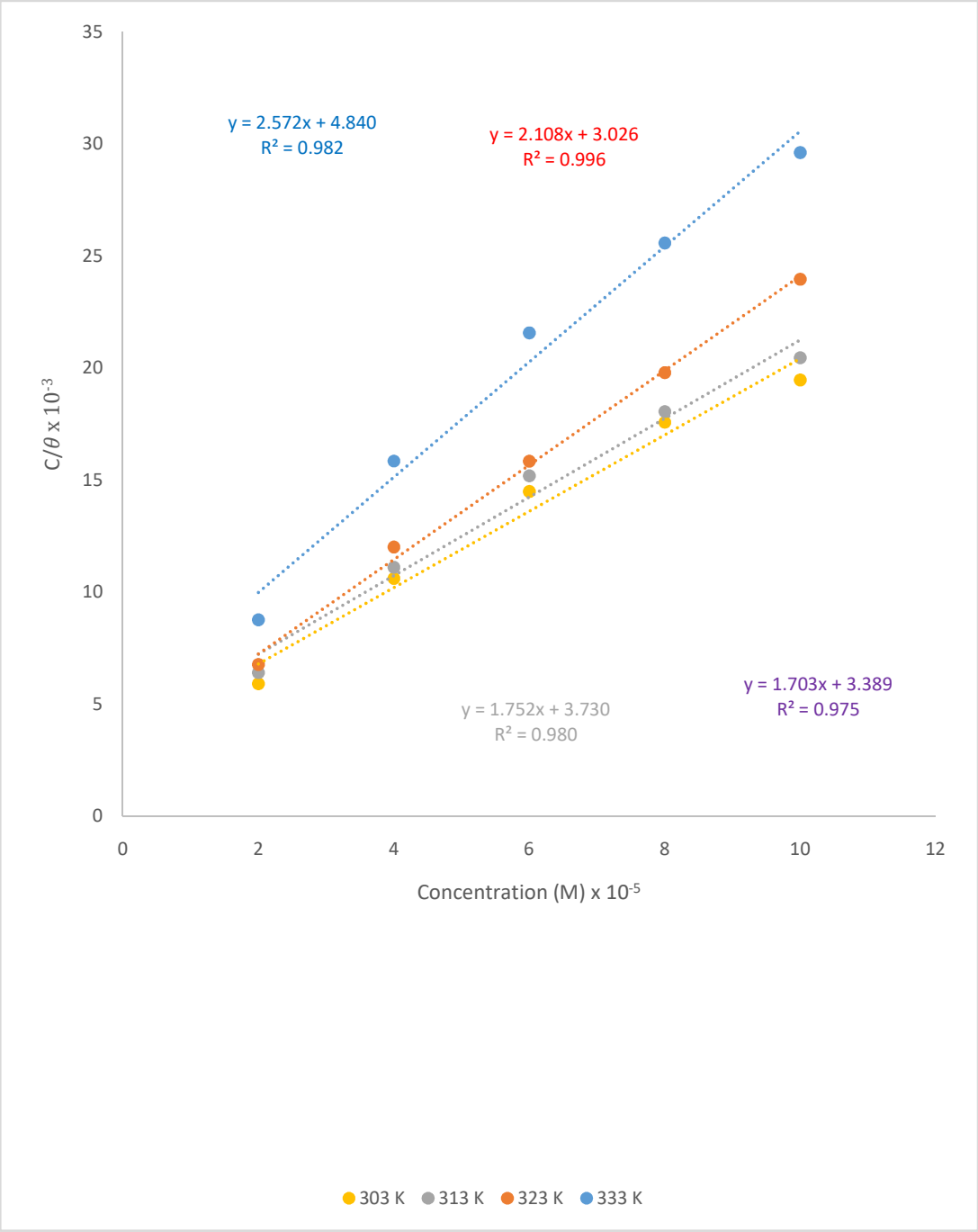

Fig 4.65: Langmuir isotherm for the adsorption of 3 nitro aniline on low carbon steel in 1 mol/dm^3 HCl

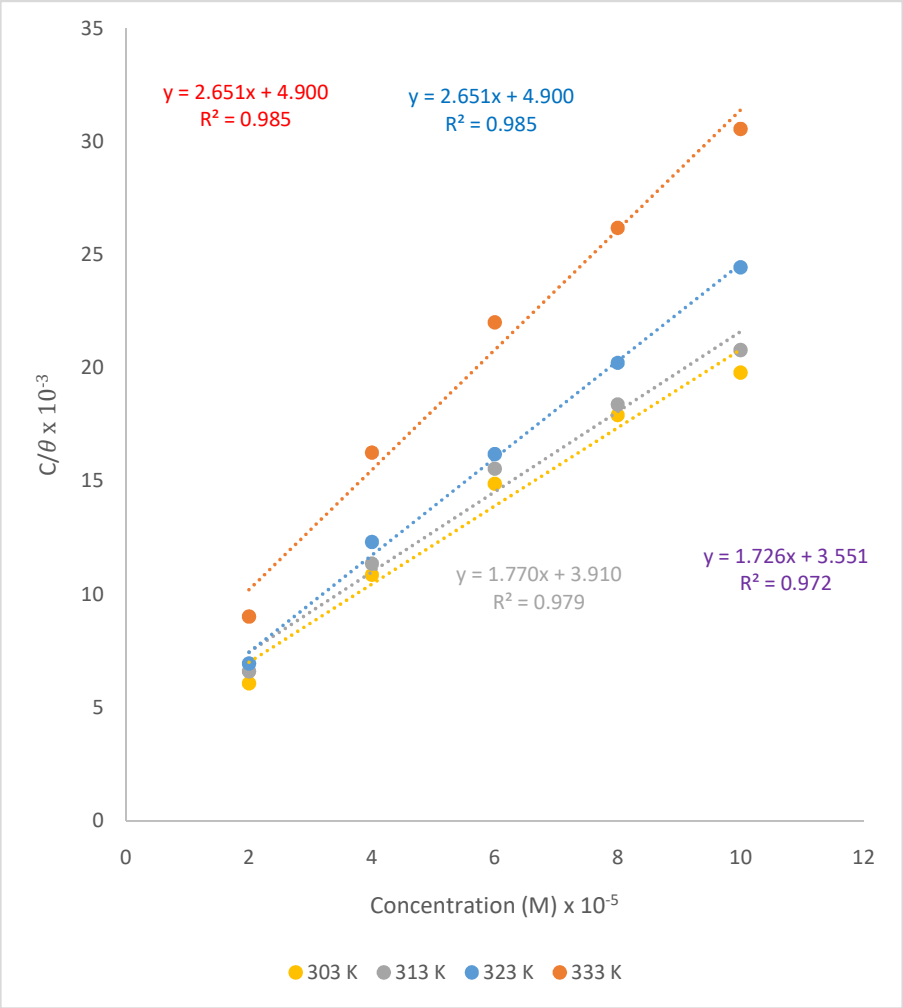

Fig 4.66: Langmuir isotherm for the adsorption of 4 nitro aniline on low carbon steel in 1 mol/dm^3 HCl

Table 4.18: Langmuir indices for the adsorption of 2 nitro aniline on low carbon steel surface

Temperature (^oC)	Kads	ΔG^oads (KJ)	Slope	R^2	R	Intercept
30	0.2991	-7.0773	1.6743	0.9749	0.9874	3.3431
40	0.2995	-7.3143	1.7641	0.9767	0.9883	3.3391
50	0.3404	-7.8918	2.0832	0.9964	0.9982	2.9381
60	0.2076	-6.7670	2.5462	0.9823	0.9911	4.8180

Where $\boldsymbol{R = \sqrt{R^2}}$

Table 4.19: Langmuir indices for the adsorption of 3 nitro aniline on low carbon steel surface

Temperature (^oC)	K_{ads}	ΔG^o_{ads} (KJ)	Slope	R^2	R	Intercept
30	0.2951	-7.0434	1.7063	0.9753	0.9876	3.3431
40	0.2681	-7.0261	1.7527	0.9805	0.9902	3.7301
50	0.3305	-7.8125	2.1086	0.9967	0.9983	3.0260
60	0.2066	-6.7537	2.5728	0.9828	0.9914	4.8406

Where $\boldsymbol{R = \sqrt{R^2}}$

Table 4.20: Langmuir indices for the adsorption of 4 nitro aniline on low carbon steel surface

Temperature (^oC)	Kads	ΔG^oads (KJ)	Slope	R^2	R	Intercept
30	0.2816	-6.9254	1.7261	0.9728	0.9863	3.5514
40	0.2557	-6.9029	1.7708	0.9792	0.9895	3.9108
50	0.2041	-6.5182	2.6512	0.9854	0.9927	4.9007
60	0.2041	-6.7200	2.6512	0.9854	0.9927	4.9007

Where $\boldsymbol{R = \sqrt{R^2}}$

4.12 Adsorption Isotherm of nitro aniline compounds

The graph of C/θ against C was linear as showninFigures 4.64 – 4.66 with a correlation greater than 0.9, with aninsignificant deviation of the slopes from unity (Tables 4.18 - 4.20). This suggest that the Langmuir adsorption isotherm model correctly describes the adsorption behavior of the nitro aniline compounds.

Free energy values for the nitro aniline compounds are shown in Tables 4.18 to4.20. The free energy values ranged from -7.08 to -6.77 KJ/mol^{-1} for 2 nitro aniline, -7.04 to -6.75KJ/mol^{-1} for 3 nitro aniline and -6.93 to -6.72 KJ/mol^{-1}for 4 nitro aniline.

ΔG^{o}_{ads} values up to -20kJmol^{-1} usually indicates physical adsorption, the inhibition comes to play as a result of electrostatic interaction between the charge molecules and the charged metal, while values up to or more than -40kJmol^{-1} indicates chemisorption which occurs due to sharing or transfer of electrons from the organic molecules to the metal surface to form a coordinate type of bond (Ebenso *et al.,* 2010a). The values gotten from this research ranged from -7.08 to -6.72 kJmol^{-1}, which agrees with the mechanism of physiosorption (Ashassi-Sorkhabi et al, 2005).

Table 4.21: Thermodynamic indices for the adsorption of 2 nitro aniline viagravimetric method

Concentration mol/dm^3	Activation Energy (KJmol^{-1})	Heat of adsorption (Q_{ads}) KJ mol^{-1}
Blank	12.21	-
2 x 10^{-3}	16.64	-15.27
4 x 10^{-3}	17.26	-16.73
6 x 10^{-3}	18.32	-17.91
8 x 10^{-3}	18.95	-17.93
10 x 10^{-3}	21.20	-20.64

Table 4.22: Thermodynamic indices for the adsorption of 3 nitro aniline viagravimetric method

Concentration mol/dm^3	Activation Energy (KJmol^{-1})	Heat of adsorption (Q_{ads}) KJ mol^{-1}
Blank	12.21	-
2 x 10^{-5}	16.50	-14.89
4 x 10^{-5}	17.31	-16.42
6 x 10^{-5}	18.02	-17.45
8 x 10^{-5}	18.70	-17.60
10 x 10^{-5}	20.87	-20.37

Table 4.23: Thermodynamic indices for the adsorption of 4 nitro aniline viagravimetric method

Concentration mol/dm^3	Activation Energy (KJmol^{-1})	Heat of adsorption (Q_{ads}) KJ mol^{-1}
Blank	12.21	-
2 x 10^{-5}	16.38	-14.59
4 x 10^{-5}	16.97	-16.18
6 x 10^{-5}	17.71	-16.96
8 x 10^{-5}	18.56	-17.59
10 x 10^{-5}	20.81	-20.67

4.13 Thermodynamic Considerations of nitro aniline compounds

A greater value of the activation energy (E_a) of the corrosion process in the presence of inhibitor when compared to an uninhibited corrosion process is suggest that the adsorption mode is physiosorption, while the other way round suggest chemisorption.

To further show that the indole derivatives adsorbed to low carbon steel through physiosorption, the values of activation energy (E_a) were calculated using Arrhenius equation(refer to equation 4.17)

The values are as shown in Tables 4.21 to4.23. Arise in the value of activation energy (E_a)when the indole derivatives are present as compared when they are absent and the reduction of its IE% with temperature rias can be understood as a sign of physiosorption. With reference to Ameh *et al.,* 2012, it is likely that for chemisorption, the values of activation energy should be more than 80kJmol^{-1} for the mechanism of physiosorption. With the activation energy (E_a) values as shown in Table 4.21 (16.64 -21.20 kJmol^{-1}) for2 nitro aniline, Table 4.22 (16.50 – 20.87 kJmol^{-1}) for 3 nitro aniline and Table 4.23 (16.38 - 20.81 kJmol^{-1}) for 4 nitro aniline, it further confirms the process of physiosorption.

An estimation of heat of adsorption (Q_{ads}) wascalculatedusing equation 4.18. The values calculated for Q_{ads} are shown in Tables 4.21 and 4.23Calculated values of Q_{ads} using equation 4.18 ranged from -15.27 to -20.64 kJmol^{-1} for for 2 nitro aniline, -14.89 to -20.37 kJmol^{-1} for 3 nitro aniline and -14.59 to -20.67 kJmol^{-1} for 4 nitro aniline. The values obtained are negative values are obtained which suggest that the adsorption of these indole derivatives on low carbon steel is exothermic (Ameh *et al.,* 2012).

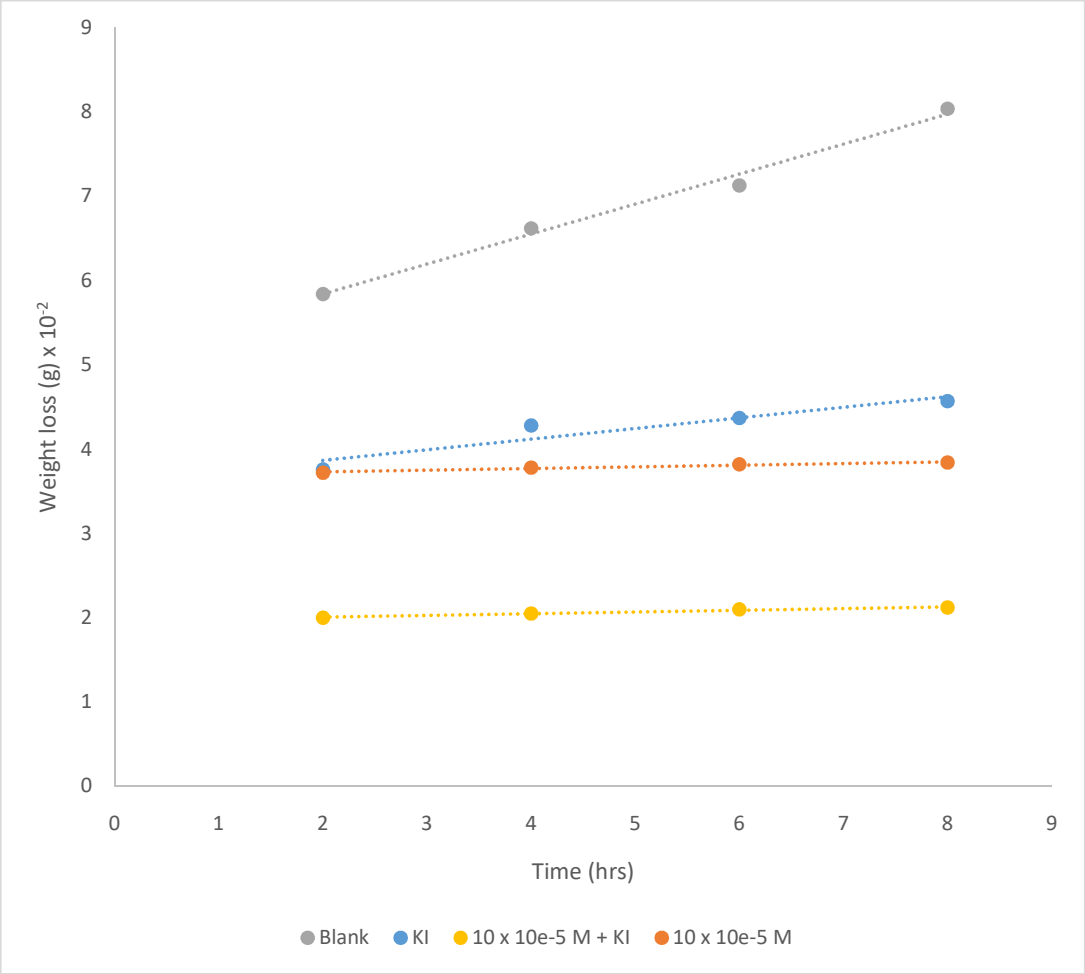

Fig 4.67: Weight loss vs time for low carbon steel corrosion in 1 mol/dm^3 HCl in the absence and presence of both KI and 2 nitro aniline and absence of either KI or 2 nitro aniline at 303K.

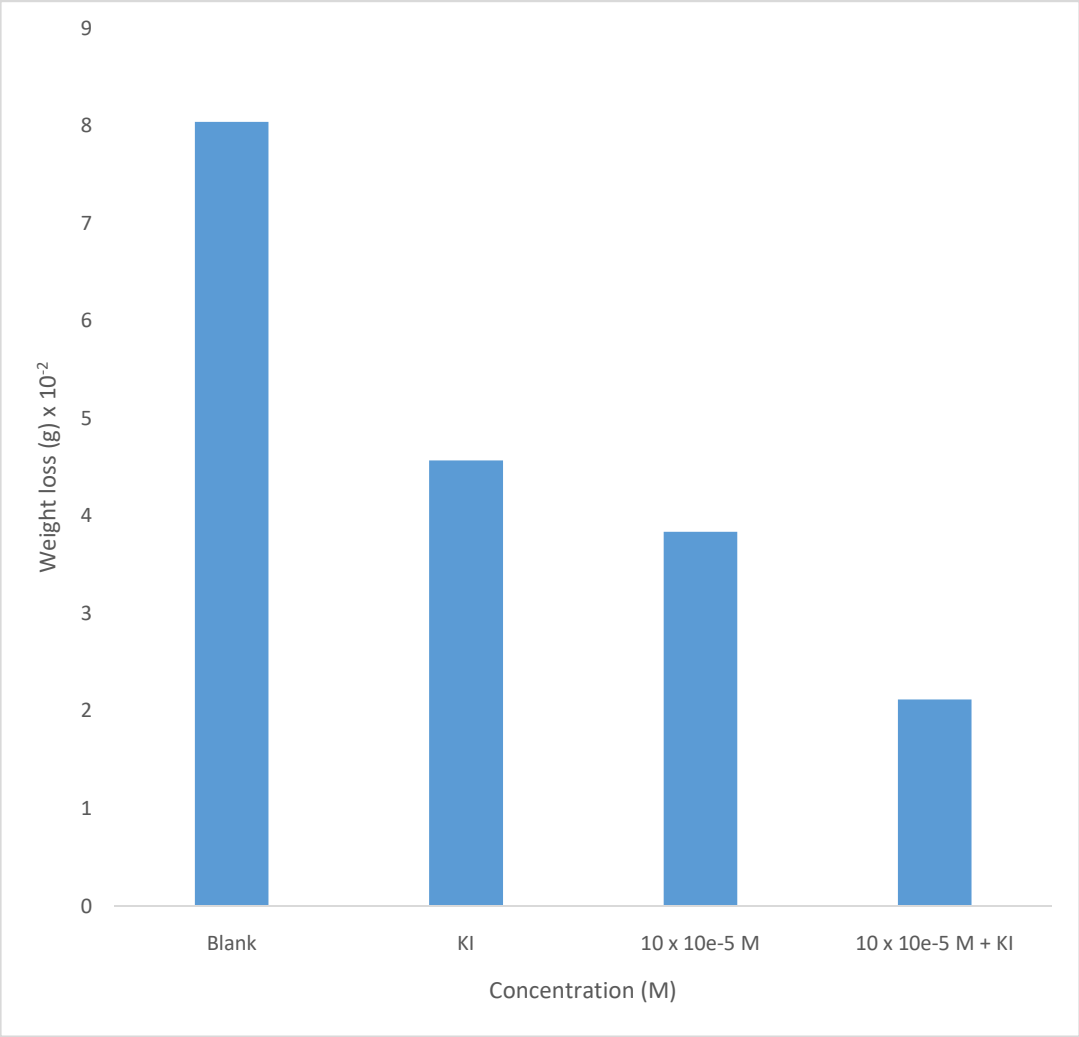

Fig 4.68: Weight loss values vs 1 mol/dm^3 HCl in the absence and presence of both KI and 2 nitro aniline and absence of either KI or 2 nitro aniline after 8 hours of immersion time at 303K.

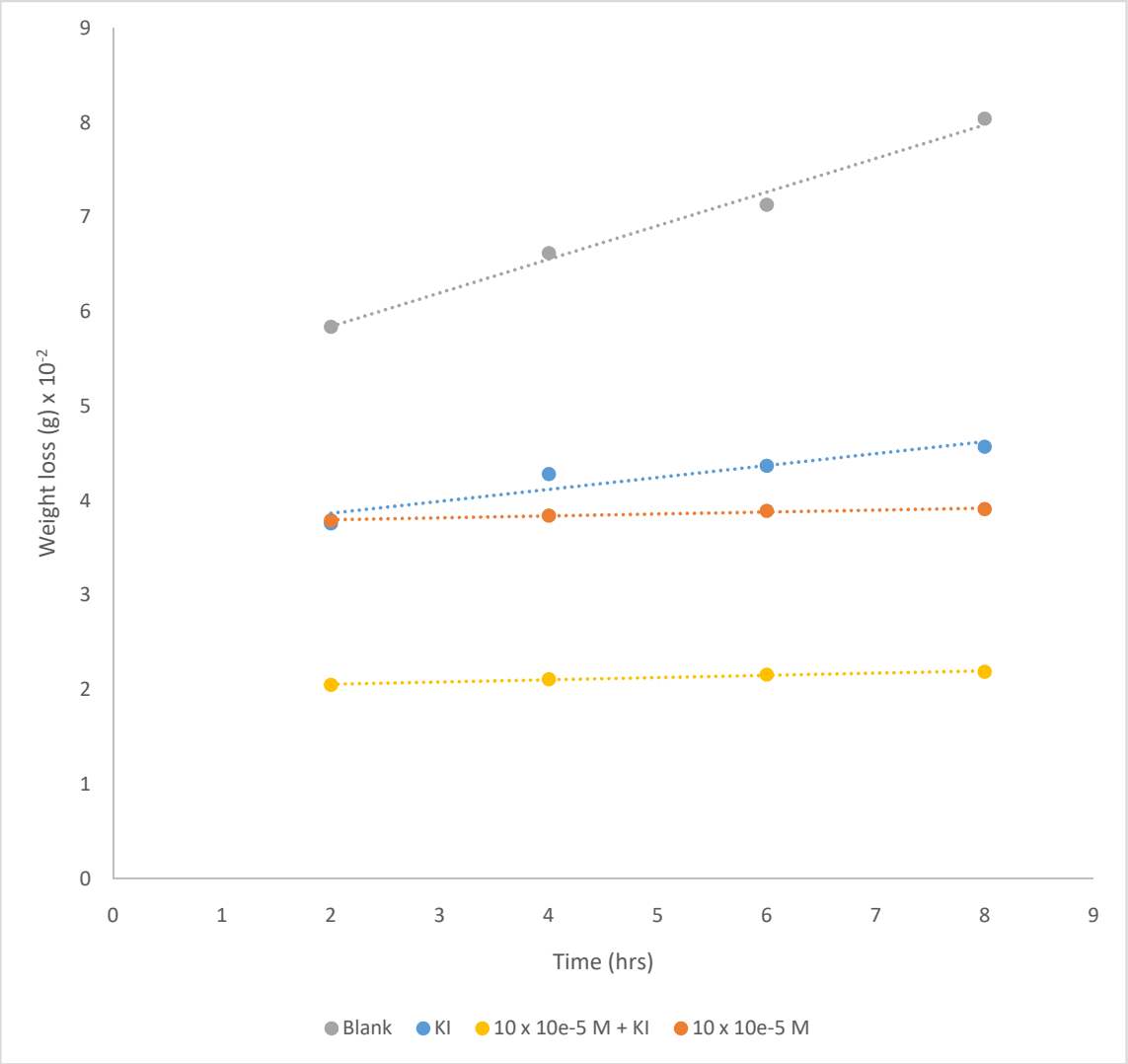

Fig 4.69: Weight loss vs time for low carbon steel corrosion in 1M HCl in the absence and presence of both KI and 3 nitro aniline and absence of either KI or 3 nitro aniline at 303K.

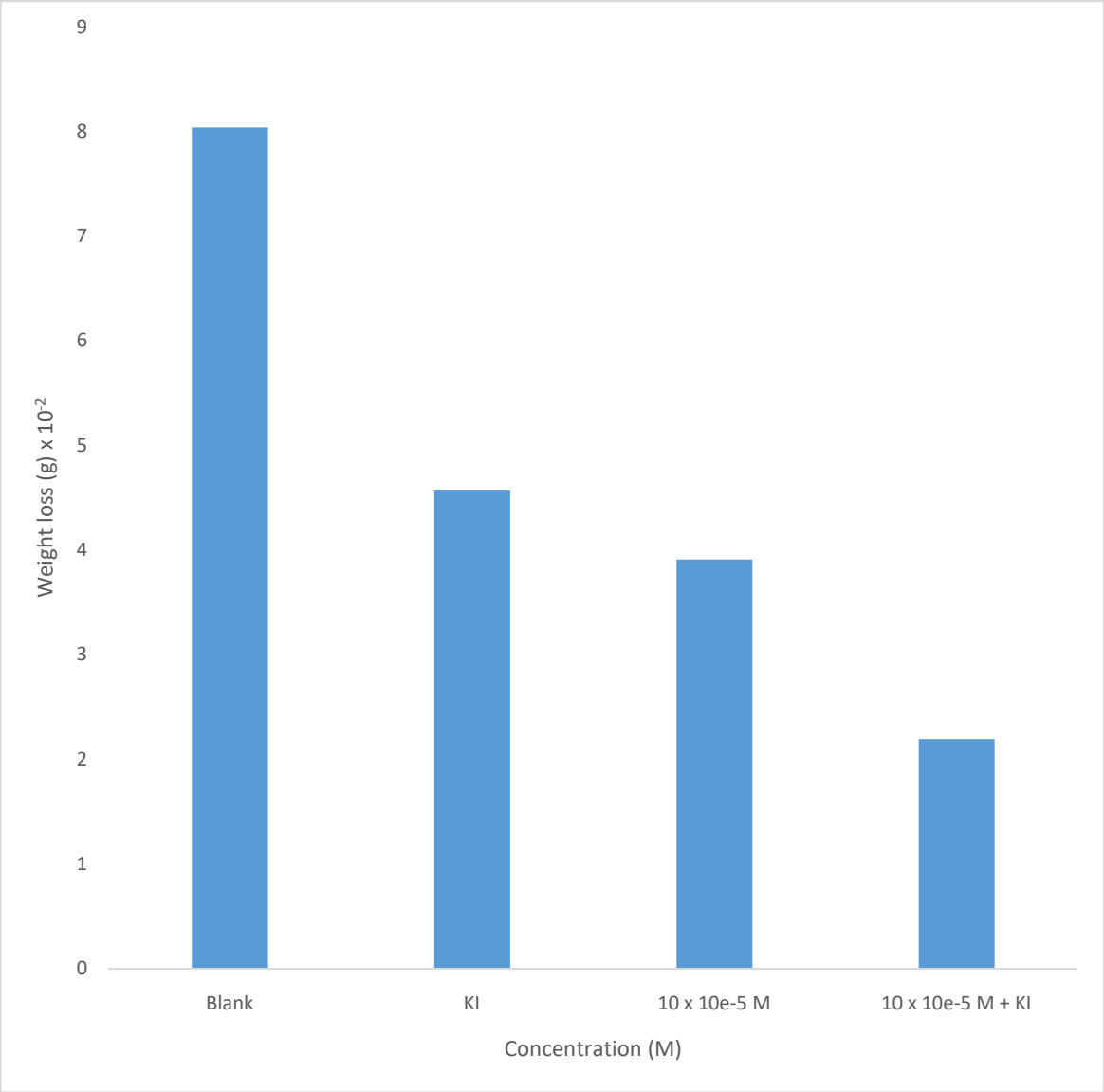

Fig 4.70: Weight loss values vs 1 mol/dm^3 HCl in the absence and presence of both KI and 3 nitro aniline and absence of either KI or 3 nitro aniline after 8 hours of immersion time at 303K.

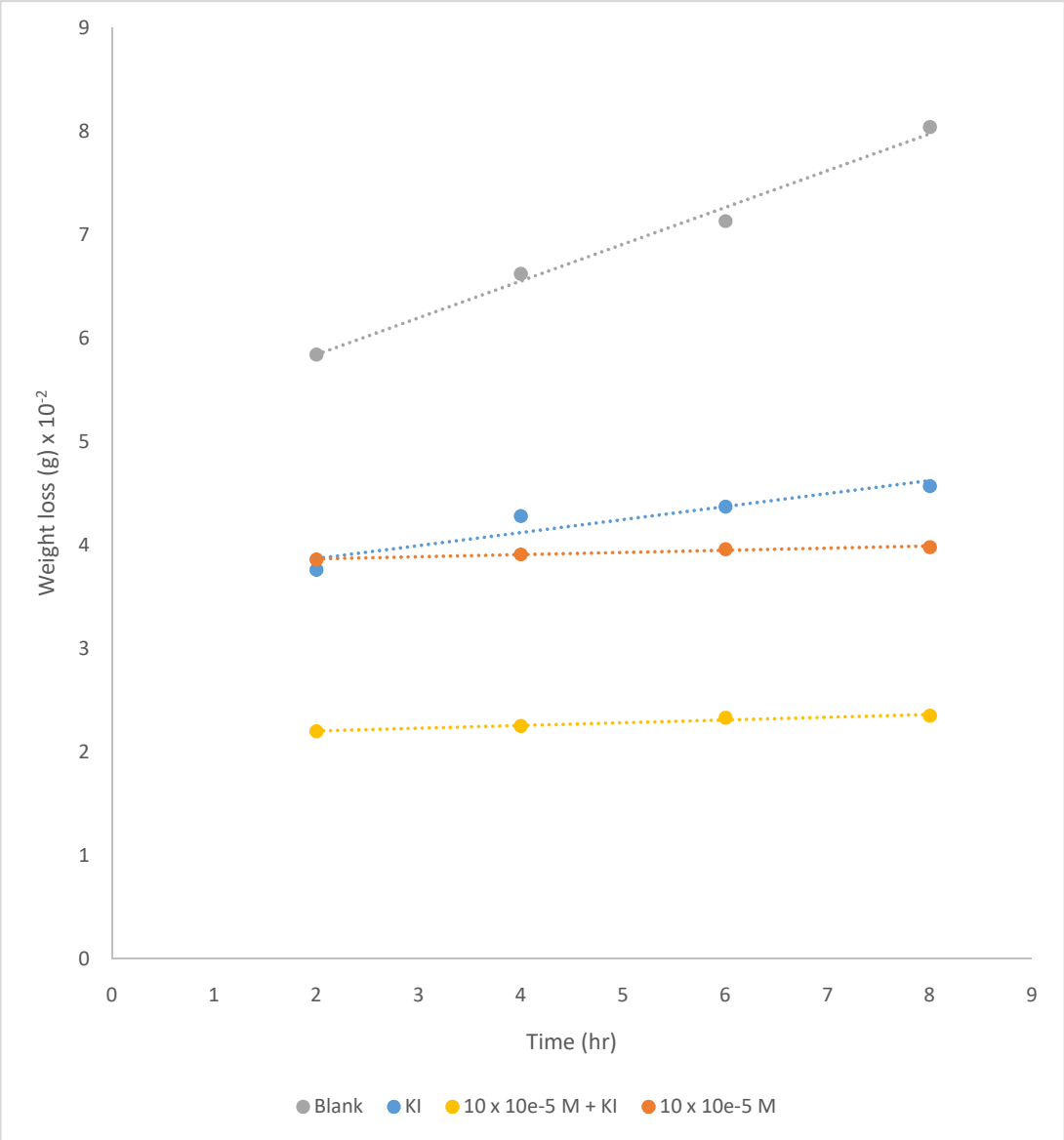

Fig 4.71: Weight loss against time for low carbon steel corrosion in 1 mol/dm^3 HCl in the absence and presence of both KI and 4 nitro aniline and absence of either KI or 4 nitro aniline at 303K.

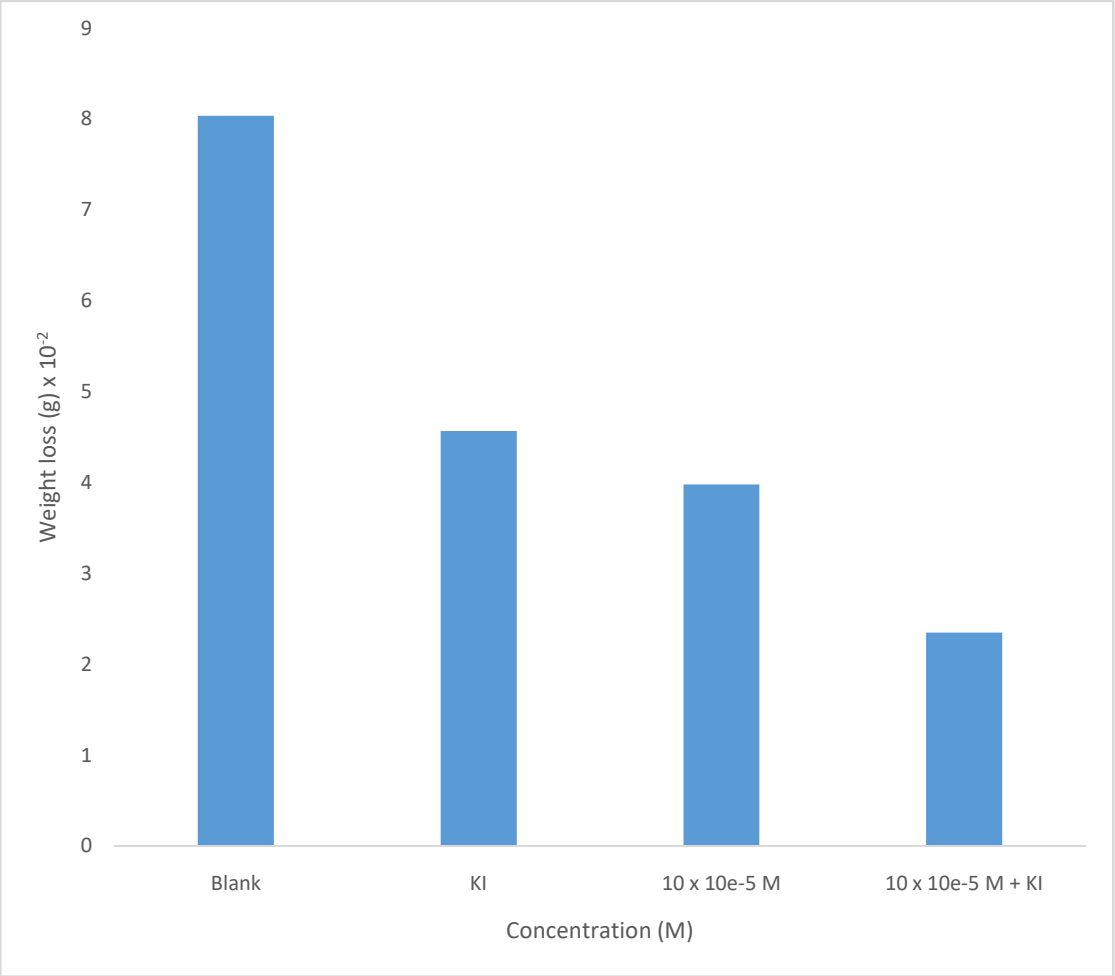

Fig 4.72 Weight loss values vs 1 mol/dm^3 HCl in the absence and presence of both KI and 4 nitro aniline And absence of either KI or 4 nitro aniline after 8 hours of immersion time at 303K.

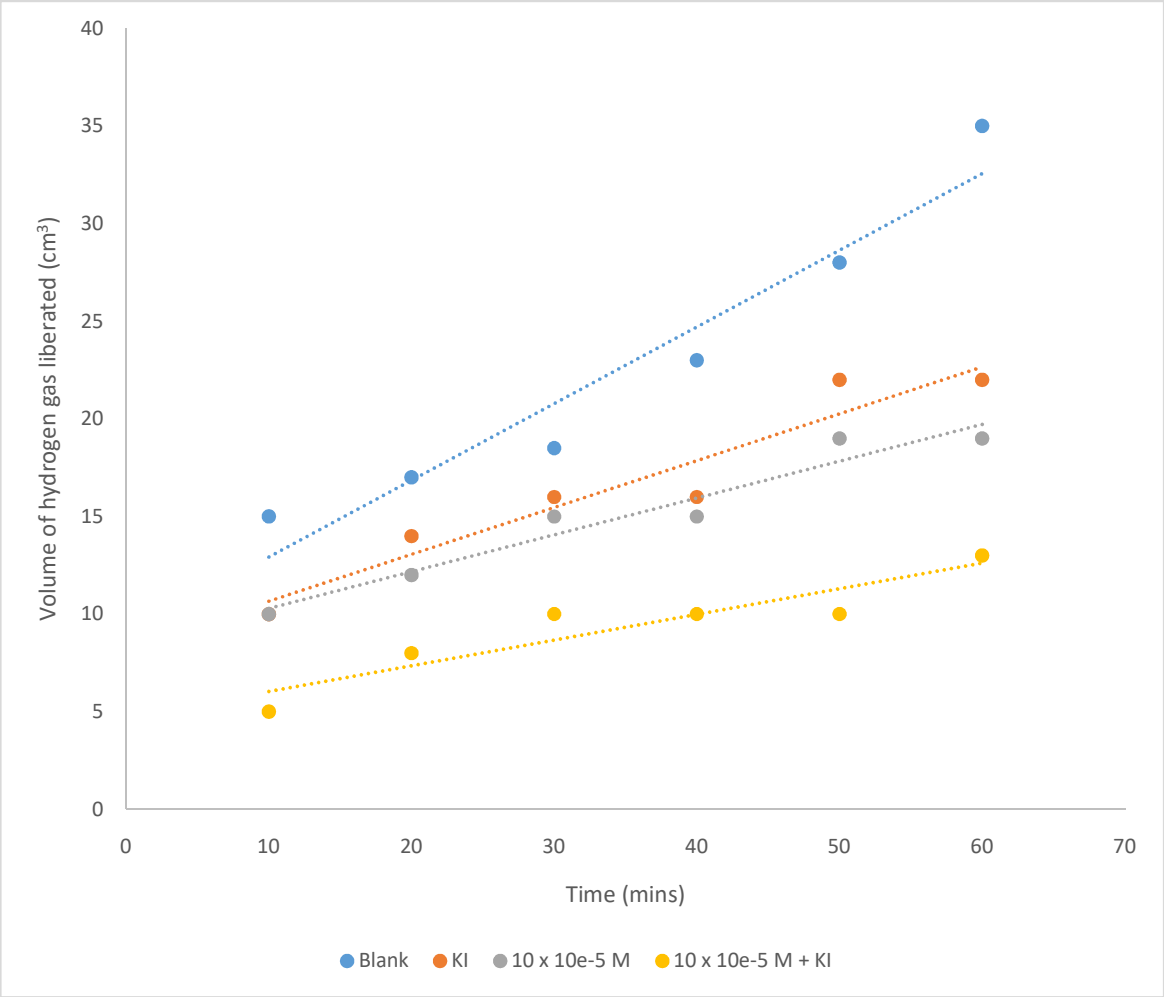

Fig 4.73: Volume of H_2 liberated vs time for low carbon steel corrosion in 1 mol/dm^3 HCl in the absence and presence of both KI and 2 nitro aniline and absence of either KI or 2 nitro aniline at 303K.

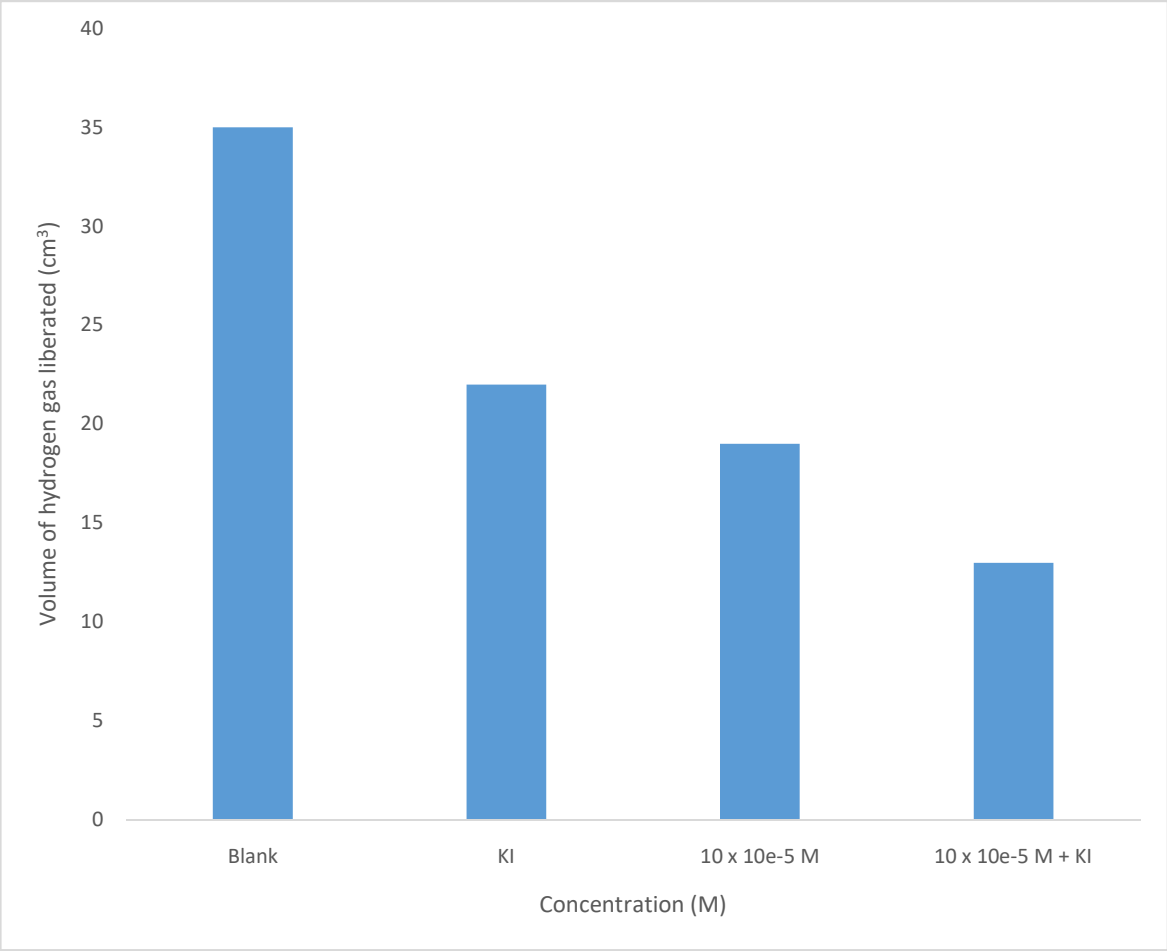

Fig 4.74: Volume of H_2 liberated against 1 mol/dm^3 HCL in the absence and presence of both KI and 2 nitro aniline and absence of either KI or 2 nitro aniline after 60 minutes of immersion time at 303K.

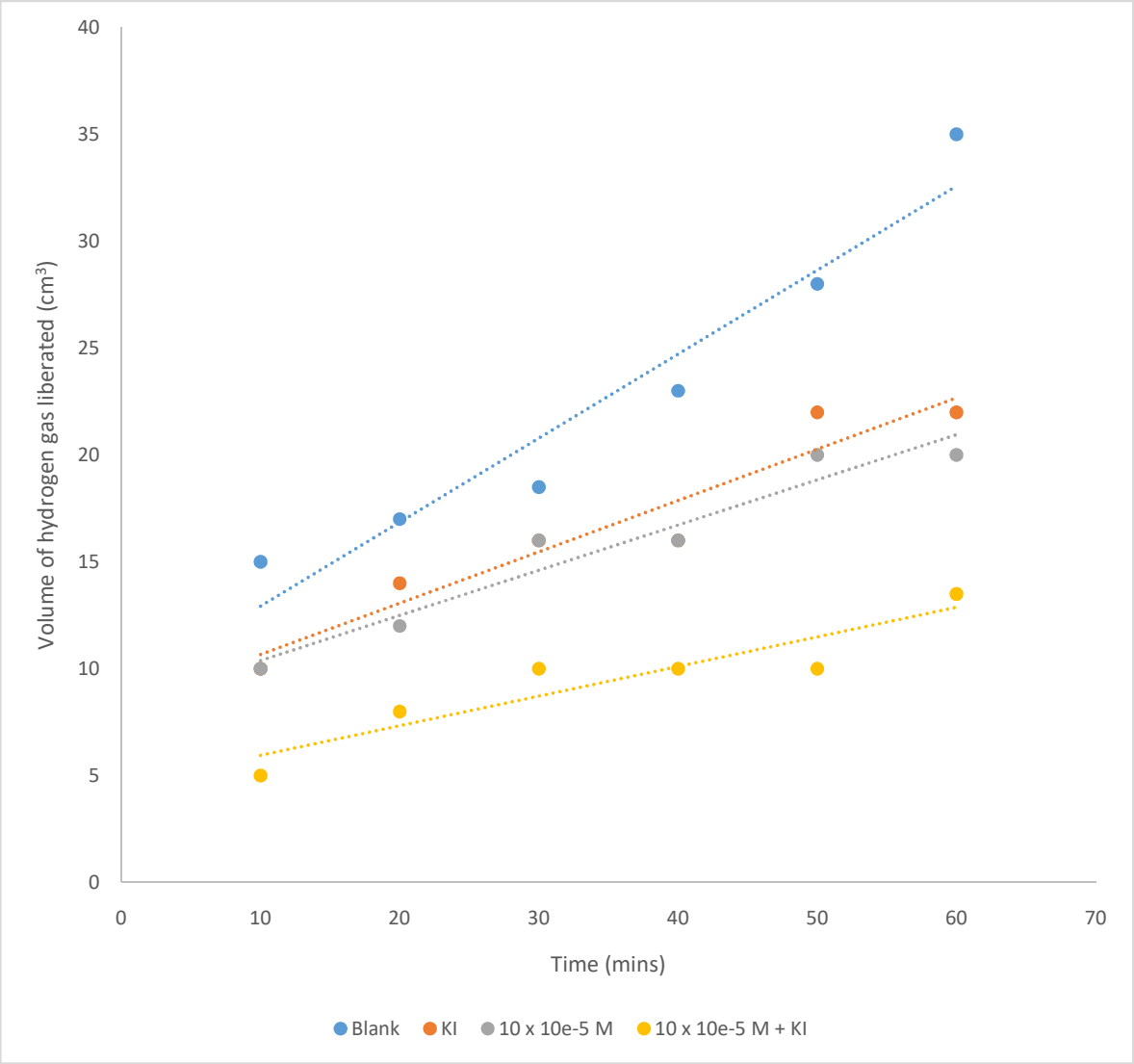

Fig 4.75: Volume of H_2 evolved against time for low carbon steel corrosion in 1 mol/dm^3 HCl in the absence and presence of both KI and 3 nitro aniline and absence of either KI or 3 nitro aniline at 303K.

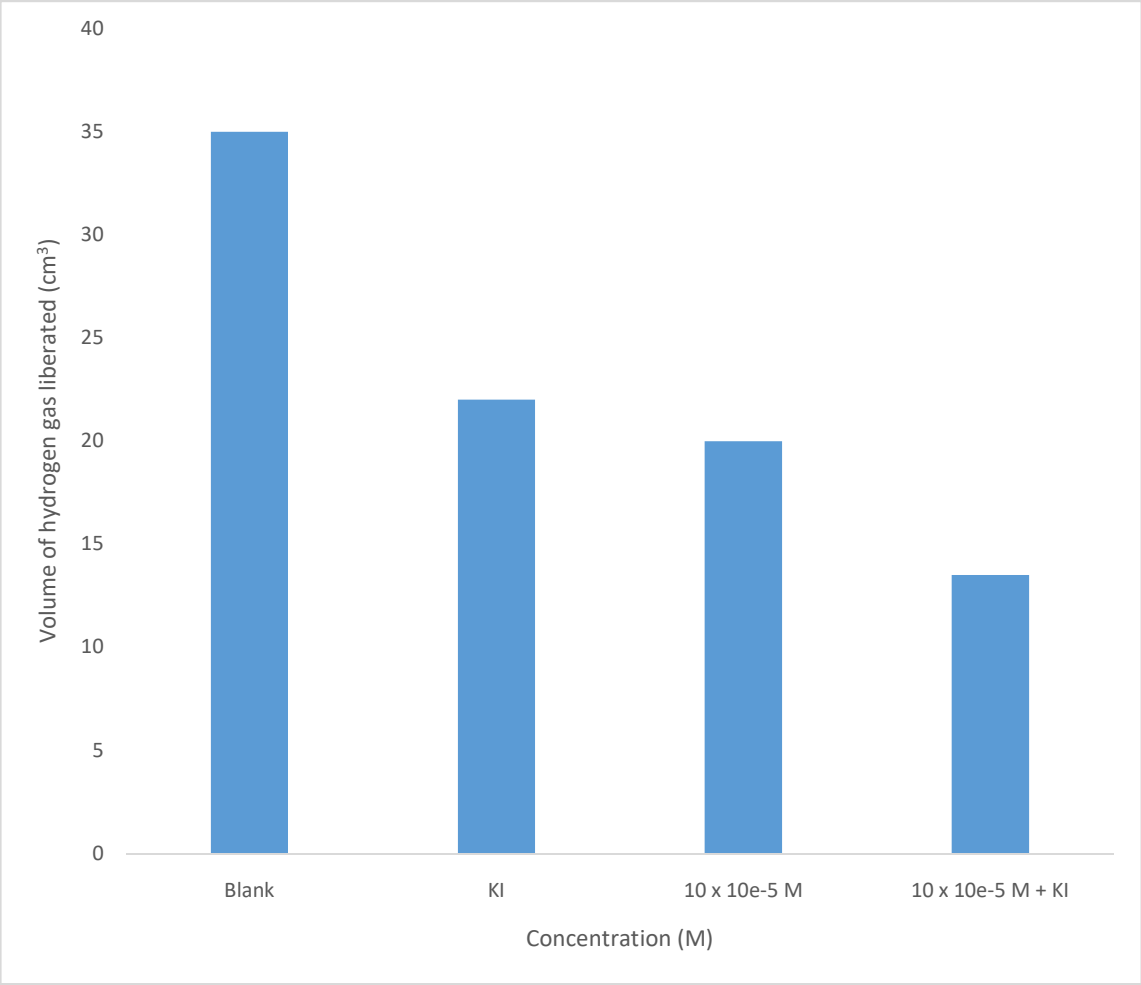

Fig 4.76: Volume of H_2 evolved vs 1 mol/dm^3 HCl in the absence and presence of both KI and 3 nitro aniline and absence of either KI or 3 nitro aniline after 60 minutes of immersion time at 303K.

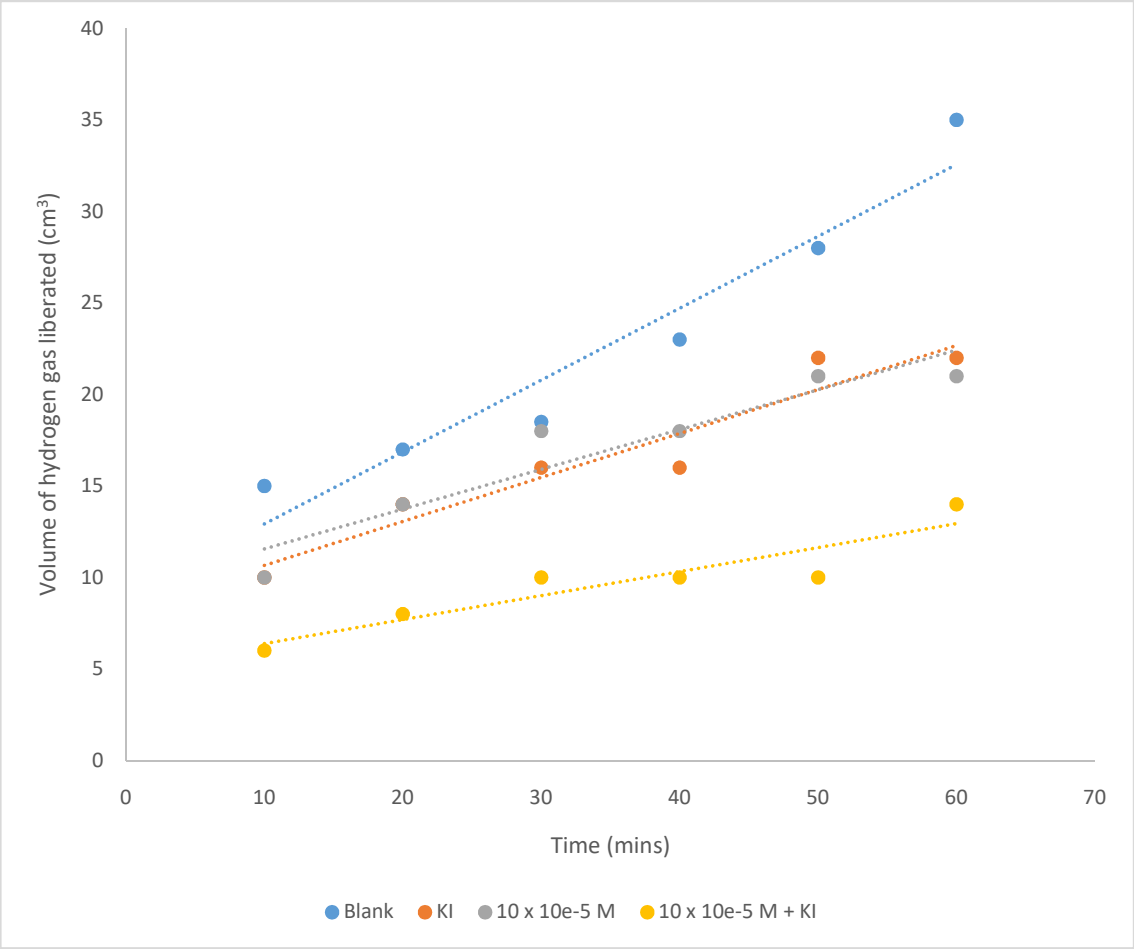

Fig 4.77: Volume of H_2 evolvedvs time for low carbon steel corrosion in 1 mol/dm^3 HCl in the absence and presence of both KI and 4 nitro aniline and absence of either KI or 4 nitro aniline at 303K.

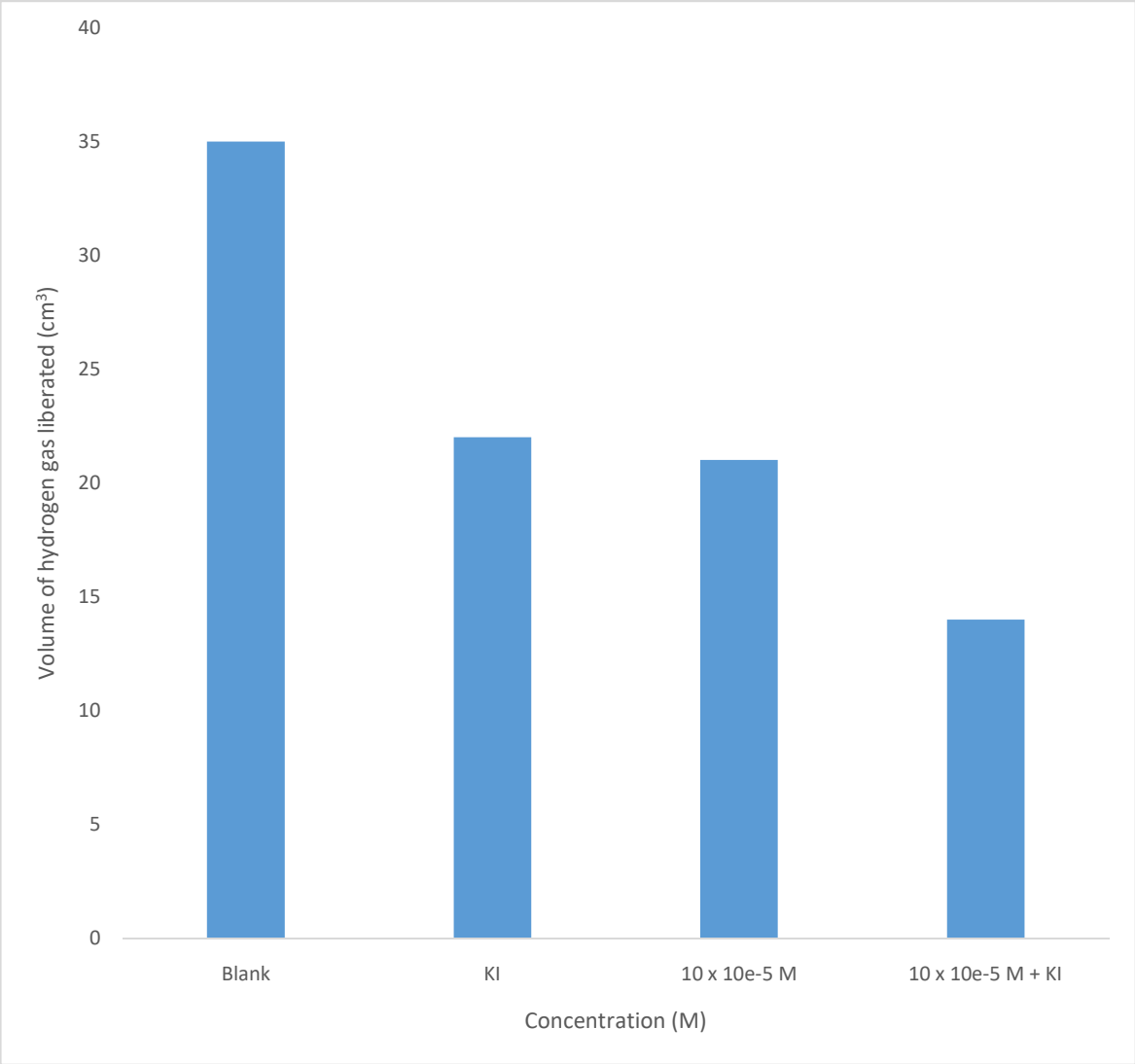

Fig 4.78: Volume of H_2 evolved against 1 mol/dm^3 HCl in the absence and presence of both KI and 4 nitro aniline and absence of either KI or 4 nitro aniline after 60 minutes of immersion time at 303K.

Table 4.24: Inhibition efficiencies (I.E%) for low carbon steel in 1 mol/dm^3 HCl in the presence and absence of 10 x 10^{-5} mol/dm^3 nitro aniline compounds and 5 x 10^{-3} mol/dm^3 potassium iodide (KI) at 303K using gravimetric technique and hydrogen evolution technique.

Molecule	Inhibition efficiency (% I.E) by weight loss method	Inhibition efficiency (% I.E) by hydrogen gas evolution method
2 nitro aniline	52.24	45.71
3 nitro aniline	51.37	42.86
4 nitro aniline	50.50	40.00
KI	43.16	37.14
2 nitro aniline + KI	73.63	62.86
3 nitro aniline + KI	72.64	61.43
4 nitro aniline + KI	70.77	60.00

Table 4.25: Synegistic parameters (S_1) of 10 x 10^{-5} mol/dm^3 nitro aniline compounds with 5 x 10^{-3} mol/dm^3 potassium iodide in 1 mol/dm^3 HCl at 303K using gravimetric technique and hydrogen gas evolution technique.

Molecule	$\mathbf{S_1}$ (weight loss method)	$\mathbf{S_1}$ (hydrogen gas evolution method)
2 nitro aniline	2.31	2.34
3 nitro aniline	2.32	2.33
4 nitro aniline	2.34	2.31

4.14 Effect of iodide ion addition on nitro aniline compounds

Corrosion inhibition of metals in strong acids by halides is well documented.This effect rest on the ionic size and charge, the electrostatic field set up by the negative charge of the anion on the adsorption sites and the nature and concentration of the halide ion (Lei*et al.,* 2017). It was also reported that the inhibitive effect increases in the order Cl- < Br- < I- (Ebenso, 2003).The iodide ion (radius: 135 pm) is more susceptible to adsorption than is the bromide ion (radius: 114 pm) or chloride ion (radius: 90 pm). InTable 4.24, it is perceived that the inhibition efficiency of nitro aniline derivatives are further enhanced by the addition of 5 x 10^{-3}mol/dm^3 KI to the nitro aniline derivatives respectively. The inhibition efficiency significantly increased to 62.86 % for 2 nitro aniline, 61.43 for 3 nitro aniline and 60.00 % for 4 nitro aniline at 303K. The strong adsorptions of iodide ions on the metal surface is responsible for the additional inhibitive effect(Lei*et al.,* 2017). The inhibitors are then absorbed by coulombic attraction on the metal surface where iodide ions are already adsorbed. Stabilization of adsorbed iodide ions with inhibitors in cationic form on low carbon steel lead to greater surface coverage and thereby greater inhibition (Ebenso, 2003).

The synergistic parameters were calculated using equation 4.19 reported by Lei*et al.,* 2017.

$$S_{1=}\frac{1-I_{1+2}}{1-I'_{1+2}} \qquad 4.19$$

Where I_{1+2} = (I_1 + I_2); I_1 = inhibition efficiency of the halides, I_2 = inhibition efficiency of the nitro aniline compounds, I'= measured inhibition efficiency for the nitro aniline derivatives in combination with iodide ions. S_1 approaches 1 when no interaction between the inhibitor compounds exist, while $S_1 > 1$ indicates a synergistic effect. In the case of $S_1 < 1$, the antagonistic interaction prevails, which may be attributed to competitive adsorption. Values of S_1 for the nitro aniline derivatives in combination with potassium iodide (KI) are presented in Table 4.25. The S_1 values obtained are greater than one ($S_1 > 1$), thusindicating better inhibition efficiency triggered by the synergistic inhibitive effect of iodide ions in combination with nitro aniline compounds. Thus it can be suggested that nitro aniline compounds in the cationic form are adsorbed by the coulombic attraction on the metal surface, where the iodide ions were already adsorbed and the corrosion rate is further suppressed as a

result of the stabilization of the adsorbed anion due to the increase in surface coverage. The adsorption of the organic cation on the low carbon steel surface is weak, since the metal surface is positively charged in HCl solution. However, with initial adsorption of iodide ion there is a reduction in the positive charge of Fe because of the formation of Fe-anion surface bond which yields a negative pole facilitating the adsorption of the organic cation.

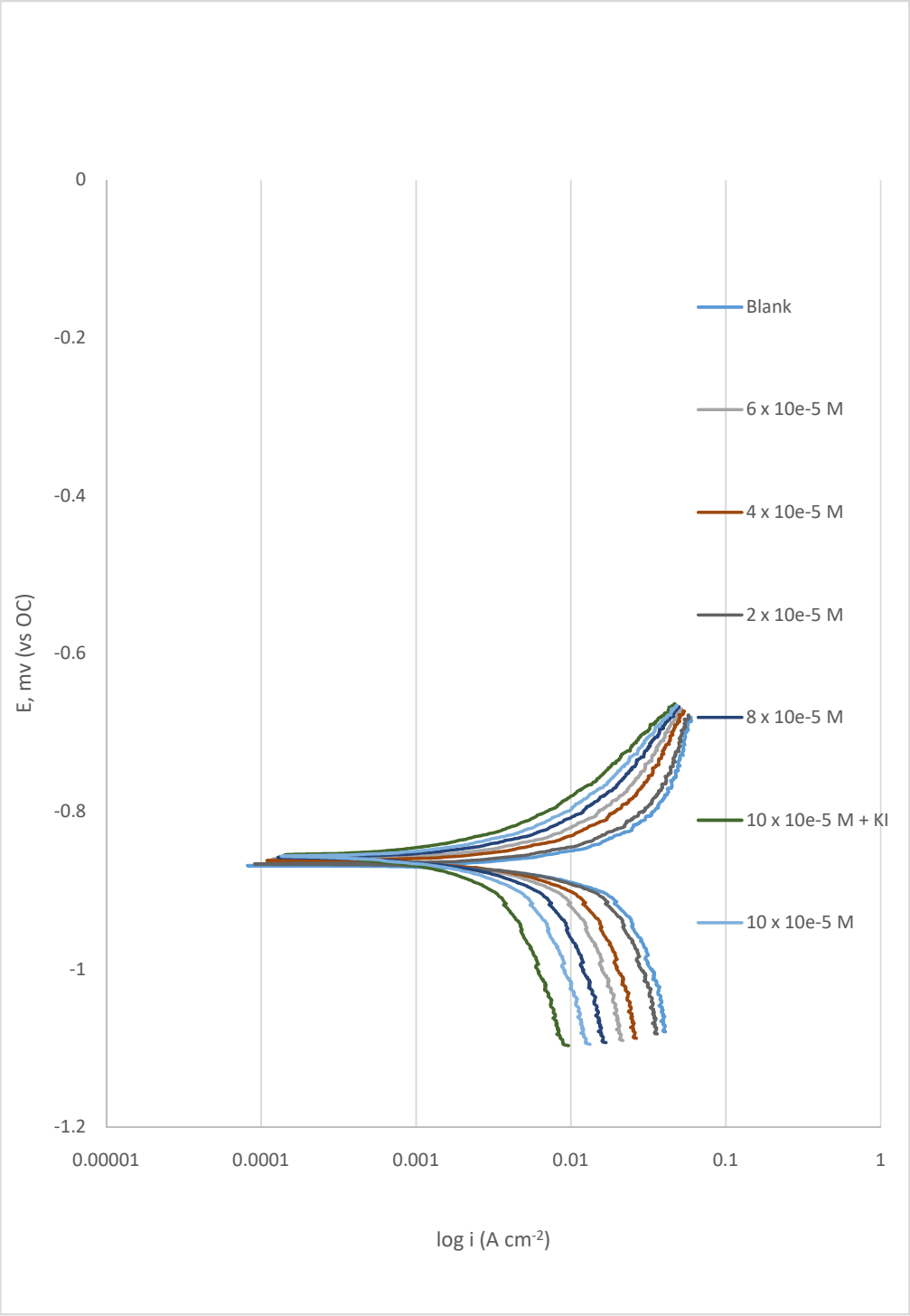

Figure 4.79: Potentiodynamic poilarization curves for low carbon steel in 1 mol/dm^3 HCl containing various concentrations of 2 nitro aniline

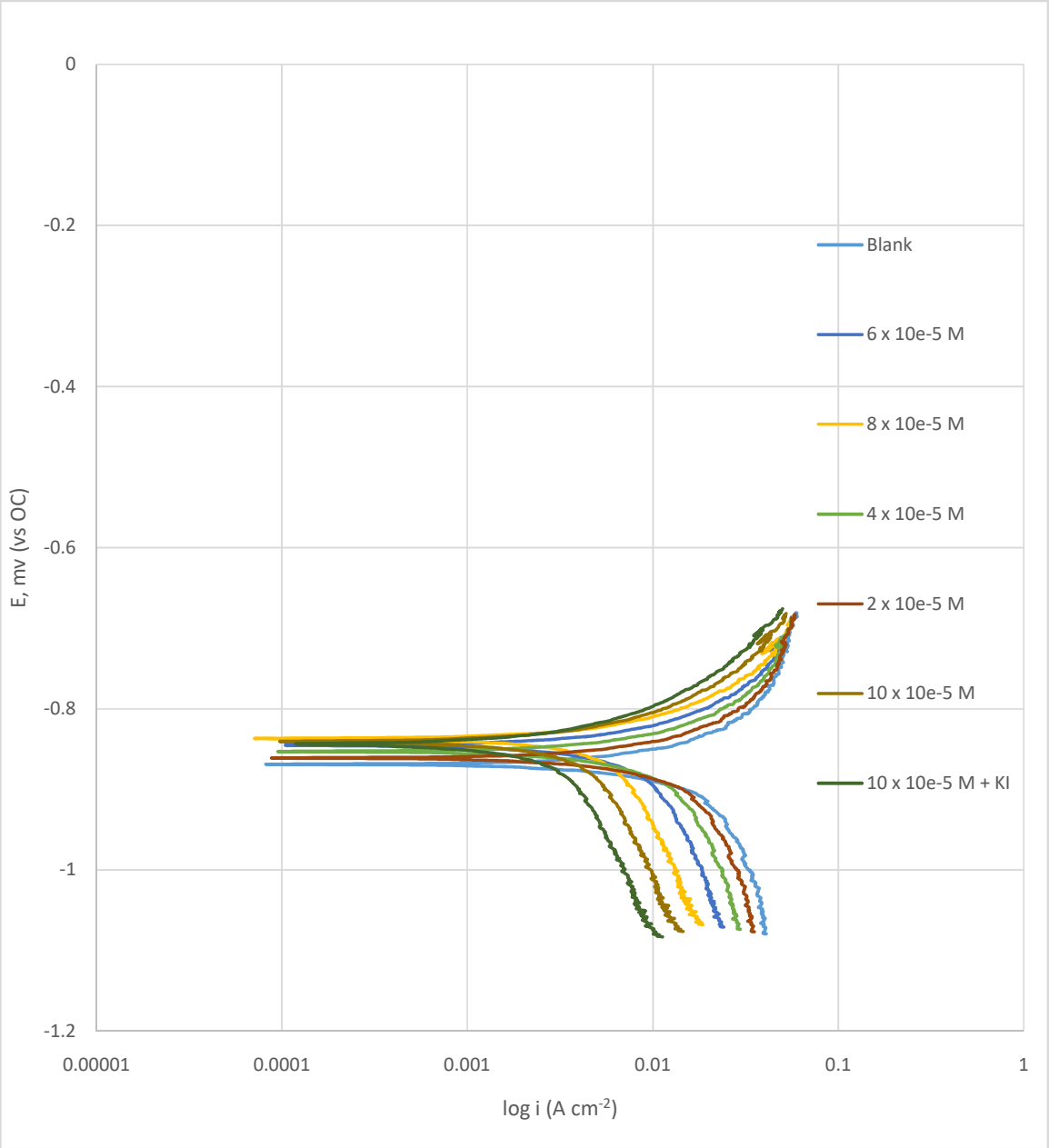

Figure 4.80: Potentiodynamic poilarization curves for low carbon steel in 1 mol/dm^3 HCl containing various concentrations of 3 nitro aniline

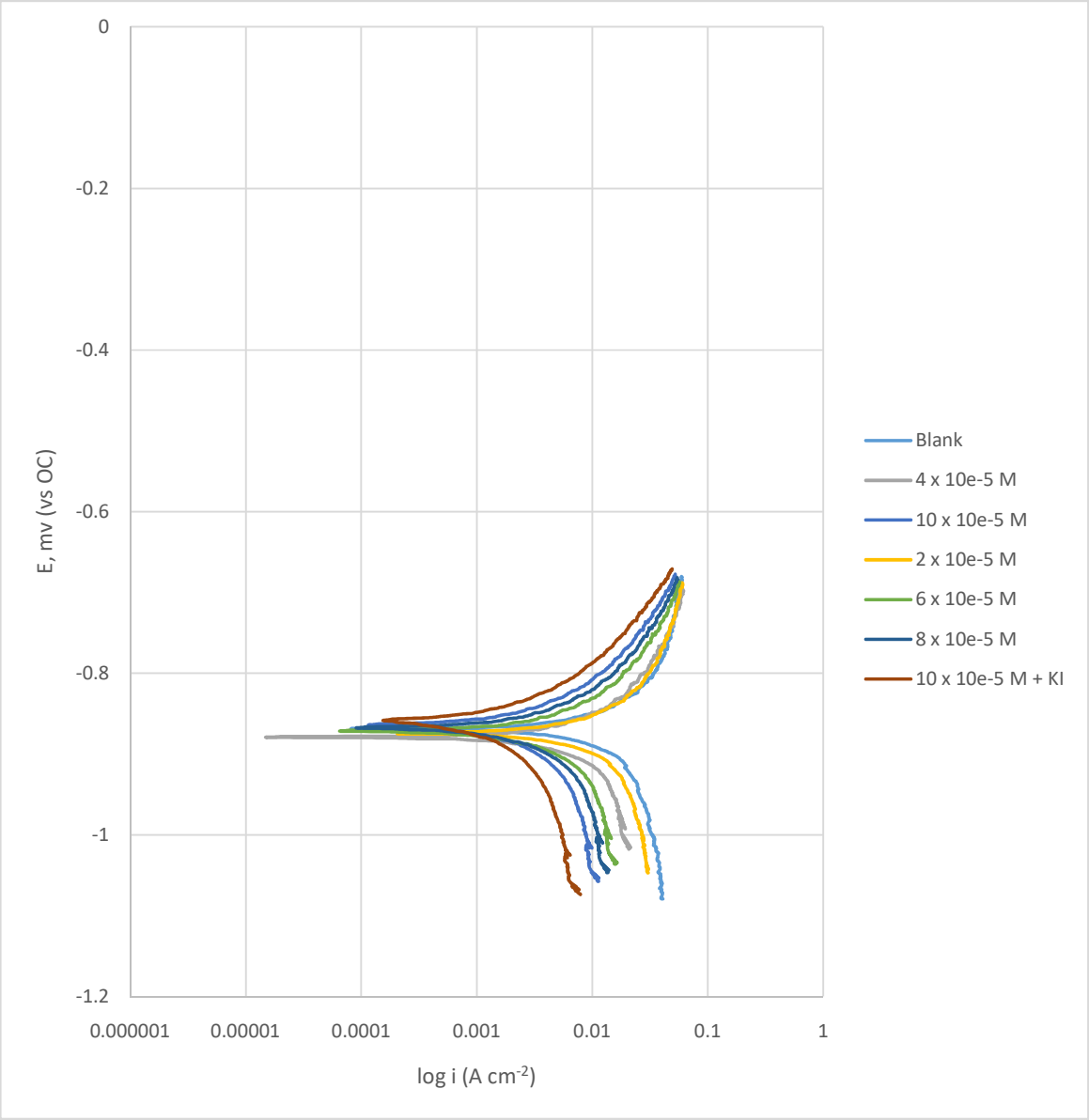

Figure 4.81: Potentiodynamic poilarization curves for low carbon steel in 1 mol/dm^3 HCl containing various concentrations of 4 nitro aniline

Table 4.26: Potentiodynamic polarization (PDP) parameters for low carbon steel in 1mol/dm^3 HCl with various concentrations of 2 nitro aniline.

Concentration (mol/dm^3)	i_{cor} (A cm^{-2})	CR (mmpy)	I.E (%)	Ɵ
Blank	70.948	588.04	-	-
2 x 10^{-5}	47.898	396.994	32.49	0.325
4 x 10^{-5}	44.117	365.656	37.82	0.378
6 x 10^{-5}	40.253	333.630	43.26	0.433
8 x 10^{-5}	34.792	288.370	50.96	0.510
10 x 10^{-5}	29.214	242.135	58.82	0.588
10 x 10^{-5} + KI	15.873	131.561	77.63	0.776

Table 4.27: Potentiodynamic polarization (PDP) parameters for low carbon steel in 1mol/dm^3 HCl with various concentrations of 3 nitro aniline.

Concentration (mol/dm^3)	i_{cor} (A cm^{-2})	CR (mmpy)	I.E (%)	Θ
Blank	70.948	588.04	-	-
2 x 10^{-5}	48.095	398.627	32.21	0.322
4 x 10^{-5}	44.462	368.515	37.33	0.373
6 x 10^{-5}	40.587	336.397	42.79	0.428
8 x 10^{-5}	35.115	291.045	50.51	0.505
10 x 10^{-5}	29.557	244.977	58.34	0.583
10 x 10^{-5} + KI	16.225	134.478	77.13	0.771

Table 4.28: Potentiodynamic polarization (PDP) parameters for low carbon steel in 1mol/dm^3 HCl with various concentrations of 4 nitro aniline.

Concentration (mol/dm^3)	i_{cor} (A cm^{-2})	CR (mmpy)	I.E (%)	Ɵ
Blank	70.948	588.04	-	-
2 x 10^{-5}	48.475	401.777	31.68	0.317
4 x 10^{-5}	44.851	371.740	36.78	0.368
6 x 10^{-5}	40.985	339.677	42.23	0.422
8 x 10^{-5}	35.503	294.261	49.96	0.500
10 x 10^{-5}	29.985	248.525	57.74	0.577
10 x 10^{-5} + KI	16.628	137.818	76.56	0.766

4.15 Potentiodynamic Polarization Measurements of nitro aniline compounds

Figures 4.79, 4.80 and 4.81 illustratesthe Tafel polarization curves for low carbon steel in 1 mol/dm^3 HCl in the absence and presence of different concentrations of nitro aniline compounds and in the absence and presence of 5 x 10^{-3} mol/dm^3 KI at 303K, respectively. From Figures 4.79, 4.80 and 4.81, it is shown that both anodic reaction (i.e metal dissolution) and cathodic reaction (i.e H_2evolution) were inhibited when nitro aniline compounds in the absence and presence of 5 x 10^{-3} mol/dm^3 KI at 303K, respectively were introduced to 1 mol/dm^3 HCl with the strength of inhibition increasing as inhibitor concentration increases. Tafel lines of inhibited systems in comparism with the uninhibited system are deflected to more negative and more positive potentials which increases with rise ininhibitor concentration. This act suggest that the organic moleculesbehave as mixed-type inhibitors (Fouda *et al.,* 2006).

The results in Table 4.26, 4.27 and 4.28 reveals that the rise in concentration of inhibitor leads to decrease in corrosion current density (icorr) and corrosion rates, (Migahed et al, 2009). The addition of KI further decreases the icorr values and increases the inhibition efficiency of the nitro aniline compounds considerably. The results obtained from polarization measurements are in agreement with that from weight loss and hydrogen evolution methods. The order of reducing inhibition efficiency of the studied molecules is as follows: 2 nitro aniline >3 nitro aniline >4 nitro aniline.

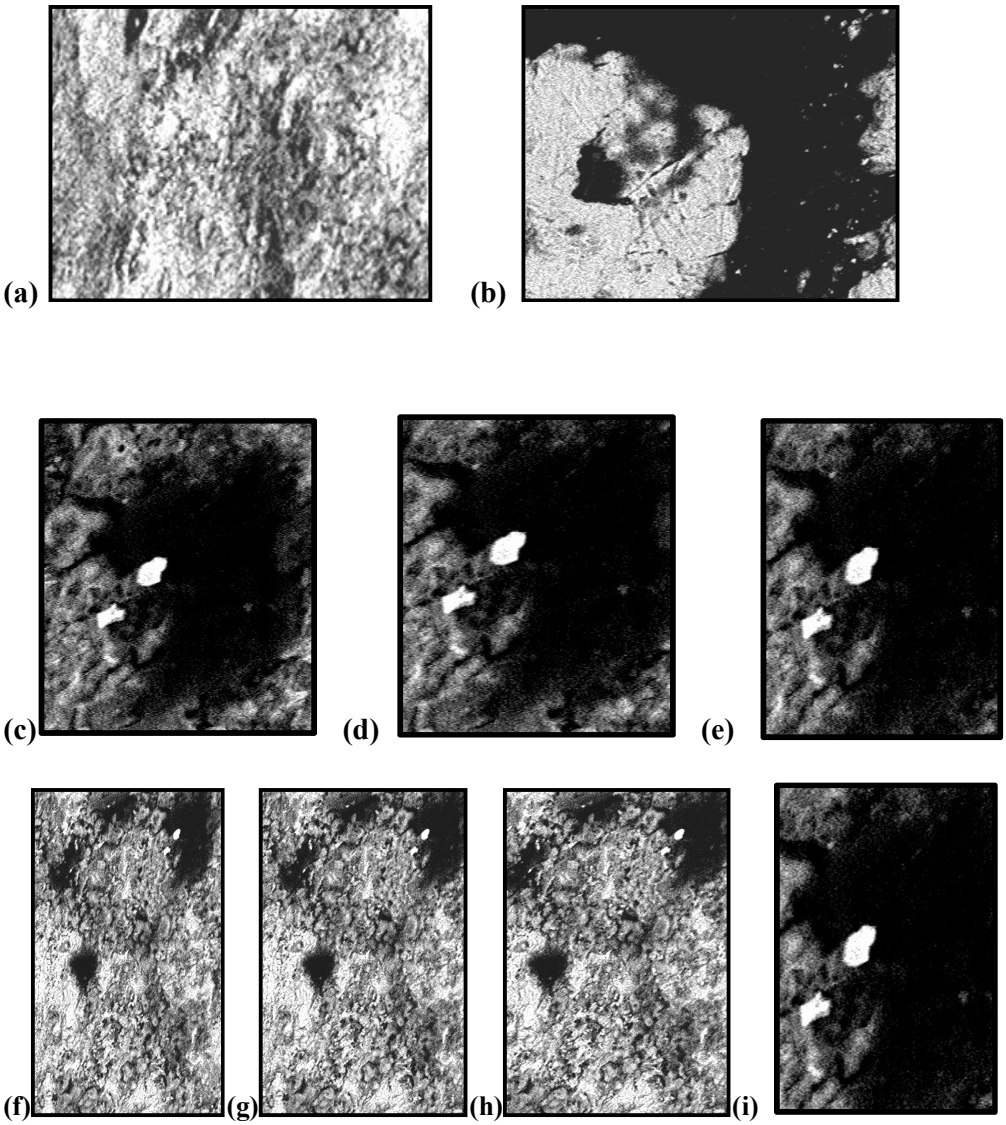

Fig 4.82: SEM characteristics of the low carbon steel in 1.0 mol/dm^3 HCl in (a) low carbon steel in the absence of inhibitor and acid, (b) low carbon steel in the presence of acid only (c) low carbon steel in the presence of 2 nitro aniline and acid, (d) low carbon steel in the presence of 3 nitro aniline and acid (e) low carbon steel in the presence of 4 nitro aniline and acid (f) low carbon steel in the presence of 2 nitro aniline, KI and acid, (g) low carbon steel in the presence of 3 nitro aniline KI and acid, (h) low carbon steel in the presence of 4 nitro aniline, KI and acid (i) low carbon steel in the presence of KI and acid.

4.16 Scanning electron microscopy of nitro aniline compounds

The scanning electron microscopy (SEM) image in Fig 4.82 reveals that corrosion does not occur homogeneously over the surface of low carbon steel in 1 mol/dm^3 HCl solution. However, the surface is significantly protected by the nitro aniline compounds in comparism to the inhibitor – free solution. The inhibition efficiency of the nitro aniline compounds are further enhanced by the addition of 5 x 10^{-3}mol/dm^3 KI asshown in Fig 4.82.

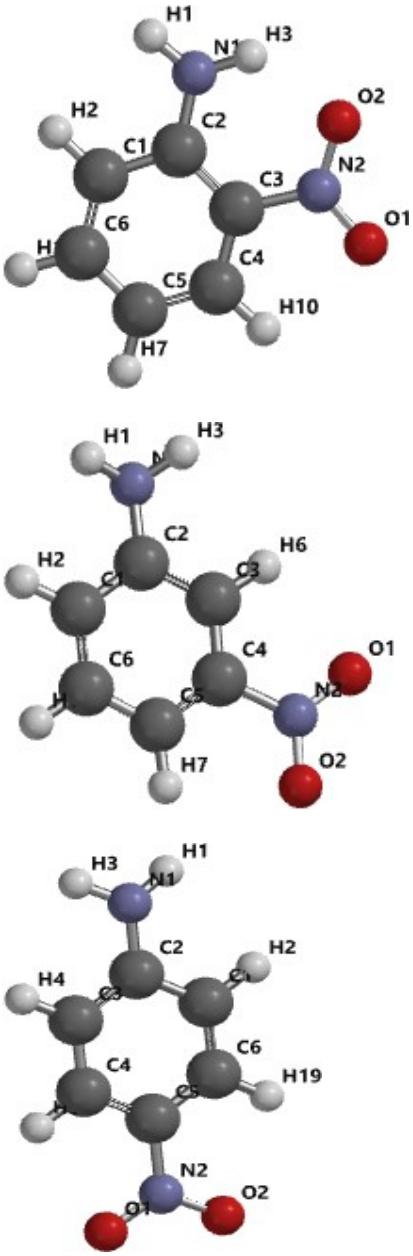

Fig 4.83: Labelled optimised structures of nitro aniline compounds

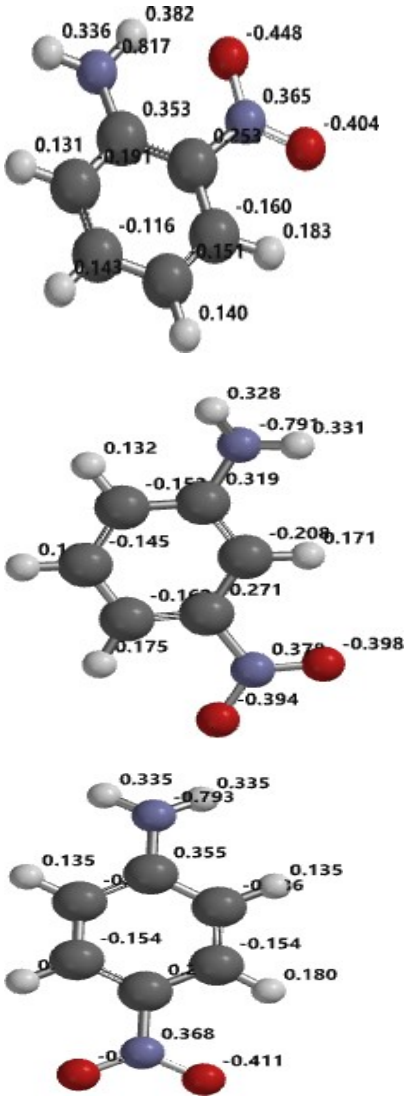

Fig 4.84: Optimised molecular structures of nitro aniline compounds showing mulliken charges.

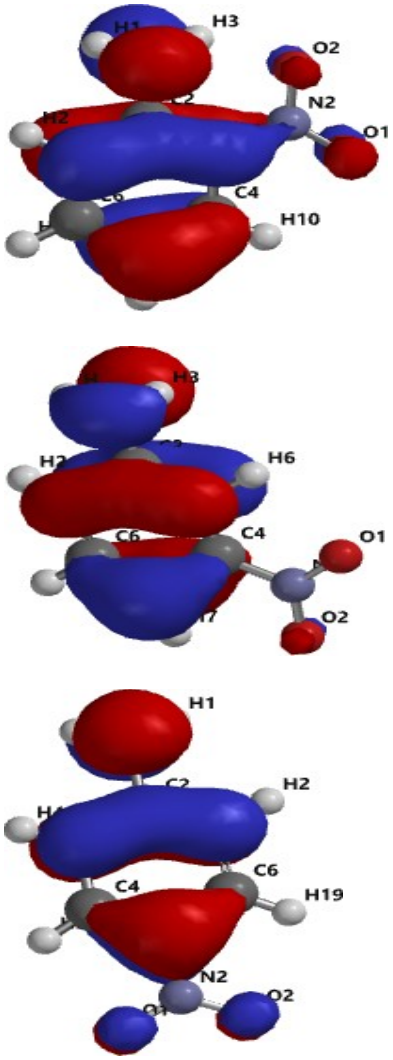

Fig 4.85: HOMO plot of optimised molecules of nitro aniline compounds

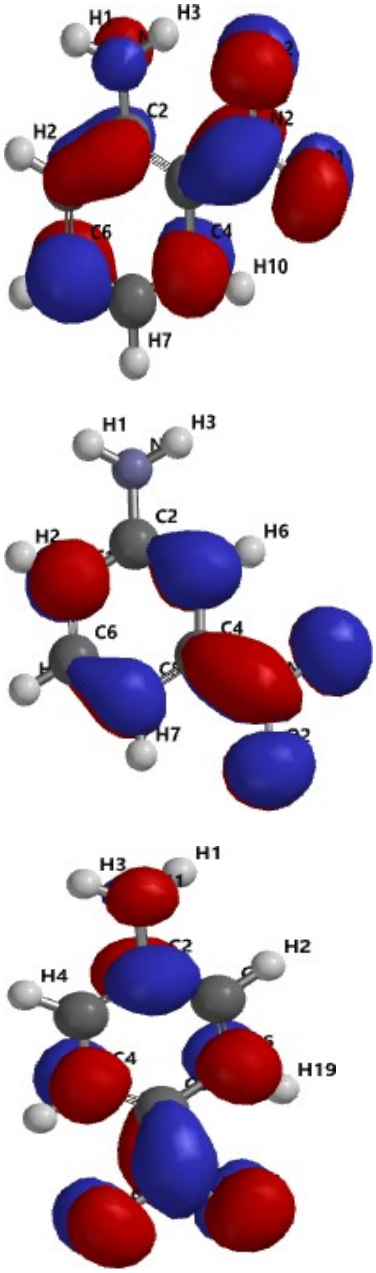

Fig 4.86: LUMO plot of optimised molecules of nitro aniline compounds

Table 4.29: Quantum chemical parameters of Nitro aniline derivatives using DFT method

Quantum chemical parameters	2 nitro aniline	3 nitro aniline	4 nitro aniline
E_{Homo} (eV)	-6.06	-6.14	-6.25
E_{Lumo} (eV)	-2.17	-2.24	-1.96
$E_{Lumo} - E_{Homo}$ (eV)	3.89	3.90	4.29
Dipole moment (μ)	4.74	5.65	7.12
Log P	-4.35	-4.35	-4.35
Polarizability	51.02	51.10	50.99
Volume ($Å^3$)	130.30	131.19	131.12
Weight (amu)	138.126	138.126	138.126
Ionisation Potential (*I*)	6.06	6.14	6.25
Electron Affinity (*A*)	2.17	2.24	1.96
Hardness(η)	1.94	1.95	2.145
Softness (*S*)	0.514	0.513	0.466
Electronegativity(χ)	4.115	4..190	4.105
Chemical potential (μ)	-4.115	-4.190	-4.105
Electrophilicity Index (ω)	4.353	4.502	3.928

4.17 Quantum chemical study of orto, meta and 4 nitro aniline

The inhibition efficiency of the aniline derivatives have been measured experimentally. Quantum chemical indices calculated includes: energies of frontier molecular orbitals (E_{HOMO} and E_{LUMO}), separation energy ($E_{LUMO} - E_{HOMO}$), dipole moment, substituent constant (log p), polarizability, molecular volumes and molecular weights are tabulated in Table 4.29.

It is seen from the molecular structure that the nitro aniline compounds have the amino group which pocess basic properties because of the available lone pair of electrons of the nitrogen atom. The significance of this basic properties of NH_2 group is that complexes of amine with metal ions could be foarmed (Adejoro *et al.,* 2016).

The quantum indices calculated reveal that 2 nitro aniline with E_{HOMO} and the E_{LUMO} energies at -6.06eV and -2.17eV, respectively and separation energy of 3.89eV this clearly marks 2 nitro aniline a corrosion inhibitor with slightly higher reactivity toward the metal surface as compared to 3 nitro aniline and 4 nitro aniline. The effect of nitro substituent on the meta and para position in the nitro aniline shows that the separation energy increases to 3.90eV for 3 nitro aniline and 4.29eV for 4 nitro aniline. Similar quantum chemical values were calculated for log p, polarizability, molecular weight and molecular volume except for dipole moment. These results are consistent with experimental results. This great inhibiting potential could also be attributed to the aromatic ring having sufficient π electrons thereby reducing the gap between the E_{HOMO} and E_{LUMO} orbitals. The calculated Mulliken charge shows that the nitrogen atom of the amine group and the oxygen atom could act as active centres for the adsorption of the nitro aniline compounds on the surface of the metal. The charge distribution charge over the entire molecule is presented in Figure 4.84.

Molecular orbital calculations weredone to determine the coefficients of the HOMO and LUMO levels for the investigated indole derivatives as corrosion inhibitors to further throw more light on the mechanism of their adsorptions on the surface of the metal. Fig 4.85 shows the plot of the HOMO electronic density distribution for the nitro aniline compounds. It is observed from calculations that the highest coefficients are found on the nitrogen atom of the amino group and the phenyl moiety which can be denoted as active adsorption sites of the inhibitors. The adsorption of nitro aniline compoundstook place via the lone pairs of electrons of the nitrogen (N_1) atom, oxygen

atom and π charges of the phenyl moiety.It is obvious that more than one adsorbed site could be obtained from one molecule of nitro aniline compounds. It was understood from Langmuir isotherm plots, which indicates a multi-centre adsorption on the iron surface. The deviation of the slope from unity suggest that active centres influencing adsorption per molecule were more than one. This result agreest with quantum calculations (Valdez *et al.,* 2005).

The LUMO plot is shown in Fig 4.86. The highest coefficient is localised on the nitrogen atom which can enable the back donation from the amino group of the inhibitor to the metal. Thus increasing its adsorption on the surface of the metaland consequently the inhibition efficiency increases. The adsorption mechanism of the nitro aniline compounds on the metal surface can be explained as electron donation from inhibitor molecule to the vacant d orbitals of the Fe atom and back donation from the d-orbital of the Fe atom to the π antibonding counterpart of the organic molecule. In summary the results suggest that the nitro aniline compounds are adsorbed on the surface of the metal via the nitro group, amine group and highly electronegative nitrogen atom, the oxygen atom and the π charge of the phenyl moieties.

Table 4.30 Inhibition Efficiency: Experimental and Predicted Values

Molecules	**Experimental (%)**	**Predicted (%)**
6-benzyloxyindole	92.29	91.55
3-methylindole	86.32	85.65
2-nitroaniline	52.24	52.24
3-nitroaniline	51.37	51.69
4-nitroaniline	50.50	50.94

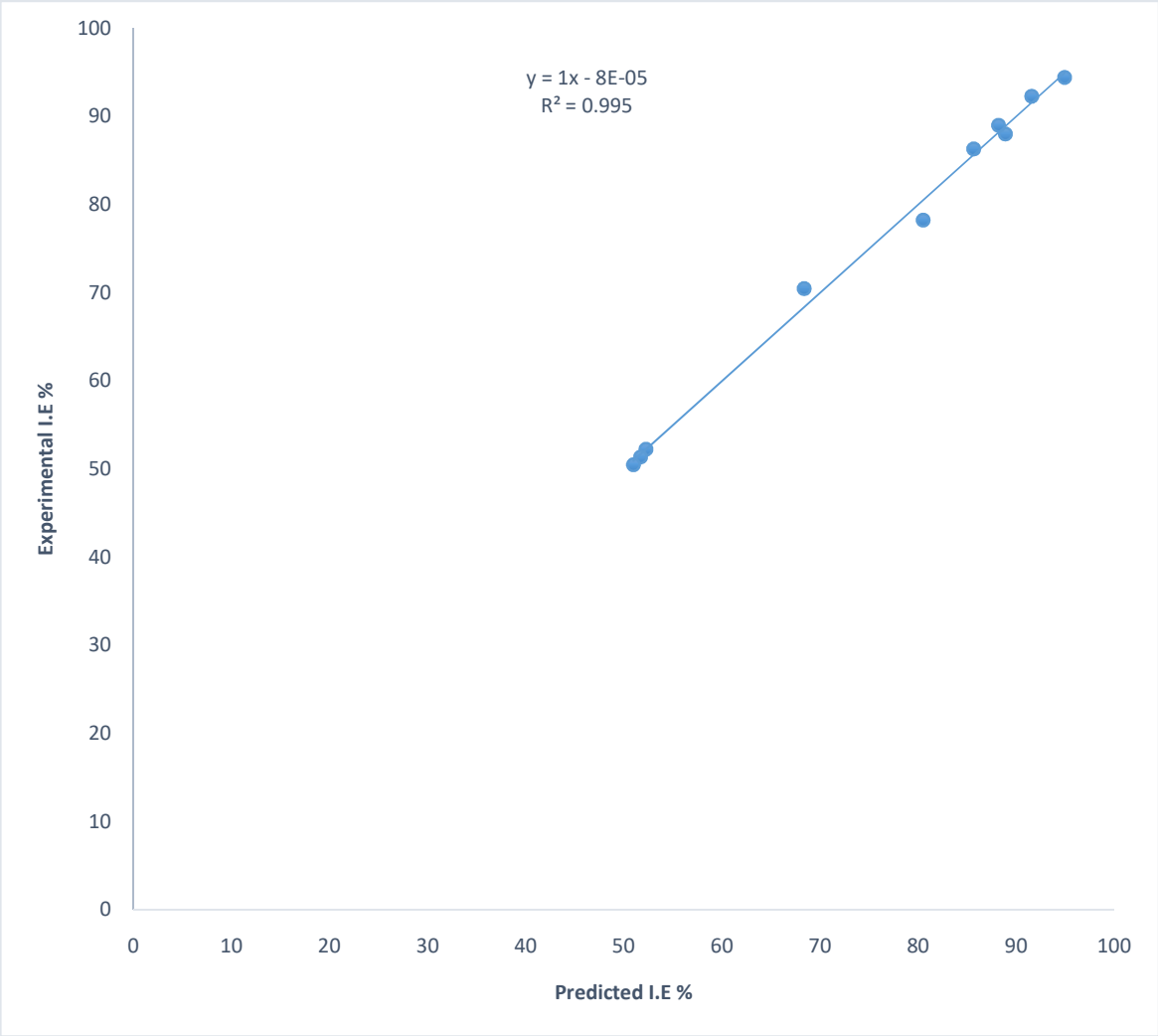

Fig 4.87: Plot ofExperimental inhibitionefficiency vs Theoretical inhibition efficiency

4.18 QuantitativeStructuralActivityRelationshipModelling (QSAR).

The significance of QSAR model hangs on the fitting and prediction ability. Since each molecular index calculated does not correlate with the %IE of the molecule, thus it was necessary to combine some of the quantumchemical indices into QSAR model, this is done because there could be several inter-related factors contributing to the molecules as corrosion inhibitors. In this approach, an equation which relates the quantum chemical parameters to the observed activity is formulated. The linear equation shown in equation 2.5, is often used in the study of corrosion inhibitors to relate the quantum molecular parameters with the experimental inhibition efficiency of the inhibitors (Lukovits, *et al.,* 2001). The QSAR model represented in equation 4.20 shows that the combination of the E_{HOMO}, E_{LUMO}, separation energy (ΔE), dipole moment (μ), log P, polarizability (pol), softness (*S*) and hardness (η)are the quantum chemical indices that describe the corrosion inhibition efficiency of the molecules.

$$\%IE = -337.913 - 5.96\,\mu - 116.63\,S - 59482.4\,\eta + 29742.6\,\Delta E + 1.98\log P + 6.55\mathrm{pol} - 24.72\,E_{HOMO} \qquad 4.20$$

This QSAR model was used to predict percentage inhibition efficiency, the predicted %IE were compared with the experimental %IE of the compounds as revealed in Table 4.30. A good fit (R^2 = 0.996) between the experimental and theoretical inhibition efficiencies was observed as shown in Fig 4.87.

CHAPTER FIVE

CONCLUSION AND RECOMMENDATION

5.1 Conclusions

The corrosion inhibition studies of low carbon steel in 1 mol/dm^3 HCl using some indole derivatives (Set A inhibitors) and nitro aniline derivatives (Set B inhibitors) namely 6 benzyl oxy indole, 3 methyl indole, 2 nitro aniline, 3 nitro aniline and 4 nitro aniline were investigated using weight loss method (gravimetric), hydrogen gas evolution method (gasometric), potentiodynamic polarization method (electrochemical) and quantum chemical studies (theoretical). The Set B inhibitors were observed to be fairly effective corrosion inhibitors as such synergistic effect with iodide ions was undertaken. The scanning electron microscope (SEM) was also employed to show the rate of corrosion. The quantum chemical indices of set A and B organic inhibitors were also investigated.

The following conclusions can be drawn from this study:

i. All the organic compounds studied act as effective corrosion inhibitor of low carbon steel in 1 mol/dm^3 HCl.
ii. Inhibition efficiency (I.E %) values rises with rise in inhibitor concentration and drops with rise in temperature.
iii. The activation energies gotten for the inhibited corrosion of low carbon steel are within the limit expected (< 80 KJ/mol) for the mechanism of physiosorption.
iv. ΔG^{o}_{ads} valuesgotten from this research ranged from -8.80 to -4.514kJmol^{-1}, which supports the mechanism of physiosorption.
v. Q_{ads} values calculated are all negative, suggesting that the adsorption of these indole derivatives and nitro aniline compounds on low carbon steel is exothermic.

vi. The inhibition of low carbon steel in 1 mol/dm^3 HCl solution was found to obey Langmuir adsorption isotherm.

vii. The rates of hydrogen gas evolution were observed to reduce with rising inhibitor concentration, indicating that the inhibition depends on concentration.

viii. Tafel polarization curves reveals that both anodic metal dissolution and cathodic hydrogen gas evolution reactions were inhibited when studied inhibitors were added to 1 mol/dm^3 HCl at 303K and this inhibition increases with rising inhibitor concentration.

ix. Tafel lines are shifted to more negative and more positive potentials with respect to the blank curve by raising the concentration of the studied inhibitors. This act indicates that the organic moleculesbehave as mixed-type inhibitors.

x. The results from electrochemical method reveal that the rise in inhibitor concentration results to reduction in the corrosion current density (icorr) and corrosion rates.

xi. The inhibition efficiency obtained from all the experimental methods are consistent and follows the order: 6 benzyl oxy indole > 3 methyl indole > 2 nitro aniline > 3 nitro aniline > 4 nitro aniline.

xii. It was established that the synergistic inhibitive influencedue to the presence of nitro aniline compounds in combination with potassium iodide (KI) on the corrosion of low carbon steel in 1 mol/dm^3 HCl at 303K further enhanced the inhibition efficiency of nitro aniline derivatives.

xiii. The scanning electron microscopy (SEM) images reveal that the corrosion process did not take place homogeneously over the surface of low carbon steel in 1 mol/dm^3 HCl solution.

xiv. SEM images also show that the surface of low carbon steel is protected by the investigated organic molecules in comparism to the inhibitor – free solution and it reveals that the inhibition efficiency of the nitro aniline compounds are further enhanced by the addition of 5 x 10^{-3}mol/dm^3 KI.

xv. Quantum chemical indicescorrelated well with the experimental inhibition efficiency as observed.

xvi. The inhibition efficiency of the studied organic molecules rises with rising E_{HOMO}, decreasing E_{LUMO}, decreasing E_{LUMO}-E_{HOMO}, increasing Dipole moment, increasing Log p, increasing Polarizability, increasing Softness and decreasing Hardness.

5.2 Recommendations

1. Detailed study of the molecular structure of the organo-iron complexes responsible for the inhibition should be undertaken.
2. Other electrochemical methods such as Electrochemical Impedance Spectroscopy (EIS) and Electrochemical frequency modulation measurements (EFM) techniques should be use to futher ascertain the validity of the results obtained.
3. The corrosion inhibition studies of theses investigated organic inhibitors should be carried out in other aqueous media such as alkaline and neutral media.
4. The inhibitory action of studied inhibitors should be tested on other metals/alloys e.g aluminum, zinc, copper and brass.

REFERENCES

Abboud, Y., Abourriche, A., Saffaj, T., Berrada, M., Charrouf, M., Bennamara, A. and Hannache, H. 2009. A novel azo dye, 8-quinolinol-5-azoantipyrine as corrosion inhibitor for low carbon steel in acidic media. *Desalination*. 247: 175-188

Abdallah, M. 2004. Antibacterial drugs as corrosion inhibitors for corrosion of aluminium in hydrochloric solution. *Corrosion Science*. 46: 1981-1992.

Abiola, O.K. 2006. Adsorption of 3-(4-amino-2-methyl-5-pyrimidyl methyl)-4-methyl thiazolium chloride on low carbon steel, *Corros. Sci.* 48: 3078–3090.

Adejoro, I.A., Ojo, F.K. and Lori, J.A. 2016. Theoretical Study of the Efficiency of Some Nitro Aniline Derivatives in Acidic Medium to Serve as Excellent Organic Corrosion Inhibitors of Low carbon Steel. *International Research Journal of Pure & Applied Chemistry* 10.1: 1-10.

Adejoro, I.A., Ojo, F.K. and Obafemi, S.K. 2015. Corrosion inhibition potentials of ampicillin for low carbon steel in hydrochloric acid solution. *Journal of Taibah University for Science* 9: 196–202.

Ait Chikh, A., Chebabe, D., Dermaj, A., Hajjaji, N., Srhiri, A., Montemor, M.F., Ferreira, M.G.S. and Bastos, A.C. 2005. Electrochemical and analytical study of corrosion inhibition on carbon steel in HCl medium by 1,12-bis(1,2,4-triazolyl)dodecane, *Corros. Sci.* 47: 447–459.

Ali, S., Reyes, J.S., Samuel, M.M. and Auzerais, F.M. 2010. Self-Diverting Acid Treatment with Formic-Acid-Free Corrosion Inhibitor, in: US Patent 2010/0056405 A1, Schlumberger Technology Corporation, 2010.

Aljourani, J., Raeissi, K. and Golozar, M.A. 2009. Benzimidazole and its derivatives as corrosion inhibitors for low carbon steel in 1 M HCl solution, *Corros. Sci.* 51: 1836–1843.

Ameena, M.A. 2014. Cefadroxil as Save Corrosion Inhibitor for Carbon Steel in Hydrochloric Acid Solutions. *International Journal of Advanced Research* 2.5 522-534.

Ameh, P.O., Magaji, L. and Salihu, T. 2012. Corrosion inhibition and adsorption behavior for low carbon steel by Ficus glumosa gum in H_2SO_4 solution, *J. Pure Appl.Chem.* 6: 100–106.

Arslan, T., Kandemirli, F., Ebenso, E.E., Love, I. and Alemu, H. 2009. Quantum chemical studies on the corrosion inhibition of some sulphonamides on low carbon steel in acidic medium. *Corros. Sci.* 51: 35-47.

Ashassi-Sorkhabi, H., Shaabani, B. and Seifzadeh, D. 2005. Effect of some pyrimidinic Schiff bases on the corrosion of low carbon steel in HCl solution. *Electrochim. Acta* 50: 3446-3452.

Awad, M.K., Issa, R. M., Atlam, F.M. 2009.Theoretical investigation of the inhibition of corrosion by some triazolle Schiff bases. *Material and Corrosion*.60:813-819.

Aydin, R. and Koleli, F. 2006. Hydrogen evolution on conducting polymer electrodes in acidic media. Progress in Organic Coatings. 31: 285.

Aydin, R., Koleli, F. (2006) Hydrogen evolution on conducting polymer electrodes in acidic media. Progress in organic coatings 31: 285

Babic-Samardzija, K., Lupu, C., Hackerman, N. and Barron, A.R. 2005. Inhibitive properties, adsorption and surface study of butyn-1-ol and pentyn-1-olalcohols as corrosion inhibitors for iron in HCl, *J. Mater. Chem.* 15: 1908–1916.

Baddini, A.L.D.Q., Cardoso, S.P., Hollauer, E. and Gomes, J.A.D.C.P. 2007. Statistical analysis of a corrosion inhibitor family on three steel surfaces (duplex, super-13 and carbon) in hydrochloric acid solutions, *Electrochim. Acta* 53: 434–446.

Baeckmann, W.V. 1997. Handbook of cathodic corrosion protection, 3rd edition. McGraw Hill, New York.

Barmatov, E., Geddes, J., Hughes, T. and Nagl, M. 2012. Research on corrosion inhibitors for acid stimulation, in: NACE. C2012–0001573.

Barouni, K., Kassale, A., Albourine, A., Jbara, O., Hammouti, B. and Bazzi. L. 2014. Amino acids as corrosion inhibitors for copper in nitric acid medium: Experimental and theoretical study. *J. Mater. Environ.Sci.* 5.2: 456-463.

Bentiss, F., Lagrenee, M., Traisnel, M. and Homez. J.C. 1999. Corrosion inhibition of low carbon steel in 1 M hydrochloric acid by 2,5-Bis(2-aminophenyl)-1,3,4-oxadiazole. NACE International, corrosion science section, p. 968

Bhardwaj, M. and Balasubramaniam, R. 2008. Uncoupled non-linear equations method for determining kinetic parameters in case of hydrogen evolution reaction following Volmer-Heyrovsky-Tafel mechanism and Volmer-Heyrovsky mechanism. *International journal of Hydrogen Energy*. 33: 2178-2190

Brondel, D., Edwards, R., Hayman, A., Hill, D Mehta, S. and Semerad, T. 1994. Corrosion in the oil industry, *Oilfield Rev.* 6: 4–18.

Cardoso, S.P., Gomes, J.A.C.P., Borges, L.E.P. and Hollauer, E. 2007. Predictive QSPR analysis of corrosion Inhibitors for super 13% Cr steel in Hydrochloric acid, *Braz. J. Chem. Eng.* 24: 547–559.

Cardoso, S.P., Hollauer, E., Borges, L.E.P., Gomes, J.A. 2006. QSPR prediction analysis of corrosion inhibitors in hydrochloric acid on 22%-Cr stainless steel. *J. Braz. Chem. Soc.* 17: 1241–1249.

Chilingar, G.V. and Beeson C.M. 1969. Surface operations in petroleum production. American Elsevier, New York, p 397

Cruz, J., Martı ´nez, R., Genesca, J. and Garcı´a-Ochoa, E. 2004. Experimental and theoretical study of 1-(2-ethylamino)-2-methylimidazoline as an inhibitor of carbon steel corrosion in acid media, *J. Electroanal. Chem.* 566: 111–121.

Cruz, J., Pandiyan, T. and García-Ochoa, E. 2005. A new inhibitor for low carbon carbon steel: electrochemical and DFT studies, *J. Electroanal. Chem.* 583: 8–16.

De Waard, C. and Lotz, U. 1994. Prediction of CO_2 corrosion of carbon steel. EFC publication number 13. The Institute of Materials, London

Dewar M.J.S. Zoebisch E.G., Healy E.H. and Stewart J.P. 1985. The development and use of quantum mechanical molecular models. 76. AMI: a new general purpose quantum mechanical molecular model. *J. Am. Chem Soc*.107: 3902.

Dewar, M.J.S. and Thiel, W. 1977. Ground states of molecules.38. The MNDO method. Approximations and parameters, J. Am. Chem. Soc. 107:3902-3909.

Dewar, M.J.S., Butterworths. 1971. Elementary Electrochemistry, (2nd ed).

Dugstad, A. 1992. The importance of $FeCO_3$ supersaturation on the CO_2 corrosion of carbon steels, corrosion″92, paper 14. NACE, Houston

Dunlop, A., Hassel H.L. and Rhodes P.R. 1984. Fundamental considerations in sweet gas well corrosion, 1st edition. NACE, Houston, p 52

Ebenso, E. 2003. Effect of Halide ions on the corrosion inhibition of low carbon steel in H_2SO_4 using methyl red. Part 1, *Bull Electrochem.*19: 209-216.

Ebenso, E.E., Alemu, H., Umoren, S.A. and Obot, I.B.2008. Inhibition of mild steel corrosion in sulphuric acid using alizarin yellow GG dye and synergistic iodide additive. *International Journal of Electrochemical Science* 3: 1325-1340

Ebenso, E.E., Arslan, T., Fatma, K., Love, I., Cemil, O., Murat, S. and Umoren, S.A. 2010. Theoretical studies of some sulphonamides as corrosion inhibitors. International Journal of Quantum Chemistry. 110: 2614–2636.

Ebenso, E.E., Ibok, U.J., Umoren, S.A., Jackson, E., Abiola, O.K., Oforka, N.C. and Martinez, S. 2004. Corrosion inhibition studies of some plant extracts on aluminium in acidic medium. Trans. SAEST, 39: 117-123

Ebenso, E.E., Isabirye, D.A. and Eddy, N.O. 2010. Potentials of Some Thiosemicarbazides for the Corrosion of Low carbon Steel in Acidic Medium. *Int. J. Mol. Sci.* 11: 2473-2498.

Ebenso, E.E., Isabirye, D.A. and Eddy, N.O. 2010.Adsorption and quantum chemical studies on the inhibition potentials of some thiosemicarbazides for the corrosion of low carbon steel in acidic medium, *Int.J. Mol. Sci.* 11: 2473–2498.

Eddy, N.O. and Ebenso, E.E. 2010. Adsorption and Quantum Chemical Studies on Cloxacillin and Halides for the Corrosion of Low carbon Steel in Acidic Medium.*Int. J. Electrochem. Sci.* 5: 731 – 750

Eddy, N.O. and Ebenso, E.E. 2010. Adsorption and Quantum Chemical Studies on Cloxacillin and Halides for the Corrosion of Low carbon Steel in Acidic Medium.*Int. J. Electrochem. Sci.* 5: 731 – 750

El Maghraby, A.A. and Soror, T.Y. 2003. Quaternary ammonium salt as effective corrosion inhibitor for carbon steel dissolution in sulphuric acid media, *Adv. Appl. Sci. Res.* 1 2: 143–155.

Elachouri, M., Hajji, M.S., Kertit, S., Essassi, E.M., Salem, M. and Coudert, R. 1995. Somesurfactants in the series of 2-(alkyldimethylammonio) alkanol bromides as inhibitors of the corrosion of iron in acid chloride solution, *Corros. Sci.* 37: 381–389.

Erika, C. (2012) Development of Accelerated Corrosion Tests Involving Alternative Exposure to Hostile Gases, Neutral Salt Spray and Drying. M.Sc. Dissertation, Chalmers University of Technology, Goteborg.

Fekry, A.M. and Ameer, M.A. 2010. Corrosion inhibition of low carbon steel in acidic media using newly synthesized heterocyclic organic molecules. *International Journal of Hydrogen Energy.* 35: 7641-7652

Flores, E.A. Olivares, O., Likhanova, N.V., Domínguez-Aguilar, M.A., Nava, N., Guzman-Lucero, D. and Corrales, M. 2011. Sodium phthalamates as corrosion inhibitors for carbon steel in aqueous hydrochloric acid solution, *Corros. Sci.* 53: 3899–3913.

Fouda A.S., Al-Sarawy A.A. and El-Katori E.E. 2006. pyrazolone derivatives as corrosion inhibitor for C-steel HCl solution, *Desalination.* 201: 1-13

Fouda, A.S., Shalabi, K. and Elmogazy, H. 2014. Corrosion inhibition of α-brass in HNO_3 by indole and 2-oxyindole. *J. Mater. Environ. Sci.* 5 (6) 1691-1702

French, E. C., Martin, R. L., Dougherty, J. A. 1993. Corrosion and Its Inhibition in Oil and Gas Wells, in Raman, A., and Labine, P. (eds.), *Reviews on Corrosion InhibitorScience and Technology,* Houston, Tex., NACE International, , pp. II-1-1–II-1-25.

Frenier, W.W. 1992. Process and Composition for Inhibiting High-Temperature Iron and Steel Corrosion, in: US Patent 5,096,618, Dowell Schlumberger Incorporated, Tulsa, Okla,

Fukui K., 1975. Theory of Orientation and Stereo selection, Springer-Verlag, New York.

Gatzky, LK. and Hausler, R.H. 1984. A novel correlation of tubing corrosion rates and gas production rates. Adv in CO_2 Corro 1:87

Gece, G. 2011. Drugs a review of promising novel. *Corrosion science.* 53: 3873-3898

Gokhan, G. 2008. The use of quantum chemical methods in corrosion inhibitor studies. *Corrosion Science.* 50: 2981-2992.

Graeme, W. 2010. Corrosion protection of metals in marine environment. J. Metal Corrosion Protection, Chemistry Department, University of Auckland

Gruber, C. and Buss, V. 1989. Quantum-mechanically calculated properties for the development of quantitative structure-activity relationships (QSA'S). pKA values of phenols and aromatics aliphatic carboxylic acids, *Chemosphere* 19:1595-1609.

Guyer, J.P. 2009. An introduction to cathodic protection. Continuing Education and Development Inc., New York

Hill, D.G. and Jones, A. 2003. An engineered approach to corrosion control during matrix acidizing of HTHP sour carbonate reservoir, Corrosion. Paper No. 03121.

Hill, D.G. and Romijn, H. 2000. Reduction of risk to the marine environment from oilfield chemicals: environmentally improved acid corrosion inhibition for well stimulation, Corrosion (2000). Paper No. 00342.

Hmamou, D.B., Salghi, R., Zarrouk, A., Messali, M., Zarrok, H., Errami, M., Hammouti, B., Bazzi, L. and Chakir, A. 2012. Inhibition of steel corrosion in hydrochloric acid solution by chamomile extract, *Der Pharma Chem.* 4: 1496–1505.

Hohenberg, P. and Kohn, W. 1964. Inhomogeneous electron gas, Phys.Rev. 136 : 864-871.

Hovsepian, P.E., Lewis, D.B., Munz, W.D., Lyon, S.B. and Tomlinson, M. 1999. Combined cathodic arc/unbalanced magnetron growth CrN/NbN super lattice coatings for corrosion resistant applications. *Surf Coat Tech* 120(121):535–541

Huizinga, S. and Liek, W.E. 1994. Corrosion behavior of 13% chromium steel in acid stimulations, *Corrosion* 50: 555–566.

Iran, S. and Hossein, N. 2009. Theoretical study on the structural effect of some organic compounds as corrosion inhibitors on low carbon steel in acid media.*Chem. soc. of Ethiop*.23(2):309-313.

Issa, R.M., Award, M.K. and Atlam, F.M. 2009. DFT theoretical studies of antipyrine schiff bases as corrosion inhibitors. *Materials and Corrosion* 60:1-6.

Ita, B.I and Offiong, O.E. 1997. The inhibition of low carbon steel corrosion in hydrochloric acid by 2,2' -pyridil anda-pyridoin, *Mater. Chem. Phys.* 51: 203–210.

Ita, B.I., Offiong, O.E. 2001. The study of the inhibitory properties of benzoin, benzil, benzoin-(4-phenylthiosemicarbazone) and benzil-(4-phenylthiosemicarbazone) on the corrosion of low carbon steel in hydrochloric acid, *Mater. Chem. Phys.* 70: 330–335.

Jayaperumal, D. 2010. Effects of alcohol-based inhibitors on corrosion of low carbon steel in hydrochloric acid, *Mater. Chem. Phys.* 119: 478–484.

Johansson, E., Pettersson, R., Alfonsson, E. and Weisang-Hoinard, F. 2010. Specialty stainless for solving corrosion problems in the oil and gas industry. Offshore World 40

Karelson, M., Lobanov, V.S. 1996. Quantum-Chemical descriptors in QSAR/QSPR studies. *Chem. Rev.* 96: 1027–1043.

Kermani, MB, Harrop D. 1996. The impact of corrosion on the oil and gas industry. SPE Production Facilities 11, pp 186–190

Kermani, MB, Smith LM 1997. CO_2 corrosion control in oil and gas production: design considerations. The Institute of Materials, European Federation of Corrosion Publications, London

Khaled, K.F., Amin, M.A. 2009. Electrochemical and molecular dynamics steel simulation studies on the corrosion inhibition of aluminum in molar hydrochloric acid using some imidazole derivatives. *Journal of Applied Electrochemistry*, 39(12): 2553–2568.

Kharshan, M. and Furman, A. 1998. Incorporating vapor corrosion inhibitors (VCI) in oil and gas pipeline additive formulations. NACE, Corrosion 98(236)

Kikuchi, O. 1987. Systematic QSAR procedures with quantum chemical descriptors, Quant. Struct.-Act. Relat. 6: 179-184.

Laoun, B., Niboucha, K. and Serir, L. 2008. Cathodic protection of a buried pipeline by solar energy. Revue des Energies *Renouvelables* 12(1):99–104

Lazzari, L. and Pedeferri, P. 2006. Cathodic protection, 1st edition. McGraw Hill, New York

Lei, G., Guang, Y., Ime, B.O., Xiaohong, L., Xun, S., Wei, S. and Xingwen, Z. 2017. Synergistic Effect of Potassium Iodide with L-Tryptophane on the Corrosion Inhibition of Low carbon Steel: A Combined Electrochemical and Theoretical Study.*Int. J. Electrochem. Sci.,* 12: 166 – 177

Levine, I.N 1991.Quantum Chemistry, Prentice Hall, New Jersey.

Lewis, D.F.V., loannides, C. and Parke, D.V. 1994. Interaction of a series of nitriles with the alcohol-inducible isoform of P450: Computer analysis of structure-activity relationships, Xenobiotica 24:401-408.

Lewis, D.F.V., loannides, C. and Parke, D.V. 1994. Interaction of a series of nitriles with the alcohol-inducible isoform of P450: Computer analysis of structure-activity relationships, *Xenobiotica* 24:401-408.

Lukovits, I., Kalman, E., Zucchi, F. 2001. LKP model of the inhibition mechanism of thiourea compounds, *corrosion* 57: 3-15

Mannan, S. and Patel, S. 2008. A new high strength corrosion resistant alloy for oil and gas applications. Paper presented at NACE Corrosion, New Orleans

Marcus, P., Maurice V. and Strehblow, H.H. 2008. Localized corrosion (pitting): A model of pas-sivity breakdown including the role of the oxide layer nanostructure. *Corrosion Sci-ence.* 50(9) 2698-2704.

Masoud, M.S., Awad, M.K., Shaker, M.A. and El-Tahawy. 2010. The role of structural chemistry in the inhibitive performance of some amino pyrimidines on the corrosion of steel. *Corro. Sci.* 52:2387-2397

Matjaz, F. and Jennifer, J. 2014. Application of corrosion inhibitors for steels in acidic media for the oil and gas industry: A review. *Corrosion Science* 86: 17–41.

Mattson, E. 1996. Basic Corrosion Technology for Scientist and Engineers, second ed., *the Institute of materials*.p 168

Mehdi, E., Wan, J.B., Hamid, K. and Hapipah, M.A. 2012. Corrosion inhibition properties of pyrazolylindolenine compounds on copper surface in acidic media. *Chemistry Central Journal.* 6:163-173.

Migahed M.A., Azzam E.M.S. and Morsy S.M.I. 2009. Electrochemical behaviour of carbon steel in acid chloride solution in the presence of dodecyl cysteine hydrochloride self-assembled on gold nanoparticles, *Corros.Sci.* 51: 1636-1644.

Migahed, M.A. and Nassar, I.F. 2008. Corrosion inhibition of Tubing steel during acidization of oil and gas wells, *Electrochim. Acta* 53 (2008) 2877–2882.

Miksic, B.M., Kharshan, M.A. and Furman, A.Y. 2005. Proceeding of 10th European Symposium of Corrosion and scale inhibitors

Mohamed, K.A. 2013. Quantum chemical studies and molecular modeling of the effect of polyethylene glycol as corrosion inhibitors of an aluminum surface. Canadian Journal of Chemistry 91: 283-291,

Mohd, A. C. 2010. Corrosion Inhibition of 6061 Aluminum Alloy in Acidic Media by Honey. B.Sc. Thesis, University of Malaysia, Pahang.

Morgan, J.H. 1987. Cathodic protection, 2nd edition. McGraw Hill, New York

Murrell, J.N., Kettle, S.F. and Tedder, J.M. 1985. The Chemical Bond, John Wiley & Sons Chichester.

Musa, E.M. and Kamal, K.T. 2015. Computational simulation of the molecular structure of benzimidazole and substituted benzimidazoles as corrosion inhibitors for brass in perchloric acid. *American Journal of Research Communication* 3.4: 143-152.

Nalli, K. 2010. Corrosion and its mitigation in the oil and gas industry. An overview. PM-Pipeliner Report

Nasr-El-Din, H.A., Al-Othman, A.M. Taylor, K.C. and Al-Ghamdi, A.H. 2004. Surface tension of HCl-based stimulation fluids at high temperatures, *J. Petrol. Sci. Eng.* 43: 57–73.

Niamein, P.M., Koffi, A.A. and Trokourey, A. 2012. Adsorption and inhibitive effects of 2-thiobenzylbenzimidazole (TBBI) at aluminum alloy AA3003/1 M hydrochloric acid interface, Int. Res. 429 *J. Pure Appl.Chem.* 4: 268–304.

Nnabuk, O.E., Eno, E.E. and Udo, J.I. 2009. Adsorption and Quantum chemical studies of the inhibitive properties of the Tetracycline for the corrosion of low carbon steel in 0.1M H_2SO_4. *J. Argent. Chem.* Soc.97(2):178-194

Noor, E. A. 2009. Potential of aqueous extract of Hibiscus sabdariffa leaves for inhibiting the corrosion of aluminium in alkaline solutions. *J. Appl. Electrochem.* 39: 1465-1475.

Obot, I.B., Obi-Egbedi N.O. and Umoren S. A. 2009. Adsorption Characteristicsand Corrosion Inhibitive Properties of Clotrimazole for Aluminum Corrosion in Hydrochloric Acid. *Int. J. Electrochem. Sci.*, *4*: 863-877.

Patel, N.S., Jauhariand, S., Mehta, G.N., Al-Deyab, S.S., Warad, I. and Hammouti, B. 2013. Low carbon steel corrosion inhibition by various plant extracts in 0.5M sulphuric acid. *Int. J. Electrochem. Sci.*, *8*: 2635-2655.

Pearson, R.G. 1989. Absolute electronegativity and hardness: applications of organic chemistry, *J. Org. Chem.* 54: 1423-1430

Pearson, R.G. 1989. Absolute electronegativity and hardness: applications of organic chemistry, *J. Org. Chem.* 54: 1423-1430

Popoola, L.T., Grema, A.S., Latinwo, G.K. Gutti, B and Balogun, A.S. 2013. Corrosion problems during oil and gas production and its mitigation. International *Journal of Industrial Chemistry.* 4:35-47

Popova, A., Christov, M. and Zwetanova, A. 2007. Effect of the molecular structure on the inhibitor properties of azoles on low carbon steel corrosion in 1 M hydrochloric acid, *Corros. Sci.* 49: 2131–2143.

Popova, A., Christov, M., Raicheva, S. and Sokolova, E. 2004. Adsorption and inhibitive properties of benzimidazole derivatives in acid low carbon steel corrosion, *Corros. Sci.* 46: 1333–1350.

Popova, A., Sokolova, E., Raicheva, S. and Christov, M. 2003. AC and DC study of the temperature effect on low carbon steel corrosion in acid media in the presence of benzimidazole derivatives, *Corros. Sci.* 45 (2003) 33–58.

Quraishi, M. A., Sardar, N. and Ali, H. 2002. A study of some new acidizing inhibitors on corrosion of N-80 alloy in 15% boiling hydrochloric acid, *Corrosion* 58: 317–321.

Quraishi, M.A. and Jamal, D. 2000. Technical note: CAHMT—a new and eco-friendly acidizing corrosion inhibitor, *Corrosion* 56: 983–985.

Rajeev, P., Surendranathan, A.O. and Murthy, C.S.N. 2012. Corrosion mitigation of the oil well steels using organic inhibitors –a review. *J Mater Environ Sci* 3(5):856–869

Ray, J.D., Randall, B.V. and Parker J.C. 1978. Use of reactive iron oxide to remove H_2S from drilling fluid. 53rd Annu. Fall Tech. Conf. of AIME, Houston

Schmitt, G. 1984. Fundamental aspects of CO_2 corrosion, 1st edition. NACE, Houston, p 10

Shiwei, W.G., Gritis, N., Jackson, A. and Singh, P. 2005. Advanced onshore and offshore pipeline coating technologies. 2005 China international oil and gas technology conference and expo, Shangai, China

Siddiqi, W.A. and Chaubey, V.M. 2008 Corrosion Inhibition Efficiency of 3-Hydroxy-2-Methylquinazoline-4-one on Low carbon Steel in 1 M H_2SO4 and 1 M HCl Acid at Different Temperatures. *J Portugaliae Electrochimica Acta* 26: 221-233

Sieradzki, K. and Newman R.C. 1987. Stress-corrosion cracking. *Journal of Physics and Chemistry of Solids*. 48(11) 1101-1113.

Smith, C. F., Dollarhide, F.E. and Byth, N.B. 1978. Acid corrosion inhibitor: are we getting what we need?, *J Petrol. Technol.* 30: 737–746.

Smith, L. 1999. Control of corrosion in oil and gas production tubing. British Corro J 34(4):247-246

Snavely, E.S. 1971. Chemical removal of oxygen from natural waters. *J Petrol Technol* 23(4):443–446

Solmaz, R. 2010. Investigation of inhibition effect of 5-((E)-4-phenylbuta-1,3-dienylideneamino)-1,3,4-thiadiazole-2-thiol schiff base on low carbon steel corrosion in hydrochloric acid. *Corrosion Science* 52: 3321.

Song, G., Johannesson, B., Hapugoda, S. and St.John D. 2004. Galvanic corrosion of magnesium al-loy AZ91D in contact with an aluminium alloy, steel and zinc. *Corrosion Science*. 46(4) 955-977.

Stewart, J.J.P. 1989. Optimisation of parameters for semiemperical methods I. Method, *J. Comput. Chem.* 10: 209-220

Stoyanova, A.E. and Peyerimhoff, S.D. 2002. On the relationship between corrosion inhibiting effect and molecular structure. *Electrochim. Acta.* 47:1365-1371.

Tang, L., Li, X., Li, L., Qu, Q., Mu, G. and Liu, G. 2005. The effect of 1-(2-pyridylazo)-2-naphthol on the corrosion of cold rolled steel in acid media: Part 1: inhibitive action in 1.0 M hydrochloric acid, *Mater. Chem. Phys.* 94: 353–359.

Theodore, L.B. 2000. Chemistry – the central science new jersey, USA. Pretentice Hall Inc. 67-110.

Trainor, T.P., Chaka, A.M., Eng, P.J., Newville, M., Waychunas, G.A., Catalano, J.G. and Brown, G.E. 2004. Structure and reactivity of the hydrated haematite (0001) surface. *Surf. Sci.* 573: 204–224.

Udhayakala, P., Maxwell, A.S., Rajendiran, T.V. and Gunasekaran, S. 2013. DFT study on the adsorption mechanism of some phenyltetrazole substituted compounds as effective corrosion inhibitors for low carbon steel. *Der Pharma Chemica*. 5(6): 111-124.

Udhayakala, P., Rajendiran, T.V. and Gunasekaran, S. 2012. Theoretical approach to the corrosion inhibition efficiency of some pyrimidine derivatives using DFT method. *Journal of Computational Methods in Molecular Design,* 2(1): 1-15.

Umoren, S.A. and Ebenso, E.E. 2008. Studies of the anti-corrosive effect of Raphia hookeriexudate gum-halide mixtures for aluminium corrosion in acidic medium. *Pigment and Resin Technology.* 37: 173

Valdez, L.M.R., Villafane, A.M. and Mitnik, D.G. 2005. CHIH-DFT theoretical study of isomeric thiatriazoles and their potential activity as corrosion inhibitors. *J. Mol. Struct.: Theochem.* 716:61-65.

Vishwanatham, S. and Haldar, N. 2008. Furfuryl alcohol as corrosion inhibitor for N80 steel in hydrochloric acid, *Corros. Sci.* 50: 2999–3004.

Walker, M.L. 1994. Method and Composition for Acidizing Subterranean Formations, in: US Patent 5,366,643, Halliburton Company, Duncan, Okla.

Wang, C.T., Chen, S.H., Ma, H.Y. and Qi, C.S. 2003. Protection of copper corrosion by carbazole and N-vinylcarbazoleself assembled films in NaCl solution. *J.Appl. Electrochem.* 33: 179-186

Weeter, R.F. 1965. Desorption of oxygen from water using natural gas for counter-current stripping. *J Petrol Technol* 17(5):51-64

Westood, J. 2011. Macro factors driving the global oil and gas industry and the subsea pipelines sector. Toronto

Xia, S., Qiu, M., Yu, L., Liu, F. and Zhao, H. 2008. Molecular dynamics and density functional theory study on relationship between structure of imidazoline derivatives and inhibition performance. *Corros. Sci.* 50: 2021-2029.

Zhou Z. and Parr R.G. 1990. Activation hardness: new index for describing the orientation of electrophilic aromatic substitution, *J. Am. Chem. Soc.* 112: 5720-5724.

APPENDICES

A1: First pages of published articles

Available online at www.sciencedirect.com

ScienceDirect

Journal of Taibah University for Science 9 (2015) 196–202

Journal of Taibah University for Science

www.elsevier.com/locate/jtusci

Corrosion inhibition potentials of ampicillin for mild steel in hydrochloric acid solution

I.A. Adejoro [a], F.K. Ojo [a,b,*], S.K. Obafemi [b]

[a] *Chemistry Department, University of Ibadan, Ibadan, Nigeria*
[b] *Wesley University of Science and Technology Ondo, Nigeria*

Available online 4 November 2014

Abstract

Ampicillin [(2S,6R)-6-(2-(aminomethyl)benzamido)-3,3-dimethyl-7-oxo-4-thia-1-azabicyclo(3.2.0) heptanes-2-carboxylic acid], an antibiotic drug was investigated as corrosion inhibitor for mild steel in HCl using gravimetric method. The results obtained showed that various concentrations of ampicillin studied inhibited the corrosion of mild steel in solutions of HCl. The inhibition efficiency increased with increase in the concentrations of ampicillin and decreased with increase in temperature of which the inhibitor of concentration 5×10^{-3} M at 30 °C had the highest inhibition efficiency of 75.85%. Its adsorption was found to be physical, exothermic and spontaneous as confirmed by values of activation energy and free energy of adsorption (around -20 kJ mol^{-1} for adsorption and below 80 kJ mol^{-1} for activation energy) and also fitted the Langmuir adsorption model. Quantum chemical calculations results show that ampicillin possesses a number of active centers concentrated mainly on the nitrogen atoms and the neighboring C atoms. The HOMO and LUMO plots of ampicillin further present ampicillin as an effective corrosion inhibitor.

Keywords: Corrosion; Ampicillin; Mild steel; Isotherm; Austin model (AM1); Adsorption

1. Introduction

Corrosion is the deterioration of metal by chemical attack or reaction with its environment. It is a constant and continuous problem, often difficult to eliminate completely. Prevention would be more practical and achievable than complete elimination. Corrosion processes develop fast after disruption of the protective barrier and are accompanied by a number of reactions that change the composition and properties of both the metal surface and the local environment, for example, formation of oxides, diffusion of metal cations into the coating matrix, local pH changes, and electrochemical potential. The study of corrosion of mild steel and iron is a matter of tremendous theoretical and practical concern and as such has received a considerable amount of interest. Acid solutions, widely used in industrial acid cleaning, acid descaling, acid pickling, and oil well acidizing, require the use of corrosion inhibitors in order to restrain their corrosion attack on metallic materials [1].

The use of inhibitors is one of the best options of protecting metals against corrosion. Several inhibitors in use are either synthesized from cheap raw material or chosen from compounds having heteroatoms in their aromatic or long-chain carbon system [2]. However, most

* Corresponding author at: Wesley University of Science and Technology Ondo, Nigeria. Tel.: +234 8066052507; fax: +234 073463665.
E-mail address: fktdavid@yahoo.com (F.K. Ojo).

Peer review under responsibility of Taibah University.

Production and hosting by Elsevier

http://dx.doi.org/10.1016/j.jtusci.2014.10.002

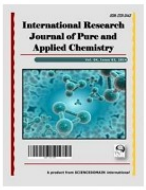

International Research Journal of Pure & Applied Chemistry
10(1): 1-10, 2016, Article no.IRJPAC.20772
ISSN: 2231-3443

SCIENCEDOMAIN *international*
www.sciencedomain.org

Theoretical Study of the Efficiency of Some Nitro Benzenamine Derivatives in Acidic Medium to Serve as Excellent Organic Corrosion Inhibitors of Mild Steel

I. A. Adejoro[1], F. K. Ojo[1*] and J. A. Lori[2]

[1]Department of Chemistry, University of Ibadan, Ibadan, Nigeria.
[2]Department of Chemistry, Bingham University, Karu, Nigeria.

Authors' contributions

This work was carried out in collaboration between all three authors. Author IAA designed the study and wrote the protocol. Author FKO preformed the statistical analysis, managed the literature search and wrote the first draft of the manuscript with assistance from author JAL. All three authors read and approved the final manuscript.

Article Information

DOI: 10.9734/IRJPAC/2016/20772
Editor(s):
(1) Li Cai, Department of Chemistry, University of South Carolina Salkehatchie, USA.
Reviewers:
(1) Anonymous, Institut Teknologi Bandung, Indonesia.
(2) Anonymous, Anhui Normal University, China.
(3) P. Krishnamoorthy, Madras University, India.
Complete Peer review History: http://sciencedomain.org/review-history/11474

Original Research Article

Received 7th August 2015
Accepted 2nd September 2015
Published 19th September 2015

ABSTRACT

A quantum chemical study of the efficiency of some nitro benzenamine derivatives as corrosion inhibitors of mild steel in acidic medium was investigated. Density Functional Theory (DFT) at the B3LYP/6-31G* level was used for the calculation. The calculated quantum chemical parameters related to the inhibition efficiencies are the orbital energies (E_{HOMO} and E_{LUMO}), Separation Energy (E_{LUMO}-E_{HOMO}), Dipole moment (μ), Substituent constant (Log P), Polarizability, molecular volume, molecular weight and mulliken charge of atom. The results showed that the Inhibition Efficiency was closely related to these quantum chemical parameters. Results revealed that 5-(deca-1,3,5,7,9-pentyl)-2-nitrobenzenamine (molecule 6) showed the greatest Inhibition Efficiency (IE) of the Nitro benzenamine derivatives.

**Corresponding author: E-mail: josephlori@yahoo.co.uk;*

JASEM ISSN 1119-8362 Full-text Available Online at https://www.ajol.info/index.php/jasem http://ww.bioline.org.br/ja
J. Appl. Sci. Environ. Manage. Vol. 22 (5) 775– 782 May 2018

Effect of Iodide Ions on the Inhibitive Performance of O-, M-, P-Nitroaniline on Mild Steel in Hydrochloric Acid Solution

[1,2]OJO, FK;[1]ADEJORO, IA;*[3]AKPOMIE, KG;[1,4]OGUNYEMI, BT; [3]OYEKA, EE

[1]*Department of Chemistry (Physical Unit), University of Ibadan, Ibadan, Nigeria*
[2]*Department of Chemical Sciences, Bingham University, Karu, Nigeria*
[3]*Department of Pure & Industrial Chemistry, University of Nigeria, Nsukka, Nigeria*
[4]*Department of Chemistry, Federal University Otuoke, Bayelsa, Nigeria*
*Corresponding Author Email: kovo.akpomie@unn.edu.ng

ABSTRACT: The effect of iodide ions on the inhibitive performance of ortho, meta and para nitro aniline in 1M HCl for mild steel has been studied using weight loss method (gravimetric) measurements at 303 and 333K. Results obtained show that the presence of the nitro aniline compounds in 1M HCl solution inhibits the corrosion process of mild steel. Its adsorption was found to be physical, exothermic and spontaneous as confirmed by values of activation energy and free energy of adsorption (not up to –20 kJ mol^{-1} for free energy of adsorption and below 80 kJ $mol^{-1}$for activation energy) and also fitted the Langmuir adsorption model. Addition of iodide ions synergistically increased the inhibition efficiency of the nitro aniline compounds. Quantitative Structure Activity Relationship (QSAR) approach was used on a composite index of some quantum chemical parameters. The results showed that the Inhibition Efficiency was closely related to some of the quantum chemical parameters.

DOI: https://dx.doi.org/10.4314/jasem.v22i5.32

Dates: Received: 12 April 2018; Revised: 22 April: 2018; Accepted: 26 April 2018

Keywords: Corrosion, Nitroaniline, Iodide ions, Theoretical study.

There has been a growing interest in the use of organic compounds as inhibitors for the aqueous corrosion of metals. The protection of metal surfaces against corrosion is an important industrial and scientific topic. The use of Inhibitor is one of the practical means of preventing corrosion (Adejoro *et al.*, 2015). In acidic media inhibitors can adhere to a metal surface to form a protective barrier against corrosive agent in contact with metal. The effectiveness of inhibitors to provide corrosion protection depends to a large extent on the interaction between the inhibitor and the metal surface (Ameena, 2014). The adsorbed inhibitors can affect the corrosion reaction, either by the blocking effect of the adsorbed inhibitor on the metal surface or by the effect attributed to the change in the activation barriers of the anodic and cathodic reactions of the corrosion process (Eno *et al.*, 2010).

Organic compounds, which can donate electrons to unoccupied *d* orbital of metal surface to form coordinate covalent bonds, can also accept free electrons from the metal surface by using their anti bonding orbital to form feedback bonds, thus constituting excellent corrosion inhibitors. The most effective organic inhibitors are those compounds containing hetero atoms like nitrogen, oxygen, sulfur and phosphorus (Barouni *et al.*, 2014). The presence of aromatic rings and conjugated double bonds could further enhance the effectiveness of these organic compounds as excellent corrosion inhibitors. The inhibitory activity of these molecules is accompanied by their adsorption to the metal surface. The free electron pairs on heteroatom or π electrons are readily available for sharing to form bonds and act as nucleophile centers of inhibitors molecules and greatly facilitate the adsorption process over the metal surface, whose atoms acts as electrophiles.

Recently, the effectiveness of an inhibitor molecule has been related to its spatial as well as its electronic structure. Quantum chemical methods are ideal tools for investigating these parameters and can provide insight into the inhibitor – surface interaction (Musa and Kamal, 2015). The use of orto, meta and para nitro aniline as effective organic inhibitors is interesting and can offer a great deal of solution to the unending corrosion challenge. However, it has not being extensively reported as such few reports exist in literature to date. Thus the aim of this study is to investigate the efficiency of this nitro aniline in combination with potassium iodide with the view of

*Corresponding Author Email: kovo.akpomie@unn.edu.ng

International Research Journal of Pure & Applied Chemistry
12(4): 1-9, 2016, Article no.IRJPAC.28357
ISSN: 2231-3443, NLM ID: 101647669

SCIENCEDOMAIN *international*
www.sciencedomain.org

Theoretical Studies on the Efficiencies of Some Triazolopyrimidine Derivatives as Corrosion Inhibitors of Mild Steel in Acidic Medium Using AM1 and DFT Approach

I. A. Adejoro[1], F. K. Ojo[1] and O. F. Akinyele[2*]

[1]Department of Chemistry, University of Ibadan, Nigeria.
[2]Department of Chemistry, Obafemi Awolowo University, Ile-Ife, Nigeria.

Authors' contributions

This work was carried out in collaboration between all authors. Author IAA designed the study and supervised the work. Author FKO wrote the protocol, preformed the statistical analysis, managed the literature search and wrote the first draft of the manuscript with assistance from author OFA. All authors read and approved the final manuscript.

Article Information

DOI: 10.9734/IRJPAC/2016/28357
Editor(s):
(1) Wenzhong Shen, State Key Laboratory of Coal Conversion, Institute of Coal Chemistry, CAS, China.
Reviewers:
(1) C. Mary Anbarasi, Jayaraj Annapackiam College for Women (A), Periyakulam, Theni, Tamil Nadu, India.
(2) Hao Wang, Northeastern University, China.
Complete Peer review History: http://www.sciencedomain.org/review-history/16167

Review Article

Received 15th July 2016
Accepted 30th August 2016
Published 12th September 2016

ABSTRACT

A quantum chemical study of the efficiency of some Triazolopyrimidine derivatives as corrosion inhibitors of mild steel in H_2SO_4 was investigated. The AM1 semi-empirical method and Density Functional Theory (DFT) at the B3LYP/6-31G* level were used. The calculated quantum chemical parameters related to the inhibition efficiencies are the orbital energies (EHOMO and ELUMO), Separation Energy (ELUMO-EHOMO), Dipole moment (μ), Log P, Polarizability, Hardness (η) and Softness (S). A good correlation between the quantum chemical parameters and the experimental inhibition efficiency was observed. Quantitative Structure Activity Relationship (QSAR) approach was used on a composite index of some quantum chemical parameters to characterize the inhibition performance of the studied molecules. The results showed that the Inhibition Efficiency was closely related to some of the quantum chemical parameters. The calculated (theoretical)

**Corresponding author: E-mail: ofakins@yahoo.com;*

A2: Statistical analysis of the model

Statistical analysis

Model 51: OLS, using observations 1-10
Dependent variable: IE

	Coefficient	*Std. Error*	*t-ratio*	*p-value*	
const	-337.913	78.5543	-4.3017	0.05002	*
U	-5.95789	1.24391	-4.7896	0.04093	**
S	-116.628	22.3989	-5.2069	0.03496	**
H	-59482.4	12825.3	-4.6379	0.04348	**
L_E	29742.6	6414.22	4.6370	0.04350	**
logp	1.97999	0.610259	3.2445	0.08330	*
pol	6.54801	0.838434	7.8098	0.01600	**
Homo	-24.7237	5.22265	-4.7339	0.04184	**

Mean dependent var	75.28700	S.D. dependent var	17.87760
Sum squared resid	12.42609	S.E. of regression	2.492598
R-squared	0.995680	Adjusted R-squared	0.980560
F(7, 2)	65.85340	P-value(F)	0.015038
Log-likelihood	-15.27545	Akaike criterion	46.55090
Schwarz criterion	48.97158	Hannan-Quinn	43.89542

where: * significant

** highly significant

$\alpha = 0.05$

A3: Molecular structure of simulated indole derivatives

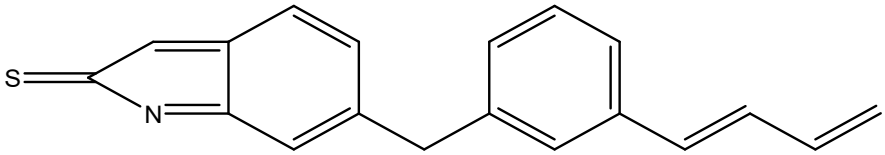

6-(3-((*E*)-buta-1,3-dienyl)benzyl)-2*H*-indole-2-thione [A]

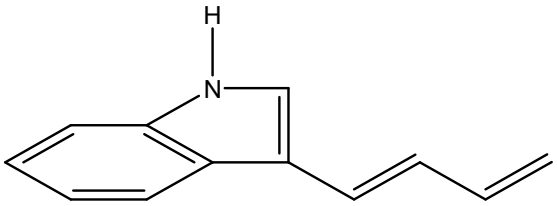

3-((*E*)-buta-1,3-dienyl)-1*H*-indole [B]

A4: Optimised structures of the modified indole derivatives

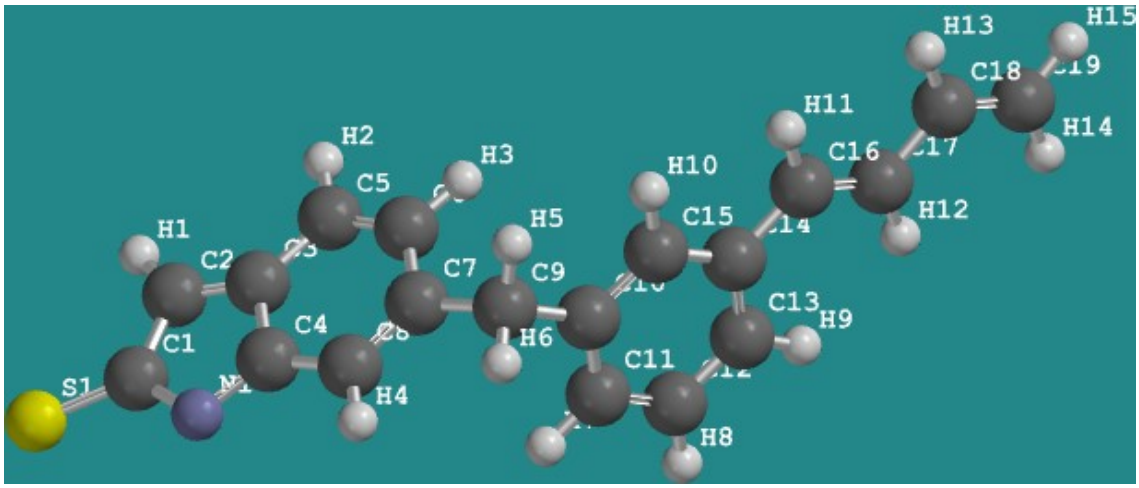

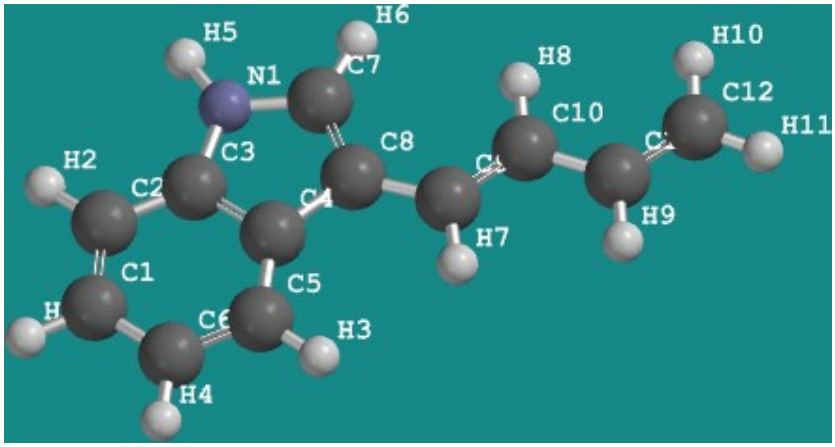

A5: Optimised molecular structures of modified indole derivatives showing mulliken charges

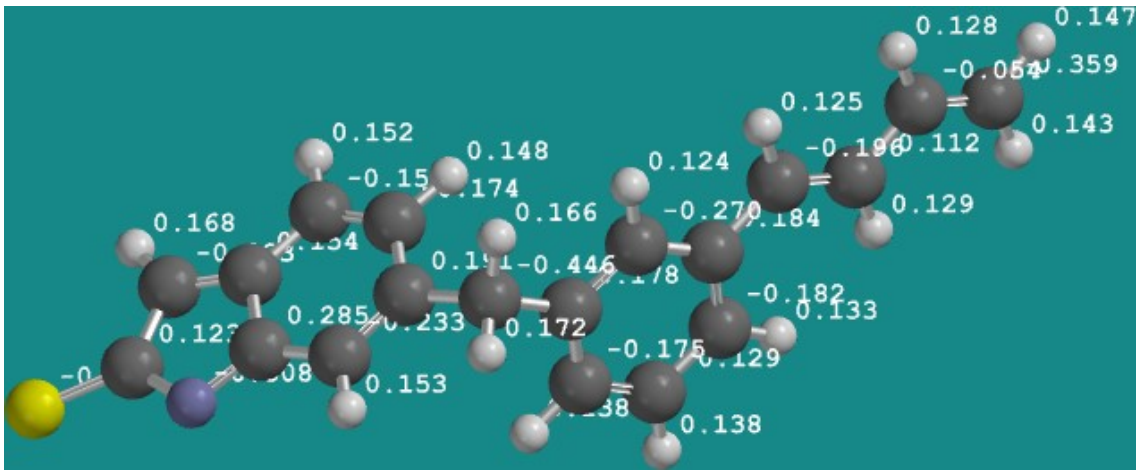

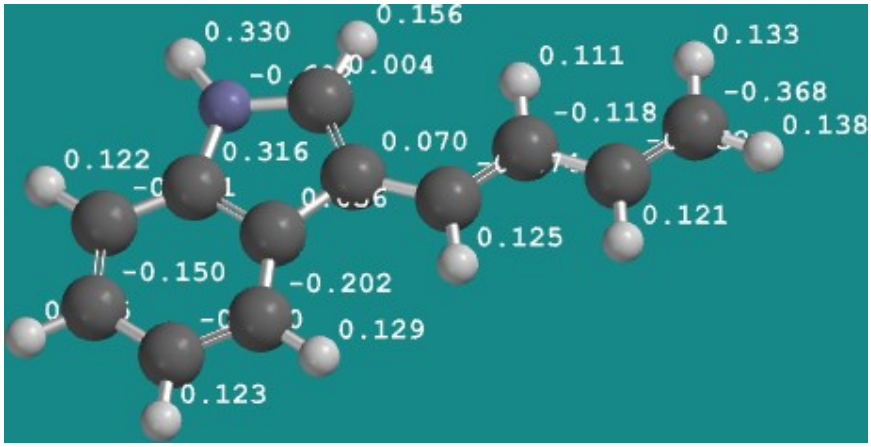

A6: HOMO plot of optimised indole derivatives

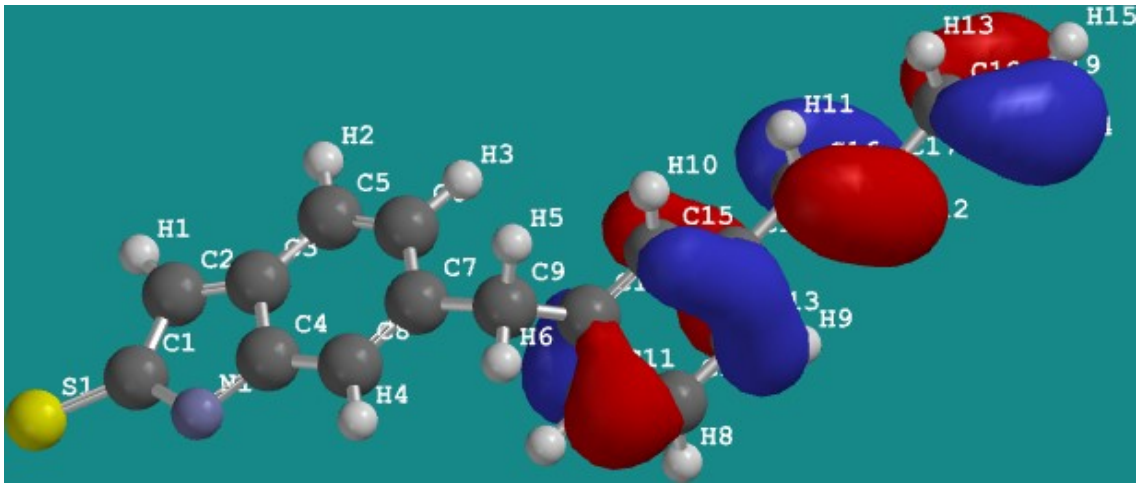

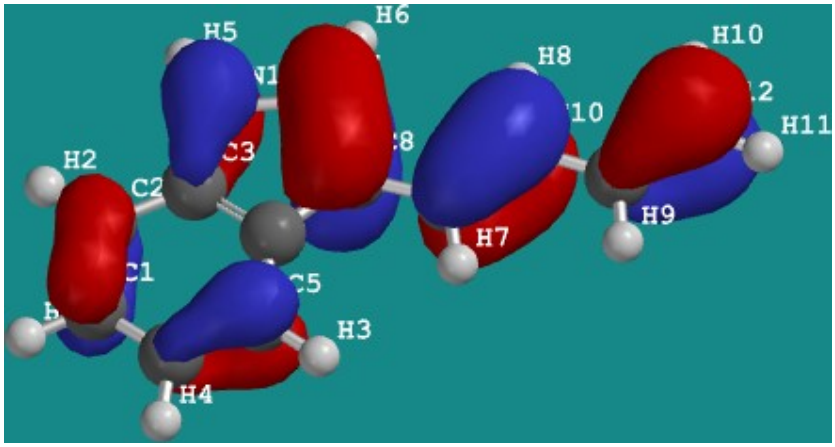

A7: LUMO plot of optimised indole derivatives

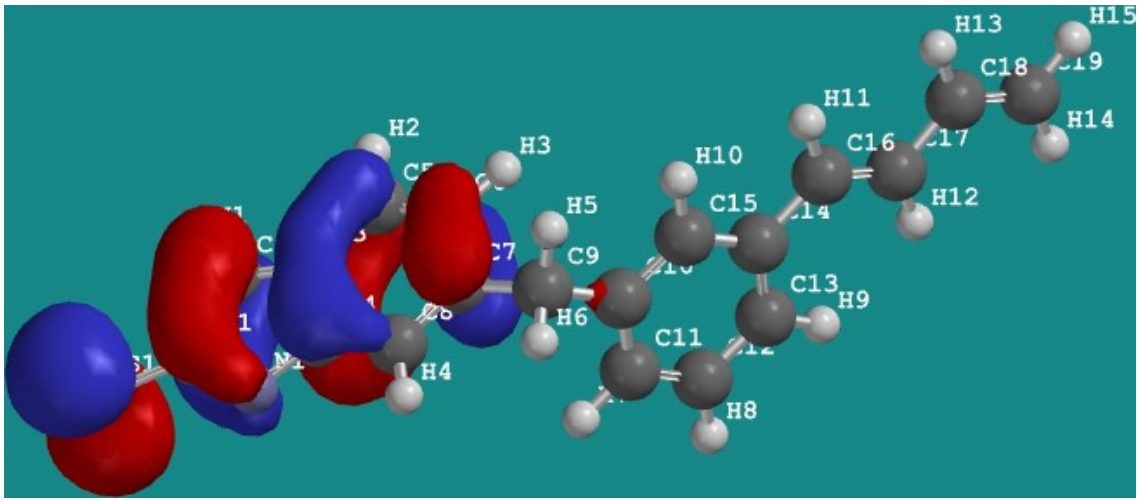

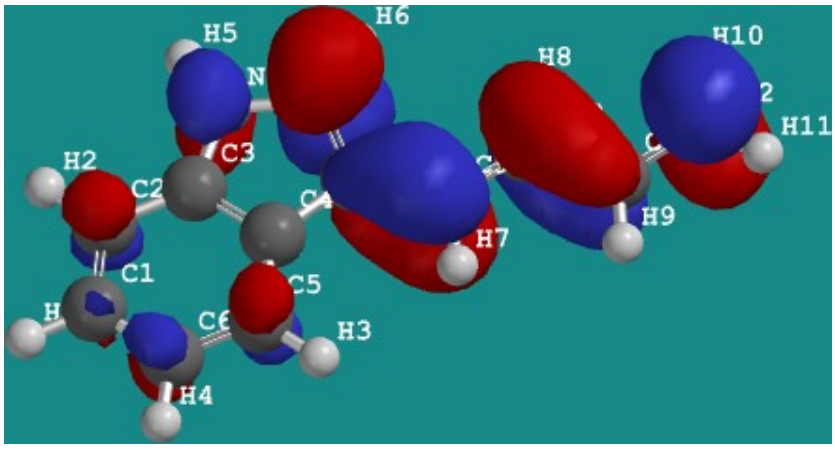

A8: Quantum chemical parameters of modified indole derivatives using DFT method

Quantum chemical parameters	A	B
E_{Homo} (eV)	-5.84	-4.95
E_{Lumo} (eV)	-3.90	-0.88
$E_{Lumo} - E_{Homo}$ (eV)	1.94	4.07
Dipole moment (μ)	5.93	2.57
Log P	3.92	0.98
Polarizability	66.22	56.43
Volume ($Å^3$)	311.87	197.43
Weight (amu)	289.40	169.23
Ionisation Potential (*I*)	5.84	4.95
Electron Affinity (*A*)	3.90	0.88
Hardness(η)	0.97	2.035
Softness (*S*)	1.0309	0.491
Electronegativity(χ)	4.87	2.915
Chemical potential (μ)	-4.87	-2.915
Electrophilicity Index (ω)	12.2252	2.0878

A9: Molecular structure of simulated 2 nitro aniline derivatives

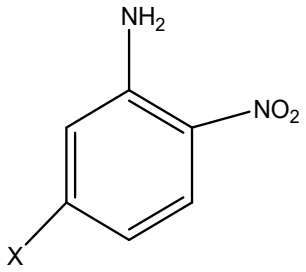

(1) X = C_2H_3 2 nitro-5-vinyl aniline (S)

(2) X = C_4H_5 5-(buta-1,3,-dienyl)-2-nitroaniline (T)

(3) X = $C_{10}H_{11}$ 5-(deca-1,3,5,7,9-pentyl)-2-nitroaniline (U)

A10: Optimised structures of the modified 2 nitro aniline derivatives

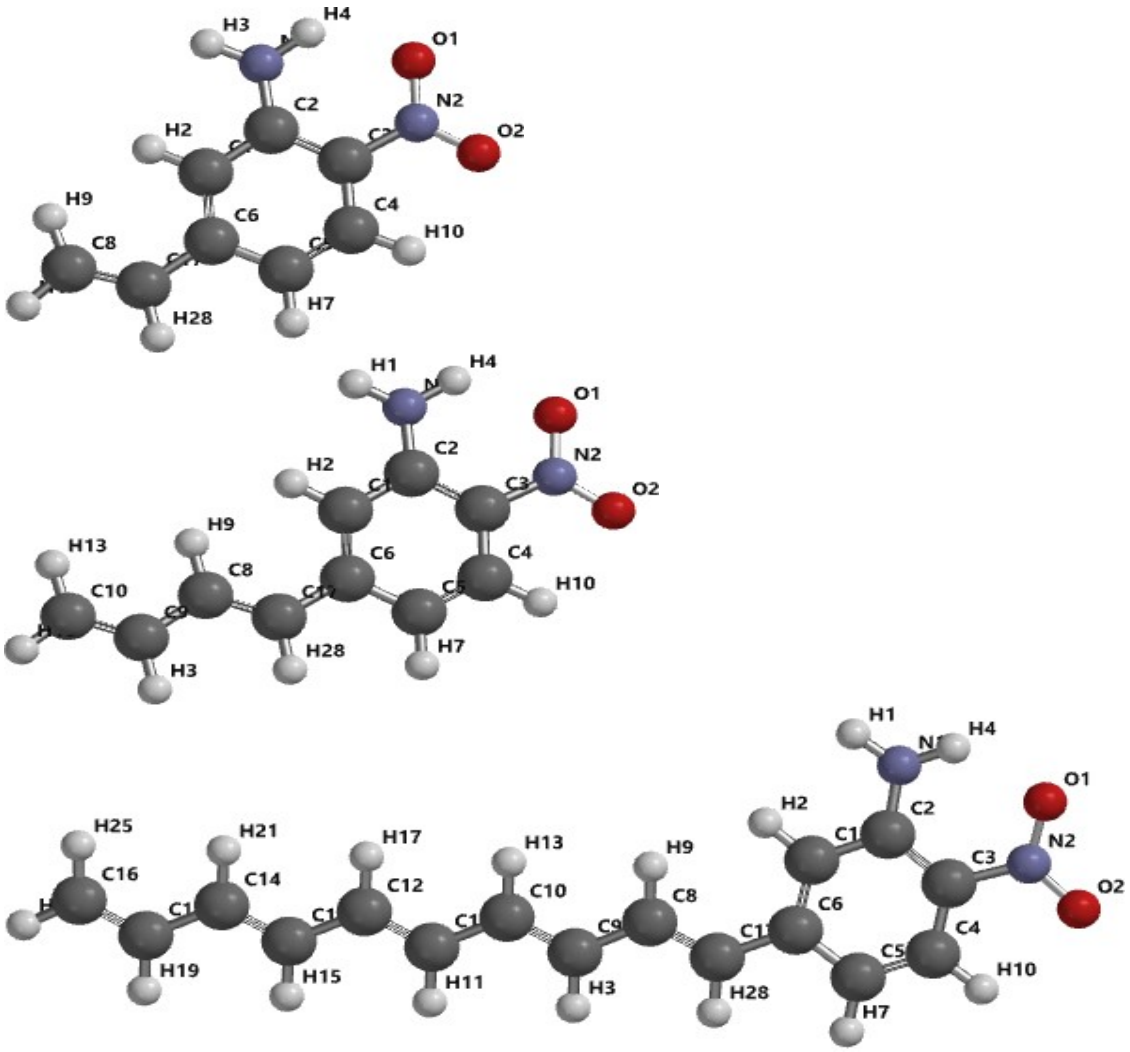

A11: Optimised molecular structures of nitro aniline showing mulliken charges

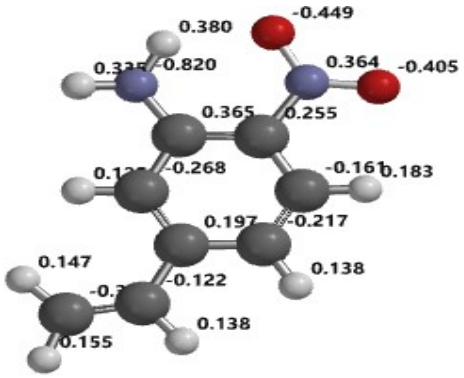

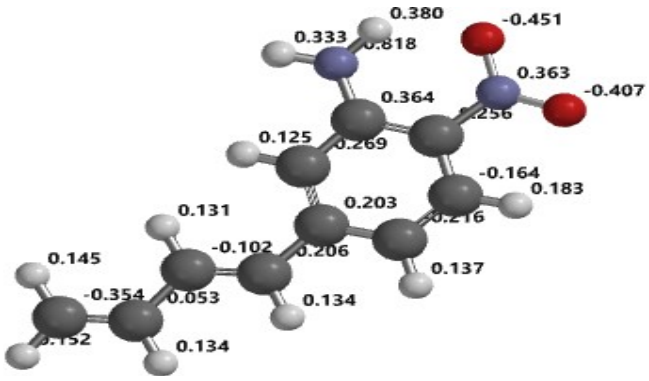

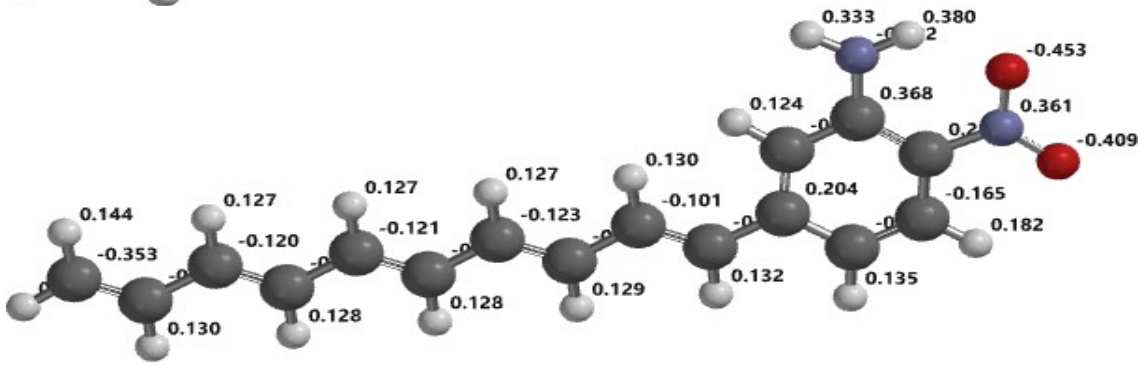

A12: HOMO plot of optimised 2 nitro aniline derivatives

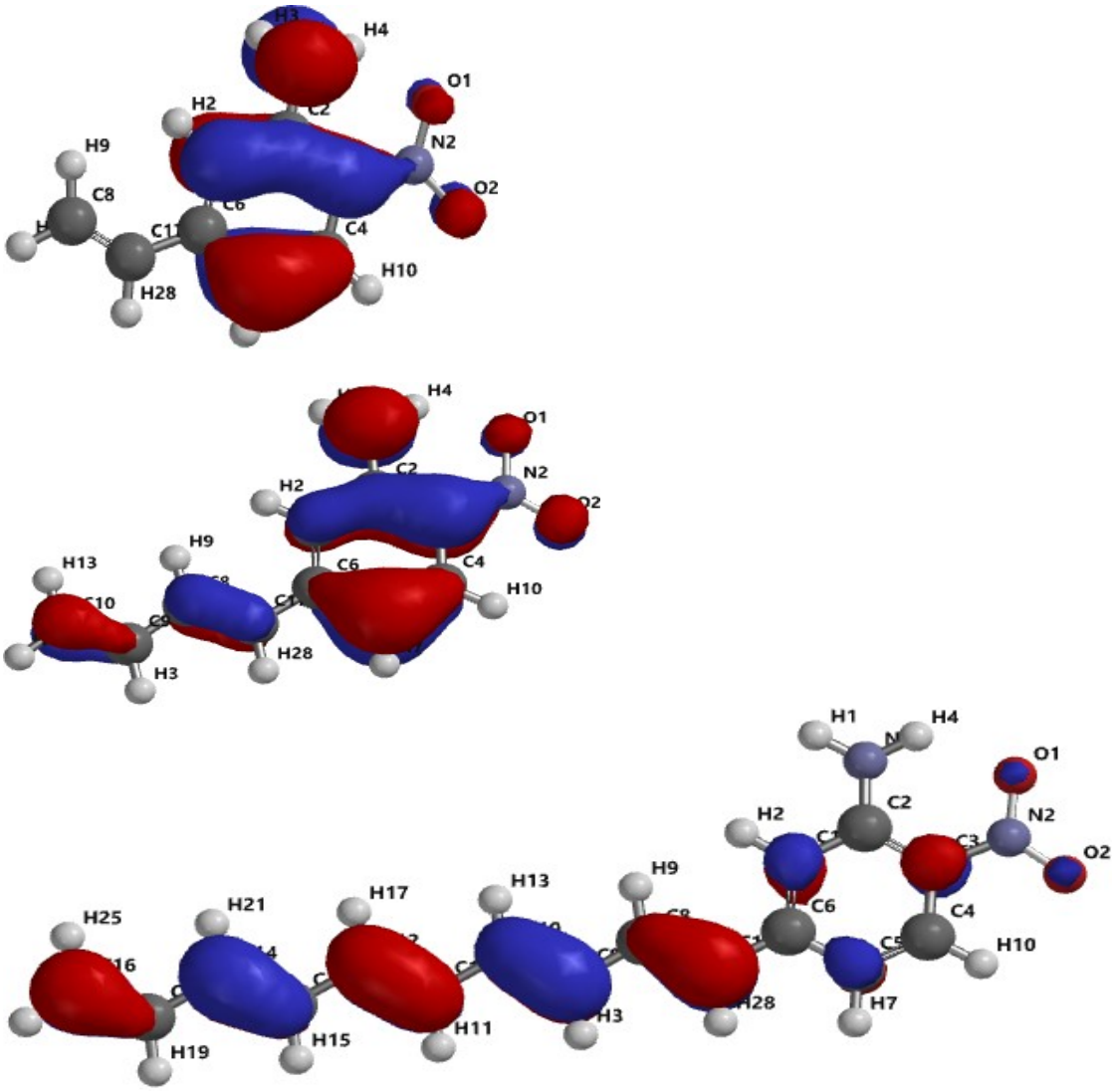

A13: LUMO plot of optimised 2 nitro aniline derivatives

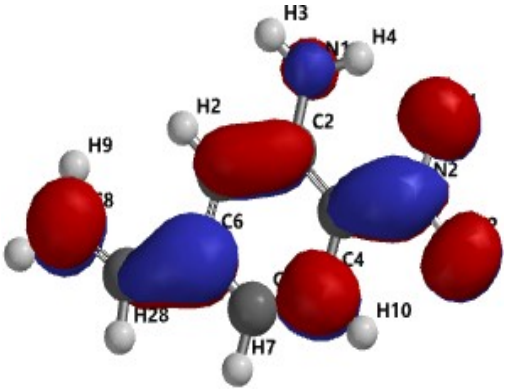

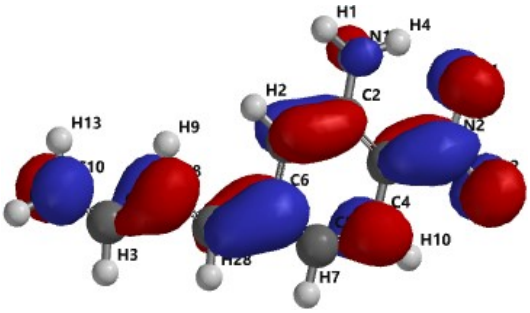

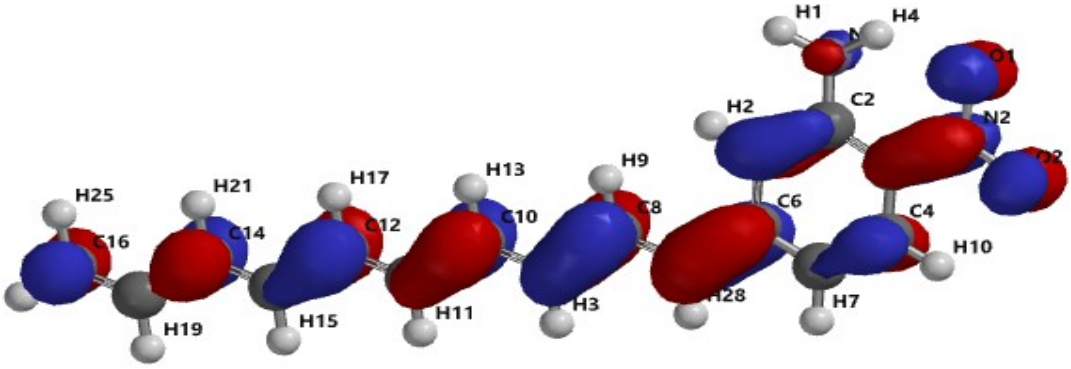

A14: Quantum chemical parameters of modified 2 nitro aniline derivatives using DFT method

Quantum chemical parameters	S	T	U
E_{Homo} (eV)	-6.07	-6.02	-5.29
E_{Lumo} (eV)	-2.34	-2.42	-2.59
$E_{Lumo} - E_{Homo}$ (eV)	3.73	3.60	2.7
Dipole moment (μ)	5.04	5.48	6.79
Log P	-4.03	-3.51	-1.97
Polarizability	53.70	56.37	64.51
Volume ($Å^3$)	162.77	195.34	293.04
Weight (amu)	164.164	190.202	268.316
Ionisation Potential (*I*)	6.07	6.02	5.29
Electron Affinity (*A*)	2.34	2.42	2.59
Hardness(η)	1.865	1.80	1.35
Softness (*S*)	0.536	0.556	0.741
Electronegativity(χ)	4.205	4.220	3.94
Chemical potential (μ)	-4.205	-4.220	-3.94
Electrophilicity Index (ω)	4.740	4.947	5.749

A15: Weight loss values after three runs for 6 benzyl oxy indole

Temperature	Concentration (mol/dm^3) x 10^{-5}	W_a (mg)	W_b (mg)	W_c (mg)	Mean value (mg)	St Dev
30 °C	Blank	0.0925	0.0654	0.0833	0.0804	0.013780784
	2	0.0428	0.0159	0.0340	0.0309	0.013715320
	4	0.0377	0.0108	0.0289	0.0258	0.013715320
	6	0.0318	0.0045	0.0222	0.0195	0.013848827
	8	0.0127	0.0128	0.0129	0.0128	0.000100000
	10	0.0065	0.0063	0.0058	0.0062	0.000360555
40 °C	Blank	0.0704	0.1062	0.0916	0.0894	0.018001111
	2	0.0192	0.0550	0.0404	0.0382	0.018001111
	4	0.0151	0.0508	0.0364	0.0341	0.017960791
	6	0.0090	0.0410	0.0340	0.0280	0.016822604
	8	0.0258	0.0255	0.0255	0.0256	0.000173205
	10	0.0140	0.0120	0.0130	0.0130	0.001000000
50 °C	Blank	0.1163	0.0785	0.1007	0.0985	0.018995789
	2	0.0674	0.0295	0.0516	0.0495	0.019037069
	4	0.0602	0.0221	0.0440	0.0421	0.019120931
	6	0.0530	0.0153	0.0376	0.0353	0.018954947
	8	0.0485	0.0105	0.0325	0.0305	0.019078784
	10	0.0426	0.0045	0.0264	0.0245	0.019120931
60 °C	Blank	0.1084	0.1360	0.1288	0.1244	0.014316424
	2	0.0575	0.0850	0.0780	0.0735	0.014291606
	4	0.0488	0.0762	0.0694	0.0648	0.014267445
	6	0.0437	0.0714	0.0640	0.0597	0.014341897
	8	0.0338	0.0616	0.0540	0.0498	0.014368020
	10	0.0287	0.0567	0.0487	0.0447	0.014422205

W_a = *1st run*

W_b = *2nd run*

W_c = *3rd run*

St Dev = Standard deviation

$$Mean\ value = \frac{W_a + W_b + W_c}{3}$$

A16: Weight loss values from gravimetric method after three runs for 3 methyl indole

Temperature	Concentration (mol/dm^3) x 10^{-5}	W_a (mg)	W_b (mg)	W_c (mg)	Mean value (mg)	St Dev
30 °C	2	0.0308	0.0665	0.0521	0.0498	0.017961
	4	0.0242	0.06	0.0454	0.0432	0.018001
	6	0.0174	0.0531	0.0387	0.0364	0.017961
	8	0.0172	0.0175	0.0172	0.0173	0.000173
	10	0.013	0.012	0.008	0.011	0.002646
40 °C	2	0.071	0.0442	0.0624	0.0592	0.013684
	4	0.0655	0.0389	0.0573	0.0539	0.013622
	6	0.0566	0.0299	0.0482	0.0449	0.013652
	8	0.0462	0.0198	0.0384	0.0348	0.013563
	10	0.0412	0.0144	0.0326	0.0294	0.013684
50 °C	2	0.0875	0.0498	0.0721	0.0698	0.018955
	4	0.0811	0.0432	0.0653	0.0632	0.019037
	6	0.0735	0.0359	0.0583	0.0559	0.018915
	8	0.0656	0.0277	0.0498	0.0477	0.019037
	10	0.0579	0.0201	0.0423	0.0401	0.018996
60 °C	2	0.0892	0.117	0.1094	0.1052	0.014368
	4	0.0741	0.1018	0.0944	0.0901	0.014342
	6	0.0658	0.0931	0.0865	0.0818	0.014244
	8	0.0586	0.0863	0.0789	0.0746	0.014342
	10	0.0482	0.076	0.0684	0.0642	0.014368

W_a = *1st run*

W_b = *2nd run*

W_c = *3rd run*

St Dev = Standard deviation

$$Mean\ value = \frac{W_a + W_b + W_c}{3}$$

A17: Weight loss values from gravimetric method after three runs for 2nitro aniline

Temperature	Concentration (mol/dm^3) x 10^{-5}	W_a (mg)	W_b (mg)	W_c (mg)	Mean value (mg)	St Dev
30 °C	2	0.0647	0.0375	0.0559	0.0527	0.013879
	4	0.0617	0.0342	0.0532	0.0497	0.01408
	6	0.0585	0.0312	0.0498	0.0465	0.013946
	8	0.0552	0.0282	0.0462	0.0432	0.013748
	10	0.0504	0.0233	0.0415	0.0384	0.013813
40 °C	2	0.04	0.0761	0.0612	0.0591	0.018141
	4	0.0374	0.0737	0.059	0.0567	0.018259
	6	0.0341	0.0704	0.0557	0.0534	0.018259
	8	0.0256	0.0621	0.0476	0.0451	0.018378
	10	0.025	0.062	0.048	0.045	0.018682
50 °C	2	0.0867	0.0485	0.0709	0.0687	0.019195
	4	0.0832	0.0451	0.0673	0.0652	0.019137
	6	0.0787	0.0405	0.0629	0.0607	0.019195
	8	0.0761	0.038	0.0602	0.0581	0.019137
	10	0.0748	0.0366	0.059	0.0568	0.019195
60 °C	2	0.0797	0.1076	0.0998	0.0957	0.014395
	4	0.0768	0.1045	0.0971	0.0928	0.014342
	6	0.0735	0.1015	0.0935	0.0895	0.014422
	8	0.0691	0.0971	0.0891	0.0851	0.014422
	10	0.066	0.091	0.089	0.082	0.013892

W_a = *1st run*

W_b = *2nd run*

W_c = *3rd run*

St Dev = Standard deviation

$$Mean\ value = \frac{W_a + W_b + W_c}{3}$$

A18: Weight loss values from gravimetric method after three runs for 3nitro aniline

Temperature	Concentration (mol/dm^3) x 10^{-5}	W_a (mg)	W_b (mg)	W_c (mg)	Mean value (mg)	St Dev
30 °C	2	0.0648	0.0382	0.0566	0.0532	0.013622
	4	0.0619	0.0351	0.0533	0.0501	0.013684
	6	0.0587	0.0321	0.0505	0.0471	0.013622
	8	0.0555	0.0288	0.0471	0.0438	0.013652
	10	0.0507	0.0241	0.0425	0.0391	0.013622
40 °C	2	0.0425	0.0781	0.0639	0.0615	0.017921
	4	0.0382	0.074	0.0594	0.0572	0.018001
	6	0.0351	0.0711	0.0561	0.0541	0.018083
	8	0.0298	0.0655	0.0511	0.0488	0.017961
	10	0.0297	0.0652	0.0512	0.0487	0.017882
50 °C	2	0.0872	0.0494	0.0716	0.0694	0.018996
	4	0.0834	0.0457	0.0680	0.0657	0.018955
	6	0.0788	0.0412	0.0636	0.0612	0.018915
	8	0.0764	0.0387	0.0610	0.0587	0.018955
	10	0.0752	0.0374	0.0596	0.0574	0.018996
60 °C	2	0.0800	0.1080	0.1000	0.0960	0.014422
	4	0.0770	0.1030	0.0990	0.0930	0.014000
	6	0.0738	0.1017	0.0939	0.0898	0.014395
	8	0.0695	0.0973	0.0897	0.0855	0.014368
	10	0.0664	0.0941	0.0867	0.0824	0.014342

W_a = *1st run*

W_b = *2nd run*

W_c = *3rd run*

St Dev = Standard deviation

$$Mean\ value = \frac{W_a + W_b + W_c}{3}$$

A19: Weight loss values from gravimetric method after three runs for 4nitro aniline

Temperature	Concentration (mol/dm^3) x 10^{-5}	W_a (mg)	W_b (mg)	W_c (mg)	Mean value (mg)	St Dev
30 °C	2	0.0655	0.0389	0.0573	0.0539	0.013622
	4	0.0625	0.0358	0.0541	0.0508	0.013652
	6	0.0600	0.0330	0.0510	0.0480	0.013748
	8	0.0563	0.0295	0.0477	0.0445	0.013684
	10	0.0517	0.0248	0.0429	0.0398	0.013715
40 °C	2	0.0433	0.0789	0.0647	0.0623	0.017921
	4	0.0389	0.0745	0.0603	0.0579	0.017921
	6	0.0359	0.0716	0.0572	0.0549	0.017961
	8	0.0315	0.0672	0.0528	0.0505	0.017961
	10	0.0274	0.0633	0.0485	0.0464	0.018042
50 °C	2	0.0881	0.0501	0.0721	0.0701	0.019079
	4	0.0843	0.0465	0.0687	0.0665	0.018996
	6	0.0800	0.0420	0.0640	0.0620	0.019079
	8	0.0773	0.0395	0.0617	0.0595	0.018996
	10	0.0761	0.0382	0.0603	0.0582	0.019037
60 °C	2	0.0808	0.1082	0.1014	0.0968	0.014267
	4	0.0778	0.1053	0.0983	0.0938	0.014292
	6	0.0745	0.1021	0.0949	0.0905	0.014316
	8	0.0704	0.0981	0.0907	0.0864	0.014342
	10	0.0677	0.0955	0.0879	0.0837	0.014368

W_a = *1st run*

W_b = *2nd run*

W_c = *3rd run*

St Dev = Standard deviation

$$Mean\ value = \frac{W_a+W_b+W_c}{3}$$

A20: Volume of H_2 gas loss from gasometric method after three runs at 30 ^oC

Molecule	Concentration (mol/dm^3) x 10^{-5}	V_a (cm^3)	V_b (cm^3)	V_c (cm^3)	Mean value (cm^3)	St Dev
6 benzyl oxy indole	Blanc	37	32	36	35	2.645751
	2	20	19	15	18	2.645751
	4	14	14	17	15	1.732051
	6	13	10	10	11	1.732051
	8	10	10	7	9	1.732051
	10	6	6	9	7	1.732051
3 methyl indole	2	26	22	21	23	2.645751
	4	19	19	22	20	1.732051
	6	15	19	17	17	2.000000
	8	14	14	17	15	1.732051
	10	13	12	11	12	1.000000
2 nitro aniline	2	27	22	23	24	2.645751
	4	24	24	21	23	1.732051
	6	22	23	21	22	1.000000
	8	19	22	19	20	1.732051
	10	18	21	18	19	1.732051
3 nitro aniline	2	24.5	25	24	24.5	0.500000
	4	26	23	23	24	1.732051
	6	23	22.5	22	22.5	0.500000
	8	23	19	21	21	2.000000
	10	22	20	18	20	2.000000
4 nitro aniline	2	26	25	24	25	1.00000
	4	24.5	24	25	24.5	0.50000
	6	24	23	25	24	1.00000
	8	22.5	23	22	22.5	0.50000
	10	22	21	20	21	1.00000

V_a = *1st run*

V_b = *2nd run*

V_c = *3rd run*

St Dev = Standard deviation

$$Mean\ value = \frac{V_a+V_b+V_c}{3}$$